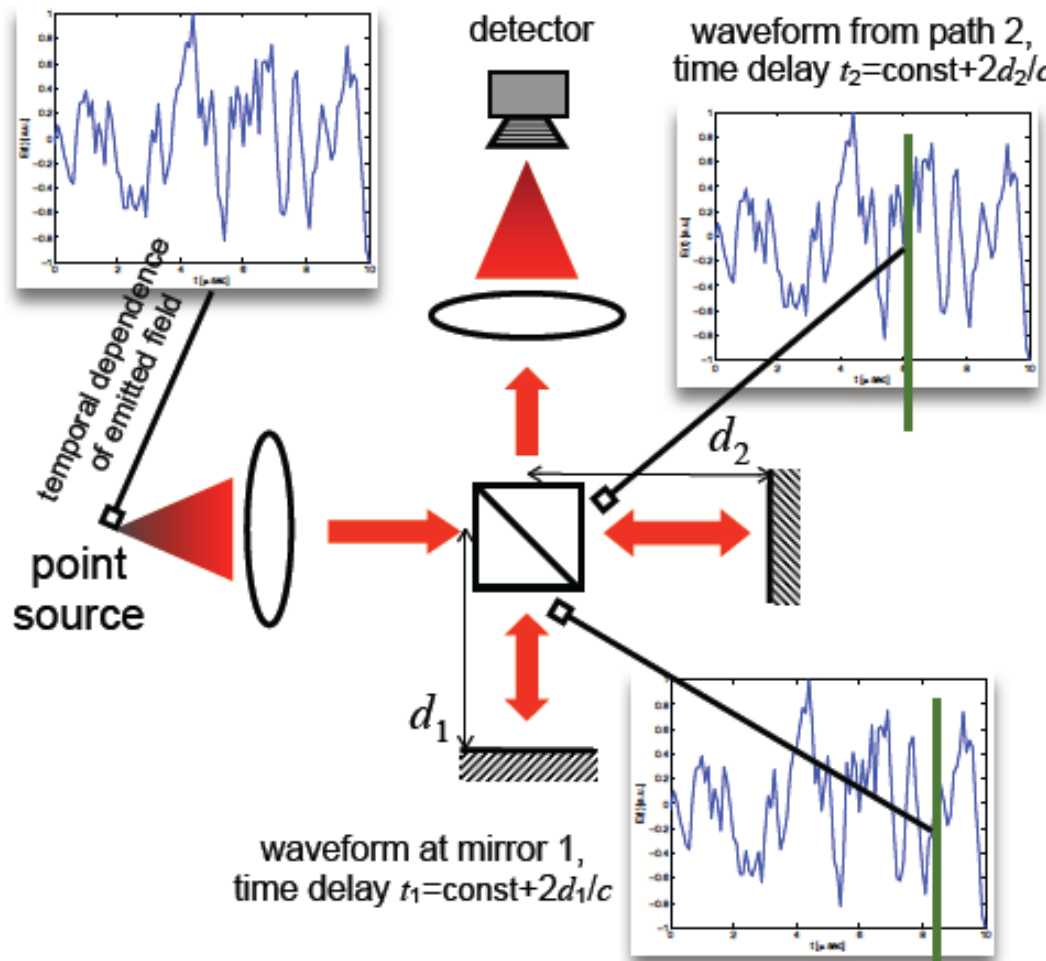


Temporal coherence

Michelson interferometer

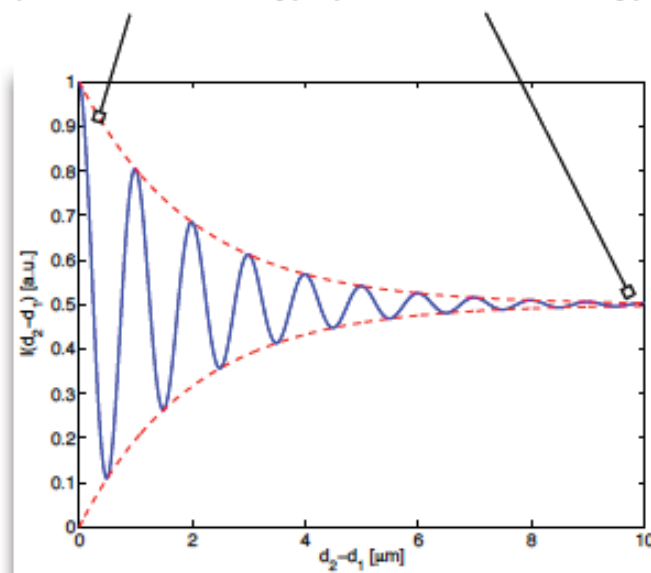
random illumination

(not single color anymore)



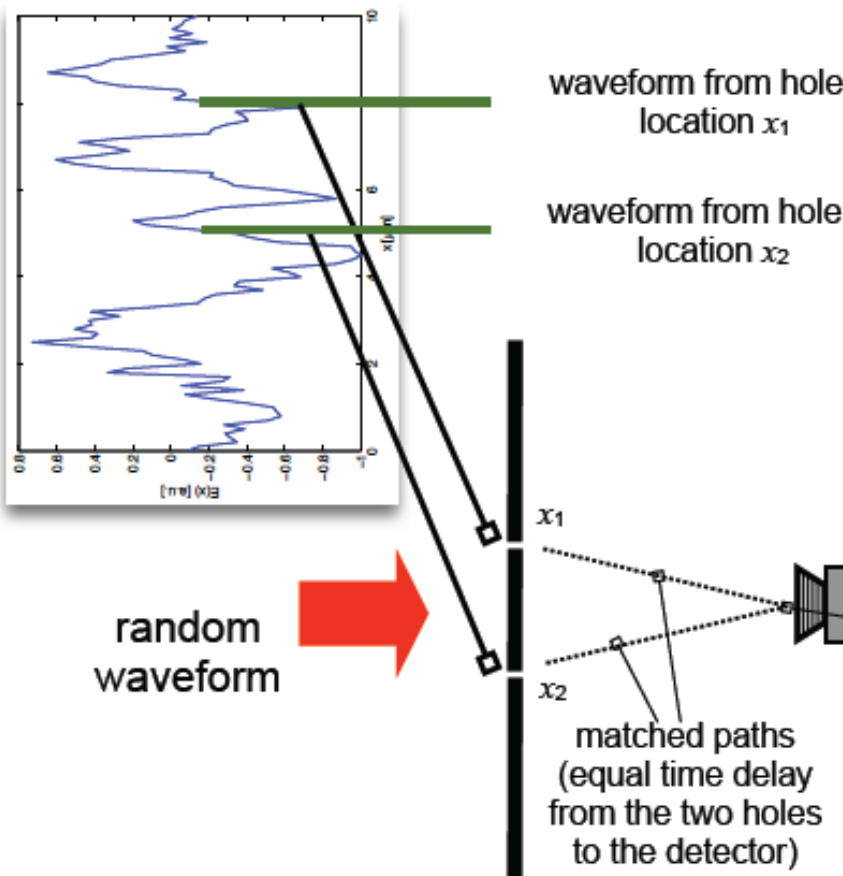
If paths 1 & 2 are matched, then the recombined waveforms at the detector are *correlated* so they produce interference fringes. However, as the difference $d_2 - d_1$ increases, the degree of correlation decreases and so does the contrast in the interference pattern.

interference
(fields add coherently) no interference
(fields add incoherently)



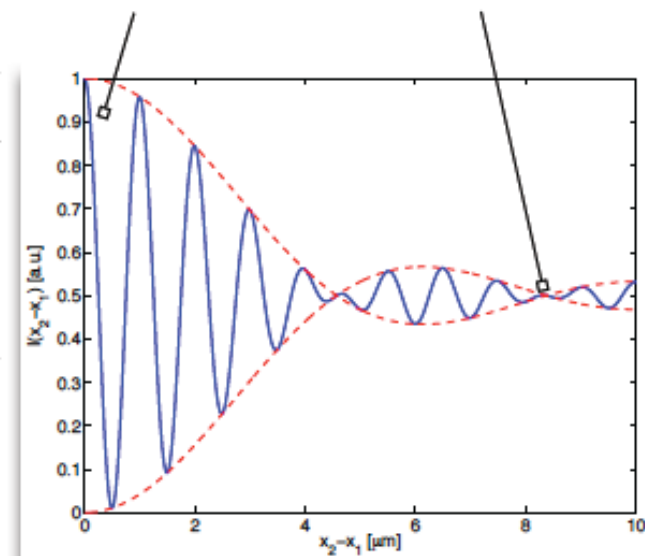
Spatial coherence

Young interferometer



If holes 1 & 2 are coincident, or very closely spaced, then the recombined waveforms at the detector are *correlated* so they produce interference fringes. However, as the difference $x_2 - x_1$ increases, the degree of correlation decreases and so does the contrast in the interference pattern.

interference
(fields add *coherently*) no interference
(fields add *incoherently*)



Coherent and incoherent sources and measurements

Temporally incoherent; spatially coherent

- ▶ White light lamp (broadband; e.g., thermal) spatially limited by a pinhole
- ▶ White light source located very far away (i.e. with extremely small NA)
e.g. sun, stars, lighthouse at long distance
- ▶ Pulsed laser sources with extremely short (<nsec) pulse duration; supercontinuum sources

Temporally & spatially coherent

- ▶ Monochromatic laser sources
e.g. doubled Nd:YAG (best), HeNe, Ar⁺ (poorer)
- ▶ Atomic transition (quasi-monochromatic) lamps (e.g. Xe) spatially limited by a pinhole

Temporally & spatially incoherent

- ▶ White light source at a nearby distance or without spatial limitation

Temporally coherent; spatially incoherent

also referred to as
**quasi-monochromatic
spatially incoherent**

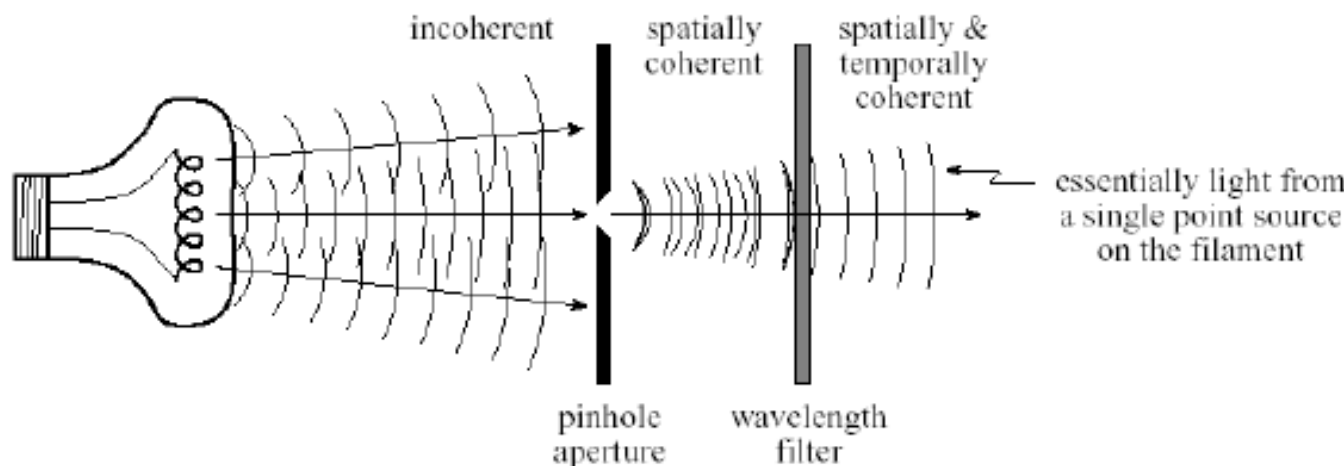
- ▶ Monochromatic laser sources (e.g. HeNe, doubled Nd:YAG) with a rotating diffuser (plate of ground glass) in the beam path
- ▶ Atomic transition (quasi-monochromatic) lamps (e.g. Xe) without spatial limitation

Optical instruments utilizing the degree of coherence for imaging

- ▶ Michelson interferometer [spatial; high resolution astronomical imaging at optical frequencies]
- ▶ Radio telescopes, e.g. the Very Large Array (VLA) [spatial; astronomical imaging at RF frequencies]
- ▶ Optical Coherence Tomography (OCT) [temporal; bioimaging with optical sectioning]
- ▶ Multipole illumination in optical lithography [spatial; sub- μm feature patterning]

NOTE : In order to get a high visibility in an interference fringe, both the temporal and spatial coherences must be good.

How to make an incoherent light **COHERENT?**



Module 4: Laser Principles and Engineering Application

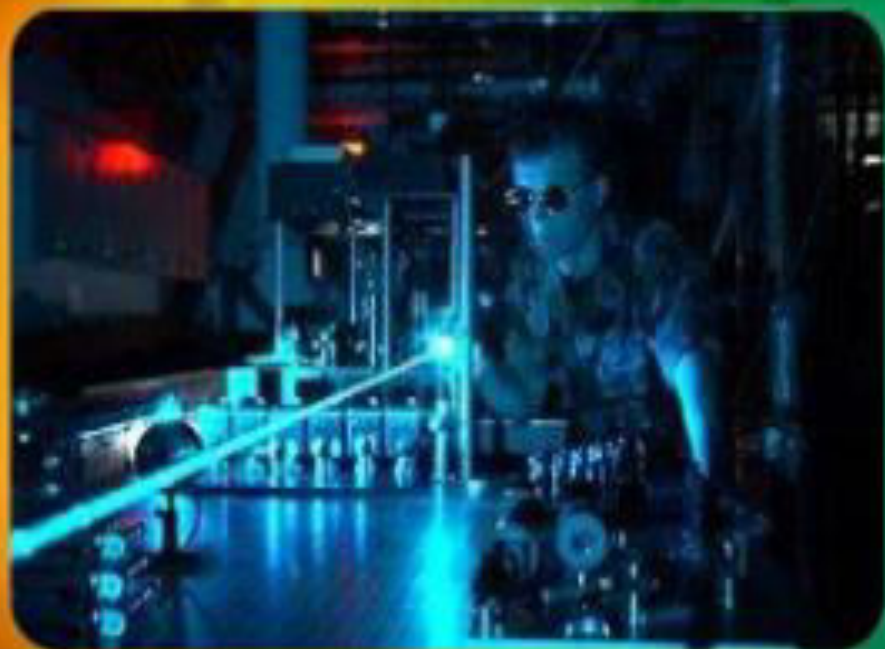
Lecture Hours 6

Laser Characteristics, Spatial and Temporal Coherence, Einstein Coefficient & its significance, Population inversion, Two, three & four level systems, Pumping schemes, Threshold gain coefficient, Components of laser, Nd-YAG, He-Ne, CO₂ and Dye laser and their engineering applications

Text books to be followed:

Laser Fundamentals, William Silfvast, Cambridge University Press (2008)

BASIC LASER

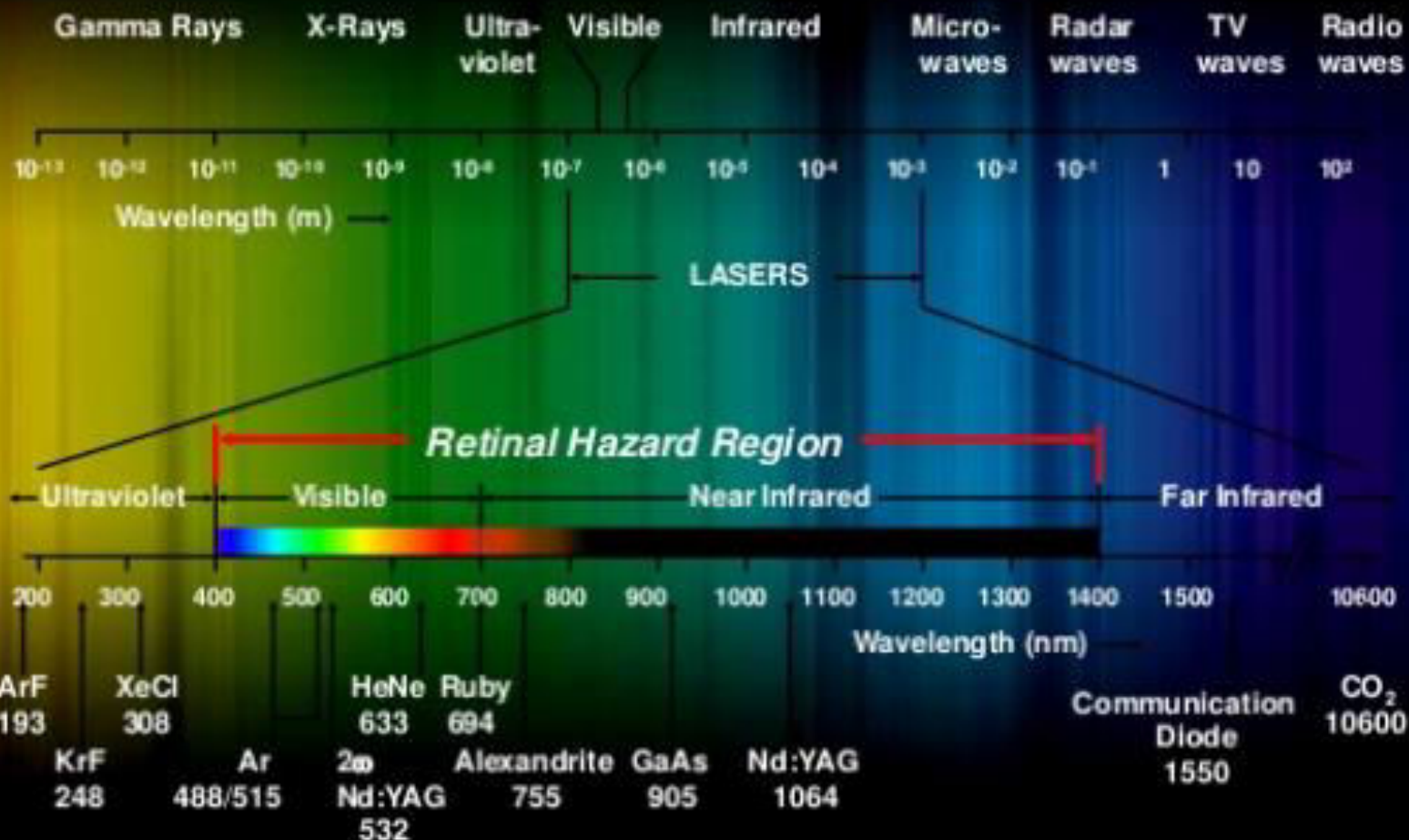


*Light
Amplification by
Stimulated
Emission of
Radiation*

Definition of **laser**

- A laser is a device that generates light by a process called **STIMULATED EMISSION**.
- The acronym LASER stands for Light Amplification by Stimulated Emission of Radiation
- Semiconducting lasers are multilayer semiconductor devices that generates a coherent beam of monochromatic light by laser action. A coherent beam resulted which all of the photons are in phase.

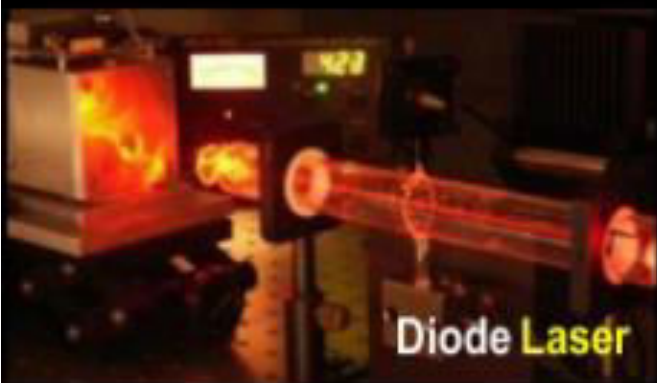
Electromagnetic Spectrum



Lasers operate in the ultraviolet, visible, and infrared.

Types of LASERS

LASERS

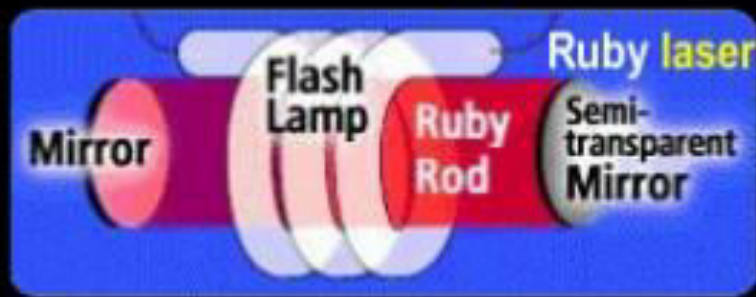


Semiconductor

Solid state

Liquid

Gas Lasers



BASIC LASER COMPONENTS

ACTIVE MEDIUM

Solid (Crystal)

Gas

Semiconductor (Diode)

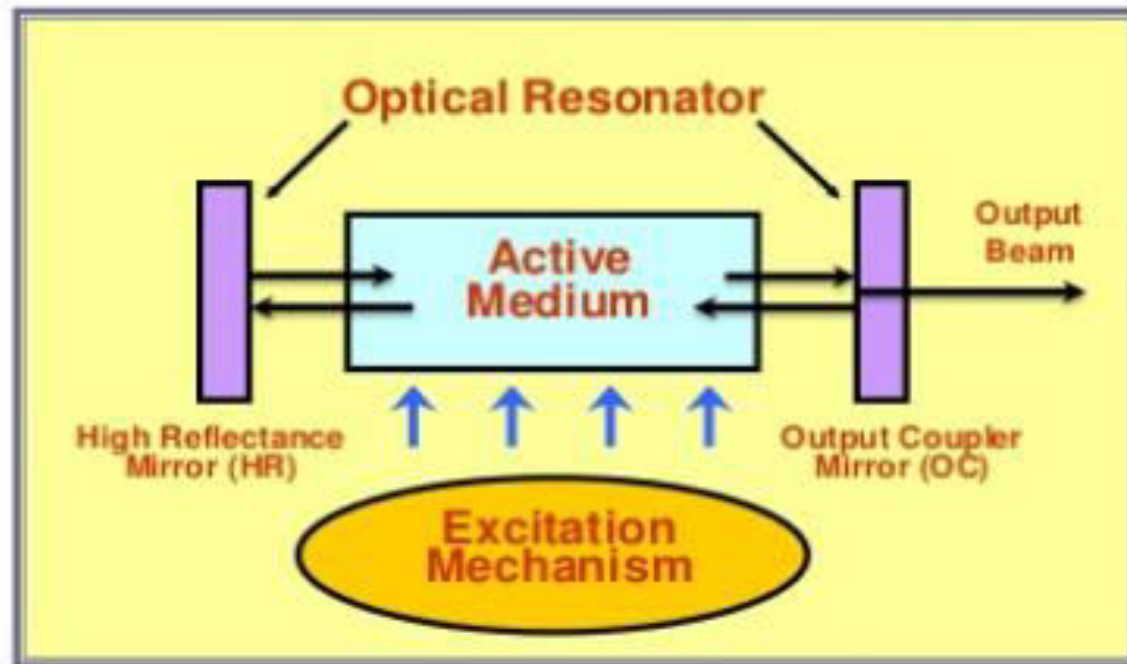
Liquid (Dye)

EXCITATION MECHANISM

*Optical
Electrical
Chemical*

OPTICAL RESONATOR

*HR Mirror and
Output Coupler*



The **Active Medium** contains atoms which can emit light by stimulated emission.

The **Excitation Mechanism** is a source of energy to excite the atoms to the proper energy state.

The **Optical Resonator** reflects the laser beam through the active medium for amplification.

History : Some important dates

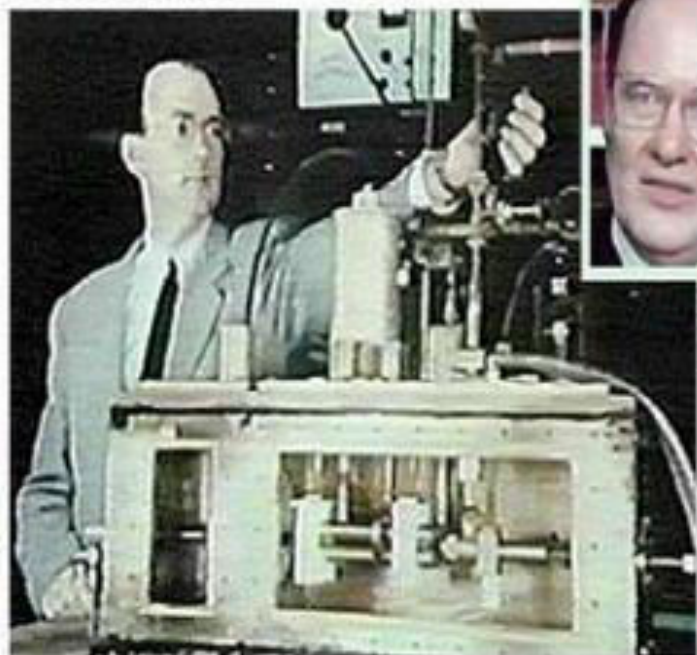
- 1917: Albert Einstein developed the theoretical concept of photons & stimulated emission
- 1954: Charles Townes & Arthur Schawlow built the first MASER using ammonia and microwave energy
- 1960: Thomas Maiman produced the first laser using a synthetic ruby rod
- 1960: Dr. Ali Javan-first continuous laser (He-Ne 632.6 nm red gas ion laser

- In 1917, Albert Einstein first theorized about the process which makes lasers possible called "Stimulated Emission."



Pioneers

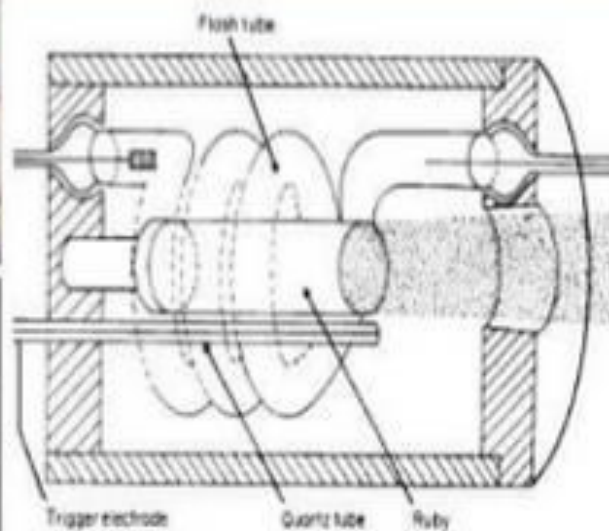
Charles Townes



Arthur Schawlow



Microwave Amplification by Stimulated Emission of Radiation
The "MASER" ... predecessor to the LASER, 1954



Thomas Maiman, 1960

This man ignored the ridicule of his peers and easily succeeded in producing history's first visible light laser from this simple photographic coiled flashlamp and his ruby crystalline rod.

History of laser

- 1960s: Dr. Leon Goldman: Father of Laser Medicine & Surgery-usage of laser in medical practice
- 1962: Bennett et al: blue-green argon laser (retinal surgery)
- 1964: Kumar Patel: CO₂ laser
- 1964: Nd:YAG laser
- 1969: Dye laser
- 1975: Excimer laser (noble gas-halide)

PIONEERS



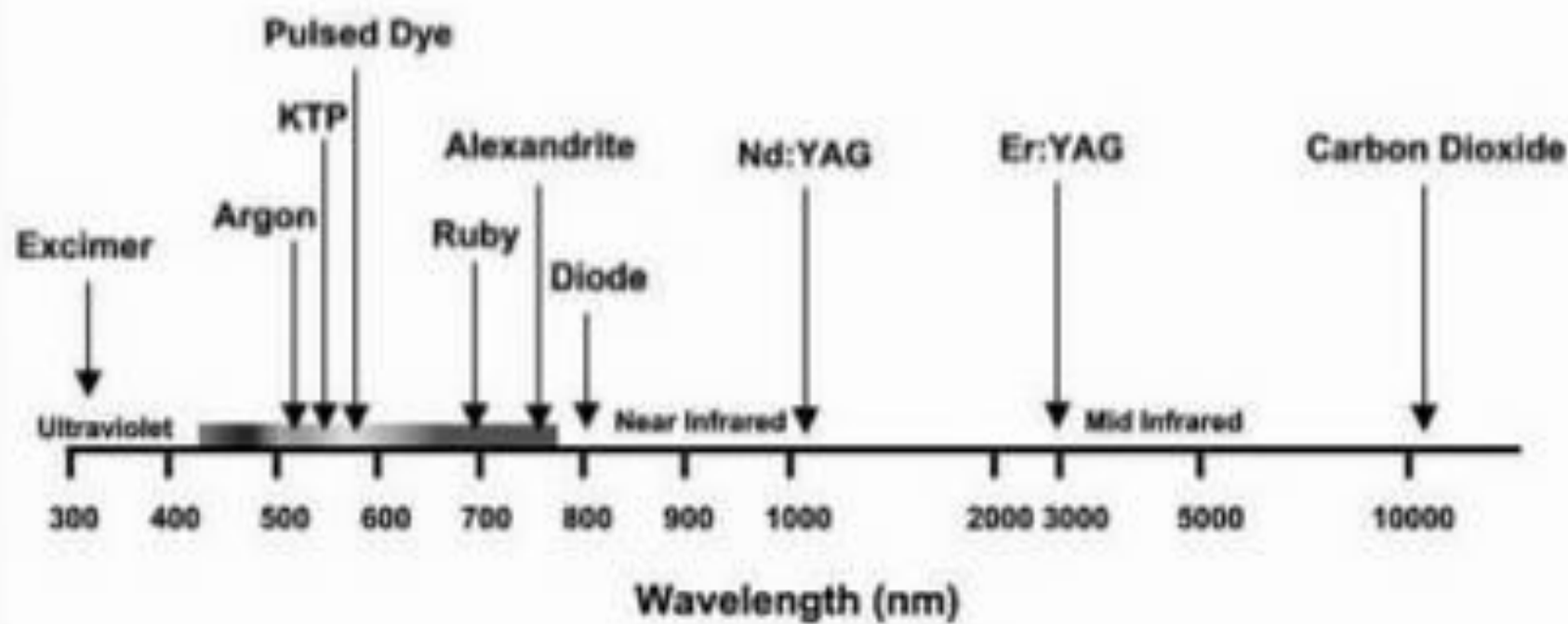
1905-1997

Dr. Leon Goldman

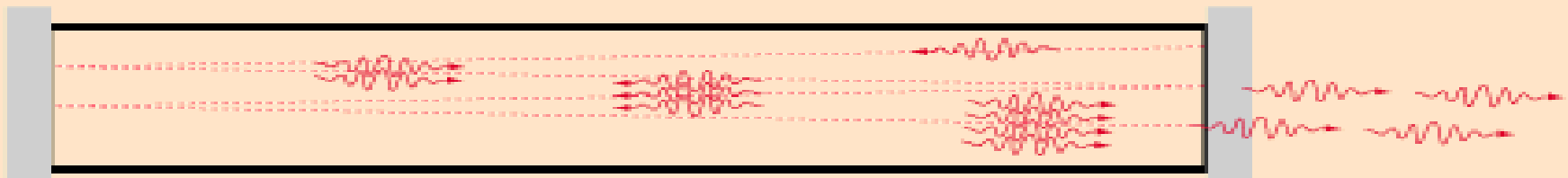
"The Father of Laser Medicine"



Identification of different types of medical lasers



Light Amplification by Stimulated Emission of Radiation



100% reflective
mirror

99% reflective
mirror



When radiation interacts with matter we have three processes to generate laser light.

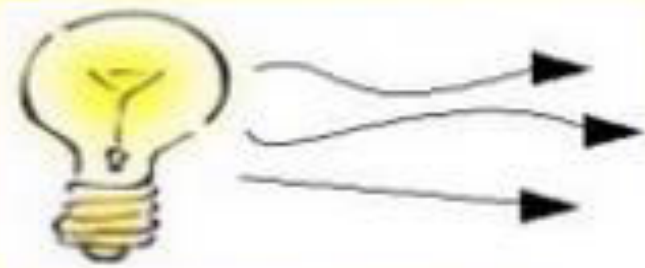
- (1) Optical Absorption*
- (2) Spontaneous Emission*
- (3) Stimulated Emission*

Characteristics of laser radiation

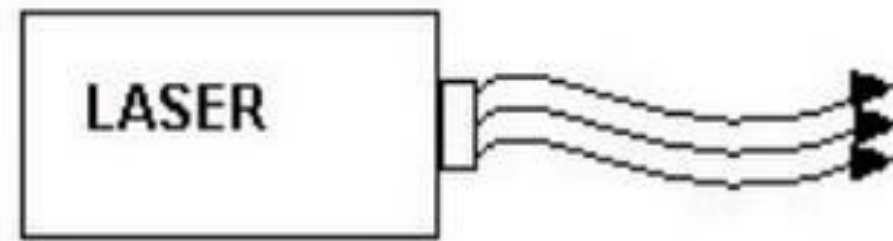
Laser radiation has the following important characteristics over ordinary light source. They are:

- i) monochromaticity
- ii) directionality
- iii) coherence
- iv) brightness

Incandescent vs. Laser Light



- **Many wavelengths**
- **Multidirectional**
- **Incoherent**



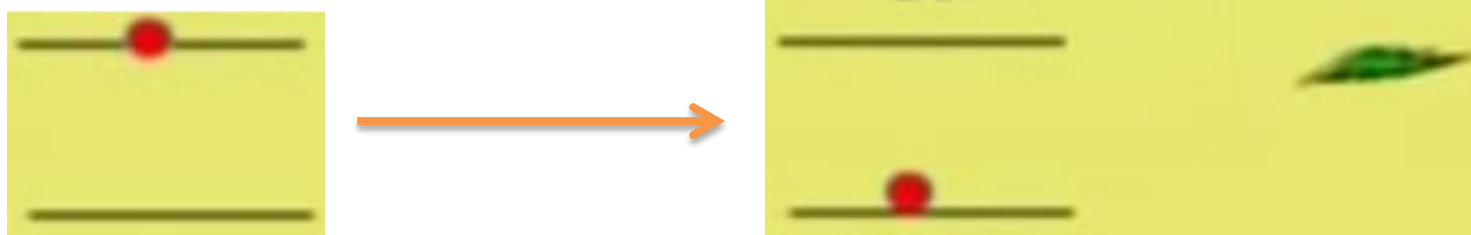
- **Monochromatic**
- **Directional**
- **Coherent**

Mono-chromaticity

- Laser is monochromatic light
i.e. Laser has mono [single] wavelength [color]

Sun, White Light

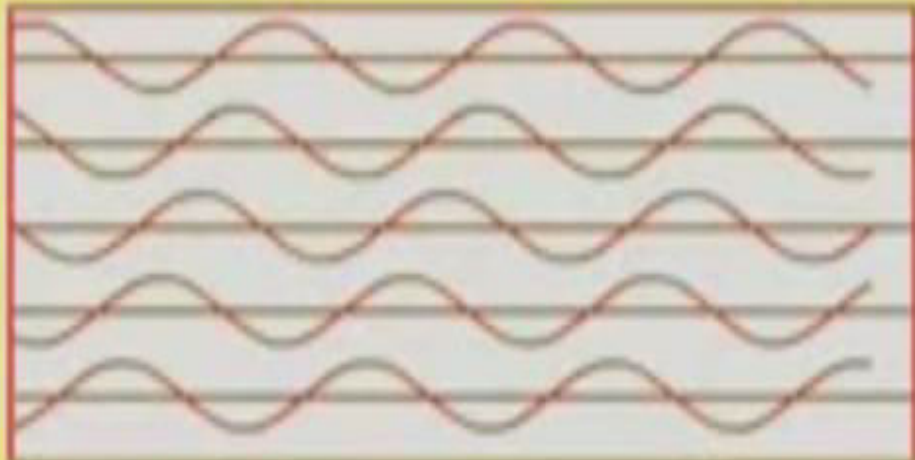
- Laser is created from the transition of electrons from definite energy levels



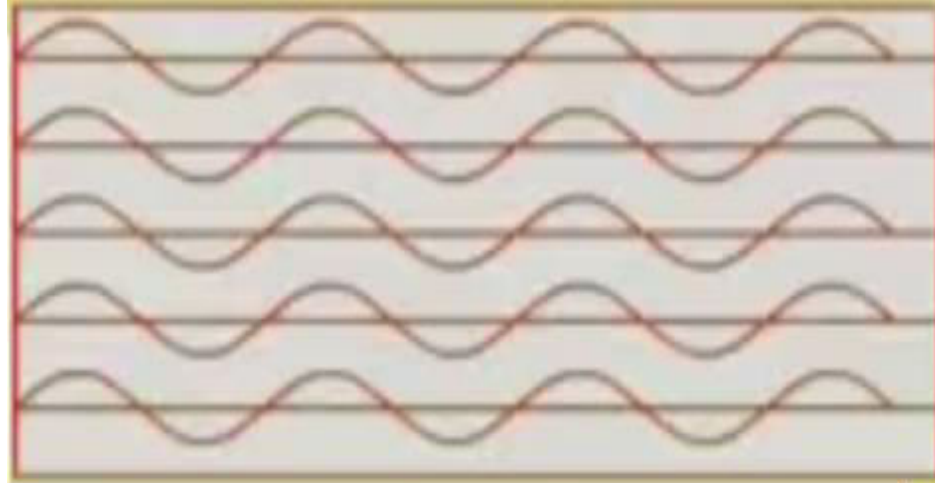
Coherence

- Laser is highly coherent light.
- Coherent light are light waves that are “in phase” with one another.

Incoherent Beams



Coherent Beams



Spatial and Temporal Coherence

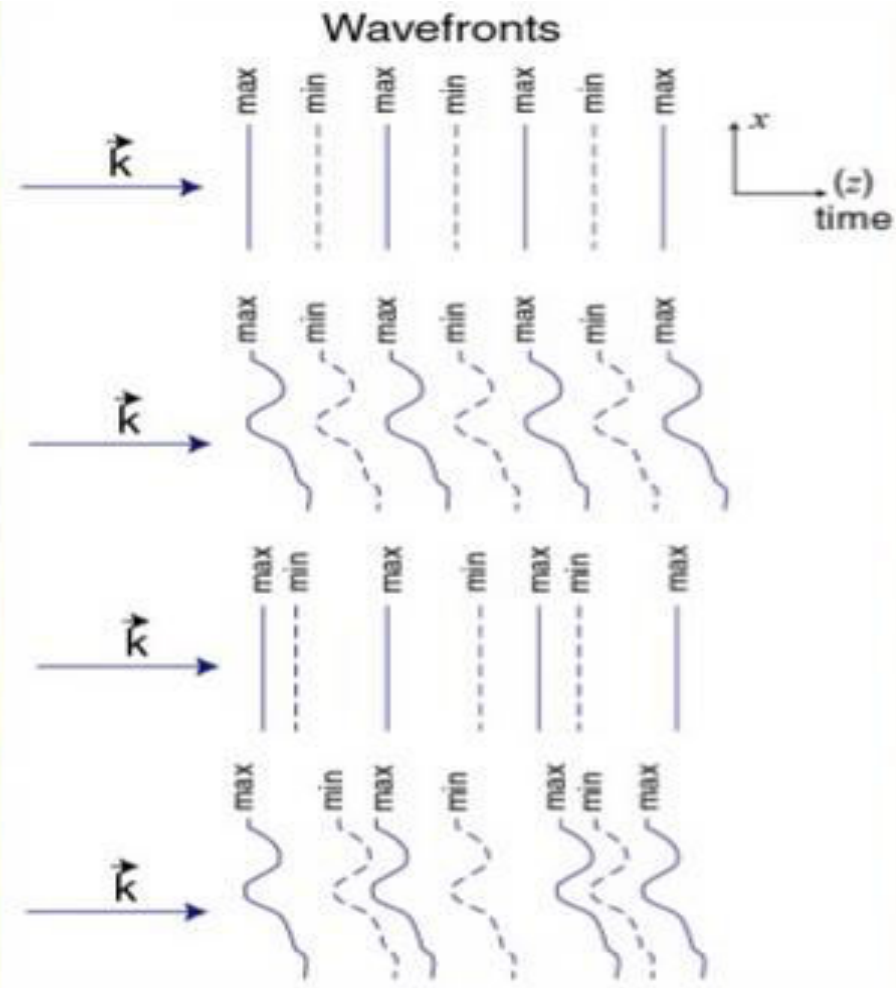
Beams can be coherent or only partially coherent (indeed, even incoherent) in both space and time.

Spatial and Temporal Coherence:

Temporal Coherence; Spatial Incoherence

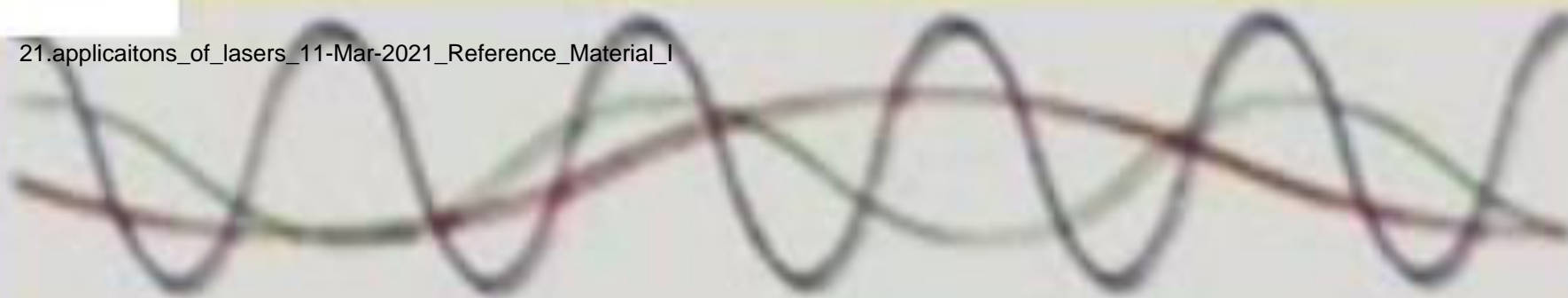
Spatial Coherence; Temporal Incoherence

Spatial and Temporal Incoherence

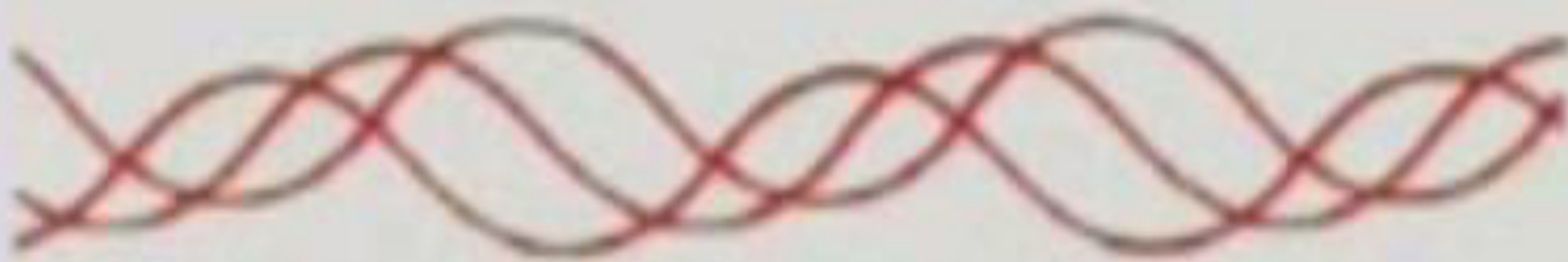


The temporal coherence time is the time the wave-fronts remain equally spaced. That is, the field remains sinusoidal with one wavelength:

The waves at different points in space are said to be space coherent if they preserve a constant phase difference over any time t .



Interference (many different colors)



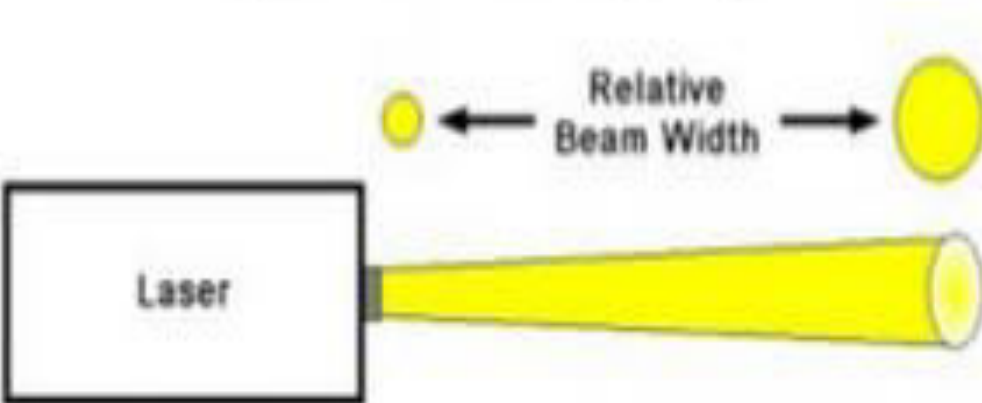
Dispersion (many colors) will result in a rainbow (rainbow)



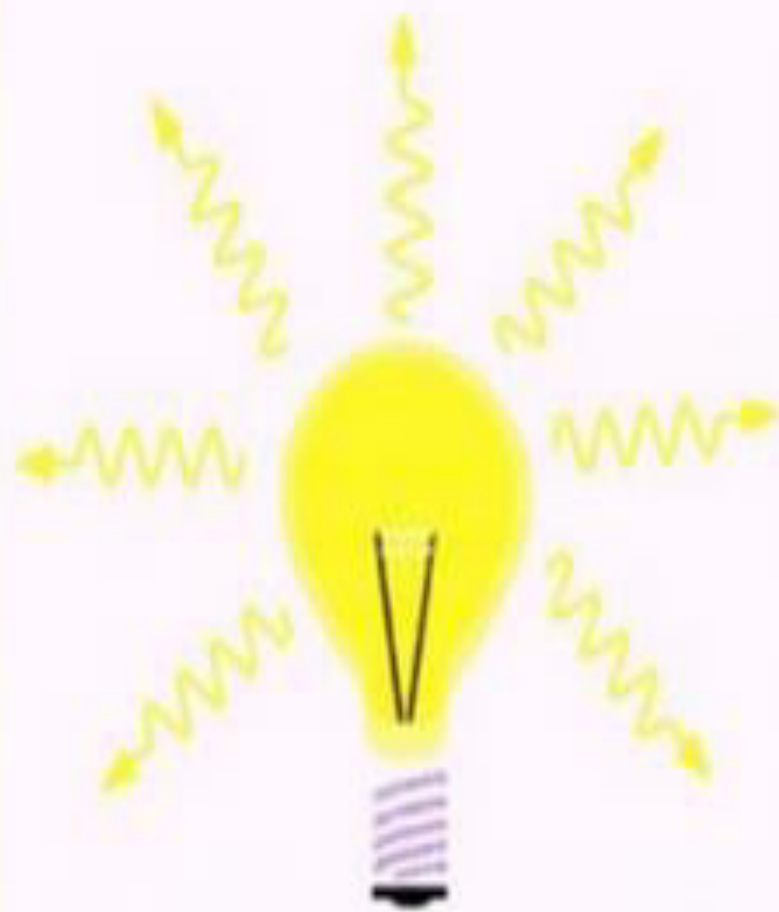
Diffraction: One color (monochromatic) and spread out (diffraction)

Directionality

Highly Directional Beam
(Narrow Cone of Divergence)

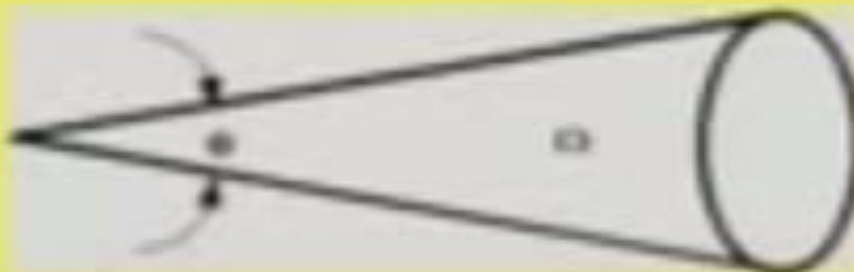


Light spreads out in all directions



Intensity

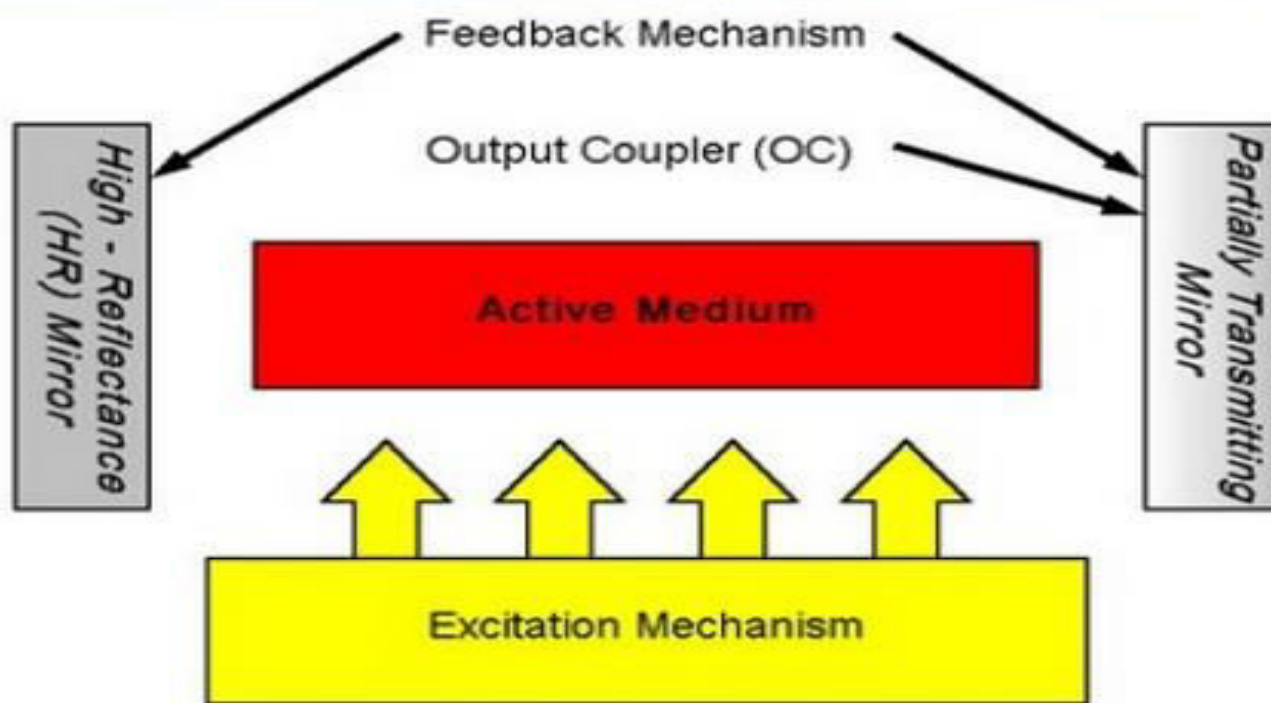
- The intensity of a light source is the power emitted per unit surface area per unit solid angle.



Basic Components

- Spontaneous emission
- Stimulated emission
- Amplification
- Population inversion
- Active medium
- Pumping
- Optical resonators

ELEMENTS OF A LASER



The three main components of any laser device are:

- (i) The active medium
- (ii) The pumping source
- (iii) The optical resonator.

Technically, the whole device is known as a **LASER OSCILLATOR**, but this term is often shortened to simply "laser".

1. AMPLIFYING OR GAIN MEDIUM (solid, liquid or gas)

- This medium is composed of atoms, molecules, ions or electrons whose energy levels are used to increase the power of a light wave during its propagation.
- The physical principle involved is called stimulated emission

2. PUMPING SYSTEM - a system to excite the amplifying medium

- This creates the conditions for light amplification by supplying the necessary energy.
- There are different kinds of pumping system:
 1. Optical (the sun, flash lamps, continuous arc lamps or tungsten-filament lamps, diode or other lasers)
 2. Electrical (gas discharge tubes, electric current in semi-conductors)
 3. Chemical

3. OPTICAL RESONATOR (OR CAVITY) in order to produce a very special radiation

- The laser oscillator uses reflecting mirrors to amplify the light source considerably by bouncing it back and forth within the cavity
- It also has an output beam mirror that enables part of the light wave in the cavity to be and its radiation used

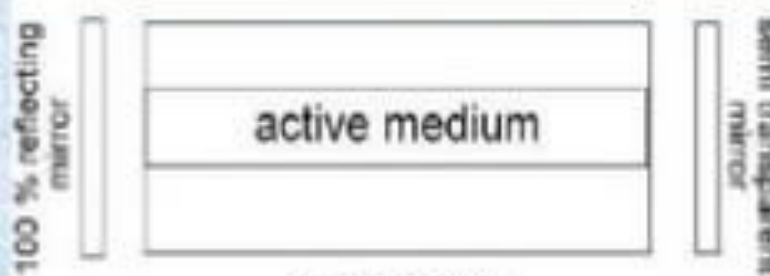


Fig : optical resonator

Spontaneous Emission Stimulated emission

- *Incoherent*
- *Less intensity*
- *Poly chromatic*
- *Less directionality*
- *More angular spread*
- *No need of external energy*
- *Coherent*
- *High intensity*
- *Mono chromatic*
- *High directionality*
- *Less angular spread*
- *External energy is required*

Distinction between spontaneous and stimulated emission of radiation

<i>Spontaneous emission</i>	<i>Stimulated emission</i>
<ul style="list-style-type: none"> • It takes place when an atom in a higher energy state transits to a lower energy state by itself. • It is independent of incident radiation density. • It takes place after 10^{-8} second. • It is a slower process as compared to stimulated emission. • A_{21} is the Einstein's coefficient of spontaneous emission. 	<ul style="list-style-type: none"> • It takes place when an atom in a higher energy state gets stimulated by the incident photon and transits to a lower energy state. • It depends upon the incident radiation density. • It takes place within a time of 10^{-8} second. • It is a faster process as compared to spontaneous emission. • B_{21} is the Einstein's coefficient of stimulated emission.

PRINCIPLE OF LASER

From the theory of interaction of radiation with matter, we can get an idea regarding the working of laser. Consider an atom that has only two energy levels, E_1 and E_2 . When it is exposed to radiation having a stream of photons, each with energy $h\nu$, three distinct processes can take place.

- (i) Absorption
- (ii) Spontaneous emission, and
- (iii) Stimulated emission.

Absorption An atom or molecule in the ground state E_1 can absorb a photon of energy $h\nu$ and go to the higher energy state E_2 . This process is known as *absorption* and is illustrated in Fig.



Fig. Absorption

The rate of upward transition R_{12} from ground state E_1 to excited state E_2 is proportional to the population of the lower energy level N_1 (number of atoms per unit volume) and to the energy density of radiation ρ_v ,

i.e.

$$R_{12} \propto \rho_v$$

$$\propto N_1$$

Thus,

$$R_{12} = B_{12} \rho_v N_1 \quad (2.1)$$

where B_{12} is the probability of absorption per unit time.

Normally, the higher energy state is an unstable state and hence, the atoms will make a transition back to the lower energy state with the emission of a photon. Such an emission can take place by one of the two methods given below.

Spontaneous Emission

21.applications_of_lasers_11-Mar-2021_Reference_Material_I
In spontaneous emission, the atoms or molecules in the higher energy state E_2 eventually return to the ground state by emitting their excess energy spontaneously. This process is independent of external radiation. The rate of the spontaneous emission is directly proportional to the population of the energy level E_2 ,

i.e.

$$R_{21} (\text{SP}) \propto N_2$$

$$R_{21} (\text{SP}) = A_{21} N_2 \quad (2.2)$$

where A_{21} is the probability per unit time that the atoms will spontaneously fall to the ground state and N_2 the number of atoms per unit volume in the state E_2 . This process is illustrated in Fig.

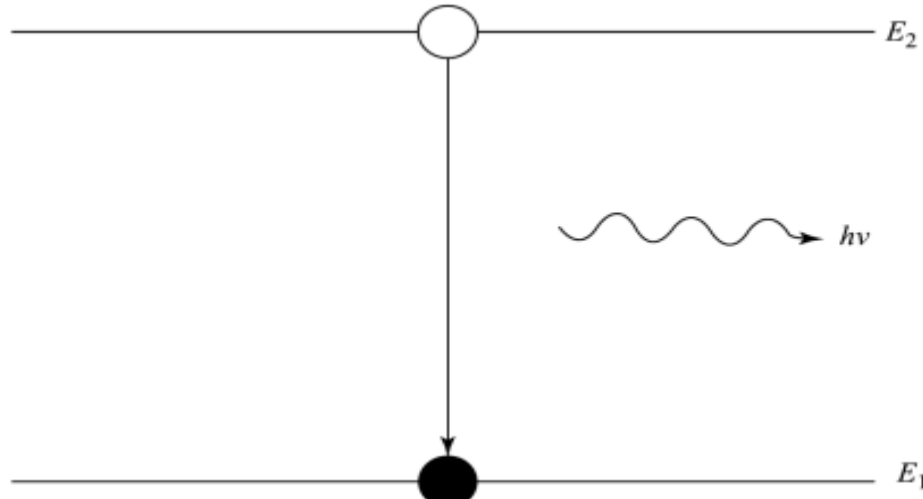


Fig. Spontaneous emission

Stimulated Emission In stimulated emission, a photon having energy E , equal to the difference in energy between the two levels E_2 and E_1 , stimulates an atom in the higher state to make a transition to the lower state with the creation of a second photon, as shown in Fig.

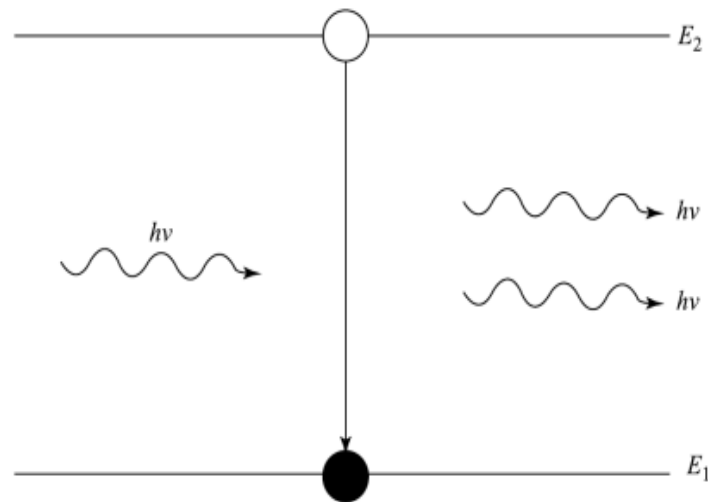


Fig. Stimulated emission

The rate of stimulated emission R_{21} (ST) is given as,

$$R_{21} (\text{ST}) = B_{21}\rho_v N_2 \quad (2.3)$$

where B_{21} is the probability per unit time that the atoms undergo transition from higher energy state to lower state by stimulated emission.

Under conditions of thermal equilibrium, the population of energy levels obey Boltzmann's distribution function.

EINSTEIN'S THEORY OF STIMULATED EMISSION

In 1917, Einstein proposed a mathematical expression for the existence of stimulated emission of light. This expression is known as *Einstein's expression*.

Consider a two-level energy system (E_1 and E_2). Let N_1 and N_2 be the number of atoms in the ground state and excited state, respectively. Let us assume that only the spontaneous emission is present and there is no stimulated emission of light.

At thermal equilibrium condition, the rate of absorption = the rate of emission of light. From Eqs. (2.1) and (2.2), we can write,

$$\rho_v \times B_{12}N_1 = A_{21}N_2$$

$$\rho_v = \frac{A_{21}N_2}{B_{12}N_1} \quad (2.4)$$

According to Boltzmann's distribution function, the population of atoms in the upper and lower energy levels are related by,

$$\frac{N_2}{N_1} = \frac{e^{-E_2/kT}}{e^{-E_1/kT}} \quad (2.5)$$

Substituting N_2/N_1 in Eq. (2.4), we get,

$$\rho_v = \frac{A_{21}}{B_{21}} e^{-(E_2 - E_1)/kT} \quad (2.6)$$

$$\rho_v = \frac{A_{21}}{B_{21}} \frac{1}{e^{hv/kT}}$$

According to black body radiation, the energy density

$$\rho_v = \frac{8\pi h v^3}{c^3} \frac{1}{e^{hv/kT} - 1} \quad (2.7)$$

where h is the Planck's constant and c the velocity of light. Comparing the above two equations [Eqs. (2.6) and (2.7)], one can observe that they are not in agreement.

To rectify this discrepancy, Einstein proposed another kind of emission known as *stimulated emission of radiation*. Therefore, the total emission is the sum of the spontaneous and stimulated emissions of radiation.

At thermal equilibrium condition, the rate of absorption = the rate of emission. From Eqs. (2.1), (2.2) and (2.3),

$$B_{12}N_1 \rho_v = A_{21}N_2 + B_{21}N_2 \rho_v$$

$$\rho_v = \frac{A_{21}N_2}{B_{12}N_1 - B_{21}N_2} \quad (2.8)$$

Dividing each and every term on the RHS of Eq. (2.8) by N_2 , we get,

$$\rho_v = \frac{A_{21}}{B_{12}(N_1/N_2) - B_{21}}$$

Substituting for N_1/N_2 from Eq. (2.5), we get,

$$\rho_v = \frac{A_{21}}{B_{12} \left[e^{(E_2 - E_1)/kT} \right] - B_{21}}$$

$$\rho_v = \frac{A_{21}}{B_{12}e^{hv/kT} - B_{21}} \quad (2.9)$$

The coefficients A_{21} , B_{12} and B_{21} are known as *Einstein's coefficients*.

Comparing the above equation with Eq. (2.7), we get,

$$B_{12} = B_{21}$$

and

$$\frac{A_{21}}{B_{21}} = \frac{8\pi hv^3}{c^3} \quad (2.10)$$

From Eqs. (2.7) and (2.9), the ratio of the stimulated emission to spontaneous emission is given by,

$$\frac{R_{21}(\text{ST})}{R_{21}(\text{SP})} = \frac{B_{21}N_2\rho_v}{A_{21}N_2} = \frac{1}{e^{hv/kT} - 1} \quad (2.11)$$

From Eq. (2.11), Einstein proved the existence of stimulated emission of radiation.

The spontaneous emission produces incoherent light, while stimulated emission produces coherent light. In an ordinary conventional light source, spontaneous emission is dominant. For laser action, stimulated emission should be predominant over spontaneous emission and absorption. To achieve this, an artificial condition known as, *population inversion* is required.

Physical Significance of Einstein coefficient

1. The probability of stimulated emission is numerically equal to probability of stimulated absorption. Their rates are different because stimulated emission is proportional to number of atoms present in excited state while stimulated absorption is proportional to number of atoms present in ground state.

2. The coefficient of stimulated emission (B_{21}) is inversely proportional to the third power of frequency of radiation or directly proportional to the third power of wavelength of radiation.

$$\frac{B_{21}}{A_{21}} = \frac{1}{8\pi h} \left(\frac{c}{\nu} \right)^3 = \frac{1}{8\pi h} (\lambda)^3$$

3. The ratio of the rate of stimulated emission to the rate of spontaneous emission

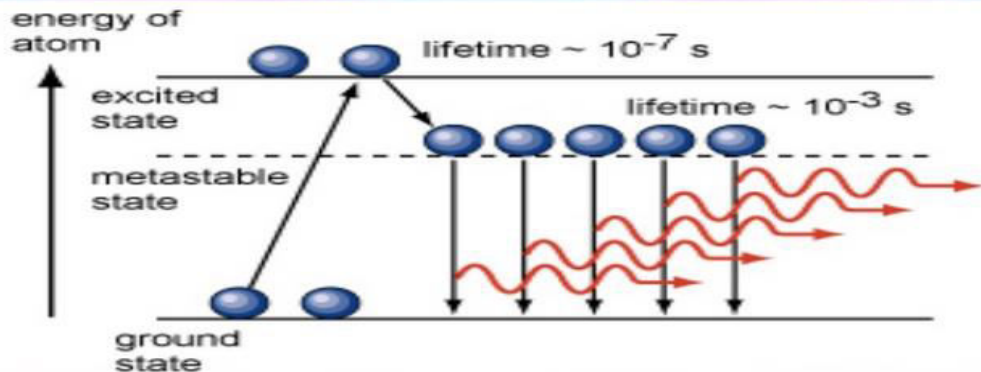
$$\frac{R_{st}}{R_{sp}} = \frac{B_{21} N_2 \rho(\nu)}{A_{21} N_2} = \left(\frac{B_{21}}{A_{21}} \right) \rho(\nu) = \frac{1}{e^{h\nu/kT} - 1} = \frac{1}{e^{hc/\lambda kT} - 1}$$

- (i) For ***larger wavelength***, the probability of stimulated emission is more compared to spontaneous emission in ***microwave region***.
- (ii) For ***Shorter wavelength***, the probability of stimulated emission is negligible compared to spontaneous emission in ***visible region***.

POPULATION INVERSION

21.applications_of_lasers_11-Mar-2021_Reference_Material_I

- A state of a medium where a higher-lying electronic level has a higher population than a lower-lying level



A state in which the number of atoms in higher energy state is greater than that in the lower energy state is called a state of population inversion.

To achieve it, consider an atom which has three energy state, which is the ground state; the excited state, E_3 in which the atom can reside only for 10^{-7} sec; and the metastable state, E_2 in which the atom can reside only for 10^{-3} sec (much longer than 10^{-8} sec).

Since the life time of metastable state E_2 is much longer than E_3 , the atom reaches state E_2 much faster than they leave state E_2 . Thus, the state E_2 is filled with a far greater number of atoms than the ground state E_1 . Consequently, we have a population inversion between the two states E_2 and E_1 . The process by which the population inversion is achieved is called optical pumping.

The population inversion can be achieved by exciting the medium with a suitable form of energy. This process is called pumping. The pumping is necessary for producing population inversion and consequently stimulated emission occurs. Some of the commonly used methods are:

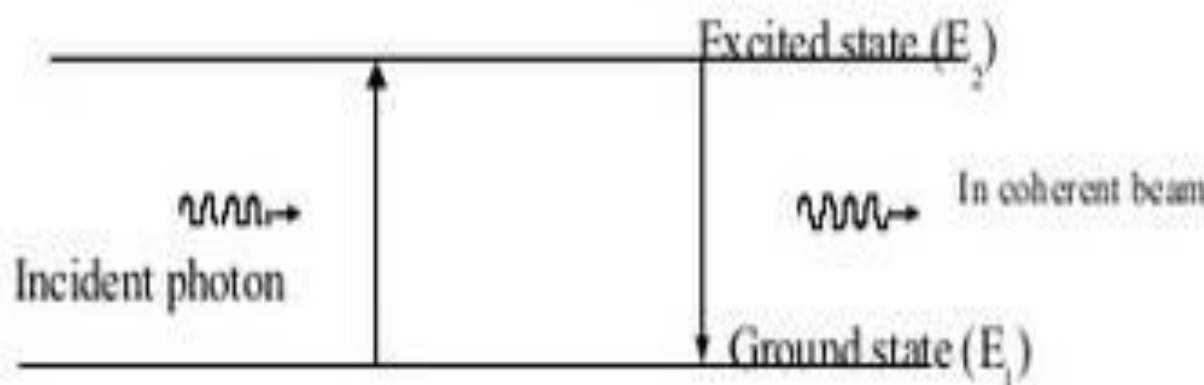
1. Optical pumping (Nd:YAG laser)
2. Electrical discharge (Argon – ion laser)
3. Inelastic atom – atom collision (He-Ne laser)
4. Direct conversion (Semiconductor laser)
5. Chemical reactions (CO₂ laser)

There are three levels in which population inversion takes place, those are

1. Two level pumping Scheme
2. Three level pumping Scheme
3. Three level pumping Scheme

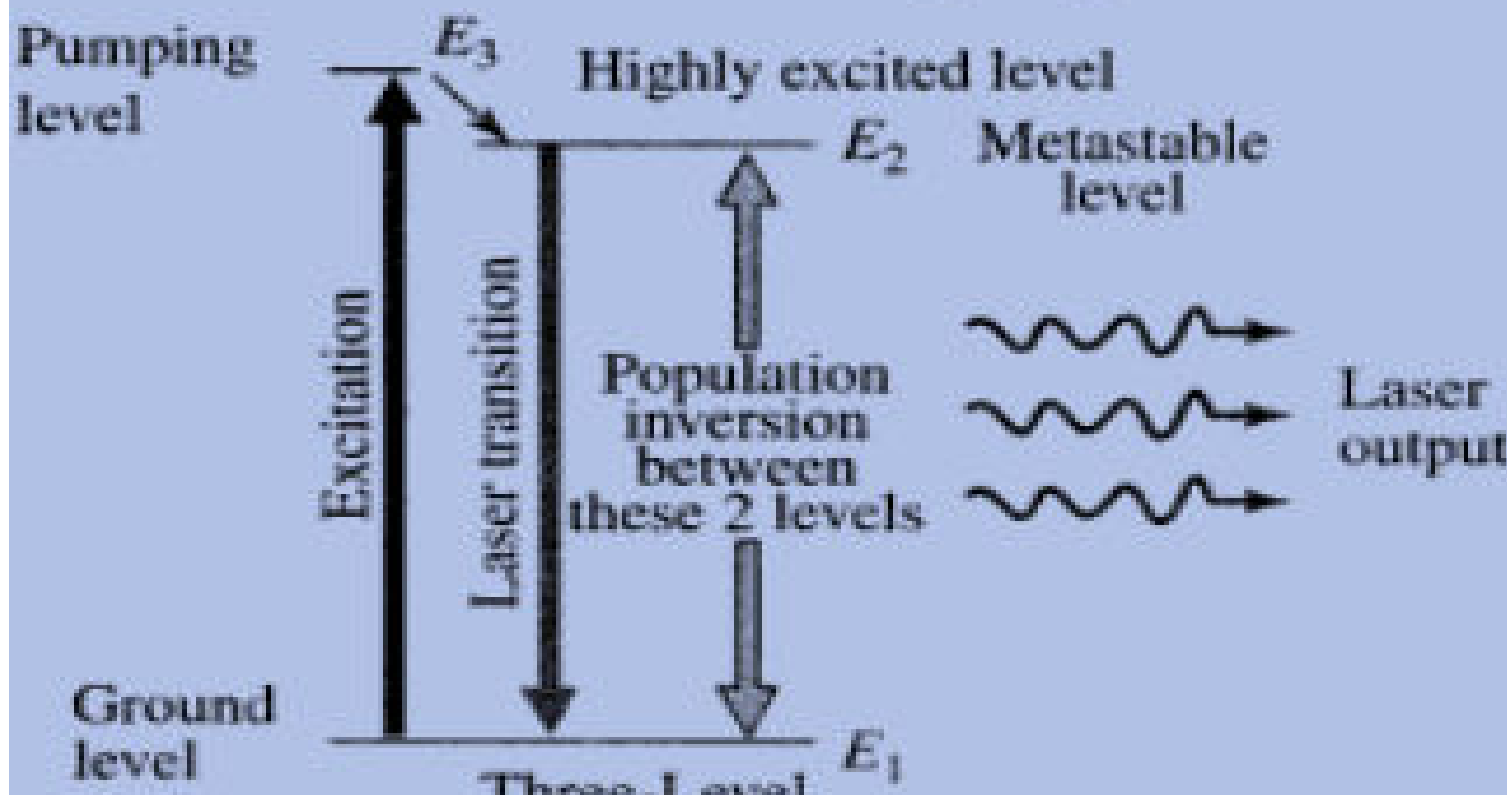
Two level pumping Scheme: This scheme contains only two energy levels i.e., ground state and excited state. The atom absorbs the photon energy and jumps to excited state from ground state. In this case it is difficult to achieve stimulated emission.

This is because, the electron spontaneously returns to ground state (time lag 10^{-8} sec) by the emission of radiation and passing photon have practically no time to stimulate excited atom.



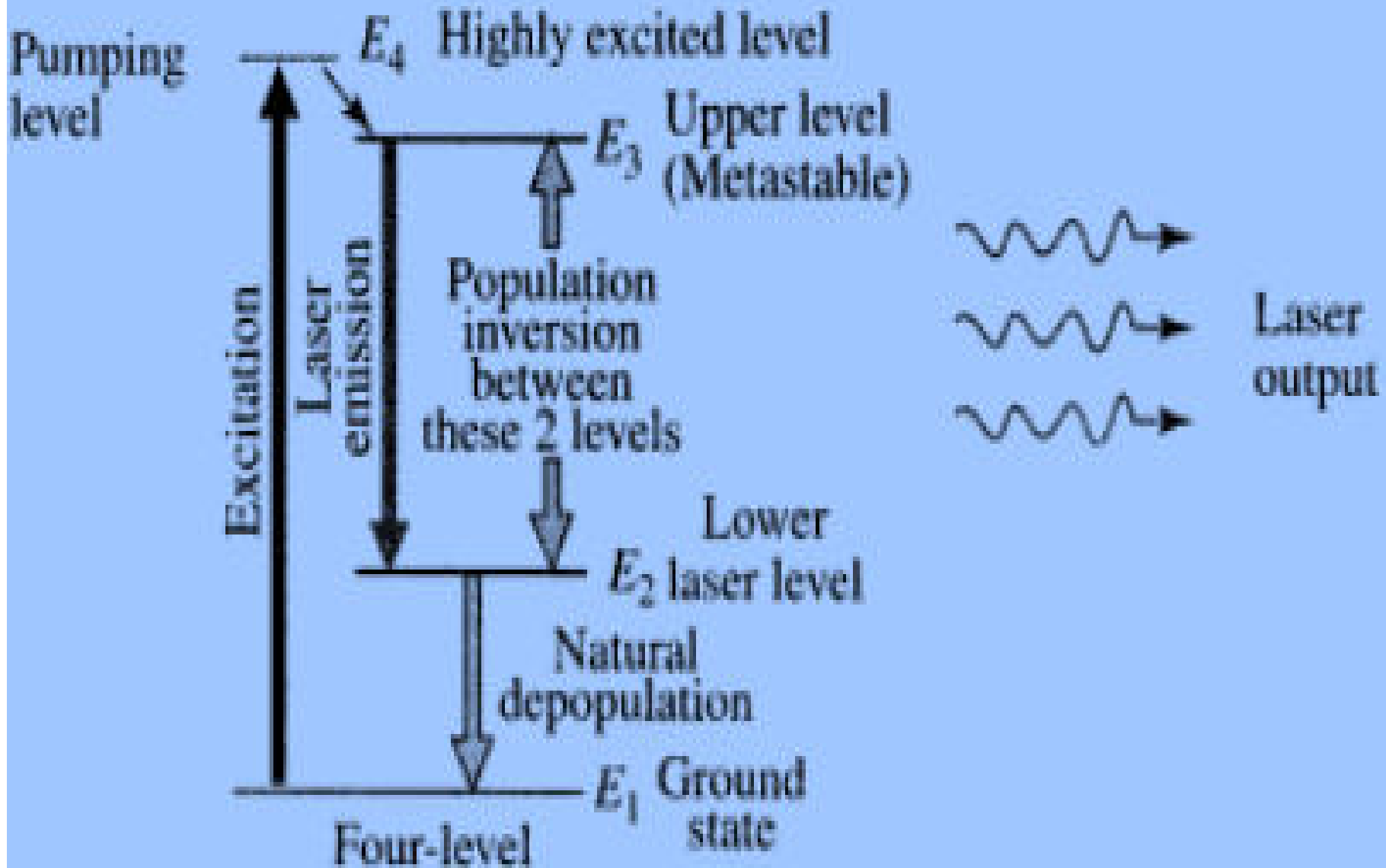
Therefore only spontaneous emission takes place in two level pumping scheme.

Three-level laser energy diagram



Metastable state: Metastable state is the energy state which lies between ground state and excited state, transition takes place to this state from excited state without emission of radiation. This state is more stable than the excited state and electron stay in this state for about 10^{-3} to 10^2 sec. and this time is sufficient undergo stimulation emission.

Four level pumping scheme or laser energy diagram



Types of LASERS

- Solid state Lasers(Nd: YAG Laser)
 - Gas Lasers(He-Ne laser)
 - Liquid lasers(Europium laser)
- Semiconducting lasers(Ga As laser)
- Dye lasers(Coumarian laser)

SOLID-STATE LASERS

Solid-state laser systems make use of a solid rod of a laser-active material. The most commonly used solid-state lasers are ruby laser and Nd-YAG laser.

Neodymium laser This laser system uses rare earth metals like neodymium. These are two types.

- Nd-YAG laser
- Nd-glass laser

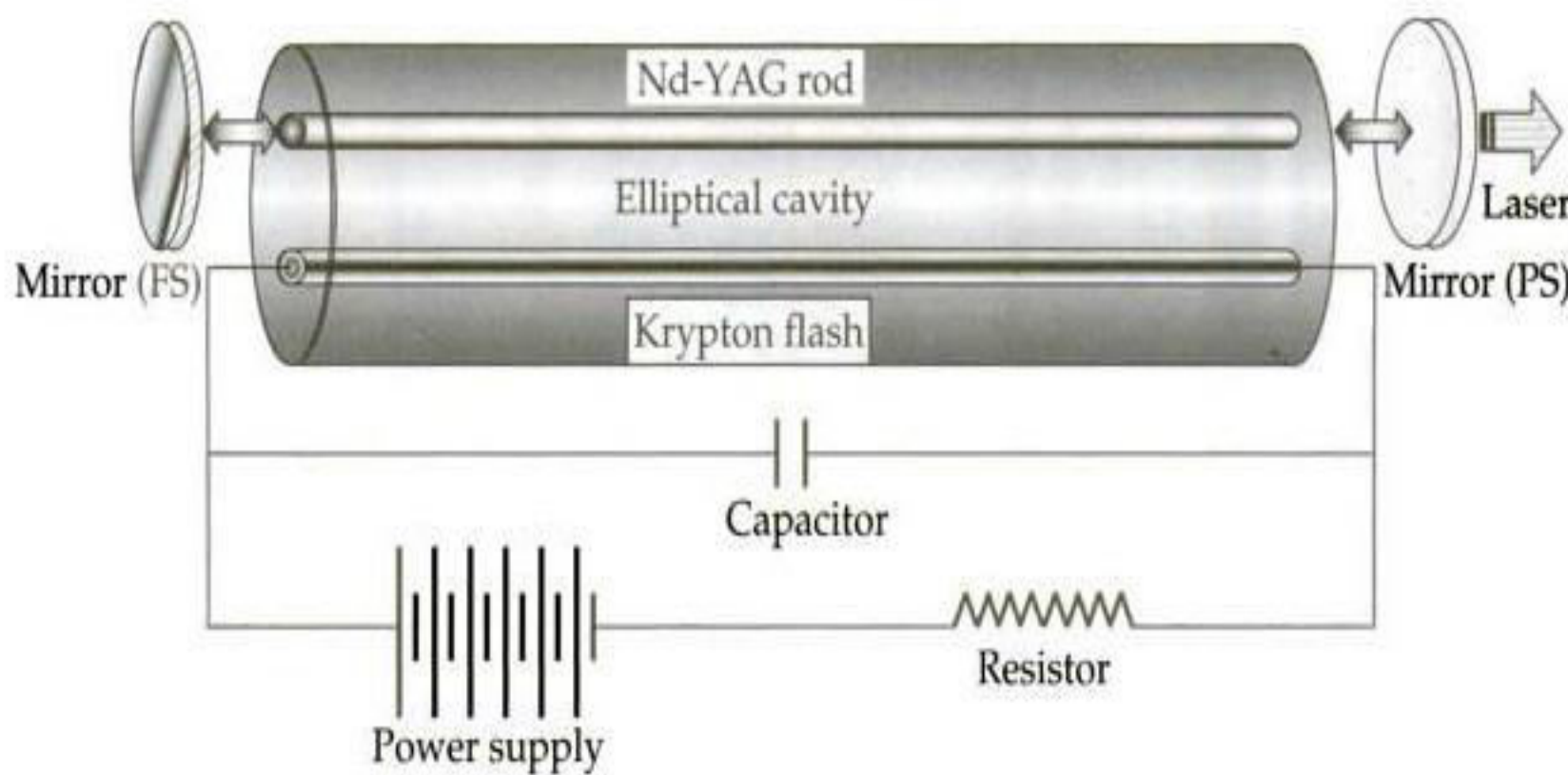
These are powerful four-level laser system with high-power pulse.

They can produce laser output both in the pulsed and the continuous modes.

Because of their high-power output, they are mostly used in industries for cutting, drilling, welding, and surface treatments like hardening of the Industrial products.

Nd-YAG Laser

As mentioned earlier, this is a four-level solid-state laser. Nd-YAG is a neodymium-doped yttrium-aluminium garnet ($\text{Nd}-\text{Y}_3\text{Al}_5\text{O}_{12}$), a compound that is used as the lasing medium for some solid-state lasers.



Experimental set-up of a Nd-YAG laser system

Pumping

As this is a solid-state laser, pumping could be done by optical means.

Nd-YAG absorbs mostly in the bands between 730–760 nm and 790–820 nm.

Krypton flash lamps,

with high output at these bands, are therefore more efficient for pumping than the xenon lamps, which produce white light resulting in a loss of energy. The output from a krypton-flash-lamp-pumped laser is mostly pulsed . To get a continuous output, a quartz-halogen lamp is used.

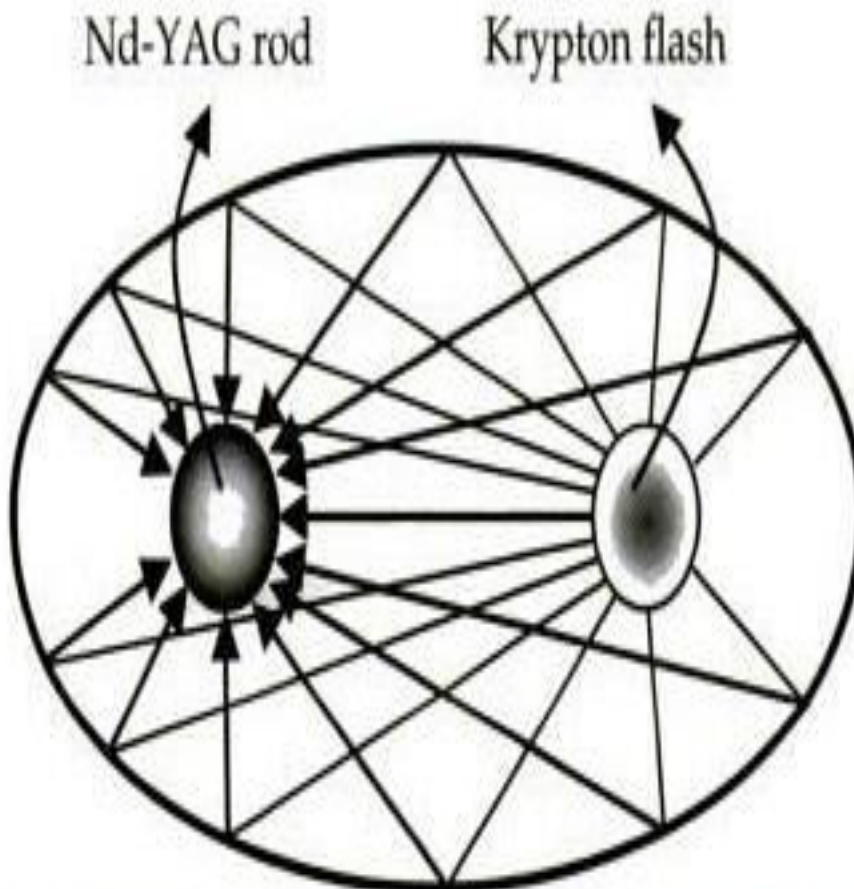
Nd-YAG lasers typically emit light of wavelength 1,064 nm in the infrared. However, there are also transitions near 940, 1,120, 1,320, and 1,440 nm.

Construction

The Nd-YAG crystal is conveniently cut in the form a cylindrical rod of desired length (5–10 cm) and diameter (6–9 mm).

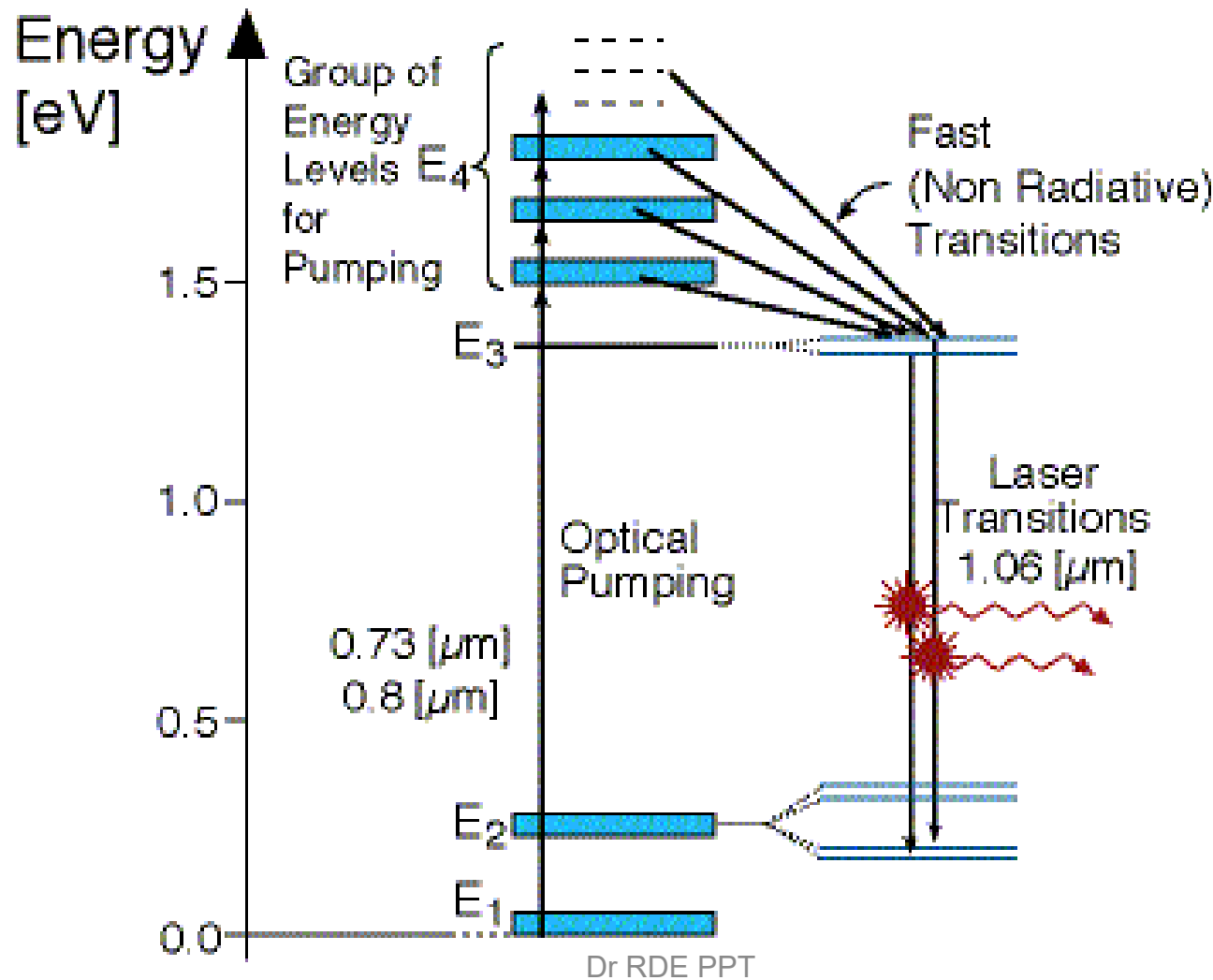
Unlike a ruby laser where the xenon flash lamp was coiled around the ruby rod, the Nd-YAG rod is placed inside at one of the foci of an elliptical reflector cavity. At the other focus, a krypton flash tube, which is connected to the power supply via a capacitor connected in parallel and a resistor connected in series, is placed. The reason for this arrangement is to maximize the pumping power (Fig.). Almost all the power emitted by the flash lamp kept at one focus reaches the rod kept at the other focus. In this way, maximum pumping takes place, and hence a large population inversion is achieved. This results in an intense laser beam.

Working The laser action is achieved by means of optical pumping utilizing a flash lamp (either a xenon flash lamp at moderate pressure or a krypton flash lamp at high pressure). Only a small fraction of the energy given out by the flash lamp is used for excitation and the rest merely heats up the apparatus. This requires a separate cooling mechanism to cool the laser apparatus.

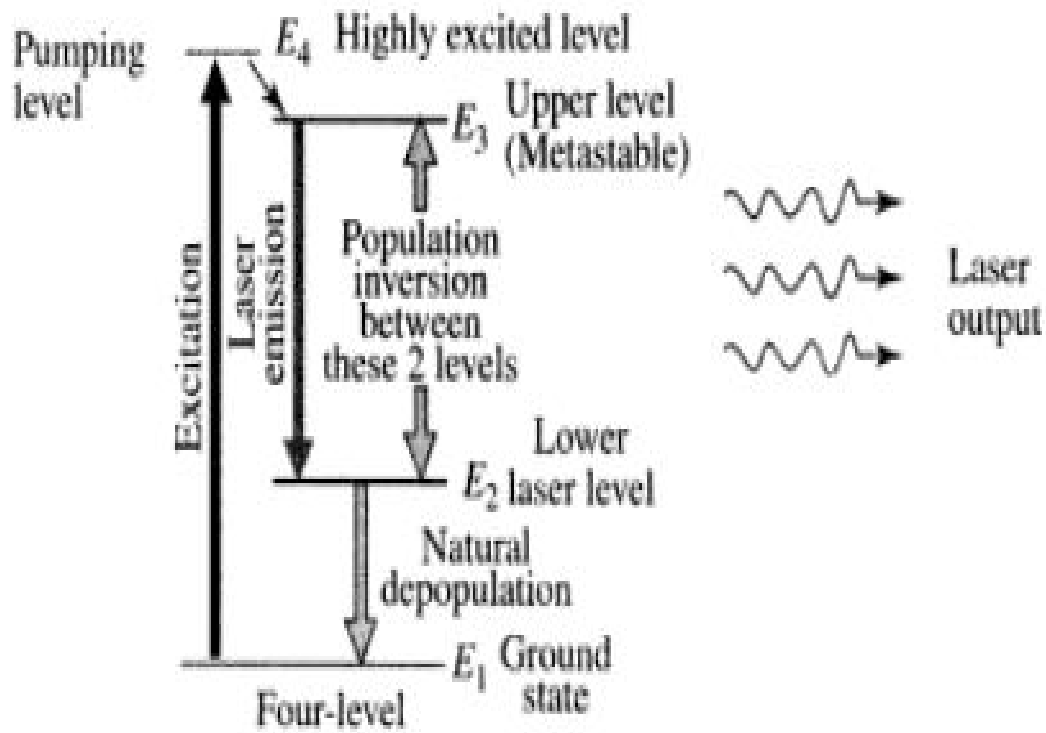


Cross-sectional view of the experimental arrangement of the Nd-YAG system

Energy Level Diagram of Nd-YAG laser



Four level pumping scheme or laser energy diagram



Finally, a laser output at 1064 nm is obtained corresponding to the transition between the levels E_3 and E_2 .

The neodymium ions absorb radiations at around 730 nm (E_1) and 800 nm (E_2) and go to the respective excited states.

From these excited absorption levels, the atoms decay by means of a rapid non-radiative transition to the metastable levels (E_4) where they populate and achieve population inversion. Once this condition is achieved, photons are emitted following stimulated emission. The emitted photons are allowed to pass back and forth upwards for a million times through a set of optical resonators where their number builds up and the amplitude increases.

Advantages

21.applications_of_lasers_11-Mar-2021_Reference_Material_I

The advantages of Nd-YAG laser are

- It has a high output and repetition rate.
- It is much easier to achieve population inversion.
- As it is crystalline, the line width is small and therefore it has lower thresholds.
- It can be used in lasers utilizing frequency doubling and frequency tripling, and high-energy Q-switching.
- Its thermal conductivity is better and its fluorescence lifetime is about twice as long as Nd-YVO₄.
- It can be operated on power levels of up to kilowatts. It can be directly Q-switched with Cr⁴⁺-YAG.
- Nd-YAG lases at 1,064 nm and its best absorption band for pumping is 1 nm wide and located at 807.5 nm.

Disadvantages

- Its electronic energy level structure is complicated.

GAS LASER

Carbon Dioxide Laser

Carbon dioxide laser is the first molecular gas laser developed by C.K.N. Patel. It produces a continuous output and is simple to construct. Unlike the solid-state lasers, in gas lasers the output is achieved when the transitions take place between the vibrational or rotational levels of the molecules. As shown in Fig. 5.9, the two types of transitions in gas laser systems are

- Type I—Transitions between the vibrational levels of the same electronic states.
- Type II—Transitions between the vibrational levels of different electronic states.

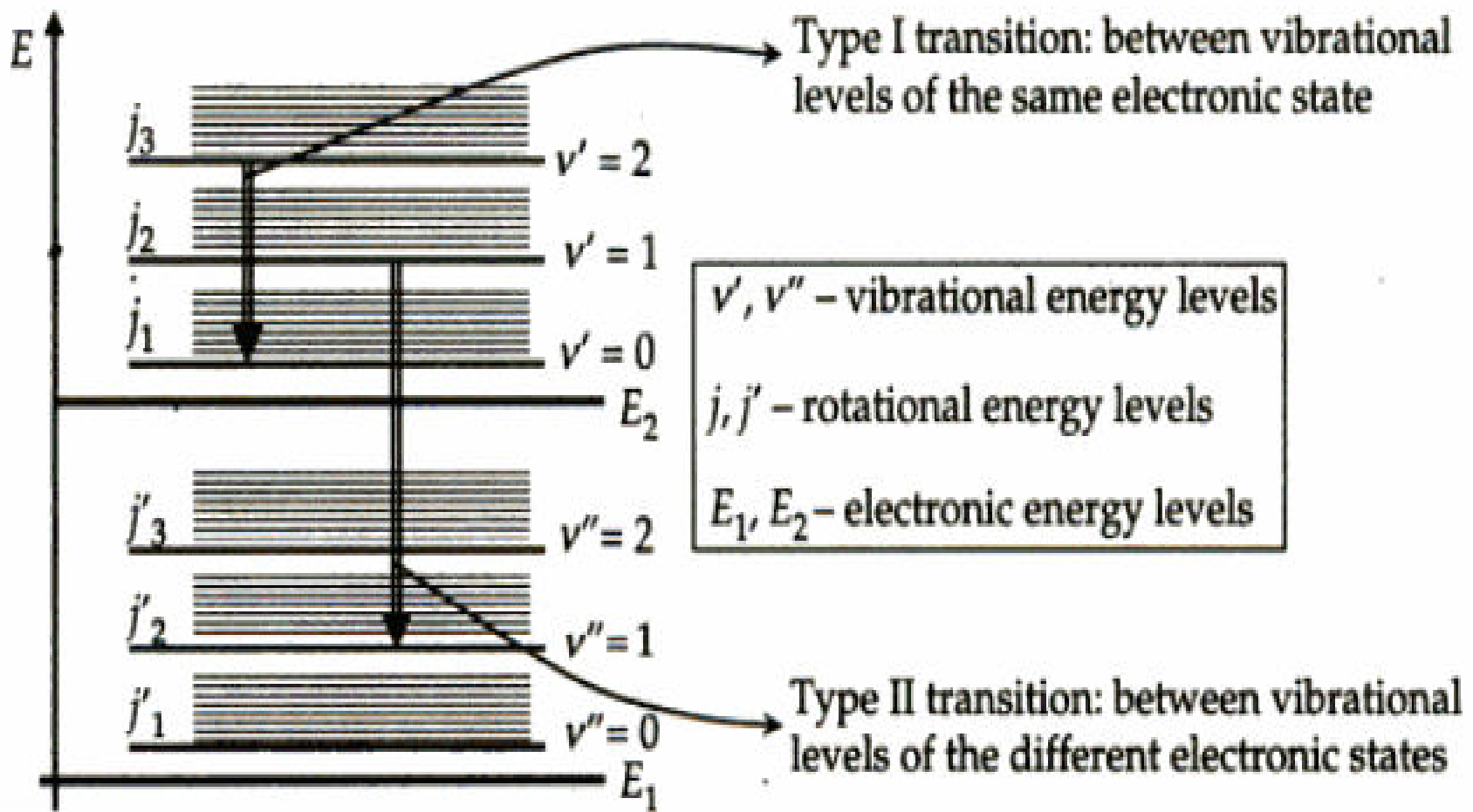
The output from a CO₂ laser is the result of type I transitions, in which the transitions take place between the vibrational levels of the same electronic levels.

Principle As a gas molecule can both rotate and vibrate along with getting excited to different electronic states, it is necessary to know the different mechanisms by which a CO₂ molecule can get excited. CO₂ is a linear molecule, with the two oxygen atoms at the ends and the single carbon atom at the middle. It can undergo three types or modes of vibrations, namely

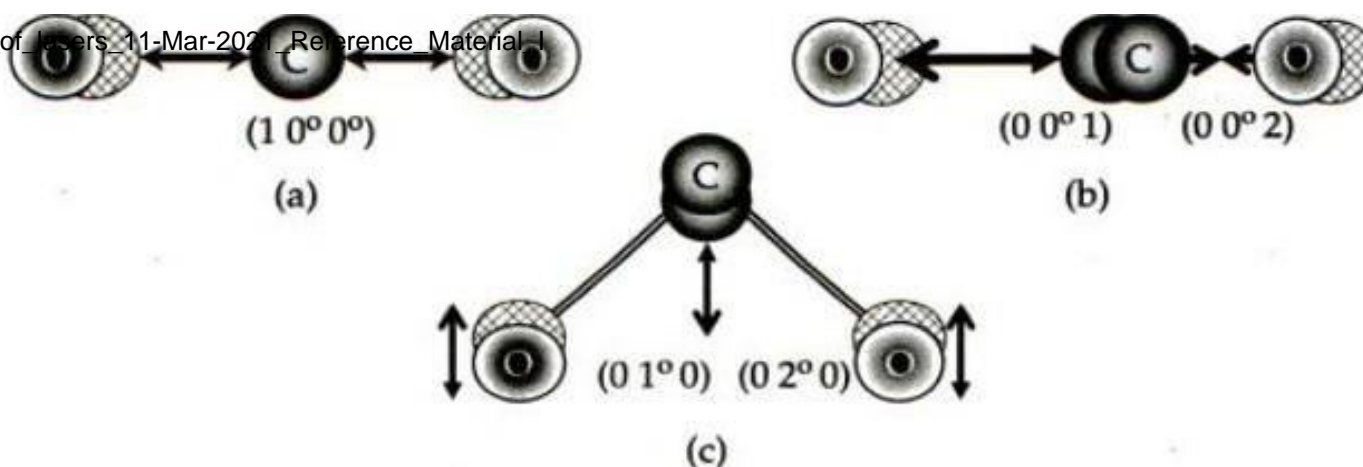
- Symmetric mode or stretching
- Asymmetric mode or stretching
- Bending mode

In all the three modes, the centre of gravity of the molecule remains fixed.

Symmetric mode In the symmetric mode, the end oxygen atoms stretch opposite to each other symmetrically either away or towards the carbon atom in a straight line (Fig. 5.10a), and the centre carbon atom remains stationary. The frequency corresponding to this stretching is known as the symmetric stretching frequency.



Different types of energy levels and transitions in a diatomic molecule

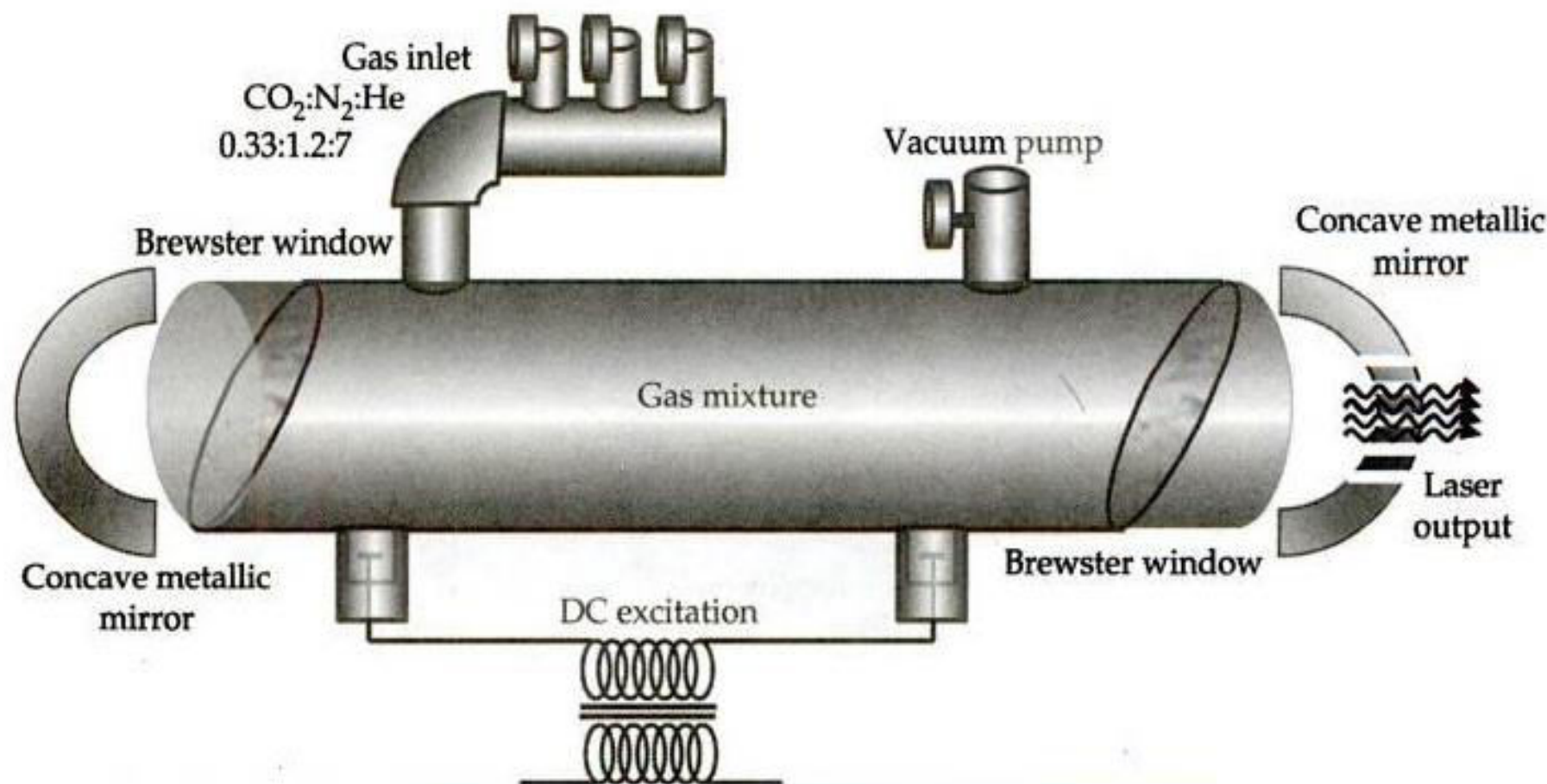


(a) Symmetric stretching (b) asymmetric stretching (c) bending mode

Asymmetric mode In this mode, the oxygen atoms move in the same direction, i.e., if one atom comes towards the carbon atom, then the other one moves away from it (Fig. 5.10b). At the same time, the carbon atom also moves in a straight line towards and away from any one of the oxygen atoms. This results in two atoms (one carbon and one oxygen) either coming together or getting away from each other. The entire stretching is along a straight line. The frequency corresponding to this stretching is known as the asymmetric stretching frequency.

Bending mode In this mode, the carbon atom and the oxygen atoms vibrate at right angles to the line joining the three atoms (centre of gravity). When the carbon atom moves up, the two oxygen atoms move down simultaneously and vice versa (Fig. 5.10c). This results in the bending of the molecule and the mode is known as bending mode. The frequency corresponding to this mode is known as bending frequency.

Construction The laser system consists of a long cylindrical tube several metres in length and several centimetres in diameter (Fig. 5.11). The feature of the CO₂ laser is

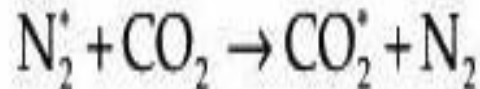
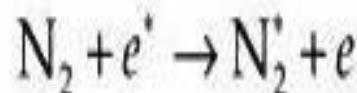


Construction of CO₂ laser system

that the output from it depends on the diameter of the tube; wider the diameter, more powerful the output. The laser is powered by a 50 Hz power supply. DC excitation or electric discharge is used to pump the laser. A mixture of CO₂, N₂, and He in the ratio 0.33:1.2:7 torr is used for producing the laser. A separate inlet for the gases with necessary valves to control the flow of the gases into the discharge tube is provided. The discharge tube is also connected to a vacuum tube to remove any unwanted trace gases present inside the tube prior to working.

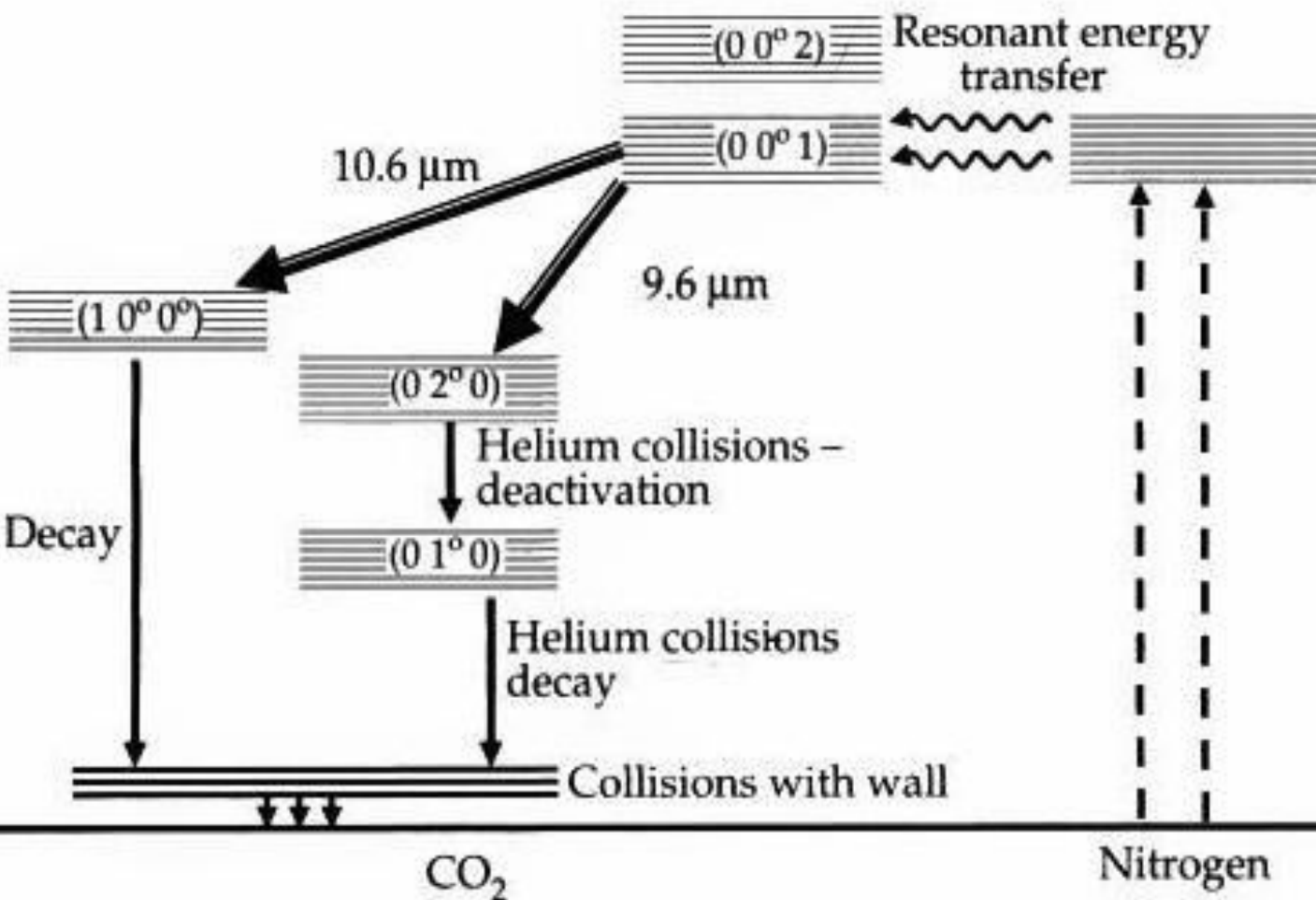
The ends of the tube contain NaCl crystal kept at Brewster angle to filter out the radiations that are not incident at the Brewster angle. The radiations are thus polarized. As the output from a CO₂ laser is in the IR range, the reflection of the incident radiation is possible only by using metallic mirrors (concave). In order to get a high-power output, a metallic mirror made of gold is employed. The mixture of gases in the discharge tube can be either longitudinal or transverse in nature. When sent in transversely (TEA laser), the output power from the laser increases tremendously.

Working The CO₂ laser utilizes a mixture of CO₂, N₂, and He for producing an output. The addition of two gases, N₂ and He, in the CO₂ laser is specifically for a purpose. As the CO₂ molecules are difficult to excite, the nitrogen atoms are excited first and then they transfer their energy to the CO₂ molecule by the following process (Fig. 5.12).



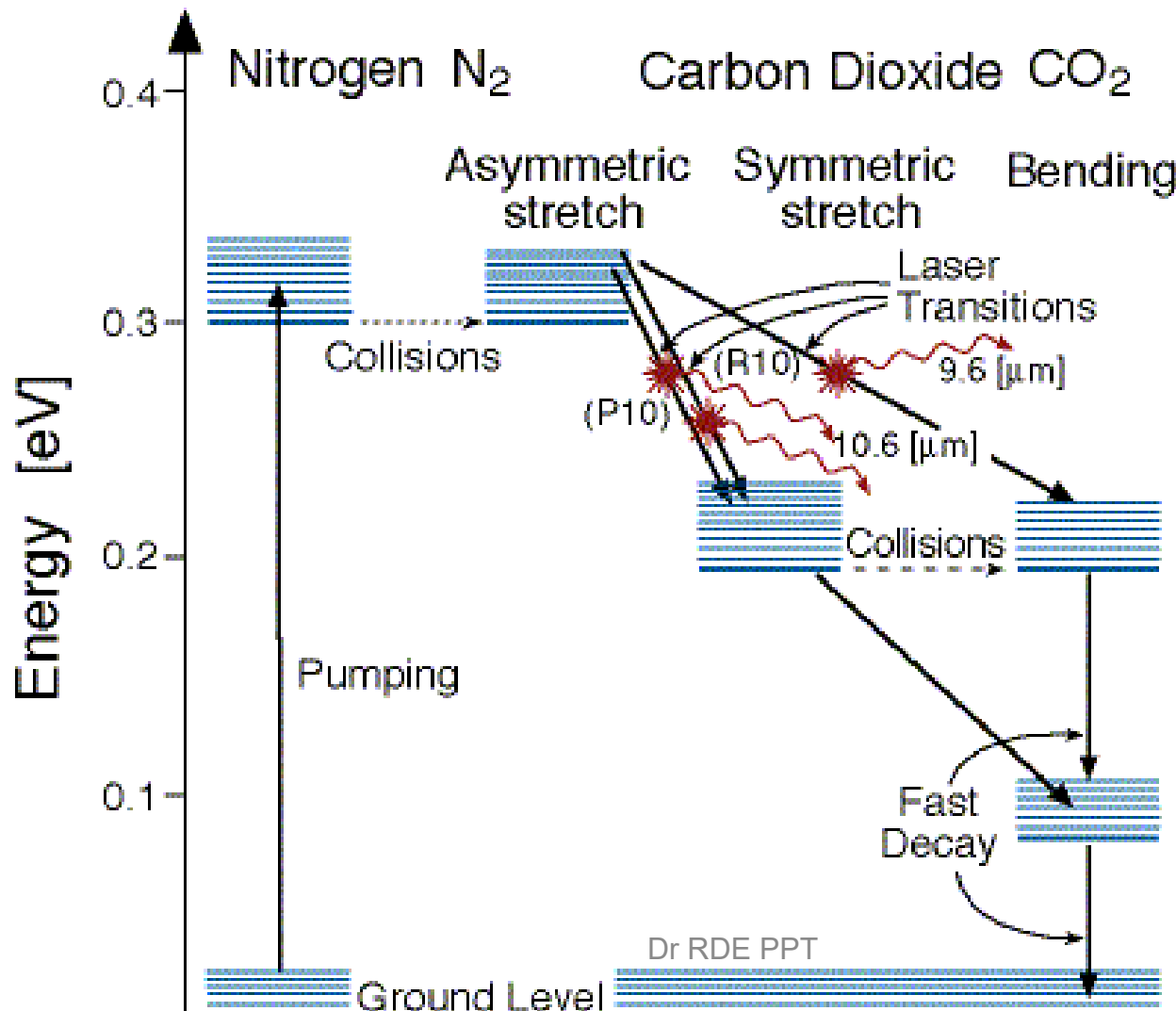
The (0 0 1) level of the asymmetric mode CO₂ molecule is close to the excited level of the N₂ atoms and hence it gets excited. The population of this level increases rapidly compared to the lower levels (0 2 0), (0 1 0), and (1 0 0). This results in a population inversion condition, which is essential for laser action to take place.

Symmetric Bending Asymmetric



Energy level diagram of CO_2 laser

Energy Level Diagram For Carbon Dioxide Laser



The excited asymmetric mode of the CO_2 molecule relaxes to the symmetric (1 0 0) and bending modes (0 2 0) by emitting radiations of 10.6^{11} and $9.6 \mu\text{m}$, respectively. After this, the symmetric mode relaxes close to the ground level by a radiation-less decay, while the bending mode utilizes the helium atoms in the mixture to deactivate themselves to the (0 1 0) level from where they decay to a level close to the ground level. As this level is just above the ground level, populating this level results in a lowered laser output, because they do not allow sufficient inversion of population in the higher levels. Hence, the helium atoms, being good conductors of heat (the reason why their ratio is far higher than the other two gases in the mixture), take away the heat of the CO_2 molecules by colliding with them. Also, the CO_2 molecules themselves collide with the walls of the tube and lose their energy and reach the ground level.

Thus, the discharge tube gets heated up rapidly and this necessitates it to be cooled by external means. Hence, air or water is used for cooling the discharge tube externally apart from the cooling produced by the He gas internally. The output from the CO_2 laser is maximum only when it is properly cooled (i.e., the operating temperature plays a major part in determining the output power). As the gases can be contaminated (CO_2 splits into CO and O_2) on continuous operation, they have to be removed from the discharge tube by means of the vacuum pump, and fresh gas mixture is introduced to maintain the output.

- CO₂ lasers emit energy in the far-infrared region.
- They emit up to 100 kW at 9.6 and 10.6 μm, and their output power can be controlled.
- As their output power depends on the diameter of the tube, increasing the tube diameter increases the power level.
- When the gases are transversely passed through the tube (conventionally the gases are passed along the length of the tube—longitudinal), the output power can be increased drastically.
- The TEA laser is an inexpensive gas laser producing UV light at 337.1 nm.

Disadvantages

- The efficiency of CO₂ laser is only 30%.
- Increasing the output power increases the heating produced.
- A higher power level results in the need for higher cooling.
- It is difficult to control and maintain the precise mixing of the gases in the desired ratio.
- For proper operation, the contaminated gases have to be removed and fresh mixture introduced.

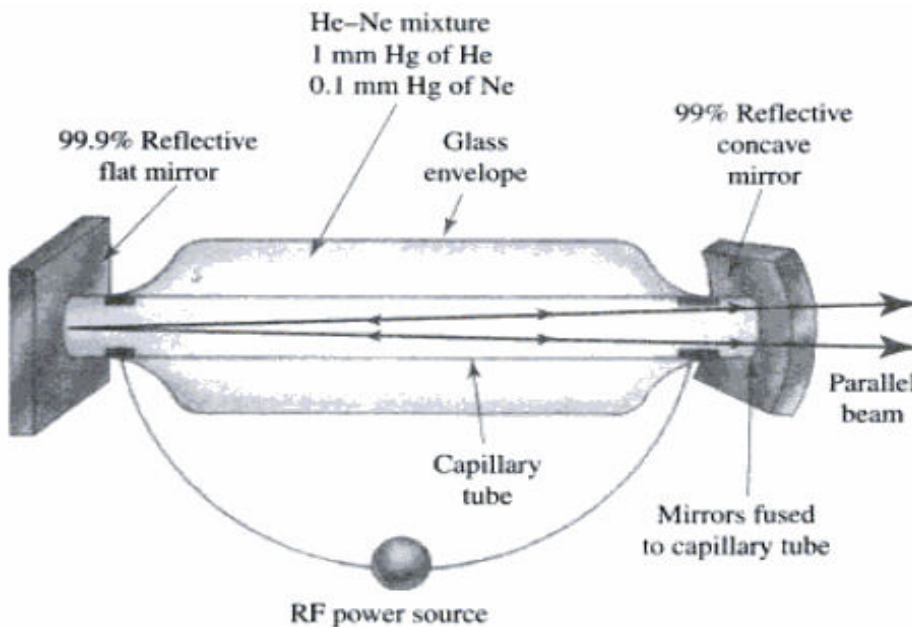
Applications They have various applications because of their ability to produce high power continuously.

- They are used in open-air communication (as the main output from the CO₂ laser is at 10.6 μm, and the wavelength has a low attenuation at that value).
- Used in military for spying (the IR radiations can travel through fog and buildings).
- Because of their high-power output, they are used in industries for cutting, drilling, welding, and other heavy applications.
- They are also used as LIDAR (Light Detection And Ranging), the operation of which is similar to RADAR.
- In medicine, they are used for bloodless surgery (highly focused laser light can cut and seal the blood vessel immediately, thereby minimizing and totally avoiding blood loss).

GAS LASER

21.applications_of_lasers_11-Mar-2021_Reference_Material_I

The Helium–Neon Laser



Schematic drawing of an He-Ne laser

It consists of a gas tube containing 15% helium gas and 85% neon gas.

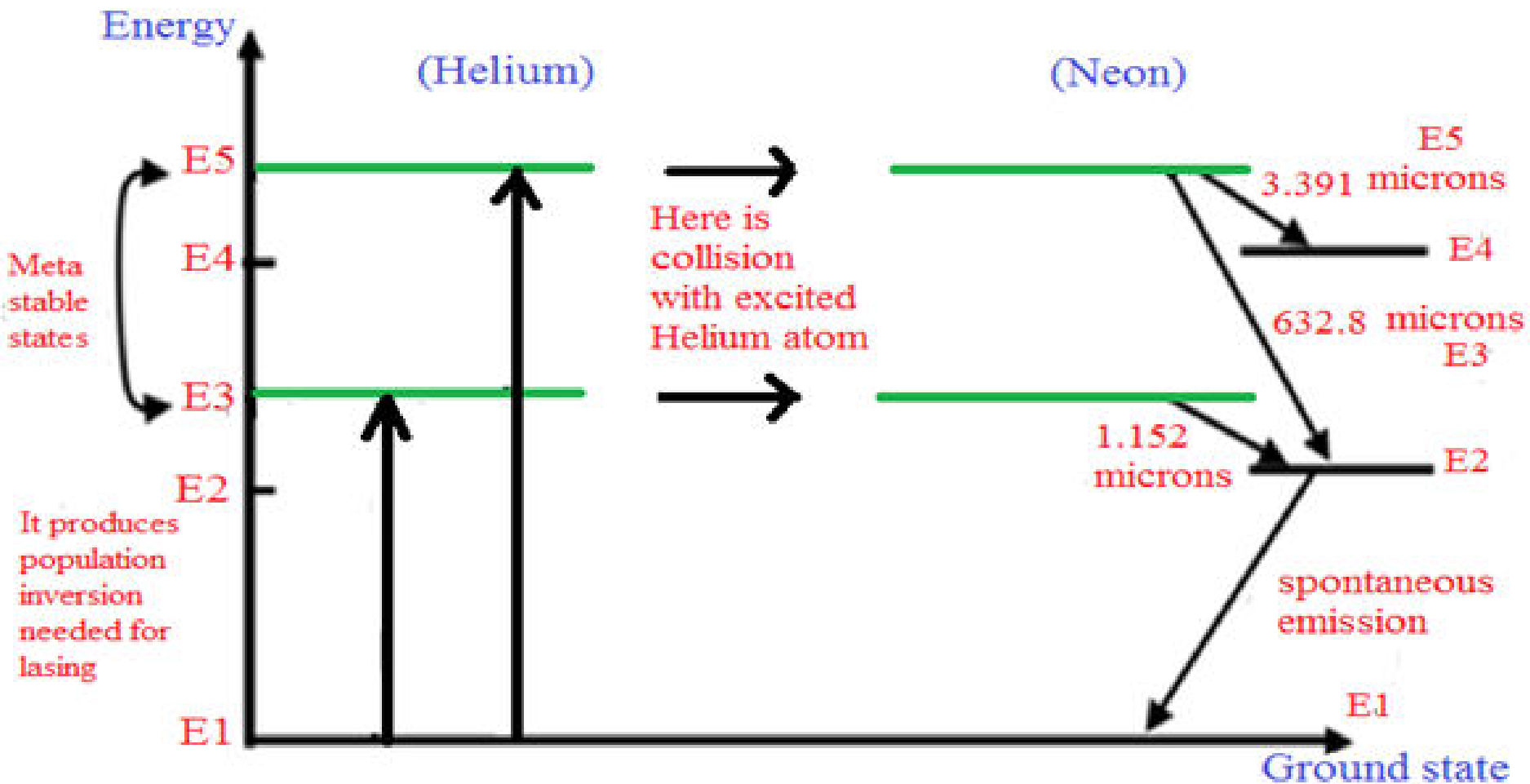
A totally reflecting flat mirror is mounted at one end of the gas tube and a partially reflecting concave mirror is placed at other end.

The helium-neon laser is a kind of neutral atom gas laser, the common wavelength of an He-Ne laser is 632.8 nm. It is tunable from infrared to various visible light frequencies.

Pumping is done by a dc electrical discharge in the low-pressure discharge tube. First, the He atom is excited. Because the Ne atom has an energy level very near to an energy level of He, through kinetic interaction, energy is readily transferred from He to Ne; and the Ne atom emits the desired laser light.

The typical power of an He-Ne laser is below 50 mW, hence it is widely used in holography, scanning measurement, optical fiber communication. It is the most popular visible light laser.

Helium Neon Laser – Energy Level Diagram



2 Find out the separation between metastable and excited levels for two wavelengths of $9.6 \mu\text{m}$ and $10.6 \mu\text{m}$ emitted from a CO_2 laser source. Calculate the frequency and hence the energy of the light photons emitted. How many photons are required to be emitted per second to obtain a laser output power of 10 kW ?

Solution

Given, two wavelengths: $9.6 \mu\text{m}$ and $10.6 \mu\text{m}$

$$h = 6.625 \times 10^{-34} \text{ Js} = 4.14 \times 10^{-15} \text{ eVs}$$

$$c = 3 \times 10^8 \text{ m/s}$$

$$k = 8.625 \times 10^{-5} \text{ eV/K}$$

$$\Delta E = E_2 - E_1 = \frac{hc}{\lambda} = \frac{1.2422 \times 10^{-6} \text{ eVm}}{9.6 \times 10^{-6} \text{ m}} = 0.129 \text{ eV}$$

and

$$\Delta E = \frac{hc}{\lambda} = \frac{1.2422 \times 10^{-6} \text{ eVm}}{10.6 \times 10^{-6} \text{ m}} = 0.117 \text{ eV}$$

So the estimated separation between the two required levels is 0.129 eV and 0.117 eV respectively. The energy of the photon is also respectively 0.129 eV and 0.117 eV . The frequency of the two different types of photons will be

$$v = \frac{c}{\lambda} = \frac{3 \times 10^8 \text{ m/s}}{9.6 \times 10^{-6} \text{ m}} = 3.125 \times 10^{13} \text{ Hz}$$

$$v = \frac{c}{\lambda} = \frac{3 \times 10^8 \text{ m/s}}{10.6 \times 10^{-6} \text{ m}} = 2.83 \times 10^{13} \text{ Hz}$$

To get 10 kW output power, 10000 J/s power is required

The energy of one photon is

$$hv = 6.625 \times 10^{-34} \times 3.125 \times 10^{13} = 2.07 \times 10^{-20} \text{ J}$$

Similarly, for other photon the energy in joules is

$$hv = 6.625 \times 10^{-34} \times 2.83 \times 10^{13} = 1.87 \times 10^{-20} \text{ J}$$

So, the number of photons per second required is

$$(10000 \text{ J/s}) / 2.07 \times 10^{-20} = 4.83 \times 10^{23} \text{ photons/second, and}$$

$$(10000 \text{ J/s}) / 1.87 \times 10^{-20} = 5.34 \times 10^{23} \text{ photons/second.}$$

So, approximately one mole of atoms are involved in the process in one second.

3 A typical laser system is capable of lasing at infrared wavelengths. The light output at $3.124\text{ }\mu\text{m}$ is very prominent. What is the difference in the energy levels of the excited state and metastable state? What will be the energy of a photon emitted? What will be the frequency of the light emitted? If 1 mole of photons are emitted per second, what is the power of the laser output? Can you predict the type of the laser produced?

Solution $\lambda = 3.124\text{ }\mu\text{m} = 3.124 \times 10^{-6}\text{ m}$

$$h\nu = E_2 - E_1 = \frac{hc}{\lambda} = \frac{1.2422 \times 10^{-6}\text{ eVm}}{3.124 \times 10^{-6}\text{ m}} = 0.398\text{ eV}$$

Energy difference between the metastable and excited states is 0.398 eV and hence the photon energy emitted is also 0.398 eV.

$$\text{The frequency of the photon is } \nu = \frac{c}{\lambda} = \frac{3 \times 10^8\text{ m/s}}{3.124 \times 10^{-6}\text{ m}} = 9.6 \times 10^{13}\text{ Hz}$$

$$\text{The energy in joules is } h\nu = 6.625 \times 10^{-34} \times 9.6 \times 10^{13} = 6.36 \times 10^{-20}\text{ J}$$

$$\text{One mole of photon } 6.022 \times 10^{23} \times 6.36 \times 10^{-20} = 38299.92 = 38.3\text{ kJ}$$

Therefore 38.3 kW of output power of laser beam is observed. Obviously, it will be a CO₂ laser light.

USES OF LASERS

21.applications_of_lasers_11-Mar-2021_Reference_Material_I

Since their invention, lasers have become ubiquitous, finding utility in thousands of highly varied applications in every section of the modern society, including consumer electronics, information technology, science, medicine, industry, law enforcement, and the military. They have been widely regarded as one of the most influential technological achievements of the 20th century. The benefits of lasers in various applications stems from their properties such as coherency, high monochromaticity, and capability of reaching extremely high powers.

Industry

- Laser is used to cut steel and other metals.
- Laser line levels are used in surveying and construction.
- Lasers are also used for guidance in aircraft (ring laser gyroscope).
- A laser of modest power can be focused to high intensities and used for cutting, burning, or even vapourizing materials.

Science

- Lasers are employed in a wide variety of interferometric devices and for Raman spectroscopy and laser-induced breakdown spectroscopy.
- They are also used in some types of thermonuclear fusion reactors.
- Other uses of lasers include atmospheric remote sensing and investigation of non-linear optics phenomena.
- Holographic methods employing lasers also contribute to a number of measurement techniques.
- Lasers are used in consumer electronics, telecommunications, data communications, and as transmitters in optical communications over optical fibre and free space.
- They are used to store and retrieve data from compact discs, DVDs, as well as magneto-optical discs.
- A highly coherent laser beam can be focused down to its diffraction limit allowing it to record gigabytes of information in the microscopic pits of a DVD.
- Laser lighting displays (Fig. 5.16) accompany many music concerts.

Medicine

21.applications_of_lasers_11-Mar-2021_Reference_Material_I

- Laser is used as a scalpel for laser vision correction (LASIK).
- Lasers are also used for dermatological procedures including removal of tattoos, birthmarks, and hair.

Law enforcement

- Lasers are widely used as LIDAR to detect the speed of vehicles.
- In military, lasers are used as target designators for other weapons; their use as directed-energy weapons is currently under research.
- Laser weapon systems under development include the air-borne laser, the air-borne technical laser, the tactical high-energy laser, the high-energy liquid laser area defence system, and the MIRACL (mid-infrared advanced chemical laser).

Dye lasers

The gain medium in a dye lasers is a solution made with an organic dye molecule. The solution is intensely coloured owing to the very strong absorption from the ground electronic state S_0 to the first excited singlet state S_1 . Fluorescence to the ground state also has a high quantum efficiency, Φ_F .

Possible processes:

- 1,2: Absorption from S_0 to S_1 , S_2
- 3,4: Rapid collisional relaxation to ground vibrational level of S_1
- 5: Fluorescence to various vibrational states of S_0 (basis for laser emission)
- 6: Vibrational relaxation to S_0 ground vibrational level
- 7: ISC to triplet state T_1
- 8: Absorption between triplet states
- 9: Phosphorescence to S_0

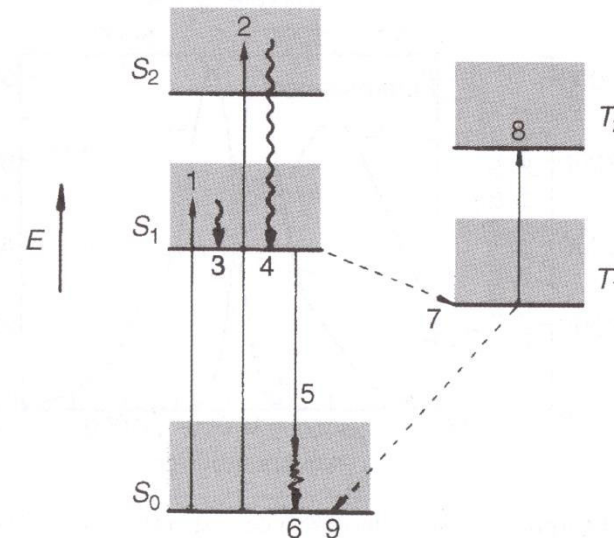


Figure 9.18 Energy level scheme for a dye molecule showing nine processes important in laser action

This is essentially a 4-level laser: pumping at 1 or 2; laser emission at 5.

The absorption and fluorescence spectra are comprised of a broad continuum of vibrational and rotational states as the following Rhodamine B/methanol spectrum shows:

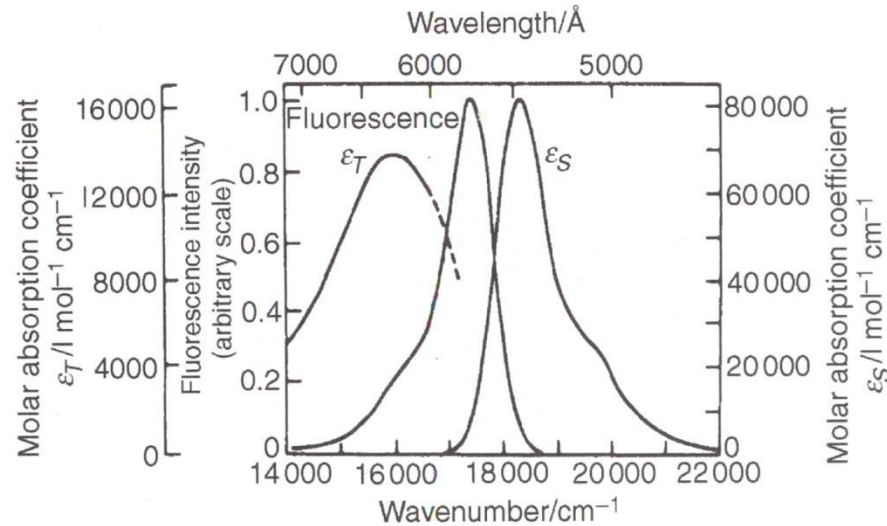
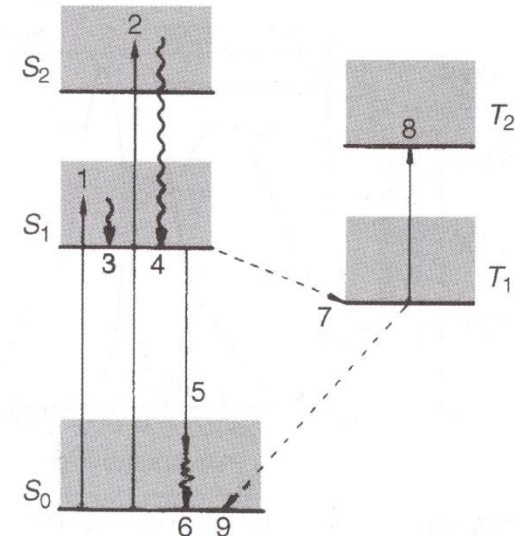


Figure 9.17 Absorption and fluorescence spectra of rhodamine B in methanol ($5 \times 10^{-5} \text{ mol l}^{-1}$). The curve marked ε_T is for the $T_2 - T_1$ absorption (process 8 in Figure 9.18) and that marked ε_S for process 1. (Reproduced, with permission, from Dienes, A. and Shank, C. V., Chapter 4 in *Creation and Detection of the Excited State* (Ed. W. R. Ware), Vol. 2, p. 154, Marcel Dekker, New York, 1972)



The fluorescence is red-shifted relative to the absorption spectrum.
Absorption by the triplet state is a significant loss process.

How is wavelength tuning accomplished?

Many laser dyes are available:

Typically, each dye can be tuned over several tens of nm.

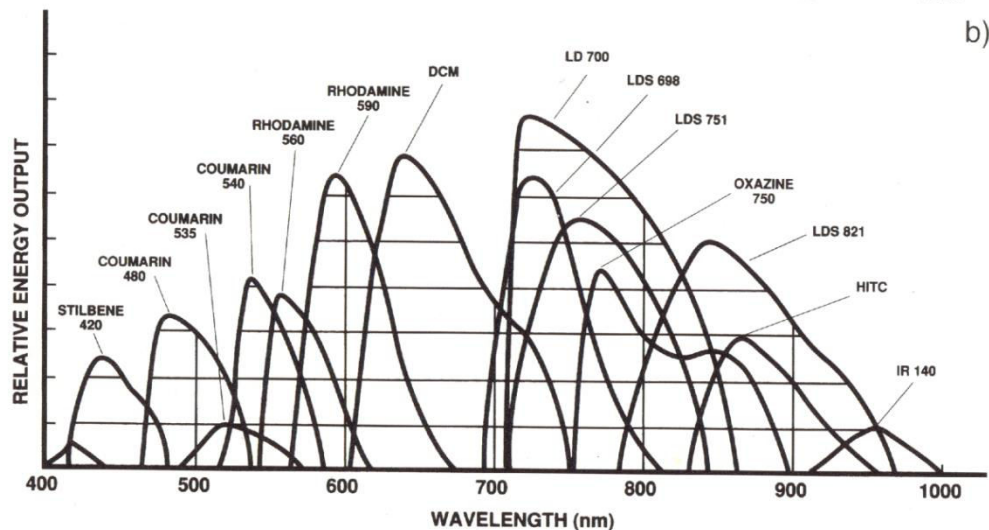


Fig. 5.80a,b. Spectral gain profiles of different laser dyes, illustrated by the output power of pulsed lasers (a) and cw dye lasers (b) (Lambda Physik and Spectra-Physics information sheets)

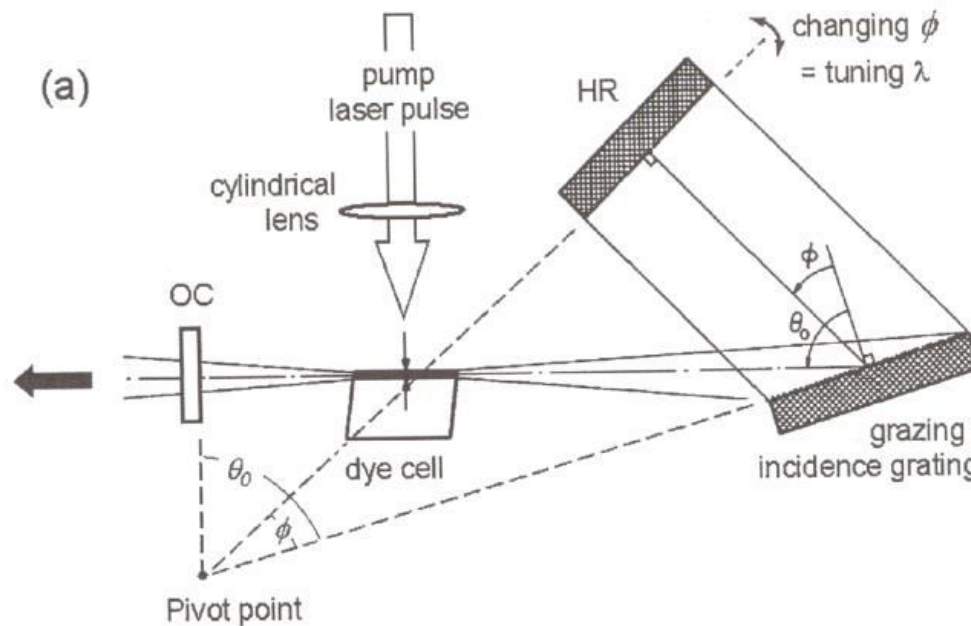
The wide tuneability range, high output power, and pulsed or CW operation make the dye laser particularly useful in many chemical studies.

Pulsed dye lasers may be pumped by flashlamps or other pulsed lasers (N_2 , excimer, Nd:YAG). CW dye lasers are usually pumped by Ar ion lasers.

The dye solution must be circulated to prevent overheating and degradation, and to replace molecules in the triplet state, T_1

Tuning the wavelength:

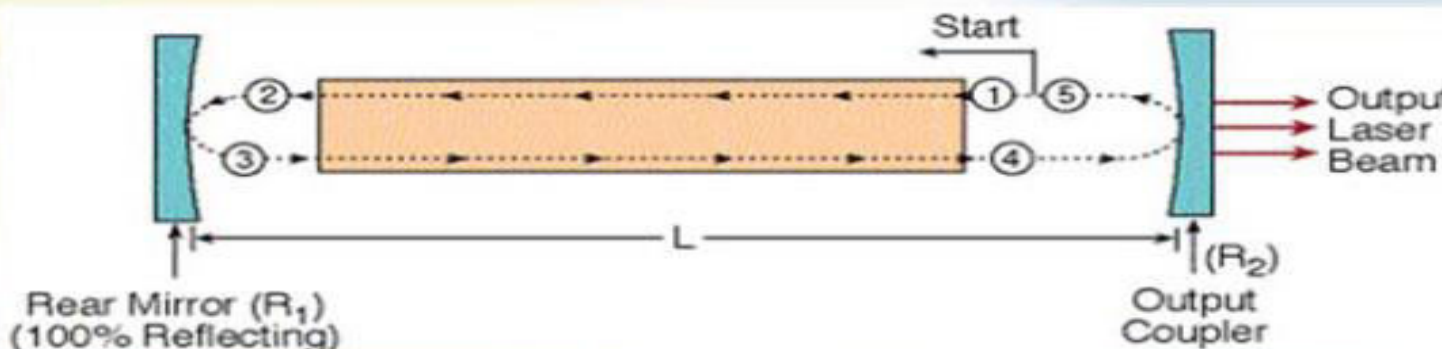
Usually a *tuning element*, such as a diffraction grating or prism, is incorporated in the cavity. This allows only light in a very narrow frequency range to resonate in the cavity and be emitted as laser emission.



Rotating a mirror or tuning element selects which wavelengths are resonant in the laser cavity.

Round trip Gain (G)

Figure below show the round trip path of the radiation through the laser cavity. The path is divided to sections numbered by 1-5, while point "5" is the same point as "1".



Round trip path of the radiation through the laser cavity.

By definition, **Round trip Gain** is given by:

$$G = I_5 / I_1$$

G = Round trip Gain.

I₁ = Intensity of radiation at the beginning of the loop.

I₅ = Intensity of radiation at the end of the loop.

we found that the intensity after one round trip

$$I_5 = R_1 * R_2 * G^2 * I_1$$

Gain (G) With Losses

We assume that the losses occur uniformly along the length of the cavity (L). In analogy to the Lambert formula for losses, we define loss coefficient (α), and using it we can define absorption factor k:

$$k = \exp(-2\alpha L)$$

k = Loss factor, describe the relative part of the radiation that remain in the cavity after all the losses in a round trip loop inside the cavity.

All the losses in a round trip loop inside the cavity are $1-k$ (always less than 1).

α = Loss coefficient (in units of 1 over length).

$2L$ = Path Length, which is twice the length of the cavity.

Adding the loss factor (k) to the equation of I_5 :

$$I_5 = R_1 * R_2 * G_A^2 * I_1 * k$$

From this we can calculate the **round trip gain**:

$$G = I_5 / I_1 = R_1 * R_2 * G_A^2 * k$$

As we assumed uniform distribution of the loss coefficient (α), we now define **gain coefficient (γ)**, and assume **active medium gain (G_A)** as distributed uniformly along the length of the cavity.

$$G_A = \exp(+\gamma L)$$

$$G(v) = e^{\gamma_o(v)L}$$

Substituting the last equation in the Loop Gain:

$$k = \exp(-2\alpha L)$$

$$G = R_1 * R_2 * \exp(2(\gamma - \alpha)L)$$

$$G = R_1 * R_2 * \exp(2(\gamma - \alpha)L)$$

When the loop gain (G) is greater than 1 ($G > 1$), the beam intensity will increase after one return pass through the laser.

When the loop gain (G) is less than 1 ($G < 1$), the beam intensity will decrease after one return pass through the laser. laser oscillation decay, and no beam will be emitted.

Conclusion:

There is a threshold condition for amplification, in order to create oscillation inside the laser.

$$G_{th} = 1$$

This Threshold Gain is marked with index "th".

For continuous laser , the threshold condition is:

$$G_{th} = 1 = R_1 R_2 G_A^2 k = R_1 * R_2 * \exp(2(\gamma - \alpha)L)$$

Example

Active medium gain in a laser is 1.05. Reflection coefficients of the mirrors are: 0.999, and 0.95. Length of the laser is 30cm. Loss coefficient is: $\alpha = 1.34 \times 10^{-4} \text{ cm}^{-1}$.

Calculate:

1. The loss factor k.
2. The round trip gain G.
3. The gain coefficient (γ).

Solution

1. The loss factor k:

$$k = \exp(-2\alpha L) = \exp[-2(1.34 \times 10^{-4}) \times 30] = 0.992$$

2. The Loop gain G:

$$G = R_1 R_2 G_A^2 k = 0.999 \times 0.95 \times 1.052 \times 0.992 = 1.038$$

Since $G_L > 1$, this laser operates above threshold.

3. The gain coefficient (γ):

$$G = \exp(\gamma L)$$

$$\ln G = \gamma L$$

$$\gamma = \ln G / L = \ln(1.05) / 30 = 1.63 \times 10^{-3} \text{ [cm}^{-1}\text{]}$$

The gain coefficient (γ) is greater than the loss coefficient (α), as expected.

Electromagnetic wave equations

Electromagnetic Wave Equations

Faraday's law (Maxwell's 3rd Equation)

$$\nabla \times \vec{E} = -\frac{\partial \vec{B}}{\partial t} . \quad \text{②}$$

$$\vec{B} = \mu \vec{H} .$$

$$\nabla \times \vec{E} = -\mu \frac{\partial \vec{H}}{\partial t} .$$

Take curl on both sides

$$\nabla \times \nabla \times \vec{E} = -\mu \nabla \times \frac{\partial \vec{H}}{\partial t} .$$

L → ①

Equation Maxwell's fourth

$$\nabla \times H = J + \frac{\partial D}{\partial t} .$$

$$\nabla \times H = \sigma E + \epsilon \frac{\partial E}{\partial t} .$$

where $D = \epsilon E$
 $J = \sigma E$
 (Ohm's law).

Differentiating

$$\nabla \times \frac{\partial H}{\partial t} = \frac{\partial (\nabla \times H)}{\partial t}$$

$$= \frac{\partial}{\partial t} \left(\sigma E + \epsilon \frac{\partial E}{\partial t} \right) .$$

$$\nabla \times \frac{\partial H}{\partial t} = \sigma \frac{\partial E}{\partial t} + \epsilon \frac{\partial^2 E}{\partial t^2} . \quad \textcircled{2}$$

Substitute eqn ① into eqn ①

$$\nabla \times \nabla \times E = -\mu \left[\sigma \frac{\partial E}{\partial t} + \epsilon \frac{\partial^2 E}{\partial t^2} \right]$$

$$= -\mu \sigma \frac{\partial E}{\partial t} - \mu \epsilon \frac{\partial^2 E}{\partial t^2} .$$

(3)

$$\nabla \times \nabla \times E = \nabla (\nabla \cdot E) - \nabla^2 E .$$

(4)

$$\nabla \cdot E = \frac{1}{\epsilon} \nabla \cdot D$$

Since there is no net charge within the conductor, the charge density $\rho = 0$.

$$\nabla \cdot D = 0$$

$$\nabla \cdot E = 0 .$$

$$\nabla \times \nabla \times E = -\nabla^2 E \quad \text{--- (5)}$$

Comparing equations ③ and ⑤

$$\nabla^2 E = \mu\sigma \frac{\partial E}{\partial t} + \mu\epsilon \frac{\partial^2 E}{\partial t^2}$$

$$\boxed{\nabla^2 E - \mu\sigma \frac{\partial E}{\partial t} - \mu\epsilon \frac{\partial^2 E}{\partial t^2} = 0}$$
⑥

This is the wave equation for electric field.

22.Electromagnetic_wave_equation_12-Mar-2021_Reference_Material_I

$$\nabla \times H = J + \frac{\partial D}{\partial t}$$

$$= \sigma E + \epsilon \frac{\partial E}{\partial t}$$

Take curl on both sides

$$\nabla \times \nabla \times H = \sigma \nabla \times E + \epsilon \nabla \times \frac{\partial E}{\partial t} \quad (7)$$

From Maxwell's third equation
(Faraday's law)

$$\nabla \times E = -\mu \frac{\partial H}{\partial t} \quad (8)$$

After Differentiating

$$\nabla \times \frac{\partial E}{\partial t} = -\mu \frac{\partial^2 H}{\partial t^2} \quad (9)$$

Use equations ⑧ & ⑨ in eqn ⑦.

$$\nabla \times \nabla \times H = -\mu\sigma \frac{\partial H}{\partial t} - \mu\epsilon \frac{\partial^2 H}{\partial t^2}.$$

$$\begin{aligned}\nabla \times \nabla \times H &= \nabla (\nabla \cdot H) - \nabla^2 H \\ &= -\nabla^2 H. \\ &\quad [\nabla \cdot B = \nabla \cdot H = 0]\end{aligned}$$

$$\nabla^2 H = \mu\sigma \frac{\partial H}{\partial t} + \mu\epsilon \frac{\partial^2 H}{\partial t^2}.$$

$$\boxed{\nabla^2 H - \mu\sigma \frac{\partial H}{\partial t} - \mu\epsilon \frac{\partial^2 H}{\partial t^2} = 0.}$$

This is the wave equation for magnetic field.

Wave Equations for free space

For free space, the conductivity of the medium is zero.

$$\sigma = 0$$

and there is no charge containing in it; $\rho = 0$.

The wave equations become

$$\nabla^2 E - \mu \epsilon \frac{\partial^2 E}{\partial t^2} = 0.$$

$$\nabla^2 H - \mu \epsilon \frac{\partial^2 H}{\partial t^2} = 0.$$

$$c = \frac{1}{\sqrt{\epsilon_0 \mu_0}} ; \mu_r = \frac{\mu}{\mu_0}$$

$$\epsilon_r = \frac{\epsilon}{\epsilon_0}$$

When $\mu_r = 1$ and $\epsilon_r = 1$.

$$c = \frac{1}{\sqrt{\epsilon_0 \mu_0}} = \frac{1}{\sqrt{\epsilon \mu}}$$

$$\Rightarrow \epsilon \mu = \frac{1}{c^2}$$

$$\nabla^2 E - \frac{1}{c^2} \frac{\partial^2 E}{\partial t^2} = 0$$

$$\nabla^2 H - \frac{1}{c^2} \frac{\partial^2 H}{\partial t^2} = 0$$

Verify that the following equations satisfy the one-dimensional wave equations :

$$E_y(x,t) = E_0 \cos(kx - \omega t);$$

$$B_z(x,t) = B_0 \cos(kx - \omega t);$$

assume $\omega = kc$.

Solution

$$E_y(x, t) = E_0 \cos(kx - \omega t) \quad \text{--- (1)}$$

$$B_z(x, t) = B_0 \cos(kx - \omega t) \quad \text{--- (2)}.$$

One dimensional wave equations

$$\frac{\partial^2 E_y(x, t)}{\partial x^2} = \frac{1}{c^2} \frac{\partial^2 E_y(x, t)}{\partial t^2} \quad \text{--- (3)}.$$

$$\frac{\partial^2 B_z(x, t)}{\partial x^2} = \frac{1}{c^2} \frac{\partial^2 B_z(x, t)}{\partial t^2} \quad \text{--- (4)}.$$

Differentiating eqn (1) w.r.t. x

$$\frac{\partial E_y(x, t)}{\partial x} = -k E_0 \sin(kx - \omega t)$$

$$\frac{\partial^2 E_y(x, t)}{\partial x^2} = -k^2 E_0 \cos(kx - \omega t). \quad \text{--- (5)}$$

Differentiating eqn ① w.r.t to 't' .

22.Electromagnetic_wave_equation_12-Mar-2021_Reference_Material_I

$$\frac{\partial E_y(x,t)}{\partial t} = \omega E_0 \sin(kx - \omega t)$$

$$\frac{\partial^2 E_y(x,t)}{\partial t^2} = -\omega^2 E_0 \cos(kx - \omega t) \quad \text{L} \rightarrow ⑥$$

$$\begin{aligned} \frac{\partial^2 E_y(x,t)}{\partial x^2} - \frac{1}{c^2} \frac{\partial^2 E_y(x,t)}{\partial t^2} \\ = \left(-k^2 + \frac{\omega^2}{c^2} \right) E_0 \cos(kx - \omega t) \quad \text{L} \rightarrow ⑦ \end{aligned}$$

Substitute $\omega = kc$.

eqn ⑦ becomes

$$\frac{\partial^2 E_y(x,t)}{\partial x^2} - \frac{1}{c^2} \frac{\partial^2 E_y(x,t)}{\partial t^2} = 0$$

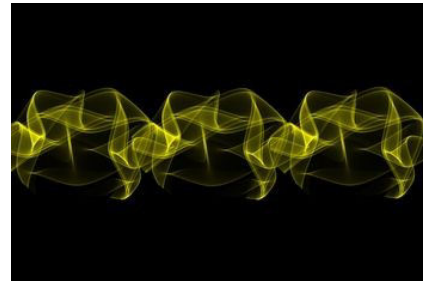
Do the same thing for eqn ② .

Both equations satisfy the wave equations .

Introduction to Electromagnetic Theory

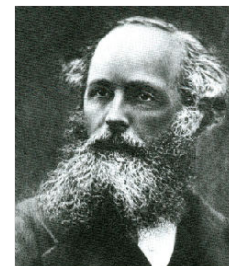
Lecture topics

- Laws of magnetism and electricity
- Meaning of Maxwell's equations
- Solution of Maxwell's equations

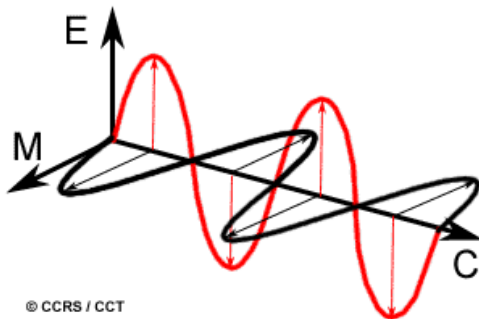


Electromagnetic radiation: wave model

- James Clerk Maxwell (1831-1879) – Scottish mathematician and physicist
- Wave model of EM energy
 - Unified existing laws of electricity and magnetism (Newton, Faraday, Kelvin, Ampère)
 - Oscillating electric field produces a magnetic field (and vice versa) – propagates an EM wave
 - Can be described by 4 differential equations
 - Derived speed of EM wave in a vacuum

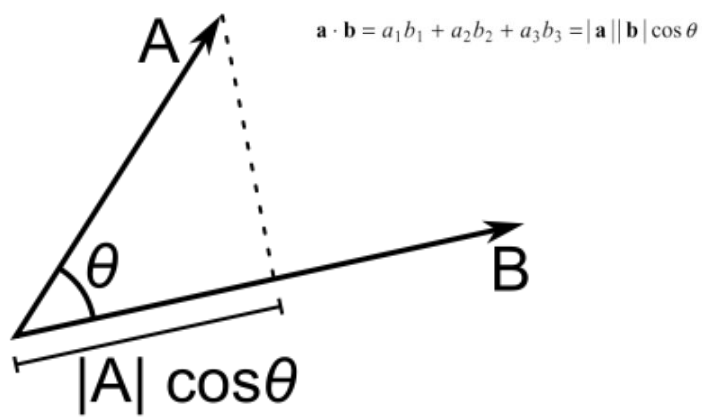


Electromagnetic radiation



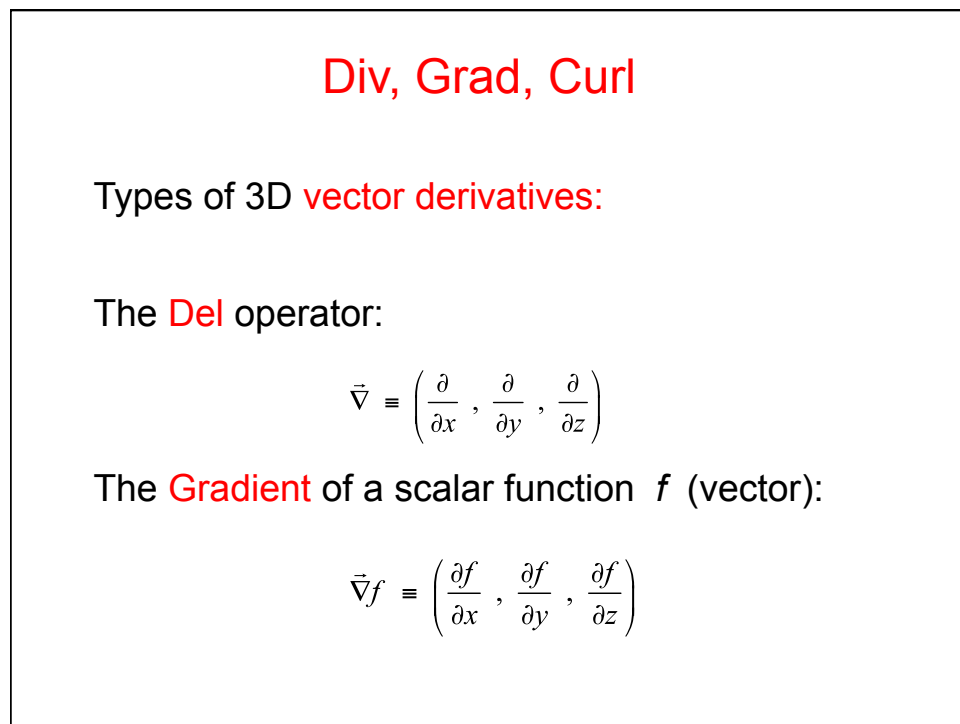
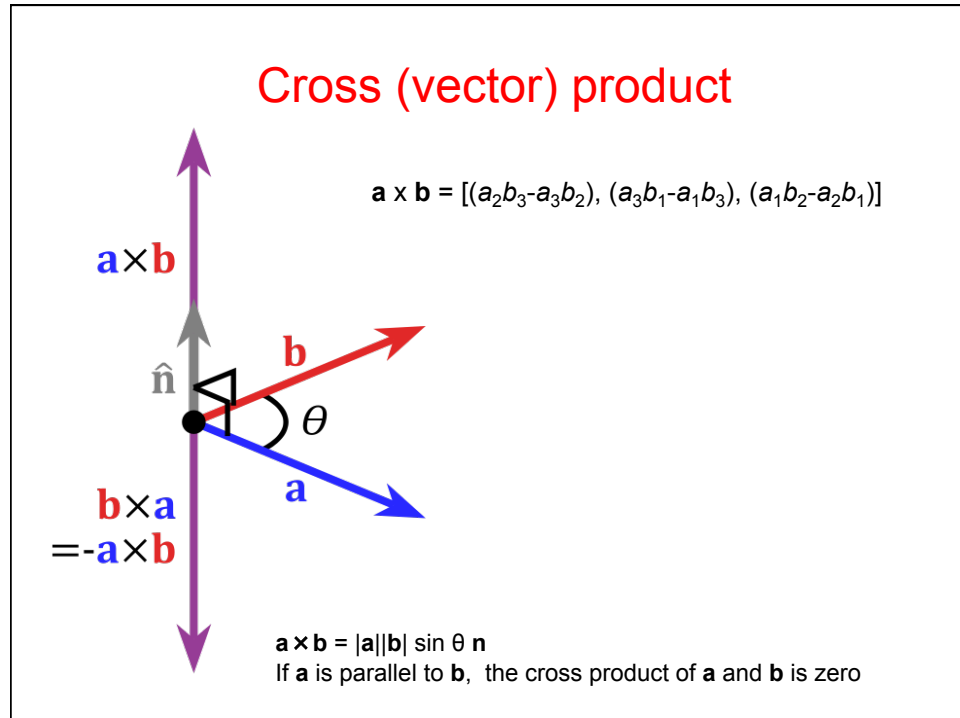
- EM wave is:
- Electric field (E) perpendicular to magnetic field (M)
- Travels at velocity, c (3×10^8 ms⁻¹, in a vacuum)

Dot (scalar) product



$$\mathbf{A} \cdot \mathbf{B} = |\mathbf{A}| |\mathbf{B}| \cos \theta$$

If **A** is perpendicular to **B**, the dot product of **A** and **B** is zero



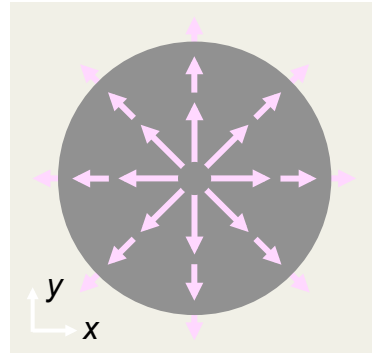
Div, Grad, Curl

The **Divergence** of a vector function (scalar):

$$\nabla \cdot \vec{f} = \frac{\partial f_x}{\partial x} + \frac{\partial f_y}{\partial y} + \frac{\partial f_z}{\partial z}$$

The **Divergence** is nonzero if there are sources or sinks.

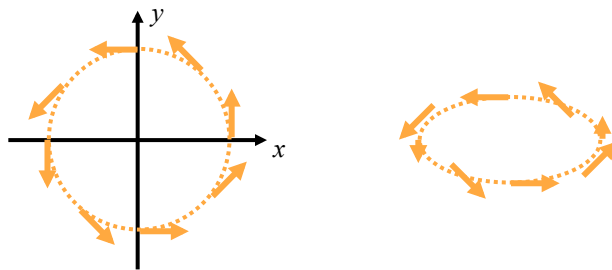
A 2D source with a large divergence:



Div, Grad, Curl

The **Curl** of a vector function \vec{f} :

$$\vec{\nabla} \times \vec{f} \equiv \left(\frac{\partial f_z}{\partial y} - \frac{\partial f_y}{\partial z}, \frac{\partial f_x}{\partial z} - \frac{\partial f_z}{\partial x}, \frac{\partial f_y}{\partial x} - \frac{\partial f_x}{\partial y} \right)$$



Functions that tend to **curl around** have large curls.

http://mathinsight.org/curl_idea

Div, Grad, Curl

The **Laplacian** of a scalar function :

$$\begin{aligned}\nabla^2 f &\equiv \vec{\nabla} \cdot \vec{\nabla} f = \vec{\nabla} \cdot \left(\frac{\partial f}{\partial x}, \frac{\partial f}{\partial y}, \frac{\partial f}{\partial z} \right) \\ &= \frac{\partial^2 f}{\partial x^2} + \frac{\partial^2 f}{\partial y^2} + \frac{\partial^2 f}{\partial z^2}\end{aligned}$$

The **Laplacian of a vector** function is the same, but for each component of f :

$$\nabla^2 \vec{f} = \left(\frac{\partial^2 f_x}{\partial x^2} + \frac{\partial^2 f_x}{\partial y^2} + \frac{\partial^2 f_x}{\partial z^2}, \frac{\partial^2 f_y}{\partial x^2} + \frac{\partial^2 f_y}{\partial y^2} + \frac{\partial^2 f_y}{\partial z^2}, \frac{\partial^2 f_z}{\partial x^2} + \frac{\partial^2 f_z}{\partial y^2} + \frac{\partial^2 f_z}{\partial z^2} \right)$$

The Laplacian tells us the curvature of a vector function.

Maxwell's Equations

- Four equations relating electric (**E**) and magnetic fields (**B**) – vector fields
- ϵ_0 is **electric permittivity of free space** (or vacuum permittivity - a constant) – *resistance to formation of an electric field in a vacuum*
- $\epsilon_0 = 8.854188 \times 10^{-12}$ Farad m⁻¹
- μ_0 is **magnetic permeability of free space** (or magnetic constant - a constant) – *resistance to formation of a magnetic field in a vacuum*
- $\mu_0 = 1.2566 \times 10^{-6}$ T.m/A (T = Tesla; SI unit of magnetic field)

$$\nabla \cdot E = \frac{\rho}{\epsilon_0}$$

$$\nabla \cdot B = 0$$

$$\nabla \times E = -\frac{\partial B}{\partial t}$$

$$\nabla \times B = \mu_0 J + \epsilon_0 \mu_0 \frac{\partial E}{\partial t}$$

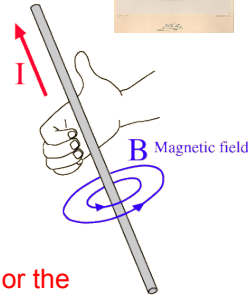
Note: $\nabla \cdot$ is 'divergence' operator and $\nabla \times$ is 'curl' operator

Biot-Savart Law (1820)



- Jean-Baptiste Biot and Felix Savart (French physicist and chemist)
- The magnetic field \mathbf{B} at a point a distance \mathbf{R} from an infinitely long wire carrying current I has magnitude:

$$B = \frac{\mu_0 I}{2\pi R}$$



- Where μ_0 is the **magnetic permeability of free space or the magnetic constant**
- Constant of proportionality linking magnetic field and distance from a current
- Magnetic field strength decreases with distance from the wire
- $\mu_0 = 1.2566 \times 10^{-6} \text{ T.m/A}$ (T = Tesla; SI unit of magnetic field)

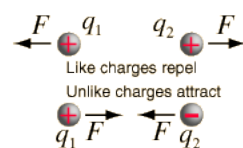
Coulomb's Law (1783)



- Charles Augustin de Coulomb (French physicist)
- The magnitude of the electrostatic force (F) between two point electric charges (q_1, q_2) is given by:

$$F = \frac{q_1 q_2}{4\pi\epsilon_0 r^2}$$

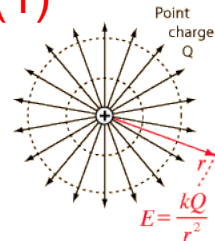
- Where ϵ_0 is the **electric permittivity or electric constant**
- Like charges repel, opposite charges attract
- $\epsilon_0 = 8.854188 \times 10^{-12} \text{ Farad m}^{-1}$





Maxwell's Equations (1)

$$\nabla \cdot E = \frac{\rho}{\epsilon_0}$$

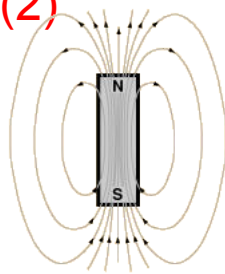


- **Gauss' law for electricity:** the electric flux out of any closed surface is proportional to the total charge enclosed within the surface; i.e. a charge will radiate a measurable field of influence around it.
- **E** = electric field, ρ = net charge inside, ϵ_0 = vacuum permittivity (constant)
- Recall: divergence of a vector field is a measure of its tendency to converge on or repel from a point.
- Direction of an electric field is the direction of the force it would exert on a positive charge placed in the field
- If a region of space has more electrons than protons, the total charge is negative, and the direction of the electric field is negative (inwards), and vice versa.

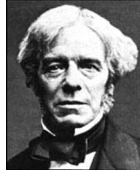


Maxwell's Equations (2)

$$\nabla \cdot B = 0$$

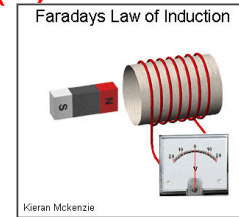


- **Gauss' law for magnetism:** the net magnetic flux out of any closed surface is zero (i.e. magnetic monopoles do not exist)
- **B** = magnetic field; magnetic flux = $\mathbf{B} \cdot \mathbf{A}$ (\mathbf{A} = area perpendicular to field **B**)
- Recall: divergence of a vector field is a measure of its tendency to converge on or repel from a point.
- Magnetic sources are dipole sources and magnetic field lines are loops – we cannot isolate N or S ‘monopoles’ (unlike electric sources or point charges – protons, electrons)
- Magnetic monopoles *could* exist, but have never been observed



Maxwell's Equations (3)

$$\nabla \times E = -\frac{\partial B}{\partial t}$$



- **Faraday's Law of Induction:** the curl of the electric field (E) is equal to the negative of rate of change of the magnetic flux through the area enclosed by the loop
- E = electric field; B = magnetic field
- Recall: curl of a vector field is a vector with magnitude equal to the maximum 'circulation' at each point and oriented perpendicularly to this plane of circulation for each point.
- Magnetic field weakens → curl of electric field is positive and vice versa
- Hence changing magnetic fields affect the curl ('circulation') of the electric field – basis of electric generators (moving magnet induces current in a conducting loop)



Maxwell's Equations (4)

$$\nabla \times B = \mu_0 J + \epsilon_0 \mu_0 \frac{\partial E}{\partial t}$$

- **Ampère's Law:** the curl of the magnetic field (B) is proportional to the electric current flowing through the loop

AND to the rate of change of the electric field. ← added by Maxwell

- B = magnetic field; J = current density (current per unit area); E = electric field
- The curl of a magnetic field is basically a measure of its strength
- First term on RHS: in the presence of an electric current (J), there is always a magnetic field around it; B is dependent on J (e.g., *electromagnets*)
- Second term on RHS: a changing electric field generates a magnetic field.
- Therefore, generation of a magnetic field does not require electric current, only a changing electric field. An oscillating electric field produces a variable magnetic field (as dE/dt changes)

Putting it all together....

- An oscillating electric field produces a variable magnetic field. A changing magnetic field produces an electric field....and so on.
- In 'free space' (vacuum) we can assume current density (J) and charge (ρ) are zero i.e. there are no electric currents or charges
- Equations become:

$$\nabla \bullet E = 0$$

$$\nabla \bullet B = 0$$

$$\nabla \times E = -\frac{\partial B}{\partial t}$$

$$\nabla \times B = \epsilon_0 \mu_0 \frac{\partial E}{\partial t}$$

Solving Maxwell's Equations

Take curl of:

$$\vec{\nabla} \times \vec{E} = -\frac{\partial \vec{B}}{\partial t}$$

$$\vec{\nabla} \times [\vec{\nabla} \times \vec{E}] = \vec{\nabla} \times [-\frac{\partial \vec{B}}{\partial t}]$$

Change the order of differentiation on the RHS:

$$\vec{\nabla} \times [\vec{\nabla} \times \vec{E}] = -\frac{\partial}{\partial t} [\vec{\nabla} \times \vec{B}]$$

Solving Maxwell's Equations (cont'd)

But (Equation 4):

$$\vec{\nabla} \times \vec{B} = \mu\epsilon \frac{\partial \vec{E}}{\partial t}$$

Substituting for $\vec{\nabla} \times \vec{B}$, we have:

$$\vec{\nabla} \times [\vec{\nabla} \times \vec{E}] = -\frac{\partial}{\partial t} [\vec{\nabla} \times \vec{B}] \Rightarrow \vec{\nabla} \times [\vec{\nabla} \times \vec{E}] = -\frac{\partial}{\partial t} [\mu\epsilon \frac{\partial \vec{E}}{\partial t}]$$

Or:

$$\vec{\nabla} \times [\vec{\nabla} \times \vec{E}] = -\mu\epsilon \frac{\partial^2 \vec{E}}{\partial t^2} \quad \text{assuming that } \mu \text{ and } \epsilon \text{ are constant in time.}$$

Solving Maxwell's Equations (cont'd)

Identity:

$$\vec{\nabla} \times [\vec{\nabla} \times \vec{f}] = \vec{\nabla}(\vec{\nabla} \cdot \vec{f}) - \nabla^2 \vec{f}$$

Using the identity, $\vec{\nabla} \times [\vec{\nabla} \times \vec{E}] = -\mu\epsilon \frac{\partial^2 \vec{E}}{\partial t^2}$

becomes: $\vec{\nabla}(\vec{\nabla} \cdot \vec{E}) - \nabla^2 \vec{E} = -\mu\epsilon \frac{\partial^2 \vec{E}}{\partial t^2}$

Assuming zero charge density (free space; Equation 1):

$$\vec{\nabla} \cdot \vec{E} = 0$$

and we're left with: $\nabla^2 \vec{E} = \mu\epsilon \frac{\partial^2 \vec{E}}{\partial t^2}$

Solving Maxwell's Equations (cont'd)

$$\nabla^2 \vec{E} = \mu\epsilon \frac{\partial^2 \vec{E}}{\partial t^2} \quad \nabla^2 \vec{B} = \mu\epsilon \frac{\partial^2 \vec{B}}{\partial t^2}$$

The same result is obtained for the magnetic field \vec{B} .

These are forms of the **3D wave equation**, describing the propagation of a sinusoidal wave:

$$\nabla^2 u = \frac{1}{v^2} \frac{\partial^2 u}{\partial t^2}$$

Where v is a constant equal to the propagation speed of the wave

$$\text{So for EM waves, } v = \frac{1}{\sqrt{\mu\epsilon}}$$

Solving Maxwell's Equations (cont'd)

$$\text{So for EM waves, } v = \frac{1}{\sqrt{\mu\epsilon}},$$

Units of $\mu = \text{T.m/A}$

The Tesla (T) can be written as $\text{kg A}^{-1} \text{s}^{-2}$

So units of μ are $\text{kg m A}^{-2} \text{s}^{-2}$

Units of ϵ = Farad m^{-1} or $\text{A}^2 \text{s}^4 \text{kg}^{-1} \text{m}^{-3}$ in SI base units

So units of $\mu\epsilon$ are $\text{m}^{-2} \text{s}^2$

Square root is $\text{m}^{-1} \text{s}$, reciprocal is m s^{-1} (i.e., velocity)

$\epsilon_0 = 8.854188 \times 10^{-12}$ and $\mu_0 = 1.2566371 \times 10^{-6}$

Evaluating the expression gives $2.998 \times 10^8 \text{ m s}^{-1}$

Maxwell (1865) recognized this as the (known) **speed of light** – confirming that **light was in fact an EM wave**.

Why light waves are transverse



Transverse waves may occur on a string, on the surface of a liquid, and throughout a solid.

Suppose a wave propagates in the x -direction. Then it's a function of x and t (and not y or z), so all y - and z -derivatives are zero:

$$\frac{\partial E_y}{\partial y} = \frac{\partial E_z}{\partial z} = \frac{\partial B_y}{\partial y} = \frac{\partial B_z}{\partial z} = 0$$

In a charge-free medium,

$$\vec{\nabla} \cdot \vec{E} = 0 \text{ and } \vec{\nabla} \cdot \vec{B} = 0$$

that is,

$$\frac{\partial E_x}{\partial x} + \cancel{\frac{\partial E_y}{\partial y}} + \cancel{\frac{\partial E_z}{\partial z}} = 0 \quad \frac{\partial B_x}{\partial x} + \cancel{\frac{\partial B_y}{\partial y}} + \cancel{\frac{\partial B_z}{\partial z}} = 0$$

Substituting the zero values, we have:

$$\frac{\partial E_x}{\partial x} = 0 \text{ and } \frac{\partial B_x}{\partial x} = 0$$

So the longitudinal fields (parallel to propagation direction) are at most **constant**, and not waves.

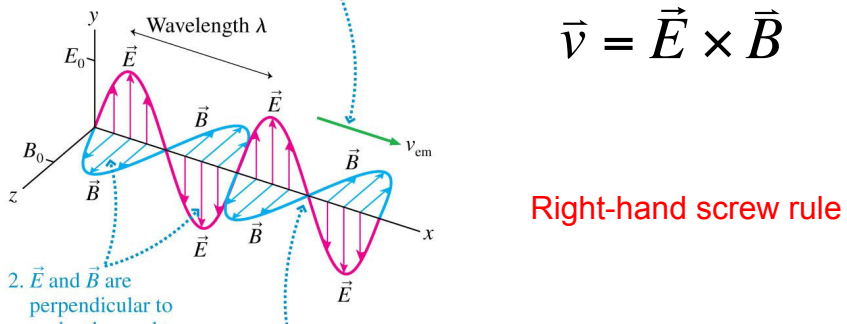
The propagation direction of a light wave

FIGURE 35.19 A sinusoidal electromagnetic wave.

1. A sinusoidal wave with frequency f and wavelength λ travels with wave speed v_{em} .

2. \vec{E} and \vec{B} are perpendicular to each other and to the direction of travel. The fields have amplitudes E_0 and B_0 .
3. \vec{E} and \vec{B} are in phase. That is, they have matching crests, troughs, and zeros.

$$\vec{v} = \vec{E} \times \vec{B}$$



Right-hand screw rule

EM waves carry energy – how much?

e.g., from the Sun to the vinyl seat cover in your parked car....

The energy flow of an electromagnetic wave is described by the **Poynting vector**:

$$\vec{S} \equiv \frac{1}{\mu_0} \vec{E} \times \vec{B}$$

The intensity (I) of a time-harmonic electromagnetic wave whose electric field amplitude is E_0 , measured normal to the direction of propagation, is the average over one complete cycle of the wave:

$$I = \frac{P}{A} = S_{\text{avg}} = \frac{1}{2c\mu_0} E_0^2 = \frac{c\epsilon_0}{2} E_0^2 \quad \text{WATTS/M}^2$$

P = Power; A = Area; c = speed of light

Key point: intensity is proportional to the square of the amplitude of the EM wave

NB. Intensity = Flux density (F) = Irradiance (incident) = Radiant Exitance (emerging)

Electric field of a laser pointer

HE-NEON POWER 1 mWatt, diameter 1 mm². How big is the electric field near the aperture (E_0)?

$$I = \frac{P}{A} = S_{\text{avg}} = \frac{1}{2c\mu_0} E_0^2 = \frac{c\epsilon_0}{2} E_0^2 \quad A = \pi r^2 = \pi(5 \times 10^{-4})^2 \text{ m}^2$$

$$E_0 = \sqrt{\frac{2I}{c\epsilon_0}} = \sqrt{\frac{2(1270 \text{ W/m}^2)}{(3.00 \times 10^8 \text{ m/s})(8.85 \times 10^{-12} \text{ C}^2/\text{N m}^2)}} \\ = 980 \text{ V/m}$$

Radiation Pressure

Radiation also exerts pressure. It's interesting to consider the force of an electromagnetic wave exerted on an object per unit area, which is called the **radiation pressure** p_{rad} . The radiation pressure on an object that absorbs all the light is:

$$F = P/c$$

$$p_{\text{rad}} = \frac{F}{A} = \frac{\overbrace{P/A}^{\triangle}}{c} = \frac{I}{c}$$

Units: N/m²

where I is the intensity of the light wave, P is power, and c is the speed of light.

$$1 \text{ Watt m}^{-2} = 1 \text{ J s}^{-1} \text{ m}^{-2} = 1 \text{ N.m s}^{-1} \text{ m}^{-2} = 1 \text{ N s}^{-1} \text{ m}^{-1}$$

Solar sailing

A low-cost way of sending spacecraft to other planets would be to use the radiation pressure on a solar sail. The intensity of the sun's electromagnetic radiation at distances near the earth's orbit is about 1300 W/m^2 . What size sail would be needed to accelerate a 10,000 kg spacecraft toward Mars at 0.010 m/s^2 ?

$$a = F / M = p_{\text{Rad}} A / M$$

$$p_{\text{Rad}} = I / c$$

$$A = Mac / I$$

$$A = 10^4 \times .01 \times 3 \times 10^8 / 1300 = 23 \text{ km}^2$$

About 4.8 km per side if square

Summary

- Maxwell unified existing laws of electricity and magnetism
- Revealed self-sustaining properties of magnetic and electric fields
- Solution of Maxwell's equations is the three-dimensional wave equation for a wave traveling at the speed of light
- Proved that light is an electromagnetic wave
- EM waves carry energy through empty space and *all remote sensing techniques exploit the modulation of this energy*
- <http://www.phy.ntnu.edu.tw/ntnужава/index.php?topic=35>

(6)

Electromagnetic Wave Equation :-

Let us apply Maxwell's electromagnetic eqns. to a homogeneous, isotropic ^{dielectric} medium. As the dielectric medium is one which offers infinite resistance to the current, and hence its conductivity $j=0$, In homogeneous isotropic medium there is no volume distribution of charge, thus the charge density $\rho=0$. Hence,

$$j=0, \rho=0, D = k\epsilon_0 E = \epsilon E \text{ and } B = \mu_0 \mu_r H = \mu H$$

Hence Maxwell's equations for a dielectric medium become

$$\nabla \cdot E = 0 \quad \text{--- (1)}$$

$$\nabla \cdot B = 0 \quad \text{--- (2)}$$

$$\nabla \times E = -\frac{\partial B}{\partial t} \quad \text{--- (3)}$$

$$\nabla \times B = \mu \epsilon \frac{\partial E}{\partial t} \quad \text{--- (4)}$$

For obtaining the eqn. of propagation of wave in dielectric medium, 'E' should be eliminated from eqns (3) & (4).

Taking curl of eqn (4),

$$\begin{aligned} \nabla \times \nabla \times B &= \nabla \times \mu \epsilon \frac{\partial E}{\partial t} \\ &= \mu \epsilon (\nabla \times \frac{\partial E}{\partial t}) \\ &= \mu \epsilon \frac{\partial}{\partial t} (\nabla \times E) \quad \text{from eqn (3)} \\ &= \mu \epsilon \frac{\partial}{\partial t} \left(-\frac{\partial B}{\partial t} \right) \end{aligned}$$

$$\nabla \times \nabla \times B = -\mu \epsilon \frac{\partial^2 B}{\partial t^2} \quad \text{--- (5)}$$

$$\nabla (\nabla \cdot B) - \nabla^2 B = -\mu \epsilon \frac{\partial^2 B}{\partial t^2}$$

$$\nabla \cdot \nabla^2 B = -\mu \epsilon \frac{\partial^2 B}{\partial t^2} \quad \text{from eqn (2)}$$

$$\therefore \nabla^2 B = \mu \epsilon \frac{\partial^2 B}{\partial t^2} \quad \text{--- (6)}$$

By from eqn (3), we can show that

$$\nabla^2 E = \mu \epsilon \frac{\partial^2 E}{\partial t^2} \quad \text{--- (7)}$$

Eqs. (6) and (7) represent the relation bet^w the space and time variation of magnetic 'B' & electric field 'E'. These are called wave eqn for B and E respectively. These eqns. have the same general form of the differential eqn. of wave motion. The general wave eqn. is represented by

$$\nabla^2 y = \frac{1}{v^2} \frac{\partial^2 y}{\partial t^2} \quad \text{--- (8)}$$

where 'v' is the velocity of wave and y is its amplitude. Comparing eqn (7) & eq (8), the factor $\mu \epsilon$ has the same significance as $1/v^2$.

So we find that the variations of E and B are propagated in homogeneous, isotropic medium with a velocity given by

$$\frac{1}{v^2} = \mu \epsilon \quad \text{or} \quad v^2 = \frac{1}{\mu \epsilon}$$

$$\boxed{v = \frac{1}{\sqrt{\mu \epsilon}}} \quad \text{--- (9)}$$

where μ and ϵ are permeability and permittivity of the medium.

$$\text{for free space } v = \frac{1}{\sqrt{\mu_0 \epsilon_0}} = \frac{1}{\sqrt{4\pi \times 10^{-7} \times \frac{1}{4\pi} \times 9 \times 10^{-9}}} \quad \text{--- (9)}$$

$$v = 3 \times 10^8 \text{ m/sec.}$$

Eqs. (6) & (7) involve periodic variations of electric & magnetic fields. So they are called electromagnetic waves. In this wave Maxwell predicted the propagation of electromagnetic waves in three dimensions and prove that they travel with the velocity of light.

8

FIBER OPTICS

8.1 STEP-INDEX FIBERS

- A. Guided Rays
- B. Guided Waves
- C. Single-Mode Fibers

8.2 GRADED-INDEX FIBERS

- A. Guided Waves
- B. Propagation Constants and Velocities

8.3 ATTENUATION AND DISPERSION

- A. Attenuation
- B. Dispersion
- C. Pulse Propagation



C O R N I N G

Dramatic improvements in the development of low-loss materials for optical fibers are responsible for the commercial viability of fiber-optic communications. Corning Incorporated pioneered the development and manufacture of ultra-low-loss glass fibers.



An optical fiber is a cylindrical dielectric waveguide made of low-loss materials such as silica glass. It has a central **core** in which the light is guided, embedded in an outer **cladding** of slightly lower refractive index (Fig. 8.0-1). Light rays incident on the core-cladding boundary at angles greater than the critical angle undergo total internal reflection and are guided through the core without refraction. Rays of greater inclination to the fiber axis lose part of their power into the cladding at each reflection and are not guided.

As a result of recent technological advances in fabrication, light can be guided through 1 km of glass fiber with a loss as low as $\approx 0.16 \text{ dB} (\approx 3.6\%)$. Optical fibers are replacing copper coaxial cables as the preferred transmission medium for electromagnetic waves, thereby revolutionizing terrestrial communications. Applications range from long-distance telephone and data communications to computer communications in a local area network.

In this chapter we introduce the principles of light transmission in optical fibers. These principles are essentially the same as those that apply in planar dielectric waveguides (Chap. 7), except for the cylindrical geometry. In both types of waveguide light propagates in the form of modes. Each mode travels along the axis of the waveguide with a distinct propagation constant and group velocity, maintaining its transverse spatial distribution and its polarization. In planar waveguides, we found that each mode was the sum of the multiple reflections of a TEM wave bouncing within the slab in the direction of an optical ray at a certain bounce angle. This approach is approximately applicable to cylindrical waveguides as well. When the core diameter is small, only a single mode is permitted and the fiber is said to be a **single-mode fiber**. Fibers with large core diameters are **multimode fibers**.

One of the difficulties associated with light propagation in multimode fibers arises from the differences among the group velocities of the modes. This results in a variety of travel times so that light pulses are broadened as they travel through the fiber. This effect, called **modal dispersion**, limits the speed at which adjacent pulses can be sent without overlapping and therefore the speed at which a fiber-optic communication system can operate.

Modal dispersion can be reduced by grading the refractive index of the fiber core from a maximum value at its center to a minimum value at the core-cladding boundary. The fiber is then called a **graded-index fiber**, whereas conventional fibers

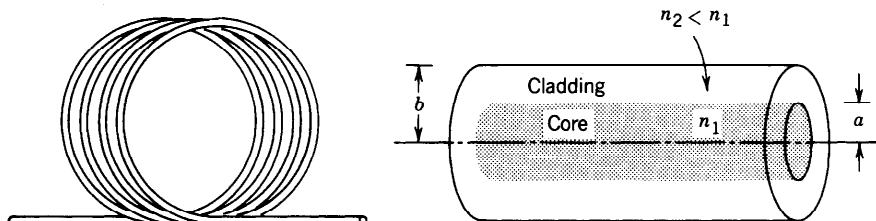


Figure 8.0-1 An optical fiber is a cylindrical dielectric waveguide.

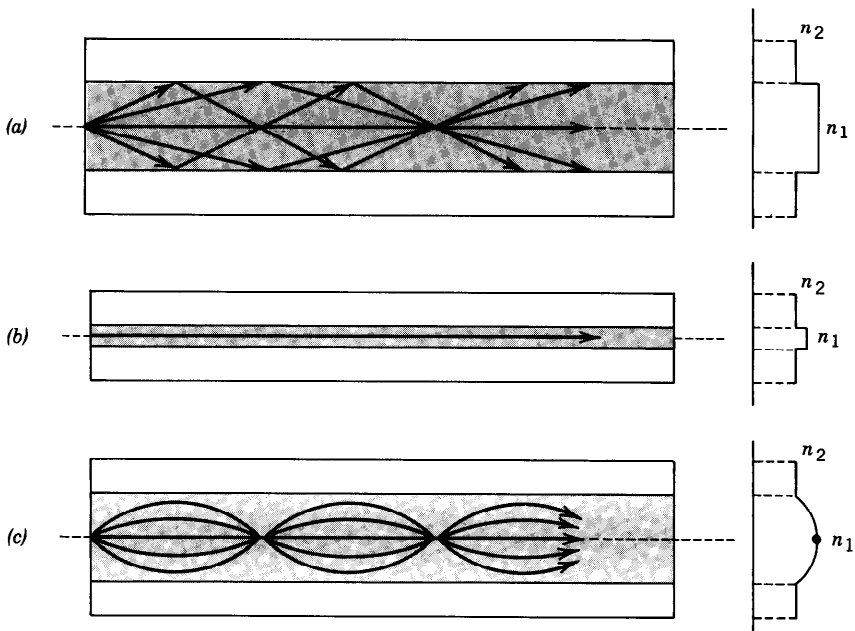


Figure 8.0-2 Geometry, refractive-index profile, and typical rays in: (a) a multimode step-index fiber, (b) a single-mode step-index fiber, and (c) a multimode graded-index fiber.

with constant refractive indices in the core and the cladding are called **step-index fibers**. In a graded-index fiber the velocity increases with distance from the core axis (since the refractive index decreases). Although rays of greater inclination to the fiber axis must travel farther, they travel faster, so that the travel times of the different rays are equalized. Optical fibers are therefore classified as step-index or graded-index, and multimode or single-mode, as illustrated in Fig. 8.0-2.

This chapter emphasizes the nature of optical modes and their group velocities in step-index and graded-index fibers. These topics are presented in Secs. 8.1 and 8.2, respectively. The optical properties of the fiber material (which is usually fused silica), including its attenuation and the effects of material, modal, and waveguide dispersion on the transmission of light pulses, are discussed in Sec. 8.3. Optical fibers are revisited in Chap. 22, which is devoted to their use in lightwave communication systems.

8.1 STEP-INDEX FIBERS

A step-index fiber is a cylindrical dielectric waveguide specified by its core and cladding refractive indices, n_1 and n_2 , and the radii a and b (see Fig. 8.0-1). Examples of standard core and cladding diameters $2a/2b$ are 8/125, 50/125, 62.5/125, 85/125, 100/140 (units of μm). The refractive indices differ only slightly, so that the fractional refractive-index change

$$\Delta = \frac{n_1 - n_2}{n_1} \quad (8.1-1)$$

is small ($\Delta \ll 1$).

Almost all fibers currently used in optical communication systems are made of fused silica glass (SiO_2) of high chemical purity. Slight changes in the refractive index are

made by the addition of low concentrations of doping materials (titanium, germanium, or boron, for example). The refractive index n_1 is in the range from 1.44 to 1.46, depending on the wavelength, and Δ typically lies between 0.001 and 0.02.

A. Guided Rays

An optical ray is guided by total internal reflections within the fiber core if its angle of incidence on the core-cladding boundary is greater than the critical angle $\theta_c = \sin^{-1}(n_2/n_1)$, and remains so as the ray bounces.

Meridional Rays

The guiding condition is simple to see for meridional rays (rays in planes passing through the fiber axis), as illustrated in Fig. 8.1-1. These rays intersect the fiber axis and reflect in the same plane without changing their angle of incidence, as if they were in a planar waveguide. Meridional rays are guided if their angle θ with the fiber axis is smaller than the complement of the critical angle $\bar{\theta}_c = \pi/2 - \theta_c = \cos^{-1}(n_2/n_1)$. Since $n_1 \approx n_2$, $\bar{\theta}_c$ is usually small and the guided rays are approximately paraxial.

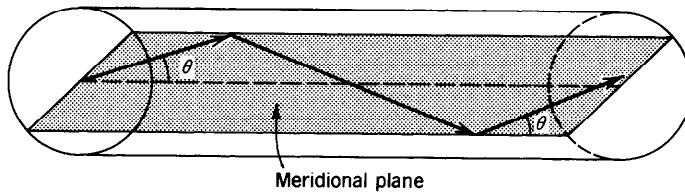


Figure 8.1-1 The trajectory of a meridional ray lies in a plane passing through the fiber axis. The ray is guided if $\theta < \bar{\theta}_c = \cos^{-1}(n_1/n_2)$.

Skewed Rays

An arbitrary ray is identified by its plane of incidence, a plane parallel to the fiber axis and passing through the ray, and by the angle with that axis, as illustrated in Fig. 8.1-2. The plane of incidence intersects the core-cladding cylindrical boundary at an angle ϕ with the normal to the boundary and lies at a distance R from the fiber axis. The ray is identified by its angle θ with the fiber axis and by the angle ϕ of its plane. When $\phi \neq 0$ ($R \neq 0$) the ray is said to be skewed. For meridional rays $\phi = 0$ and $R = 0$.

A skewed ray reflects repeatedly into planes that make the same angle ϕ with the core-cladding boundary, and follows a helical trajectory confined within a cylindrical shell of radii R and a , as illustrated in Fig. 8.1-2. The projection of the trajectory onto the transverse ($x-y$) plane is a regular polygon, not necessarily closed. It can be shown that the condition for a skewed ray to always undergo total internal reflection is that its angle θ with the z axis be smaller than $\bar{\theta}_c$.

Numerical Aperture

A ray incident from air into the fiber becomes a guided ray if upon refraction into the core it makes an angle θ with the fiber axis smaller than $\bar{\theta}_c$. Applying Snell's law at the air-core boundary, the angle θ_a in air corresponding to θ_c in the core is given by the relation $1 \cdot \sin \theta_a = n_1 \sin \theta_c$, from which (see Fig. 8.1-3 and Exercise 1.2-5) $\sin \theta_a = n_1(1 - \cos^2 \bar{\theta}_c)^{1/2} = n_1[1 - (n_2/n_1)^2]^{1/2} = (n_1^2 - n_2^2)^{1/2}$. Therefore

$$\theta_a = \sin^{-1} \text{NA}, \quad (8.1-2)$$

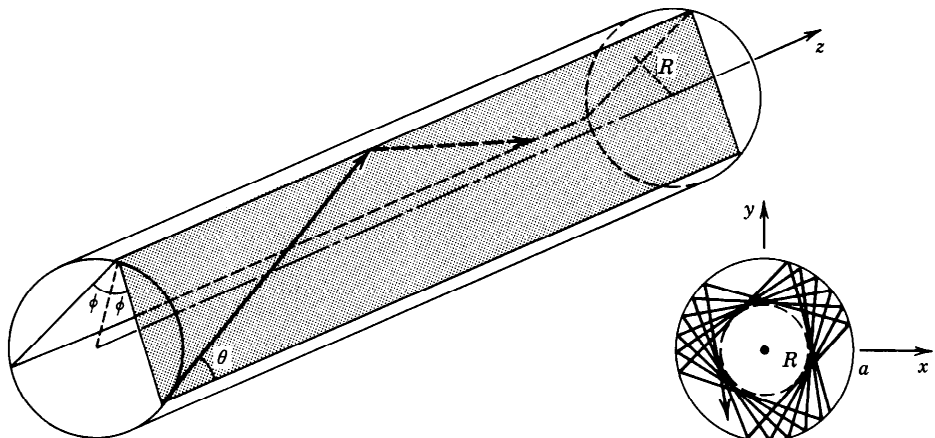


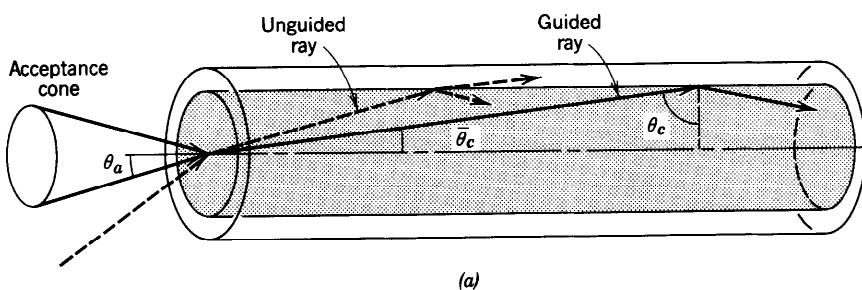
Figure 8.1-2 A skewed ray lies in a plane offset from the fiber axis by a distance R . The ray is identified by the angles θ and ϕ . It follows a helical trajectory confined within a cylindrical shell of radii R and a . The projection of the ray on the transverse plane is a regular polygon that is not necessarily closed.

where

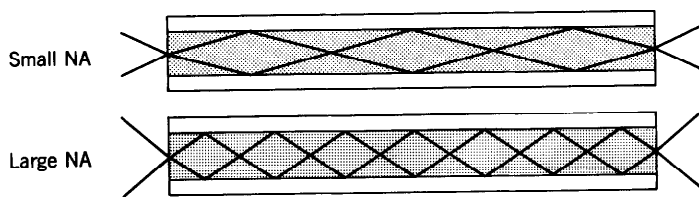
$$\text{NA} = (n_1^2 - n_2^2)^{1/2} \approx n_1(2\Delta)^{1/2} \quad (8.1-3)$$

Numerical Aperture

is the numerical aperture of the fiber. Thus θ_a is the acceptance angle of the fiber. It



(a)



(b)

Figure 8.1-3 (a) The acceptance angle θ_a of a fiber. Rays within the acceptance cone are guided by total internal reflection. The numerical aperture $\text{NA} = \sin \theta_a$. (b) The light-gathering capacity of a large NA fiber is greater than that of a small NA fiber. The angles θ_a and $\bar{\theta}_c$ are typically quite small; they are exaggerated here for clarity.

determines the cone of external rays that are guided by the fiber. Rays incident at angles greater than θ_a are refracted into the fiber but are guided only for a short distance. The numerical aperture therefore describes the light-gathering capacity of the fiber.

When the guided rays arrive at the other end of the fiber, they are refracted into a cone of angle θ_a . Thus the acceptance angle is a crucial parameter for the design of systems for coupling light into or out of the fiber.

EXAMPLE 8.1-1. Cladded and Uncladded Fibers. In a silica glass fiber with $n_1 = 1.46$ and $\Delta = (n_1 - n_2)/n_1 = 0.01$, the complementary critical angle $\bar{\theta}_c = \cos^{-1}(n_2/n_1) = 8.1^\circ$, and the acceptance angle $\theta_a = 11.9^\circ$, corresponding to a numerical aperture $NA = 0.206$. By comparison, an uncladded silica glass fiber ($n_1 = 1.46$, $n_2 = 1$) has $\bar{\theta}_c = 46.8^\circ$, $\theta_a = 90^\circ$, and $NA = 1$. Rays incident from *all* directions are guided by the uncladded fiber since they reflect within a cone of angle $\bar{\theta}_c = 46.8^\circ$ inside the core. Although its light-gathering capacity is high, the uncladded fiber is not a suitable optical waveguide because of the large number of modes it supports, as will be shown subsequently.

B. Guided Waves

In this section we examine the propagation of monochromatic light in step-index fibers using electromagnetic theory. We aim at determining the electric and magnetic fields of guided waves that satisfy Maxwell's equations and the boundary conditions imposed by the cylindrical dielectric core and cladding. As in all waveguides, there are certain special solutions, called modes (see Appendix C), each of which has a distinct propagation constant, a characteristic field distribution in the transverse plane, and two independent polarization states.

Spatial Distributions

Each of the components of the electric and magnetic fields must satisfy the Helmholtz equation, $\nabla^2 U + n^2 k_o^2 U = 0$, where $n = n_1$ in the core ($r < a$) and $n = n_2$ in the cladding ($r > a$) and $k_o = 2\pi/\lambda_o$ (see Sec. 5.3). We assume that the radius b of the cladding is sufficiently large that it can safely be assumed to be infinite when examining guided light in the core and near the core-cladding boundary. In a cylindrical coordinate system (see Fig. 8.1-4) the Helmholtz equation is

$$\frac{\partial^2 U}{\partial r^2} + \frac{1}{r} \frac{\partial U}{\partial r} + \frac{1}{r^2} \frac{\partial^2 U}{\partial \phi^2} + \frac{\partial^2 U}{\partial z^2} + n^2 k_o^2 U = 0, \quad (8.1-4)$$

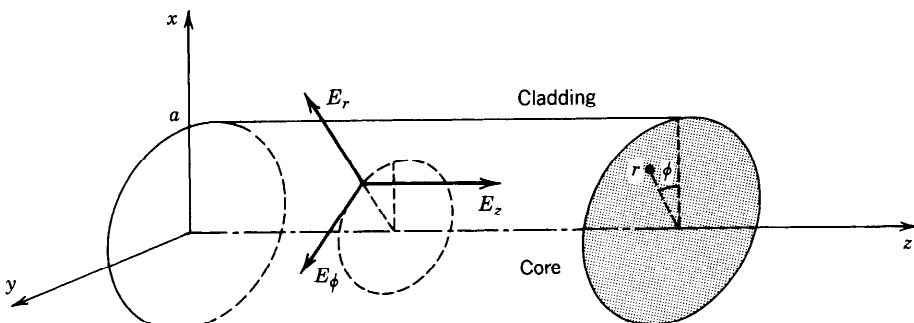


Figure 8.1-4 Cylindrical coordinate system.

278 FIBER OPTICS

where the complex amplitude $U = U(r, \phi, z)$ represents any of the Cartesian components of the electric or magnetic fields or the axial components E_z and H_z in cylindrical coordinates.

We are interested in solutions that take the form of waves traveling in the z direction with a propagation constant β , so that the z dependence of U is of the form $e^{-j\beta z}$. Since U must be a periodic function of the angle ϕ with period 2π , we assume that the dependence on ϕ is harmonic, $e^{-jl\phi}$, where l is an integer. Substituting

$$U(r, \phi, z) = u(r)e^{-jl\phi}e^{-j\beta z}, \quad l = 0, \pm 1, \pm 2, \dots, \quad (8.1-5)$$

into (8.1-4), an ordinary differential equation for $u(r)$ is obtained:

$$\frac{d^2u}{dr^2} + \frac{1}{r} \frac{du}{dr} + \left(n_1^2 k_o^2 - \beta^2 - \frac{l^2}{r^2} \right) u = 0. \quad (8.1-6)$$

As in Sec. 7.2B, the wave is guided (or bound) if the propagation constant is smaller than the wavenumber in the core ($\beta < n_1 k_o$) and greater than the wavenumber in the cladding ($\beta > n_2 k_o$). It is therefore convenient to define

$$k_T^2 = n_1^2 k_o^2 - \beta^2 \quad (8.1-7a)$$

and

$$\gamma^2 = \beta^2 - n_2^2 k_o^2, \quad (8.1-7b)$$

so that for guided waves k_T^2 and γ^2 are positive and k_T and γ are real. Equation (8.1-6) may then be written in the core and cladding separately:

$$\frac{d^2u}{dr^2} + \frac{1}{r} \frac{du}{dr} + \left(k_T^2 - \frac{l^2}{r^2} \right) u = 0, \quad r < a \text{ (core)}, \quad (8.1-8a)$$

$$\frac{d^2u}{dr^2} + \frac{1}{r} \frac{du}{dr} - \left(\gamma^2 + \frac{l^2}{r^2} \right) u = 0, \quad r > a \text{ (cladding)}. \quad (8.1-8b)$$

Equations (8.1-8) are well-known differential equations whose solutions are the family of Bessel functions. Excluding functions that approach ∞ at $r = 0$ in the core or at $r \rightarrow \infty$ in the cladding, we obtain the bounded solutions:

$$u(r) \propto \begin{cases} J_l(k_T r), & r < a \text{ (core)} \\ K_l(\gamma r), & r > a \text{ (cladding)}, \end{cases} \quad (8.1-9)$$

where $J_l(x)$ is the Bessel function of the first kind and order l , and $K_l(x)$ is the modified Bessel function of the second kind and order l . The function $J_l(x)$ oscillates like the sine or cosine functions but with a decaying amplitude. In the limit $x \gg 1$,

$$J_l(x) \approx \left(\frac{2}{\pi x} \right)^{1/2} \cos \left[x - \left(l + \frac{1}{2} \right) \frac{\pi}{2} \right], \quad x \gg 1. \quad (8.1-10a)$$

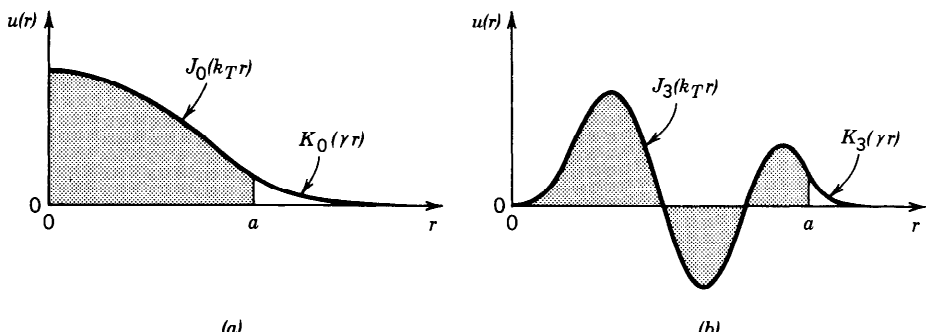


Figure 8.1-5 Examples of the radial distribution $u(r)$ given by (8.1-9) for (a) $l = 0$ and (b) $l = 3$. The shaded areas represent the fiber core and the unshaded areas the cladding. The parameters k_T and γ and the two proportionality constants in (8.1-9) have been selected such that $u(r)$ is continuous and has a continuous derivative at $r = a$. Larger values of k_T and γ lead to a greater number of oscillations in $u(r)$.

In the same limit, $K_l(x)$ decays with increasing x at an exponential rate,

$$K_l(x) \approx \left(\frac{\pi}{2x}\right)^{1/2} \left(1 + \frac{4l^2 - 1}{8x}\right) \exp(-x), \quad x \gg 1. \quad (8.1-10b)$$

Two examples of the radial distribution $u(r)$ are shown in Fig. 8.1-5.

The parameters k_T and γ determine the rate of change of $u(r)$ in the core and in the cladding, respectively. A large value of k_T means faster oscillation of the radial distribution in the core. A large value of γ means faster decay and smaller penetration of the wave into the cladding. As can be seen from (8.1-7), the sum of the squares of k_T and γ is a constant,

$$k_T^2 + \gamma^2 = (n_1^2 - n_2^2)k_o^2 = \text{NA}^2 \cdot k_o^2, \quad (8.1-11)$$

so that as k_T increases, γ decreases and the field penetrates deeper into the cladding. As k_T exceeds $\text{NA} \cdot k_o$, γ becomes imaginary and the wave ceases to be bound to the core.

The V Parameter

It is convenient to normalize k_T and γ by defining

$$X = k_T a, \quad Y = \gamma a. \quad (8.1-12)$$

In view of (8.1-11),

$$X^2 + Y^2 = V^2, \quad (8.1-13)$$

where $V = \text{NA} \cdot k_o a$, from which

$$V = 2\pi \frac{a}{\lambda_o} \text{NA}. \quad (8.1-14)$$

V Parameter

As we shall see shortly, V is an important parameter that governs the number of modes

280 FIBER OPTICS

of the fiber and their propagation constants. It is called the **fiber parameter** or **V parameter**. It is important to remember that for the wave to be guided, X must be smaller than V .

Modes

We now consider the boundary conditions. We begin by writing the axial components of the electric- and magnetic-field complex amplitudes E_z and H_z in the form of (8.1-5). The condition that these components must be continuous at the core-cladding boundary $r = a$ establishes a relation between the coefficients of proportionality in (8.1-9), so that we have only one unknown for E_z and one unknown for H_z . With the help of Maxwell's equations, $j\omega\epsilon_o n^2 \mathbf{E} = \nabla \times \mathbf{H}$ and $-j\omega\mu_o \mathbf{H} = \nabla \times \mathbf{E}$, the remaining four components E_ϕ , H_ϕ , E_r , and H_r are determined in terms of E_z and H_z . Continuity of E_ϕ and H_ϕ at $r = a$ yields two more equations. One equation relates the two unknown coefficients of proportionality in E_z and H_z ; the other equation gives a condition that the propagation constant β must satisfy. This condition, called the **characteristic equation** or **dispersion relation**, is an equation for β with the ratio a/λ_o and the fiber indices n_1, n_2 as known parameters.

For each azimuthal index l , the characteristic equation has multiple solutions yielding discrete propagation constants β_{lm} , $m = 1, 2, \dots$, each solution representing a mode. The corresponding values of k_T and γ , which govern the spatial distributions in the core and in the cladding, respectively, are determined by use of (8.1-7) and are denoted k_{Tlm} and γ_{lm} . A mode is therefore described by the indices l and m characterizing its azimuthal and radial distributions, respectively. The function $u(r)$ depends on both l and m ; $l = 0$ corresponds to meridional rays. There are two independent configurations of the \mathbf{E} and \mathbf{H} vectors for each mode, corresponding to two states of polarization. The classification and labeling of these configurations are generally quite involved (see specialized books in the reading list for more details).

Characteristic Equation for the Weakly Guiding Fiber

Most fibers are weakly guiding (i.e., $n_1 \approx n_2$ or $\Delta \ll 1$) so that the guided rays are paraxial (i.e., approximately parallel to the fiber axis). The longitudinal components of the electric and magnetic fields are then much weaker than the transverse components and the guided waves are approximately transverse electromagnetic (TEM). The linear polarization in the x and y directions then form orthogonal states of polarization. The linearly polarized (l, m) mode is usually denoted as the LP_{lm} mode. The two polarizations of mode (l, m) travel with the same propagation constant and have the same spatial distribution.

For weakly guiding fibers the characteristic equation obtained using the procedure outlined earlier turns out to be approximately equivalent to the conditions that the scalar function $u(r)$ in (8.1-9) is continuous and has a continuous derivative at $r = a$. These two conditions are satisfied if

$$\frac{(k_T a) J'_l(k_T a)}{J_l(k_T a)} = \frac{(\gamma a) K'_l(\gamma a)}{K_l(\gamma a)}. \quad (8.1-15)$$

The derivatives J'_l and K'_l of the Bessel functions satisfy the identities

$$J'_l(x) = \pm J_{l\mp 1}(x) \mp l \frac{J_l(x)}{x}$$

$$K'_l(x) = -K_{l\mp 1}(x) \mp l \frac{K_l(x)}{x}.$$

Substituting these identities into (8.1-15) and using the normalized parameters $X = k_T a$ and $Y = \gamma a$, we obtain the characteristic equation

$$X \frac{J_{l\pm 1}(X)}{J_l(X)} = \pm Y \frac{K_{l\pm 1}(Y)}{K_l(Y)}. \quad (8.1-16)$$

Characteristic
Equation

$$X^2 + Y^2 = V^2$$

Given V and l , the characteristic equation contains a single unknown variable X (since $Y^2 = V^2 - X^2$). Note that $J_{-l}(x) = (-1)^l J_l(x)$ and $K_{-l}(x) = K_l(x)$, so that if l is replaced with $-l$, the equation remains unchanged.

The characteristic equation may be solved graphically by plotting its right- and left-hand sides (RHS and LHS) versus X and finding the intersections. As illustrated in Fig. 8.1-6 for $l = 0$, the LHS has multiple branches and the RHS drops monotonically with increase of X until it vanishes at $X = V$ ($Y = 0$). There are therefore multiple intersections in the interval $0 < X \leq V$. Each intersection point corresponds to a fiber mode with a distinct value of X . These values are denoted X_{lm} , $m = 1, 2, \dots, M_l$ in order of increasing X . Once the X_{lm} are found, the corresponding transverse propagation constants k_{Tlm} , the decay parameters γ_{lm} , the propagation constants β_{lm} , and the radial distribution functions $u_{lm}(r)$ may be readily determined by use of (8.1-12), (8.1-7), and (8.1-9). The graph in Fig. 8.1-6 is similar to that in Fig. 7.2-2, which governs the modes of a planar dielectric waveguide.

Each mode has a distinct radial distribution. The radial distributions $u(r)$ shown in Fig. 8.1-5, for example, correspond to the LP₀₁ mode ($l = 0, m = 1$) in a fiber with $V = 5$; and the LP₃₄ mode ($l = 3, m = 4$) in a fiber with $V = 25$. Since the (l, m) and $(-l, m)$ modes have the same propagation constant, it is interesting to examine the spatial distribution of their superposition (with equal weights). The complex amplitude of the sum is proportional to $u_{lm}(r) \cos l\phi \exp(-j\beta_{lm}z)$. The intensity, which is proportional to $u_{lm}^2(r) \cos^2 l\phi$, is illustrated in Fig. 8.1-7 for the LP₀₁ and LP₃₄ modes (the same modes for which $u(r)$ is shown in Fig. 8.1-5).

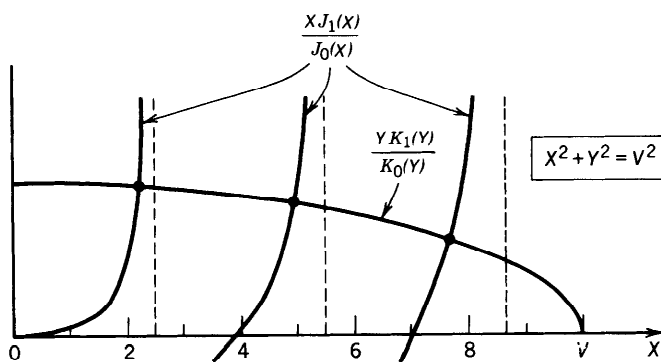


Figure 8.1-6 Graphical construction for solving the characteristic equation (8.1-16). The left- and right-hand sides are plotted as functions of X . The intersection points are the solutions. The LHS has multiple branches intersecting the abscissa at the roots of $J_{l\pm 1}(X)$. The RHS intersects each branch once and meets the abscissa at $X = V$. The number of modes therefore equals the number of roots of $J_{l\pm 1}(X)$ that are smaller than V . In this plot $l = 0$, $V = 10$, and either the $-$ or $+$ signs in (8.1-16) may be taken.

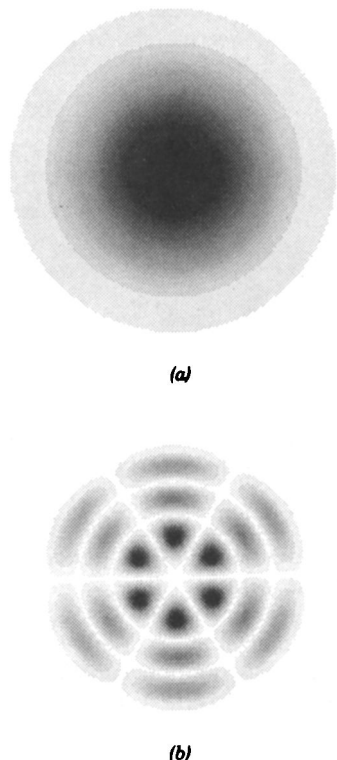


Figure 8.1-7 Distributions of the intensity of the (a) LP_{01} and (b) LP_{34} modes in the transverse plane, assuming an azimuthal $\cos l\phi$ dependence. The fundamental LP_{01} mode has a distribution similar to that of the Gaussian beam discussed in Chap. 3.

Mode Cutoff and Number of Modes

It is evident from the graphical construction in Fig. 8.1-6 that as V increases, the number of intersections (modes) increases since the LHS of the characteristic equation (8.1-16) is independent of V , whereas the RHS moves to the right as V increases. Considering the minus signs in the characteristic equation, branches of the LHS intersect the abscissa when $J_{l-1}(X) = 0$. These roots are denoted by x_{lm} , $m = 1, 2, \dots$. The number of modes M_l is therefore equal to the number of roots of $J_{l-1}(X)$ that are smaller than V . The (l, m) mode is allowed if $V > x_{lm}$. The mode reaches its cutoff point when $V = x_{lm}$. As V decreases further, the $(l, m - 1)$ mode also reaches its cutoff point when a new root is reached, and so on. The smallest root of $J_{l-1}(X)$ is $x_{01} = 0$ for $l = 0$ and the next smallest is $x_{11} = 2.405$ for $l = 1$. When $V < 2.405$, all modes with the exception of the fundamental LP_{01} mode are cut off. The fiber then operates as a single-mode waveguide. A plot of the number of modes M_l as a function of V is therefore a staircase function increasing by unity at each of the roots x_{lm} of the Bessel function $J_{l-1}(X)$. Some of these roots are listed in Table 8.1-1.

TABLE 8.1-1 Cutoff V Parameter for the LP_{0m} and LP_{1m} Modes^a

l	$m:$	1	2	3
0		0	3.832	7.016
1		2.405	5.520	8.654

^aThe cutoffs of the $l = 0$ modes occur at the roots of $J_{-1}(X) = -J_1(X)$. The $l = 1$ modes are cut off at the roots of $J_0(X)$, and so on.

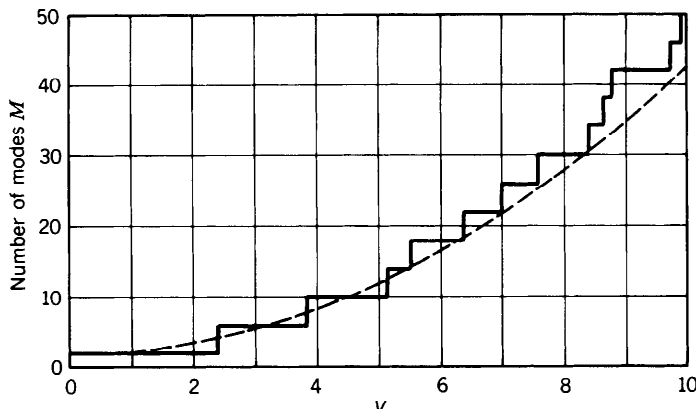


Figure 8.1-8 Total number of modes M versus the fiber parameter $V = 2\pi(a/\lambda_o)\text{NA}$. Included in the count are two helical polarities for each mode with $l > 0$ and two polarizations per mode. For $V < 2.405$, there is only one mode, the fundamental LP₀₁ mode with two polarizations. The dashed curve is the relation $M = 4V^2/\pi^2 + 2$, which provides an approximate formula for the number of modes when $V \gg 1$.

A composite count of the total number of modes M (for all l) is shown in Fig. 8.1-8 as a function of V . This is a staircase function with jumps at the roots of $J_{l-1}(X)$. Each root must be counted twice since for each mode of azimuthal index $l > 0$ there is a corresponding mode $-l$ that is identical except for an opposite polarity of the angle ϕ (corresponding to rays with helical trajectories of opposite senses) as can be seen by using the plus signs in the characteristic equation. In addition, each mode has two states of polarization and must therefore be counted twice.

Number of Modes (Fibers with Large V Parameter)

For fibers with large V parameters, there are a large number of roots of $J_l(X)$ in the interval $0 < X < V$. Since $J_l(X)$ is approximated by the sinusoidal function in (8.1-10a) when $X \gg 1$, its roots x_{lm} are approximately given by $x_{lm} - (l + \frac{1}{2})(\pi/2) = (2m - 1)(\pi/2)$, i.e., $x_{lm} = (l + 2m - \frac{1}{2})\pi/2$, so that the cutoff points of modes (l, m) , which are the roots of $J_{l\pm 1}(X)$, are

$$x_{lm} \approx \left(l + 2m - \frac{1}{2} \pm 1\right) \frac{\pi}{2} \approx (l + 2m) \frac{\pi}{2}, \quad l = 0, 1, \dots; \quad m \gg 1, \quad (8.1-17)$$

when m is large.

For a fixed l , these roots are spaced uniformly at a distance π , so that the number of roots M_l satisfies $(l + 2M_l)\pi/2 = V$, from which $M_l \approx V/\pi - l/2$. Thus M_l drops linearly with increasing l , beginning with $M_l \approx V/\pi$ for $l = 0$ and ending at $M_l = 0$ when $l = l_{\max}$, where $l_{\max} = 2V/\pi$, as illustrated in Fig. 8.1-9. Thus the total number of modes is $M \approx \sum_{l=0}^{l_{\max}} M_l = \sum_{l=0}^{l_{\max}} (V/\pi - l/2)$.

Since the number of terms in this sum is assumed large, it may be readily evaluated by approximating it as the area of the triangle in Fig. 8.1-9, $M \approx \frac{1}{2}(2V/\pi)(V/\pi) = V^2/\pi^2$. Allowing for two degrees of freedom for positive and negative l and two polarizations for each index (l, m) , we obtain

$$M \approx \frac{4}{\pi^2} V^2.$$

(8.1-18)

Number of Modes
($V \gg 1$)

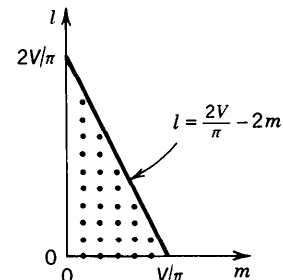


Figure 8.1-9 The indices of guided modes extend from $m = 1$ to $m \approx V/\pi - l/2$ and from $l = 0$ to $\approx 2V/\pi$.

This expression for M is analogous to that for the rectangular waveguide (7.3-3). Note that (8.1-18) is valid only for large V . This approximate number is compared to the exact number obtained from the characteristic equation in Fig. 8.1-8.

EXAMPLE 8.1-2. Approximate Number of Modes. A silica fiber with $n_1 = 1.452$ and $\Delta = 0.01$ has a numerical aperture $\text{NA} = (n_1^2 - n_2^2)^{1/2} \approx n_1(2\Delta)^{1/2} \approx 0.205$. If $\lambda_o = 0.85 \mu\text{m}$ and the core radius $a = 25 \mu\text{m}$, the V parameter is $V = 2\pi(a/\lambda_o)\text{NA} \approx 37.9$. There are therefore approximately $M \approx 4V^2/\pi^2 \approx 585$ modes. If the cladding is stripped away so that the core is in direct contact with air, $n_2 = 1$ and $\text{NA} = 1$. The V parameter is then $V = 184.8$ and more than 13,800 modes are allowed.

Propagation Constants (Fibers with Large V Parameter)

As mentioned earlier, the propagation constants can be determined by solving the characteristic equation (8.1-16) for the X_{lm} and using (8.1-7a) and (8.1-12) to obtain $\beta_{lm} = (n_1^2 k_o^2 - X_{lm}^2/a^2)^{1/2}$. A number of approximate formulas for X_{lm} applicable in certain limits are available in the literature, but there are no explicit exact formulas.

If $V \gg 1$, the crudest approximation is to assume that the X_{lm} are equal to the cutoff values x_{lm} . This is equivalent to assuming that the branches in Fig. 8.1-6 are approximately vertical lines, so that $X_{lm} \approx x_{lm}$. Since $V \gg 1$, the majority of the roots would be large and the approximation in (8.1-17) may be used to obtain

$$\beta_{lm} \approx \left[n_1^2 k_o^2 - (l + 2m)^2 \frac{\pi^2}{4a^2} \right]^{1/2}. \quad (8.1-19)$$

Since

$$M \approx \frac{4}{\pi^2} V^2 = \frac{4}{\pi^2} \text{NA}^2 \cdot a^2 k_o^2 \approx \frac{4}{\pi^2} (2n_1^2 \Delta) k_o^2 a^2, \quad (8.1-20)$$

(8.1-19) and (8.1-20) give

$$\beta_{lm} \approx n_1 k_o \left[1 - 2 \frac{(l + 2m)^2}{M} \Delta \right]^{1/2}. \quad (8.1-21)$$

Because Δ is small we use the approximation $(1 + \delta)^{1/2} \approx 1 + \delta/2$ for $|\delta| \ll 1$, and

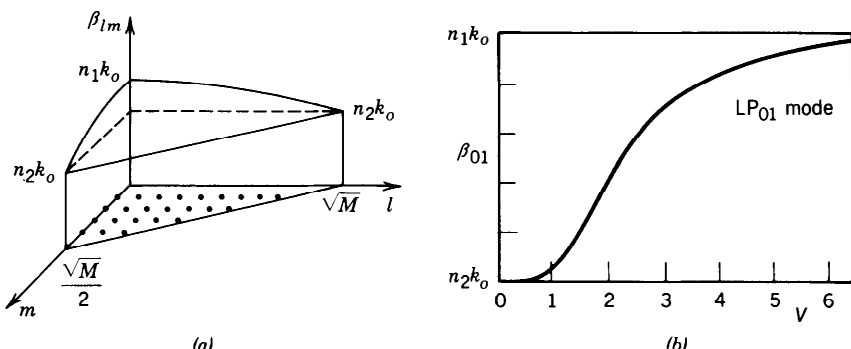


Figure 8.1-10 (a) Approximate propagation constants β_{lm} of the modes of a fiber with large V parameter as functions of the mode indices l and m . (b) Exact propagation constant β_{01} of the fundamental LP_{01} modes as a function of the V parameter. For $V \gg 1$, $\beta_{01} \approx n_1 k_o$.

obtain

$$\beta_{lm} \approx n_1 k_o \left[1 - \frac{(l + 2m)^2}{M} \Delta \right]. \quad (8.1-22)$$

Propagation Constants

$$l = 0, 1, \dots, \sqrt{M}$$

$$m = 1, 2, \dots, (\sqrt{M} - l)/2$$

$$(V \gg 1)$$

Since $l + 2m$ varies between 2 and $\approx 2V/\pi = \sqrt{M}$ (see Fig. 8.1-9), β_{lm} varies approximately between $n_1 k_o$ and $n_1 k_o(1 - \Delta) \approx n_2 k_o$, as illustrated in Fig. 8.1-10.

Group Velocities (Fibers with Large V Parameter)

To determine the group velocity, $v_{lm} = d\omega/d\beta_{lm}$, of the (l, m) mode we express β_{lm} as an explicit function of ω by substituting $n_1 k_o = \omega/c_1$ and $M = (4/\pi^2)(2n_1^2 \Delta) k_o^2 a^2 = (8/\pi^2) a^2 \omega^2 \Delta / c_1^2$ into (8.1-22) and assume that c_1 and Δ are independent of ω . The derivative $d\omega/d\beta_{lm}$ gives

$$v_{lm} \approx c_1 \left[1 + \frac{(l + 2m)^2}{M} \Delta \right]^{-1}.$$

Since $\Delta \ll 1$, the approximate expansion $(1 + \delta)^{-1} \approx 1 - \delta$ when $|\delta| \ll 1$, gives

$$v_{lm} \approx c_1 \left[1 - \frac{(l + 2m)^2}{M} \Delta \right].$$

$$(8.1-23)$$

Group Velocities
($V \gg 1$)

Because the minimum and maximum values of $(l + 2m)$ are 2 and \sqrt{M} , respectively, and since $M \gg 1$, the group velocity varies approximately between c_1 and $c_1(1 - \Delta) = c_1(n_2/n_1)$. Thus the group velocities of the low-order modes are approximately equal to the phase velocity of the core material, and those of the high-order modes are smaller.

The fractional group-velocity change between the fastest and the slowest mode is roughly equal to Δ , the fractional refractive index change of the fiber. Fibers with large Δ , although endowed with a large NA and therefore large light-gathering capacity, also have a large number of modes, large modal dispersion, and consequently high pulse spreading rates. These effects are particularly severe if the cladding is removed altogether.

C. Single-Mode Fibers

As discussed earlier, a fiber with core radius a and numerical aperture NA operates as a single-mode fiber in the fundamental LP₀₁ mode if $V = 2\pi(a/\lambda_o)NA < 2.405$ (see Table 8.1-1 on page 282). Single-mode operation is therefore achieved by using a small core diameter and small numerical aperture (making n_2 close to n_1), or by operating at a sufficiently long wavelength. The fundamental mode has a bell-shaped spatial distribution similar to the Gaussian distribution [see Figs. 8.1-5(a) and 8.1-7(a)] and a propagation constant β that depends on V as illustrated in Fig. 8.1-10(b). This mode provides the highest confinement of light power within the core.

EXAMPLE 8.1-3. Single-Mode Operation. A silica glass fiber with $n_1 = 1.447$ and $\Delta = 0.01$ (NA = 0.205) operates at $\lambda_o = 1.3 \mu\text{m}$ as a single-mode fiber if $V = 2\pi(a/\lambda_o)NA < 2.405$, i.e., if the core diameter $2a < 4.86 \mu\text{m}$. If Δ is reduced to 0.0025, single-mode operation requires a diameter $2a < 9.72 \mu\text{m}$.

There are numerous advantages of using single-mode fibers in optical communication systems. As explained earlier, the modes of a multimode fiber travel at different group velocities and therefore undergo different time delays, so that a short-duration pulse of multimode light is delayed by different amounts and therefore spreads in time. Quantitative measures of modal dispersion are determined in Sec. 8.3B. In a single-mode fiber, on the other hand, there is only one mode with one group velocity, so that a short pulse of light arrives without delay distortion. As explained in Sec. 8.3B, other dispersion effects result in pulse spreading in single-mode fibers, but these are significantly smaller than modal dispersion.

As also shown in Sec. 8.3, the rate of power attenuation is lower in a single-mode fiber than in a multimode fiber. This, together with the smaller pulse spreading rate, permits substantially higher data rates to be transmitted by single-mode fibers in comparison with the maximum rates feasible with multimode fibers. This topic is discussed in Chap. 22.

Another difficulty with multimode fibers is caused by the random interference of the modes. As a result of uncontrollable imperfections, strains, and temperature fluctuations, each mode undergoes a random phase shift so that the sum of the complex amplitudes of the modes has a random intensity. This randomness is a form of noise known as **modal noise** or **speckle**. This effect is similar to the fading of radio signals due to multiple-path transmission. In a single-mode fiber there is only one path and therefore no modal noise.

Because of their small size and small numerical apertures, single-mode fibers are more compatible with integrated-optics technology. However, such features make them more difficult to manufacture and work with because of the reduced allowable mechanical tolerances for splicing or joining with demountable connectors and for coupling optical power into the fiber.

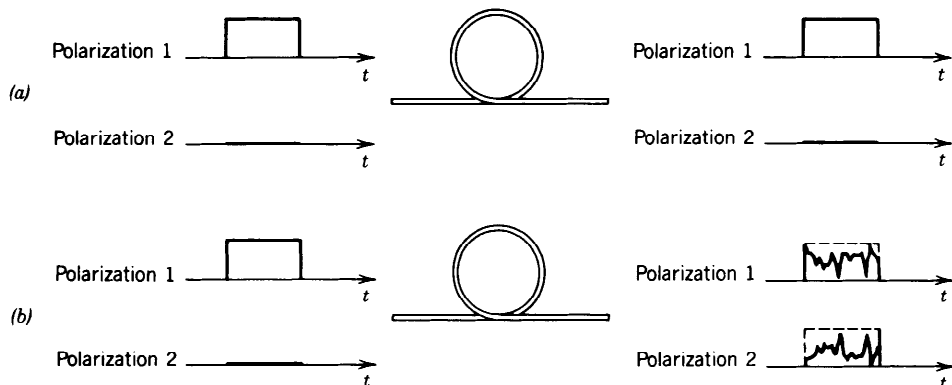


Figure 8.1-11 (a) Ideal polarization-maintaining fiber. (b) Random transfer of power between two polarizations.

Polarization-Maintaining Fibers

In a fiber with circular cross section, each mode has two independent states of polarization with the same propagation constant. Thus the fundamental LP_{01} mode in a single-mode weakly guiding fiber may be polarized in the x or y direction with the two orthogonal polarizations having the same propagation constant and the same group velocity.

In principle, there is no exchange of power between the two polarization components. If the power of the light source is delivered into one polarization only, the power received remains in that polarization. In practice, however, slight random imperfections or uncontrollable strains in the fiber result in random power transfer between the two polarizations. This coupling is facilitated since the two polarizations have the same propagation constant and their phases are therefore matched. Thus linearly polarized light at the fiber input is transformed into elliptically polarized light at the output. As a result of fluctuations of strain, temperature, or source wavelength, the ellipticity of the received light fluctuates randomly with time. Nevertheless, the total power remains fixed (Fig. 8.1-11). If we are interested only in transmitting light power, this randomization of the power division between the two polarization components poses no difficulty, provided that the total power is collected.

In many areas related to fiber optics, e.g., coherent optical communications, integrated-optic devices, and optical sensors based on interferometric techniques, the fiber is used to transmit the complex amplitude of a specific polarization (magnitude and phase). For these applications, polarization-maintaining fibers are necessary. To make a polarization-maintaining fiber the circular symmetry of the conventional fiber must be removed, by using fibers with elliptical cross sections or stress-induced anisotropy of the refractive index, for example. This eliminates the polarization degeneracy, i.e., makes the propagation constants of the two polarizations different. The coupling efficiency is then reduced as a result of the introduction of phase mismatch.

8.2 GRADED-INDEX FIBERS

Index grading is an ingenious method for reducing the pulse spreading caused by the differences in the group velocities of the modes of a multimode fiber. The core of a graded-index fiber has a varying refractive index, highest in the center and decreasing gradually to its lowest value at the cladding. The phase velocity of light is therefore minimum at the center and increases gradually with the radial distance. Rays of the

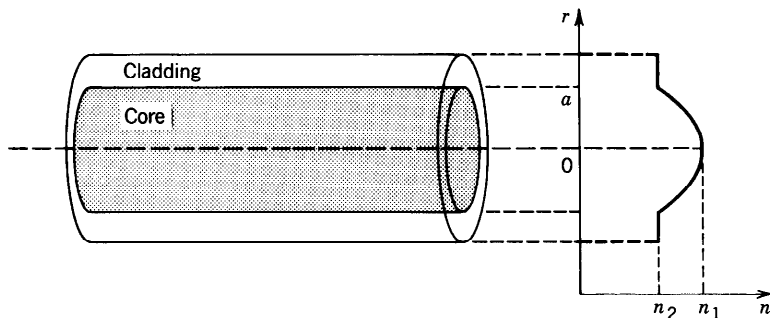


Figure 8.2-1 Geometry and refractive-index profile of a graded-index fiber.

most axial mode travel the shortest distance at the smallest phase velocity. Rays of the most oblique mode zigzag at a greater angle and travel a longer distance, mostly in a medium where the phase velocity is high. Thus the disparities in distances are compensated by opposite disparities in phase velocities. As a consequence, the differences in the group velocities and the travel times are expected to be reduced. In this section we examine the propagation of light in graded-index fibers.

The core refractive index is a function $n(r)$ of the radial position r and the cladding refractive index is a constant n_2 . The highest value of $n(r)$ is $n(0) = n_1$ and the lowest value occurs at the core radius $r = a$, $n(a) = n_2$, as illustrated in Fig. 8.2-1.

A versatile refractive-index profile is the power-law function

$$n^2(r) = n_1^2 \left[1 - 2 \left(\frac{r}{a} \right)^p \Delta \right], \quad r \leq a, \quad (8.2-1)$$

where

$$\Delta = \frac{n_1^2 - n_2^2}{2n_1^2} \approx \frac{n_1 - n_2}{n_1}, \quad (8.2-2)$$

and p , called the **grade profile parameter**, determines the steepness of the profile. This function drops from n_1 at $r = 0$ to n_2 at $r = a$. For $p = 1$, $n^2(r)$ is linear, and for $p = 2$ it is quadratic. As $p \rightarrow \infty$, $n^2(r)$ approaches a step function, as illustrated in Fig. 8.2-2. Thus the step-index fiber is a special case of the graded-index fiber with $p = \infty$.

Guided Rays

The transmission of light rays in a graded-index medium with parabolic-index profile was discussed in Sec. 1.3. Rays in meridional planes follow oscillatory planar trajec-

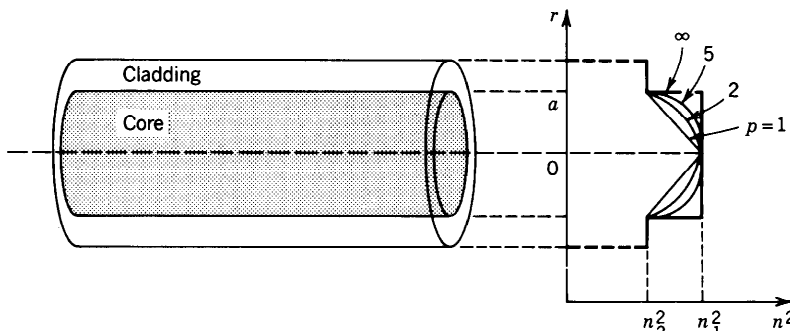


Figure 8.2-2 Power-law refractive-index profile $n^2(r)$ for different values of p .

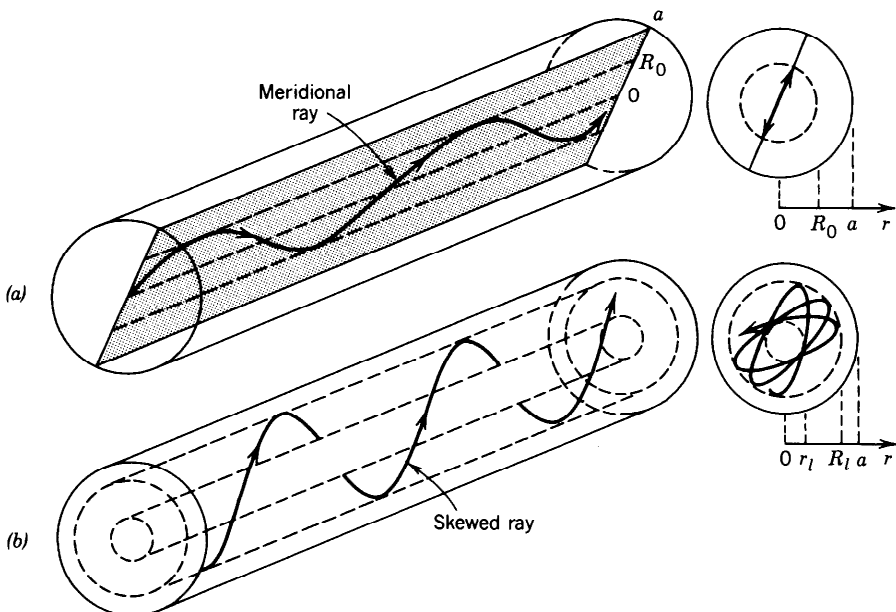


Figure 8.2-3 Guided rays in the core of a graded-index fiber. (a) A meridional ray confined to a meridional plane inside a cylinder of radius R_0 . (b) A skewed ray follows a helical trajectory confined within two cylindrical shells of radii r_i and R_i .

ries, whereas skewed rays follow helical trajectories with the turning points forming cylindrical caustic surfaces, as illustrated in Fig. 8.2-3. Guided rays are confined within the core and do not reach the cladding.

A. Guided Waves

The modes of the graded-index fiber may be determined by writing the Helmholtz equation (8.1-4) with $n = n(r)$, solving for the spatial distributions of the field components, and using Maxwell's equations and the boundary conditions to obtain the characteristic equation as was done in the step-index case. This procedure is in general difficult.

In this section we use instead an approximate approach based on picturing the field distribution as a quasi-plane wave traveling within the core, approximately along the trajectory of the optical ray. A quasi-plane wave is a wave that is locally identical to a plane wave, but changes its direction and amplitude slowly as it travels. This approach permits us to maintain the simplicity of rays optics but retain the phase associated with the wave, so that we can use the self-consistency condition to determine the propagation constants of the guided modes (as was done in the planar waveguide in Sec. 7.2). This approximate technique, called the WKB (Wentzel–Kramers–Brillouin) method, is applicable only to fibers with a large number of modes (large V parameter).

Quasi-Plane Waves

Consider a solution of the Helmholtz equation (8.1-4) in the form of a quasi-plane wave (see Sec. 2.3)

$$U(\mathbf{r}) = \alpha(\mathbf{r}) \exp[-jk_o S(\mathbf{r})], \quad (8.2-3)$$

where $\alpha(\mathbf{r})$ and $S(\mathbf{r})$ are real functions of position that are slowly varying in comparison with the wavelength $\lambda_o = 2\pi/k_o$. We know from Sec. 2.3 that $S(\mathbf{r})$ approximately

290 FIBER OPTICS

satisfies the eikonal equation $|\nabla S|^2 \approx n^2$, and that the rays travel in the direction of the gradient ∇S . If we take $k_o S(\mathbf{r}) = k_o s(r) + l\phi + \beta z$, where $s(r)$ is a slowly varying function of r , the eikonal equation gives

$$\left(k_o \frac{ds}{dr} \right)^2 + \beta^2 + \frac{l^2}{r^2} = n^2(r) k_o^2. \quad (8.2-4)$$

The local spatial frequency of the wave in the radial direction is the partial derivative of the phase $k_o S(\mathbf{r})$ with respect to r ,

$$k_r = k_o \frac{ds}{dr}, \quad (8.2-5)$$

so that (8.2-3) becomes

$$U(r) = \alpha(r) \exp\left(-j \int_0^r k_r dr\right) e^{-jl\phi} e^{-j\beta z}, \quad (8.2-6)$$

Quasi-Plane Wave

and (8.2-4) gives

$$k_r^2 = n^2(r) k_o^2 - \beta^2 - \frac{l^2}{r^2}. \quad (8.2-7)$$

Defining $k_\phi = l/r$, i.e., $\exp(-jl\phi) = \exp(-jk_\phi r\phi)$, and $k_z = \beta$, we find that (8.2-7) gives $k_r^2 + k_\phi^2 + k_z^2 = n^2(r) k_o^2$. The quasi-plane wave therefore has a local wavevector \mathbf{k} with magnitude $n(r)k_o$ and cylindrical-coordinate components (k_r, k_ϕ, k_z) . Since $n(r)$ and k_ϕ are functions of r , k_r is also generally position dependent. The direction of \mathbf{k} changes slowly with r (see Fig. 8.2-4) following a helical trajectory similar to that of the skewed ray shown earlier in Fig. 8.2-3(b).

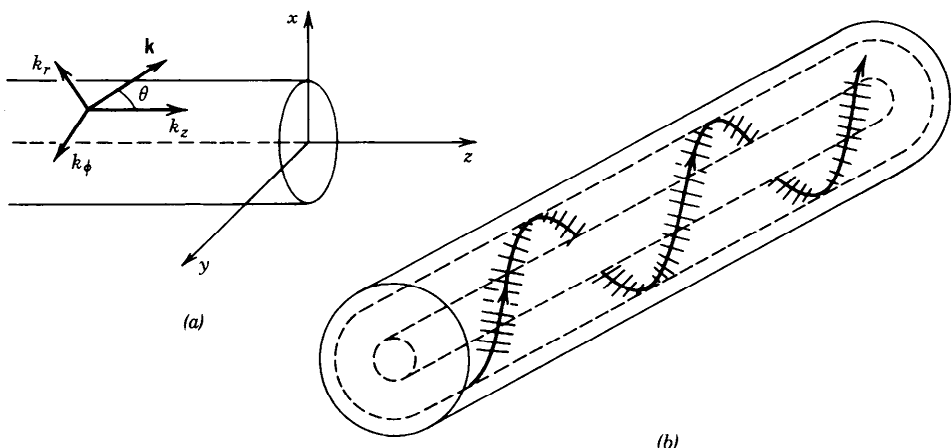


Figure 8.2-4 (a) The wavevector $\mathbf{k} = (k_r, k_\phi, k_z)$ in a cylindrical coordinate system. (b) Quasi-plane wave following the direction of a ray.

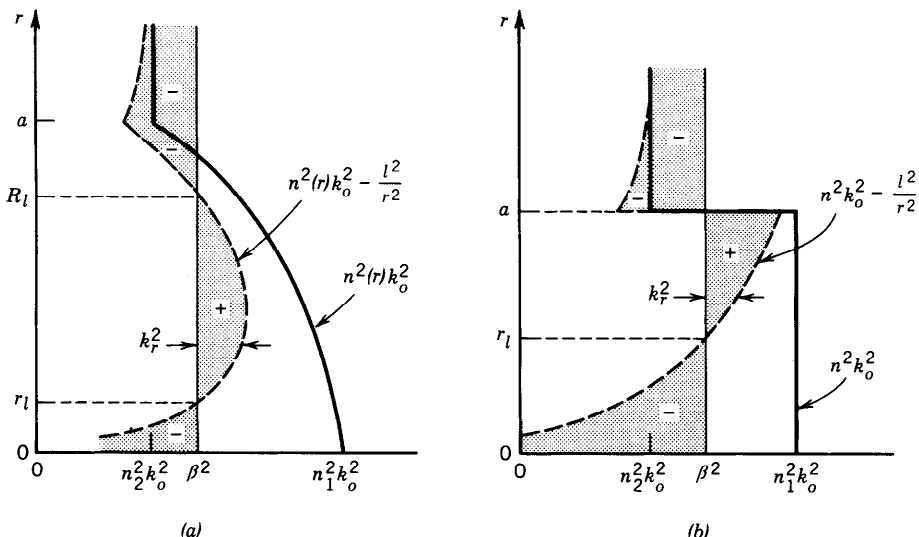


Figure 8.2-5 Dependence of $n^2(r)k_o^2$, $n^2(r)k_o^2 - l^2/r^2$, and $k_r^2 = n^2(r)k_o^2 - l^2/r^2 - \beta^2$ on the position r . At any r , k_r^2 is the width of the shaded area with the + and - signs denoting positive and negative k_r^2 . (a) Graded-index fiber; k_r^2 is positive in the region $r_l < r < R_l$. (b) Step-index fiber; k_r^2 is positive in the region $r_l < r < a$.

To determine the region of the core within which the wave is bound, we determine the values of r for which k_r is real, or $k_r^2 > 0$. For a given l and β we plot $k_r^2 = [n^2(r)k_o^2 - l^2/r^2 - \beta^2]$ as a function of r . The term $n^2(r)k_o^2$ is first plotted as a function of r [the thick continuous curve in Fig. 8.2-5(a)]. The term l^2/r^2 is then subtracted, yielding the dashed curve. The value of β^2 is marked by the thin continuous vertical line. It follows that k_r^2 is represented by the difference between the dashed line and the thin continuous line, i.e., by the shaded area. Regions where k_r^2 is positive or negative are indicated by the + or - signs, respectively. Thus k_r is real in the region $r_l < r < R_l$, where

$$n^2(r)k_o^2 - \frac{l^2}{r^2} - \beta^2 = 0, \quad r = r_l \quad \text{and} \quad r = R_l. \quad (8.2-8)$$

It follows that the wave is basically confined within a cylindrical shell of radii r_l and R_l just like the helical ray trajectory shown in Fig. 8.2-3(b).

These results are also applicable to the step-index fiber in which $n(r) = n_1$ for $r < a$, and $n(r) = n_2$ for $r > a$. In this case the quasi-plane wave is guided in the core by reflecting from the core-cladding boundary at $r = a$. As illustrated in Fig. 8.2-5(b), the region of confinement is $r_l < r < a$, where

$$n_1^2 k_o^2 - \frac{l^2}{r_l^2} - \beta^2 = 0. \quad (8.2-9)$$

The wave bounces back and forth helically like the skewed ray shown in Fig. 8.1-2. In the cladding ($r > a$) and near the center of the core ($r < r_l$), k_r^2 is negative so that k_r is imaginary, and the wave therefore decays exponentially. Note that r_l depends on β . For large β (or large l), r_l is large; i.e., the wave is confined to a thin cylindrical shell near the edge of the core.

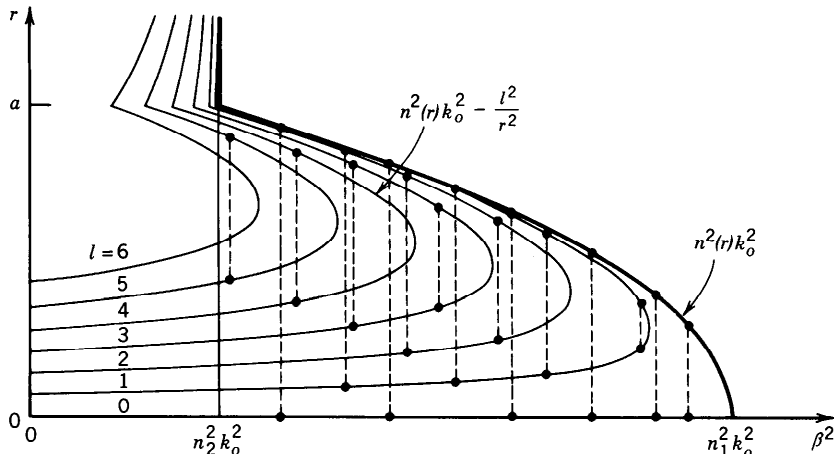


Figure 8.2-6 The propagation constants and confinement regions of the fiber modes. Each curve corresponds to an index l . In this plot $l = 0, 1, \dots, 6$. Each mode (representing a certain value of m) is marked schematically by two dots connected by a dashed vertical line. The ordinates of the dots mark the radii r_l and R_l of the cylindrical shell within which the mode is confined. Values on the abscissa are the squared propagation constants β^2 of the mode.

Modes

The modes of the fiber are determined by imposing the self-consistency condition that the wave reproduce itself after one helical period of traveling between r_l and R_l and back. The azimuthal path length corresponding to an angle 2π must correspond to a multiple of 2π phase shift, i.e., $k_\phi 2\pi r = 2\pi l$; $l = 0, \pm 1, \pm 2, \dots$. This condition is evidently satisfied since $k_\phi = l/r$. In addition, the radial round-trip path length must correspond to a phase shift equal to an integer multiple of 2π ,

$$2 \int_{r_l}^{R_l} k_r dr = 2\pi m, \quad m = 1, 2, \dots, M_l. \quad (8.2-10)$$

This condition, which is analogous to the self-consistency condition (7.2-2) for planar waveguides, provides the characteristic equation from which the propagation constants β_{lm} of the modes are determined. These values are marked schematically in Fig. 8.2-6; the mode $m = 1$ has the largest value of β (approximately $n_1 k_o$) and $m = M_l$ has the smallest value (approximately $n_2 k_o$).

Number of Modes

The total number of modes can be determined by adding the number of modes M_l for $l = 0, 1, \dots, l_{\max}$. We shall address this problem using a different procedure. We first determine the number q_β of modes with propagation constants greater than a given value β . For each l , the number of modes $M_l(\beta)$ with propagation constant greater than β is the number of multiples of 2π the integral in (8.2-10) yields, i.e.,

$$M_l(\beta) = \frac{1}{\pi} \int_{r_l}^{R_l} k_r dr = \frac{1}{\pi} \int_{r_l}^{R_l} \left[n^2(r) k_o^2 - \frac{l^2}{r^2} - \beta^2 \right]^{1/2} dr, \quad (8.2-11)$$

where r_l and R_l are the radii of confinement corresponding to the propagation constant β as given by (8.2-8). Clearly, r_l and R_l depend on β .

The total number of modes with propagation constant greater than β is therefore

$$q_\beta = 4 \sum_{l=0}^{l_{\max}(\beta)} M_l(\beta), \quad (8.2-12)$$

where $l_{\max}(\beta)$ is the maximum value of l that yields a bound mode with propagation constants greater than β , i.e., for which the peak value of the function $n^2(r)k_o^2 - l^2/r^2$ is greater than β^2 . The grand total number of modes M is q_β for $\beta = n_2 k_o$. The factor of 4 in (8.2-12) accounts for the two possible polarizations and the two possible polarities of the angle ϕ , corresponding to positive or negative helical trajectories for each (l, m) . If the number of modes is sufficiently large, we can replace the summation in (8.2-12) by an integral,

$$q_\beta \approx 4 \int_0^{l_{\max}(\beta)} M_l(\beta) dl. \quad (8.2-13)$$

For fibers with a power-law refractive-index profile, we substitute (8.2-1) into (8.2-11), and the result into (8.2-13), and evaluate the integral to obtain

$$q_\beta \approx M \left[\frac{1 - (\beta/n_1 k_o)^2}{2\Delta} \right]^{(p+2)/p}, \quad (8.2-14)$$

where

$$M \approx \frac{p}{p+2} n_1^2 k_o^2 a^2 \Delta = \frac{p}{p+2} \frac{V^2}{2}. \quad (8.2-15)$$

Here $\Delta = (n_1 - n_2)/n_1$ and $V = 2\pi(a/\lambda_o)NA$ is the fiber V parameter. Since $q_\beta \approx M$ at $\beta = n_2 k_o$, M is indeed the total number of modes.

For step-index fibers ($p = \infty$),

$$q_\beta \approx M \left[\frac{1 - (\beta/n_1 k_o)^2}{2\Delta} \right] \quad (8.2-16)$$

and

$$M \approx \frac{V^2}{2}.$$

$(8.2-17)$

Number of Modes
 (Step-Index Fiber)
 $V = 2\pi(a/\lambda_o)NA$

This expression for M is nearly the same as $M \approx 4V^2/\pi^2 \approx 0.41V^2$ in (8.1-18), which was obtained in Sec. 8.1 using a different approximation.

B. Propagation Constants and Velocities

Propagation Constants

The propagation constant β_q of mode q is obtained by inverting (8.2-14),

$$\beta_q \approx n_1 k_o \left[1 - 2 \left(\frac{q}{M} \right)^{p/(p+2)} \Delta \right]^{1/2}, \quad q = 1, 2, \dots, M, \quad (8.2-18)$$

where the index q_β has been replaced by q , and β replaced by β_q . Since $\Delta \ll 1$, the approximation $(1 + \delta)^{1/2} \approx 1 + \frac{1}{2}\delta$ (when $|\delta| \ll 1$) can be applied to (8.2-18), yielding

$$\boxed{\beta_q \approx n_1 k_o \left[1 - \left(\frac{q}{M} \right)^{p/(p+2)} \Delta \right].} \quad (8.2-19)$$

Propagation Constants
 $q = 1, 2, \dots, M$

The propagation constant β_q therefore decreases from $\approx n_1 k_o$ (at $q = 1$) to $n_2 k_o$ (at $q = M$), as illustrated in Fig. 8.2-7.

In the step-index fiber ($p = \infty$),

$$\boxed{\beta_q \approx n_1 k_o \left(1 - \frac{q}{M} \Delta \right).} \quad (8.2-20)$$

Propagation Constants
(Step-Index Fiber)
 $q = 1, 2, \dots, M$

This expression is identical to (8.1-22) if the index $q = 1, 2, \dots, M$ is replaced by $(l + 2m)^2$, where $l = 0, 1, \dots, \sqrt{M}$; $m = 1, 2, \dots, \sqrt{M}/2 - l/2$.

Group Velocities

To determine the group velocity $v_g = d\omega/d\beta_q$, we write β_q as a function of ω by substituting (8.2-15) into (8.2-19), substituting $n_1 k_o = \omega/c_1$ into the result, and evaluating $v_g = (d\beta_q/d\omega)^{-1}$. With the help of the approximation $(1 + \delta)^{-1} \approx 1 - \delta$ when

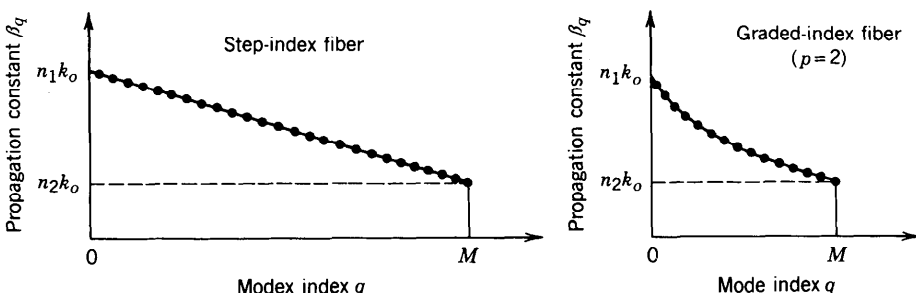


Figure 8.2-7 Dependence of the propagation constants β_q on the mode index $q = 1, 2, \dots, M$.

$|\delta| \ll 1$, and assuming that c_1 and Δ are independent of ω (i.e., ignoring material dispersion), we obtain

$$v_q \approx c_1 \left[1 - \frac{p-2}{p+2} \left(\frac{q}{M} \right)^{p/(p+2)} \Delta \right]. \quad (8.2-21)$$

Group Velocities
 $q = 1, 2, \dots, M$

For the step-index fiber ($p = \infty$)

$$v_q \approx c_1 \left(1 - \frac{q}{M} \Delta \right). \quad (8.2-22)$$

Group Velocities
(Step-Index Fiber)
 $q = 1, 2, \dots, M$

The group velocity varies from approximately c_1 to $c_1(1 - \Delta)$. This reproduces the result obtained in (8.1-23).

Optimal Index Profile

Equation (8.2-21) indicates that the grade profile parameter $p = 2$ yields a group velocity $v_q \approx c_1$ for all q , so that all modes travel at approximately the same velocity c_1 . The advantage of the graded-index fiber for multimode transmission is now apparent.

To determine the group velocity with better accuracy, we repeat the derivation of v_q from (8.2-18), taking three terms in the Taylor's expansion $(1 + \delta)^{1/2} \approx 1 + \delta/2 - \delta^2/8$, instead of two. For $p = 2$, the result is

$$v_q = c_1 \left(1 - \frac{q}{M} \frac{\Delta^2}{2} \right). \quad (8.2-23)$$

Group Velocities
($p = 2$)
 $q = 1, \dots, M$

Thus the group velocities vary from approximately c_1 at $q = 1$ to approximately $c_1(1 - \Delta^2/2)$ at $q = M$. In comparison with the step-index fiber, for which the group velocity ranges between c_1 and $c_1(1 - \Delta)$, the fractional velocity difference for the parabolically graded fiber is $\Delta^2/2$ instead of Δ for the step-index fiber (Fig. 8.2-8). Under ideal conditions, the graded-index fiber therefore reduces the group velocity

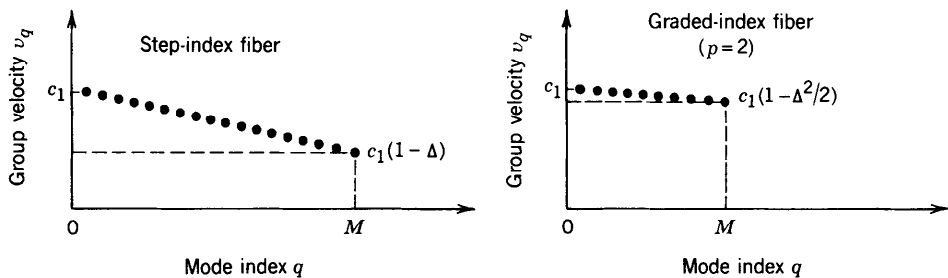


Figure 8.2-8 Group velocities v_q of the modes of a step-index fiber ($p = \infty$) and an optimal graded-index fiber ($p = 2$).

296 FIBER OPTICS

difference by a factor $\Delta/2$, thus realizing its intended purpose of equalizing the mode velocities. Since the analysis leading to (8.2-23) is based on a number of approximations, however, this improvement factor is only a rough estimate; indeed it is not fully attained in practice.

For $p = 2$, the number of modes M given by (8.2-15) becomes

$$M \approx \frac{V^2}{4}. \quad (8.2-24)$$

Number of Modes
(Graded-Index Fiber, $p = 2$)
 $V = 2\pi(a/\lambda_o)\text{NA}$

Comparing this with (8.2-17), we see that the number of modes in an optimal graded-index fiber is approximately one-half the number of modes in a step-index fiber of the same parameters n_1, n_2 , and a .

8.3 ATTENUATION AND DISPERSION

Attenuation and dispersion limit the performance of the optical-fiber medium as a data transmission channel. Attenuation limits the magnitude of the optical power transmitted, whereas dispersion limits the rate at which data may be transmitted through the fiber, since it governs the temporal spreading of the optical pulses carrying the data.

A. Attenuation

The Attenuation Coefficient

Light traveling through an optical fiber exhibits a power that decreases exponentially with the distance as a result of absorption and scattering. The attenuation coefficient α is usually defined in units of dB/km,

$$\alpha = \frac{1}{L} 10 \log_{10} \frac{1}{\mathcal{T}}, \quad (8.3-1)$$

where $\mathcal{T} = P(L)/P(0)$ is the power transmission ratio (ratio of transmitted to incident power) for a fiber of length L km. The relation between α and \mathcal{T} is illustrated in Fig. 8.3-1 for $L = 1$ km. A 3-dB attenuation, for example, corresponds to $\mathcal{T} = 0.5$, while 10 dB is equivalent to $\mathcal{T} = 0.1$ and 20 dB corresponds to $\mathcal{T} = 0.01$, and so on.

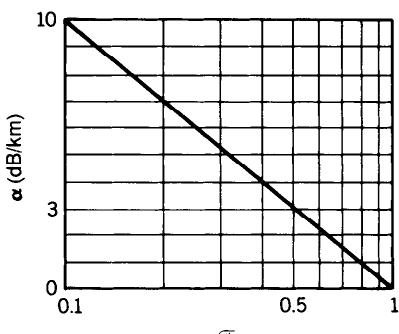


Figure 8.3-1 Relation between transmittance \mathcal{T} and attenuation coefficient α in dB units.

Losses in dB units are additive, whereas the transmission ratios are multiplicative. Thus for a propagation distance of z kilometers, the loss is αz decibels and the power transmission ratio is

$$\frac{P(z)}{P(0)} = 10^{-\alpha z/10} \approx e^{-0.23\alpha z}. \quad (\alpha \text{ in dB/km}) \quad (8.3-2)$$

Note that if the attenuation coefficient is measured in km^{-1} units, instead of in dB/km , then

$$P(z)/P(0) = e^{-\alpha z} \quad (8.3-3)$$

where $\alpha \approx 0.23\alpha$. Throughout this section α is taken in dB/km units so that (8.3-2) applies. Elsewhere in the book, however, we use α to denote the attenuation coefficient (m^{-1} or cm^{-1}) in which case the power attenuation is described by (8.3-3).

Absorption

The attenuation coefficient of fused silica glass (SiO_2) is strongly dependent on wavelength, as illustrated in Fig. 8.3-2. This material has two strong absorption bands: a middle-infrared absorption band resulting from vibrational transitions and an ultraviolet absorption band due to electronic and molecular transitions. There is a window bounded by the tails of these bands in which there is essentially no intrinsic absorption. This window occupies the near-infrared region.

Scattering

Rayleigh scattering is another intrinsic effect that contributes to the attenuation of light in glass. The random localized variations of the molecular positions in glass create random inhomogeneities of the refractive index that act as tiny scattering centers. The amplitude of the scattered field is proportional to ω^2 .[†] The scattered intensity is therefore proportional to ω^4 or to $1/\lambda_o^4$, so that short wavelengths are scattered more than long wavelengths. Thus blue light is scattered more than red (a similar effect, the

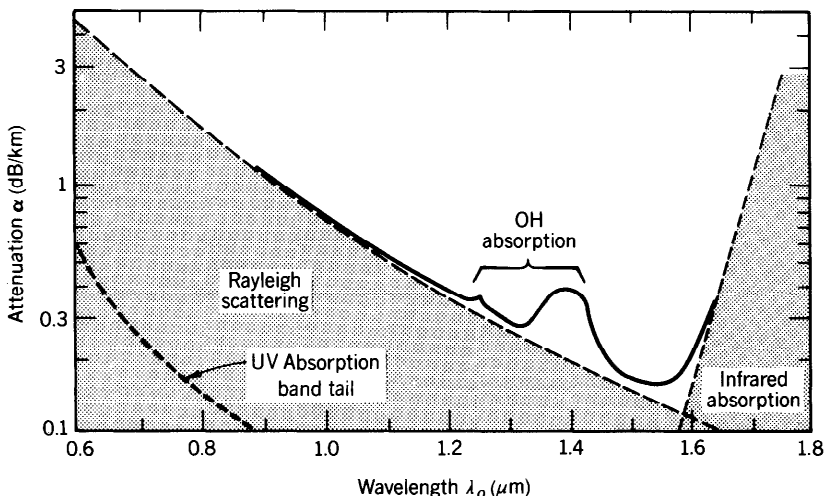


Figure 8.3-2 Dependence of the attenuation coefficient α of silica glass on the wavelength λ_o . There is a local minimum at $1.3 \mu\text{m}$ ($\alpha \approx 0.3 \text{ dB/km}$) and an absolute minimum at $1.55 \mu\text{m}$ ($\alpha \approx 0.16 \text{ dB/km}$).

[†]The scattering medium creates a polarization density \mathcal{P} which corresponds to a source of radiation proportional to $d^2\mathcal{P}/dt^2 = -\omega^2\mathcal{P}$; see (5.2-19).

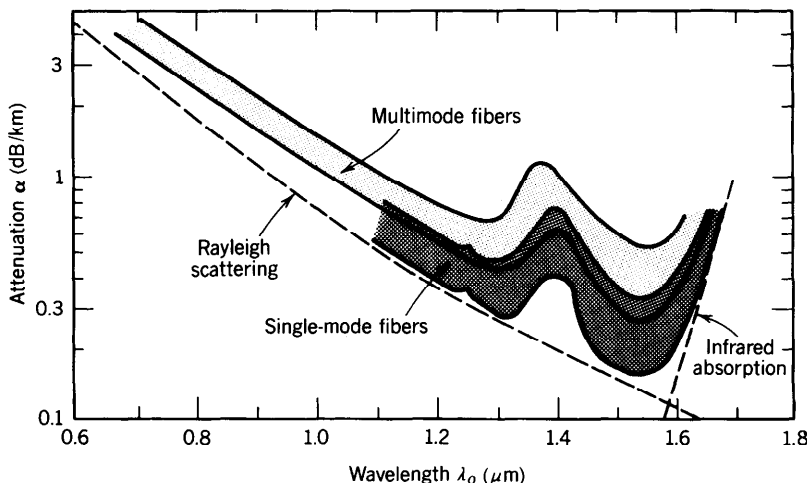


Figure 8.3-3 Ranges of attenuation coefficients of silica glass single-mode and multimode fibers.

scattering of sunlight from tiny atmospheric molecules, is the reason the sky appears blue). The attenuation caused by Rayleigh scattering therefore decreases with wavelength as $1/\lambda_0^4$, a relation known as **Rayleigh's inverse fourth-power law**. In the visible band, Rayleigh scattering is more significant than the tail of the ultraviolet absorption band, but it becomes negligible in comparison with infrared absorption for wavelengths greater than $1.6 \mu\text{m}$.

The transparent window in silica glass is therefore bounded by Rayleigh scattering on the short-wavelength side and by infrared absorption on the long-wavelength side (as indicated by the dashed lines in Fig. 8.3-2).

Extrinsic Effects

In addition to these intrinsic effects there are extrinsic absorption bands due to impurities, mainly OH vibrations associated with water vapor dissolved in the glass and metallic-ion impurities. Recent progress in the technology of fabricating glass fibers has made it possible to remove most metal impurities, but OH impurities are difficult to eliminate. Wavelengths at which glass fibers are used for optical communication are selected to avoid these absorption bands. Light-scattering losses may also be accentuated when dopants are added for the purpose of index grading, for example.

The attenuation coefficient of guided light in glass fibers depends on the absorption and scattering in the core and cladding materials. Since each mode has a different penetration depth into the cladding so that rays travel different effective distances, the attenuation coefficient is mode dependent. It is generally higher for higher-order modes. Single-mode fibers therefore typically have smaller attenuation coefficients than multimode fibers (Fig. 8.3-3). Losses are also introduced by small random variations in the geometry of the fiber and by bends.

B. Dispersion

When a short pulse of light travels through an optical fiber its power is “dispersed” in time so that the pulse spreads into a wider time interval. There are four sources of dispersion in optical fibers: modal dispersion, material dispersion, waveguide dispersion, and nonlinear dispersion.

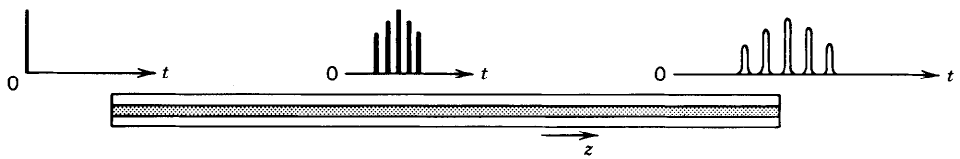


Figure 8.3-4 Pulse spreading caused by modal dispersion.

Modal Dispersion

Modal dispersion occurs in multimode fibers as a result of the differences in the group velocities of the modes. A single impulse of light entering an M -mode fiber at $z = 0$ spreads into M pulses with the differential delay increasing as a function of z . For a fiber of length L , the time delays encountered by the different modes are $\tau_q = L/v_q$, $q = 1, \dots, M$, where v_q is the group velocity of mode q . If v_{\min} and v_{\max} are the smallest and largest group velocities, the received pulse spreads over a time interval $L/v_{\min} - L/v_{\max}$. Since the modes are generally not excited equally, the overall shape of the received pulse is a smooth profile, as illustrated in Fig. 8.3-4. An estimate of the overall rms pulse width is $\sigma_\tau = \frac{1}{2}(L/v_{\min} - L/v_{\max})$. This width represents the response time of the fiber.

In a step-index fiber with a large number of modes, $v_{\min} \approx c_1(1 - \Delta)$ and $v_{\max} \approx c_1$ (see Sec. 8.1B and Fig. 8.2-8). Since $(1 - \Delta)^{-1} \approx 1 + \Delta$, the response time is

$$\boxed{\sigma_\tau \approx \frac{L}{c_1} \frac{\Delta}{2}}, \quad (8.3-4)$$

Response Time
(Multimode Step-Index Fiber)

i.e., it is a fraction $\Delta/2$ of the delay time L/c_1 .

Modal dispersion is much smaller in graded-index fibers than in step-index fibers since the group velocities are equalized and the differences between the delay times $\tau_q = L/v_q$ of the modes are reduced. It was shown in Sec. 8.2B and in Fig. 8.2-8 that in a graded-index fiber with a large number of modes and with an optimal index profile, $v_{\max} \approx c_1$ and $v_{\min} \approx c_1(1 - \Delta^2/2)$. The response time is therefore

$$\boxed{\sigma_\tau \approx \frac{L}{c_1} \frac{\Delta^2}{4}}, \quad (8.3-5)$$

Response Time
(Graded-Index Fiber)

which is a factor of $\Delta/2$ smaller than that in a step-index fiber.

EXAMPLE 8.3-1. Multimode Pulse Broadening Rate. In a step-index fiber with $\Delta = 0.01$ and $n = 1.46$, pulses spread at a rate of approximately $\sigma_\tau/L = \Delta/2c_1 = n_1\Delta/2c_o \approx 24$ ns/km. In a 100-km fiber, therefore, an impulse spreads to a width of $\approx 2.4 \mu\text{s}$. If the same fiber is optimally index graded, the pulse broadening rate is approximately $n_1\Delta^2/4c_o \approx 122$ ps/km, which is substantially reduced.

The pulse broadening arising from modal dispersion is proportional to the fiber length L in both step-index and graded-index fibers. This dependence, however, does not necessarily hold when the fibers are longer than a certain critical length because of mode coupling. Coupling occurs between modes of approximately the same propagation constants as a result of small imperfections in the fiber (random irregularities of the fiber surface, or inhomogeneities of the refractive index) which permit the optical power to be exchanged between the modes. Under certain conditions, the response time σ_τ of mode-coupled fibers is proportional to L for small L and to $L^{1/2}$ when a critical length is exceeded, so that pulses are broadened at a slower rate[†].

Material Dispersion

Glass is a dispersive medium; i.e., its refractive index is a function of wavelength. As discussed in Sec. 5.6, an optical pulse travels in a dispersive medium of refractive index n with a group velocity $v = c_o/N$, where $N = n - \lambda_o dn/d\lambda_o$. Since the pulse is a wavepacket, composed of a spectrum of components of different wavelengths each traveling at a different group velocity, its width spreads. The temporal width of an optical impulse of spectral width σ_λ (nm), after traveling a distance L , is $\sigma_\tau = |(d/d\lambda_o)(L/v)|\sigma_\lambda = |(d/d\lambda_o)(LN/c_o)|\sigma_\lambda$, from which

$$\sigma_\tau = |D_\lambda|\sigma_\lambda L, \quad (8.3-6)$$

Response Time
(Material Dispersion)

where

$$D_\lambda = -\frac{\lambda_o}{c_o} \frac{d^2n}{d\lambda_o^2} \quad (8.3-7)$$

is the material dispersion coefficient [see (5.6-21)]. The response time increases linearly with the distance L . Usually, L is measured in km, σ_τ in ps, and σ_λ in nm, so that D_λ has units of ps/km-nm. This type of dispersion is called **material dispersion** (as opposed to modal dispersion).

The wavelength dependence of the dispersion coefficient D_λ for silica glass is shown in Fig. 8.3-5. At wavelengths shorter than 1.3 μm the dispersion coefficient is negative,

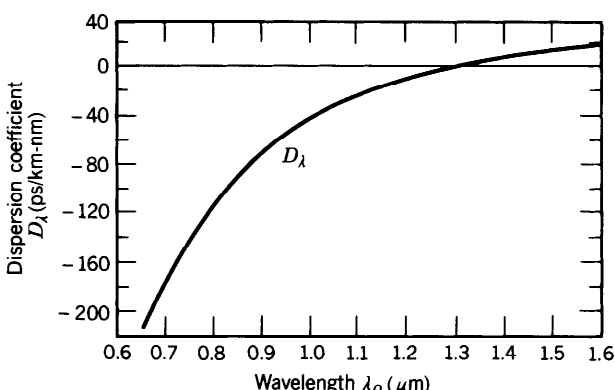


Figure 8.3-5 The dispersion coefficient D_λ of silica glass as a function of wavelength λ_o (see also Fig. 5.6-5).

[†]See, e.g., J. E. Midwinter, *Optical Fibers for Transmission*, Wiley, New York, 1979.

so that wavepackets of long wavelength travel faster than those of short wavelength. At a wavelength $\lambda_o = 0.87 \mu\text{m}$, the dispersion coefficient D_λ is approximately -80 ps/km-nm . At $\lambda_o = 1.55 \mu\text{m}$, $D_\lambda \approx +17 \text{ ps/km-nm}$. At $\lambda_o \approx 1.312 \mu\text{m}$ the dispersion coefficient vanishes, so that σ_τ in (8.3-6) vanishes. A more precise expression for σ_τ that incorporates the spread of the spectral width σ_λ about $\lambda_o = 1.312 \mu\text{m}$ yields a very small, but nonzero, width.

EXAMPLE 8.3-2. Pulse Broadening Associated with Material Dispersion. The dispersion coefficient $D_\lambda \approx -80 \text{ ps/km-nm}$ at $\lambda_o \approx 0.87 \mu\text{m}$. For a source of linewidth $\sigma_\lambda = 50 \text{ nm}$ (from an LED, for example) the pulse spreading rate in a single-mode fiber with no other sources of dispersion is $|D_\lambda|\sigma_\lambda = 4 \text{ ns/km}$. An impulse of light traveling a distance $L = 100 \text{ km}$ in the fiber is therefore broadened to a width $\sigma_\tau = |D_\lambda|\sigma_\lambda L = 0.4 \mu\text{s}$. The response time of the fiber is then $0.4 \mu\text{s}$. An impulse of narrower linewidth $\sigma_\lambda = 2 \text{ nm}$ (from a laser diode, for example) operating near $1.3 \mu\text{m}$, where the dispersion coefficient is 1 ps/km-nm , spreads at a rate of only 2 ps/km . A 100-km fiber thus has a substantially shorter response time, $\sigma_\tau = 0.2 \text{ ns}$.

Waveguide Dispersion

The group velocities of the modes depend on the wavelength even if material dispersion is negligible. This dependence, known as **waveguide dispersion**, results from the dependence of the field distribution in the fiber on the ratio between the core radius and the wavelength (a/λ_o). If this ratio is altered, by altering λ_o , the relative portions of optical power in the core and cladding are modified. Since the phase velocities in the core and cladding are different, the group velocity of the mode is altered. Waveguide dispersion is particularly important in single-mode fibers, where modal dispersion is not exhibited, and at wavelengths for which material dispersion is small (near $\lambda_o = 1.3 \mu\text{m}$ in silica glass).

As discussed in Sec. 8.1B, the group velocity $v = (d\beta/d\omega)^{-1}$ and the propagation constant β are determined from the characteristic equation, which is governed by the fiber V parameter $V = 2\pi(a/\lambda_o)\text{NA} = (a \cdot \text{NA}/c_o)\omega$. In the absence of material dispersion (i.e., when NA is independent of ω), V is directly proportional to ω , so that

$$\frac{1}{v} = \frac{d\beta}{d\omega} = \frac{d\beta}{dV} \frac{dV}{d\omega} = \frac{a \cdot \text{NA}}{c_o} \frac{d\beta}{dV}. \quad (8.3-8)$$

The pulse broadening associated with a source of spectral width σ_λ is related to the time delay L/v by $\sigma_\tau = |(d/d\lambda_o)(L/v)|\sigma_\lambda$. Thus

$$\sigma_\tau = |D_w|\sigma_\lambda L, \quad (8.3-9)$$

where

$$D_w = \frac{d}{d\lambda_o} \left(\frac{1}{v} \right) = -\frac{\omega}{\lambda_o} \frac{d}{d\omega} \left(\frac{1}{v} \right) \quad (8.3-10)$$

is the waveguide dispersion coefficient. Substituting (8.3-8) into (8.3-10) we obtain

$$D_w = -\left(\frac{1}{2\pi c_o}\right)V^2 \frac{d^2\beta}{dV^2}. \quad (8.3-11)$$

Thus the group velocity is inversely proportional to $d\beta/dV$ and the dispersion coefficient is proportional to $V^2 d^2\beta/dV^2$. The dependence of β on V is shown in Fig. 8.1-10(b) for the fundamental LP_{01} mode. Since β varies nonlinearly with V , the waveguide dispersion coefficient D_w is itself a function of V and is therefore also a function of the wavelength.[†] The dependence of D_w on λ_o may be controlled by altering the radius of the core or the index grading profile for graded-index fibers.

Combined Material and Waveguide Dispersion

The combined effects of material dispersion and waveguide dispersion (referred to here as **chromatic dispersion**) may be determined by including the wavelength dependence of the refractive indices, n_1 and n_2 and therefore NA, when determining $d\beta/d\omega$ from the characteristic equation. Although generally smaller than material dispersion, waveguide dispersion does shift the wavelength at which the total chromatic dispersion is minimum.

Since chromatic dispersion limits the performance of single-mode fibers, more advanced fiber designs aim at reducing this effect by using graded-index cores with refractive-index profiles selected such that the wavelength at which waveguide dispersion compensates material dispersion is shifted to the wavelength at which the fiber is to be used. **Dispersion-shifted fibers** have been successfully made by using a linearly tapered core refractive index and a reduced core radius, as illustrated in Fig. 8.3-6(a). This technique can be used to shift the zero-chromatic-dispersion wavelength from 1.3 μm to 1.55 μm , where the fiber has its lowest attenuation. Note, however, that the process of index grading itself introduces losses since dopants are used. Other grading profiles have been developed for which the chromatic dispersion vanishes at two wavelengths and is reduced for wavelengths between. These fibers, called **dispersion-flattened**, have been implemented by using a quadruple-clad layered grading, as illustrated in Fig. 8.3-6(b).

Combined Material and Modal Dispersion

The effect of material dispersion on pulse broadening in multimode fibers may be determined by returning to the original equations for the propagation constants β_q of the modes and determining the group velocities $v_q = (d\beta_q/d\omega)^{-1}$ with n_1 and n_2 being functions of ω . Consider, for example, the propagation constants of a graded-index fiber with a large number of modes, which are given by (8.2-19) and (8.2-15). Although n_1 and n_2 are dependent on ω , it is reasonable to assume that the ratio $\Delta = (n_1 - n_2)/n_1$ is approximately independent of ω . Using this approximation and evaluating $v_q = (d\beta_q/d\omega)^{-1}$, we obtain

$$v_q \approx \frac{c_o}{N_1} \left[1 - \frac{p-2}{p+2} \left(\frac{q}{M} \right)^{p/(p+2)} \Delta \right], \quad (8.3-12)$$

where $N_1 = (d/d\omega)(\omega n_1) = n_1 - \lambda_o (dn_1/d\lambda_o)$ is the group index of the core material. Under this approximation, the earlier expression (8.2-21) for v_q remains the same, except that the refractive index n_1 is replaced with the group index N_1 . For a step-index fiber ($p = \infty$), the group velocities of the modes vary from c_o/N_1 to

[†] For more details on this topic, see the reading list, particularly the articles by Gloge.

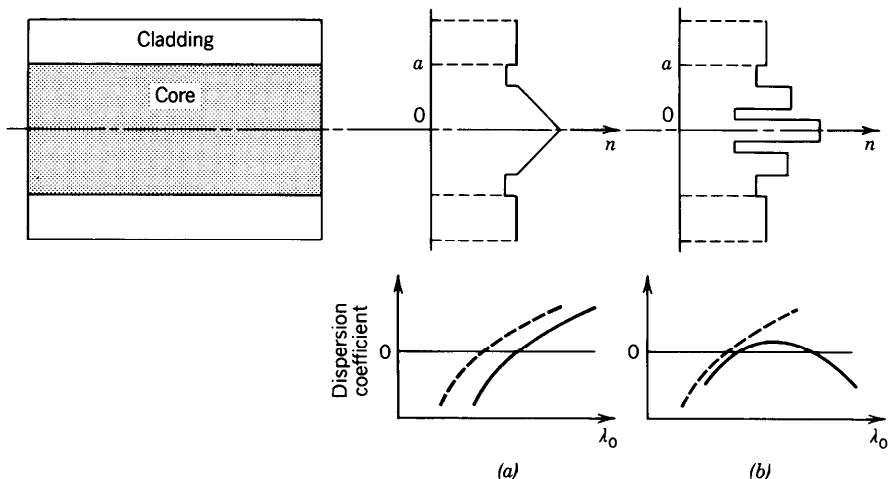


Figure 8.3-6 Refractive-index profiles and schematic wavelength dependences of the material dispersion coefficient (dashed curves) and the combined material and waveguide dispersion coefficients (solid curves) for (a) dispersion-shifted and (b) dispersion-flattened fibers.

$(c_o/N_1)(1 - \Delta)$, so that the response time is

$$\sigma_\tau \approx \frac{L}{(c_o/N_1)} \frac{\Delta}{2} \quad (8.3-13)$$

Response Time
(Multimode Step-Index Fiber
with Material Dispersion)

This should be compared with (8.3-4) when there is no material dispersion.

EXERCISE 8.3-1

Optimal Grade Profile Parameter. Use (8.2-19) and (8.2-15) to derive the following expression for the group velocity v_q when both n_1 and Δ are wavelength dependent:

$$v_q \approx \frac{c_o}{N_1} \left[1 - \frac{p - 2 - p_s}{p + 2} \left(\frac{q}{M} \right)^{p/(p+2)} \Delta \right], \quad q = 1, 2, \dots, M, \quad (8.3-14)$$

where $p_s = 2(n_1/N_1)(\omega/\Delta) d\Delta/d\omega$. What is the optimal value of the grade profile parameter p for minimizing modal dispersion?

Nonlinear Dispersion

Yet another dispersion effect occurs when the intensity of light in the core is sufficiently high, since the refractive indices then become intensity dependent and the material exhibits nonlinear behavior. The high-intensity parts of an optical pulse undergo phase shifts different from the low-intensity parts, so that the frequency is shifted by different amounts. Because of material dispersion, the group velocities are

modified, and consequently the pulse shape is altered. Under certain conditions, nonlinear dispersion can compensate material dispersion, so that the pulse travels without altering its temporal profile. The guided wave is then known as a solitary wave, or a soliton. Nonlinear optics is introduced in Chap. 19 and optical solitons are discussed in Sec. 19.8.

C. Pulse Propagation

As described in the previous sections, the propagation of pulses in optical fibers is governed by attenuation and several types of dispersion. The following is a summary and recapitulation of these effects, ignoring nonlinear dispersion.

An optical pulse of power $\tau_0^{-1}p(t/\tau_0)$ and short duration τ_0 , where $p(t)$ is a function which has unit duration and unit area, is transmitted through a multimode fiber of length L . The received optical power may be written in the form of a sum

$$P(t) \propto \sum_{q=1}^M \exp(-0.23\alpha_q L) \sigma_q^{-1} p\left(\frac{t - \tau_q}{\sigma_q}\right), \quad (8.3-15)$$

where M is the number of modes, the subscript q refers to mode q , α_q is the attenuation coefficient (dB/km), $\tau_q = L/v_q$ is the delay time, v_q is the group velocity, and $\sigma_q > \tau_0$ is the width of the pulse associated with mode q . In writing (8.3-15), we have implicitly assumed that the incident optical power is distributed equally among the M modes of the fiber. It has also been assumed that the pulse shape $p(t)$ is not altered; it is only delayed by times τ_q and broadened to widths σ_q as a result of propagation. As was shown in Sec. 5.6, an initial pulse with a Gaussian profile is indeed broadened without altering its Gaussian nature.

The received pulse is thus composed of M pulses of widths σ_q centered at time delays τ_q , as illustrated in Fig. 8.3-7. The composite pulse has an overall width σ_τ which represents the overall response time of the fiber.

We therefore identify two basic types of dispersion: **intermodal** and **intramodal**. Intermodal, or simply modal, dispersion is the delay distortion caused by the disparity among the delay times τ_q of the modes. The time difference $\frac{1}{2}(\tau_{\max} - \tau_{\min})$ between the longest and shortest delay constitutes modal dispersion. It is given by (8.3-4) and (8.3-5) for step-index and graded-index fibers with a large number of modes, respectively. Material dispersion has some effect on modal dispersion since it affects the delay times. For example, (8.3-13) gives the modal dispersion of a multimode fiber with material dispersion. Modal dispersion is directly proportional to the fiber length L , except for long fibers, in which mode coupling plays a role, whereupon it becomes proportional to $L^{1/2}$.

Intramodal dispersion is the broadening of the pulses associated with the individual modes. It is caused by a combination of material dispersion and waveguide dispersion

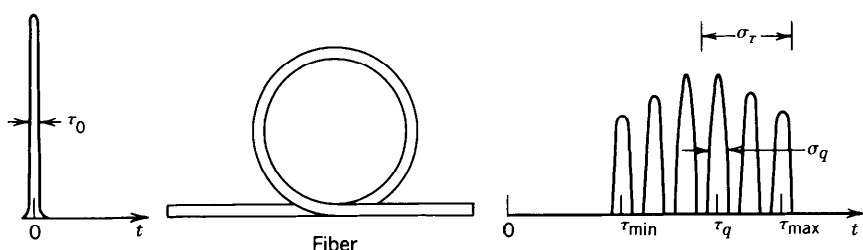


Figure 8.3-7 Response of a multimode fiber to a single pulse.

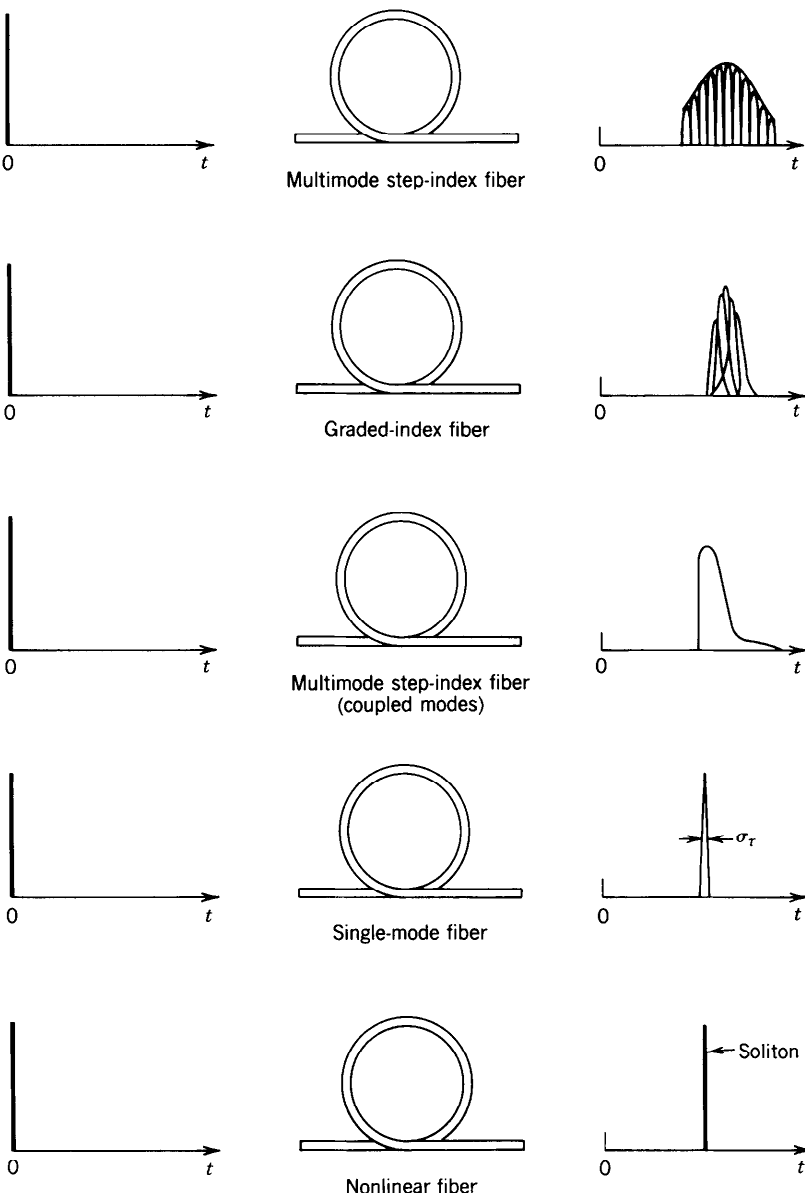


Figure 8.3-8 Broadening of a short optical pulse after transmission through different types of fibers. The width of the transmitted pulse is governed by modal dispersion in multimode (step-index and graded-index) fibers. In single-mode fibers the pulse width is determined by material dispersion and waveguide dispersion. Under certain conditions an intense pulse, called a soliton, can travel through a nonlinear fiber without broadening. This is a result of a balance between material dispersion and self-phase modulation (the dependence of the refractive index on the light intensity).

306 FIBER OPTICS

resulting from the finite spectral width of the initial optical pulse. The width σ_q is given by

$$\sigma_q^2 \approx \tau_0^2 + (D_q \sigma_\lambda L)^2, \quad (8.3-16)$$

where D_q is a dispersion coefficient representing the combined effects of material and waveguide dispersion for mode q . Material dispersion is usually more significant. For a very short initial width τ_0 , (8.3-16) gives

$$\sigma_q \approx D_q \sigma_\lambda L. \quad (8.3-17)$$

Figure 8.3-8 is a schematic illustration in which the profiles of pulses traveling through different types of fibers are compared. In multimode step-index fibers, the modal dispersion $\frac{1}{2}(\tau_{\max} - \tau_{\min})$ is usually much greater than the material/waveguide dispersion σ_q , so that intermodal dispersion dominates and $\sigma_\tau \approx \frac{1}{2}(\tau_{\max} - \tau_{\min})$. In multimode graded-index fibers, $\frac{1}{2}(\tau_{\max} - \tau_{\min})$ may be comparable to σ_q , so that the overall pulse width involves all dispersion effects. In single-mode fibers, there is obviously no modal dispersion and the transmission of pulses is limited by material and waveguide dispersion. The lowest overall dispersion is achieved in a single-mode fiber operating at the wavelength for which the combined material-waveguide dispersion vanishes.

READING LIST

Books

See also the books on optical waveguides in Chapter 7.

- P. K. Cheo, *Fiber Optics and Optoelectronics*, Prentice Hall, Englewood Cliffs, NJ, 1985, 2nd ed. 1990.
- F. C. Allard, *Fiber Optics Handbook for Engineers and Scientists*, McGraw-Hill, New York, 1990.
- C. Yeh, *Handbook of Fiber Optics: Theory and Applications*, Academic Press, Orlando, FL, 1990.
- L. B. Jeunhomme, *Single-Mode Fiber Optics*, Marcel Dekker, New York, 1983, 2nd ed. 1990.
- P. W. France, ed., *Fluoride Glass Optical Fibers*, CRC Press, Boca Raton, FL, 1989.
- P. Diament, *Wave Transmission and Fiber Optics*, Macmillan, New York, 1989.
- W. B. Jones, Jr., *Introduction to Optical Fiber Communication Systems*, Holt, Rinehart and Winston, New York, 1988.
- H. Murata, *Handbook of Optical Fibers and Cables*, Marcel Dekker, New York, 1988.
- E. G. Neuman, *Single-Mode Fibers—Fundamentals*, Springer-Verlag, New York, 1988.
- E. L. Safford, Jr. and J. A. McCann, *Fiberoptics and Laser Handbook*, Tab Books, Blue Ridge Summit, PA, 2nd ed. 1988.
- S. E. Miller and I. Kaminow, *Optical Fiber Telecommunications II*, Academic Press, Boston, MA, 1988.
- J. Gowar, *Optical Communication Systems*, Prentice Hall, Englewood Cliffs, NJ, 1984.
- R. G. Seippel, *Fiber Optics*, Reston Publishing, Reston, VA, 1984.
- ANSI/IEEE Standards 812-1984, *IEEE Standard Definitions of Terms Relating to Fiber Optics*, IEEE, New York, 1984.
- A. H. Cherin, *An Introduction to Optical Fibers*, McGraw-Hill, New York, 1983.
- G. E. Keiser, *Optical Fiber Communications*, McGraw-Hill, New York, 1983.
- C. Hentschel, *Fiber Optics Handbook*, Hewlett-Packard, Palo Alto, CA, 1983.
- Y. Suematsu and K. Iga, *Introduction to Optical Fiber Communications*, Wiley, New York, 1982.
- T. Okoshi, *Optical Fibers*, Academic Press, New York, 1982.
- C. K. Kao, *Optical Fiber Systems*, McGraw-Hill, New York, 1982.
- E. A. Lacy, *Fiber Optics*, Prentice-Hall, Englewood Cliffs, NJ, 1982.

- D. Marcuse, *Light Transmission Optics*, Van Nostrand Reinhold, New York, 1972, 2nd ed. 1982.
- D. Marcuse, *Principles of Optical Fiber Measurements*, Academic Press, New York, 1981.
- A. B. Sharma, S. J. Halme, and M. M. Butusov, *Optical Fiber Systems and Their Components*, Springer-Verlag, Berlin, 1981.
- CSELT (Centro Studi e Laboratori Telecomunicazioni), *Optical Fibre Communications*, McGraw-Hill, New York, 1981.
- M. K. Barnoski, ed., *Fundamentals of Optical Fiber Communications*, Academic Press, New York, 1976, 2nd ed. 1981.
- C. P. Sandbank, ed., *Optical Fibre Communication Systems*, Wiley, New York, 1980.
- M. J. Howes and D. V. Morgan, eds., *Optical Fibre Communications*, Wiley, New York, 1980.
- H. F. Wolf, ed., *Handbook of Fiber Optics*, Garland STPM Press, New York, 1979.
- D. B. Ostrowsky, ed., *Fiber and Integrated Optics*, Plenum Press, New York, 1979.
- J. E. Midwinter, *Optical Fibers for Transmission*, Wiley, New York, 1979.
- S. E. Miller and A. G. Chynoweth, *Optical Fiber Telecommunications*, Academic Press, New York, 1979.
- G. R. Elion and H. A. Elion, *Fiber Optics in Communication Systems*, Marcel Dekker, New York, 1978.
- H. G. Unger, *Planar Optical Waveguides and Fibers*, Clarendon Press, Oxford, 1977.
- J. A. Arnaud, *Beam and Fiber Optics*, Academic Press, New York, 1976.
- W. B. Allan, *Fibre Optics: Theory and Practice*, Plenum Press, New York, 1973.
- N. S. Kapany, *Fiber Optics: Principles and Applications*, Academic Press, New York, 1967.

Special Journal Issues

- Special issue on fiber-optic sensors, *Journal of Lightwave Technology*, vol. LT-5, no. 7, 1987.
- Special issue on fiber, cable, and splicing technology, *Journal of Lightwave Technology*, vol. LT-4, no. 8, 1986.
- Special issue on low-loss fibers, *Journal of Lightwave Technology*, vol. LT-2, no. 10, 1984.
- Special issue on fiber optics, *IEEE Transactions on Communications*, vol. COM-26, no. 7, 1978.

Articles

- M. G. Drexhage and C. T. Moynihan, Infrared Optical Fibers, *Scientific American*, vol. 259, no. 5, pp. 110–114, 1988.
- S. R. Nagel, Optical Fiber—the Expanding Medium, *IEEE Communications Magazine*, vol. 25, no. 4, pp. 33–43, 1987.
- R. H. Stolen and R. P. DePaula, Single-Mode Fiber Components, *Proceedings of the IEEE*, vol. 75, pp. 1498–1511, 1987.
- P. S. Henry, Lightwave Primer, *IEEE Journal of Quantum Electronics*, vol. QE-21, pp. 1862–1879, 1985.
- T. Li, Advances in Optical Fiber Communications: An Historical Perspective, *IEEE Journal on Selected Areas in Communications*, vol. SAC-1, pp. 356–372, 1983.
- I. P. Kaminow, Polarization in Optical Fibers, *IEEE Journal of Quantum Electronics*, vol. QE-17, pp. 15–22, 1981.
- P. J. B. Clarricoats, Optical Fibre Waveguides—A Review, in *Progress in Optics*, vol. 14, E. Wolf, ed., North-Holland, Amsterdam, 1977.
- D. Gloge, Weakly Guiding Fibers, *Applied Optics*, vol. 10, pp. 2252–2258, 1971.
- D. Gloge, Dispersion in Weakly Guiding Fibers, *Applied Optics*, vol. 10, pp. 2442–2445, 1971.

PROBLEMS

- 8.1-1 Coupling Efficiency.** (a) A source emits light with optical power P_0 and a distribution $I(\theta) = (1/\pi)P_0 \cos \theta$, where $I(\theta)$ is the power per unit solid angle in the direction making an angle θ with the axis of a fiber. Show that the power collected

308 FIBER OPTICS

by the fiber is $P = (\text{NA})^2 P_0$, i.e., the coupling efficiency is NA^2 where NA is the numerical aperture of the fiber.

(b) If the source is a planar light-emitting diode of refractive index n_s bonded to the fiber, and assuming that the fiber cross-sectional area is larger than the LED emitting area, calculate the numerical aperture of the fiber and the coupling efficiency when $n_1 = 1.46$, $n_2 = 1.455$, and $n_s = 3.5$.

- 8.1-2 Modes.** A step-index fiber has radius $a = 5 \mu\text{m}$, core refractive index $n_1 = 1.45$, and fractional refractive-index change $\Delta = 0.002$. Determine the shortest wavelength λ_c for which the fiber is a single-mode waveguide. If the wavelength is changed to $\lambda_c/2$, identify the indices (l, m) of all the guided modes.
- 8.1-3 Modal Dispersion.** A step-index fiber of numerical aperture $\text{NA} = 0.16$, core radius $a = 45 \mu\text{m}$ and core refractive index $n_1 = 1.45$ is used at $\lambda_o = 1.3 \mu\text{m}$, where material dispersion is negligible. If a pulse of light of very short duration enters the fiber at $t = 0$ and travels a distance of 1 km, sketch the shape of the received pulse:
- Using ray optics and assuming that only meridional rays are allowed.
 - Using wave optics and assuming that only meridional ($l = 0$) modes are allowed.
- 8.1-4 Propagation Constants and Group Velocities.** A step-index fiber with refractive indices $n_1 = 1.444$ and $n_2 = 1.443$ operates at $\lambda_o = 1.55 \mu\text{m}$. Determine the core radius at which the fiber V parameter is 10. Use Fig. 8.1-6 to estimate the propagation constants of all the guided modes with $l = 0$. If the core radius is now changed so that $V = 4$, use Fig. 8.1-10(b) to determine the propagation constant and the group velocity of the LP_{01} mode. *Hint:* Derive an expression for the group velocity $v = (d\beta/d\omega)^{-1}$ in terms of $d\beta/dV$ and use Fig. 8.1-10(b) to estimate $d\beta/dV$. Ignore the effect of material dispersion.
- 8.2-1 Numerical Aperture of a Graded-Index Fiber.** Compare the numerical apertures of a step-index fiber with $n_1 = 1.45$ and $\Delta = 0.01$ and a graded-index fiber with $n_1 = 1.45$, $\Delta = 0.01$, and a parabolic refractive-index profile ($p = 2$). (See Exercise 1.3-2 on page 24.)
- 8.2-2 Propagation Constants and Wavevector (Step-Index Fiber).** A step-index fiber of radius $a = 20 \mu\text{m}$ and refractive indices $n_1 = 1.47$ and $n_2 = 1.46$ operates at $\lambda_o = 1.55 \mu\text{m}$. Using the quasi-plane wave theory and considering only guided modes with azimuthal index $l = 1$:
- Determine the smallest and largest propagation constants.
 - For the mode with the smallest propagation constant, determine the radii of the cylindrical shell within which the wave is confined, and the components of the wavevector \mathbf{k} at $r = 5 \mu\text{m}$.
- 8.2-3 Propagation Constants and Wavevector (Graded-Index Fiber).** Repeat Problem 8.2-2 for a graded-index fiber with parabolic refractive-index profile with $p = 2$.
- 8.3-1 Scattering Loss.** At $\lambda_o = 820 \text{ nm}$ the absorption loss of a fiber is 0.25 dB/km and the scattering loss is 2.25 dB/km . If the fiber is used instead at $\lambda_o = 600 \text{ nm}$ and calorimetric measurements of the heat generated by light absorption give a loss of 2 dB/km , estimate the total attenuation at $\lambda_o = 600 \text{ nm}$.
- 8.3-2 Modal Dispersion in Step-Index Fibers.** Determine the core radius of a multimode step-index fiber with a numerical aperture $\text{NA} = 0.1$ if the number of modes $M = 5000$ when the wavelength is $0.87 \mu\text{m}$. If the core refractive index $n_1 = 1.445$, the group index $N_1 = 1.456$, and Δ is approximately independent of wavelength, determine the modal-dispersion response time σ_r for a 2-km fiber.
- 8.3-3 Modal Dispersion in Graded-Index Fibers.** Consider a graded-index fiber with $a/\lambda_o = 10$, $n_1 = 1.45$, $\Delta = 0.01$, and a power-law profile with index p . Determine

the number of modes M , and the modal-dispersion pulse-broadening rate σ_r/L for $p = 1.9, 2, 2.1$, and ∞ .

- 8.3-4 **Pulse Propagation.** A pulse of initial width τ_0 is transmitted through a graded-index fiber of length L kilometers and power-law refractive-index profile with profile index p . The peak refractive index n_1 is wavelength-dependent with $D_\lambda = -(\lambda_o/c_o)d^2n_1/d\lambda_o^2$, Δ is approximately independent of wavelength, σ_λ is the source's spectral width, and λ_o is the operating wavelength. Discuss the effect of increasing each of the following parameters on the width of the received pulse: $L, \tau_0, p, |D_\lambda|, \sigma_\lambda$, and λ_o .

Attenuation in fibers

Transmission characteristics of optical fibers

- The transmission characteristics of most interest: **attenuation (*loss*)** and **bandwidth**.
- Now, *silica-based* glass fibers have losses less than 0.2 dB/km (i.e. 95 % launched power remains after 1 km of fiber transmission). This is essentially the *fundamental lower limit* for attenuation in silica-based glass fibers.
- **Fiber bandwidth** is limited by the *signal dispersion* within the fiber. Bandwidth determines the number of bits of information transmitted in a given time period. Now, fiber bandwidth has reached many 10's Gbit over many km's per wavelength channel.

Attenuation

- Signal attenuation within optical fibers is usually expressed in the logarithmic unit of the decibel.

The decibel, which is used for comparing two *power* levels, may be defined for a particular optical wavelength as the *ratio* of the **output optical power P_o** from the fiber to the **input optical power P_i** .

$$\text{Loss (dB)} = -10 \log_{10} (P_o/P_i) = 10 \log_{10} (P_i/P_o)$$
$$(P_o \leq P_i)$$

*In *electronics*, $\text{dB} = 20 \log_{10} (V_o/V_i)$

Attenuation in dB/km

*The logarithmic unit has the advantage that the operations of *multiplication (and division)* reduce to *addition (and subtraction)*.

In numerical values:

$$P_o/P_i = 10^{[-\text{Loss(dB)}/10]}$$

The attenuation is usually expressed in decibels per unit length (i.e. dB/km):

$$\gamma L = -10 \log_{10} (P_o/P_i)$$

γ (dB/km): signal attenuation per unit length in decibels

L (km): fiber length

dBm

- dBm is a specific unit of power in decibels when the reference power is 1 mW:

$$\text{dBm} = 10 \log_{10} (\text{Power}/1 \text{ mW})$$

e.g. 1 mW = 0 dBm; 10 mW = 10 dBm; 100 μW = -10 dBm

$$\Rightarrow \text{Loss (dB)} = \text{input power (dBm)} - \text{output power (dBm)}$$

e.g. Input power = 1 mW (0 dBm), output power = 100 μW (-10 dBm)

$$\Rightarrow \text{loss} = -10 \log_{10} (100 \mu\text{W}/1 \text{ mW}) = 10 \text{ dB}$$

$$\text{OR } 0 \text{ dBm} - (-10 \text{ dBm}) = 10 \text{ dB}$$

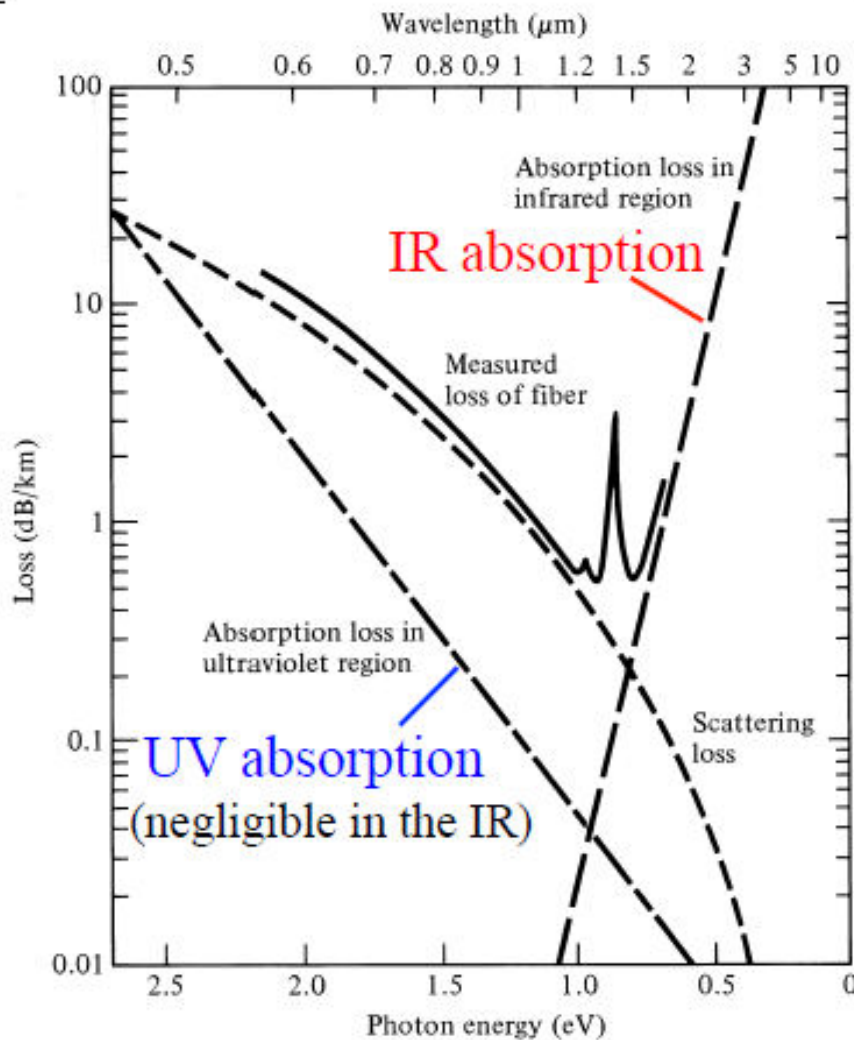
Fiber attenuation mechanisms

1. Material absorption
 2. Scattering loss
 3. Nonlinear loss
 4. Bending loss
 5. Mode coupling loss
-
- ***Material absorption*** is a loss mechanism related to both *the material composition* and the *fabrication process* for the fiber. The optical power is lost as *heat* in the fiber.
 - The light absorption can be *intrinsic* (*due to the material components of the glass*) or *extrinsic* (*due to impurities introduced into the glass during fabrication*).

Intrinsic absorption

- Pure silica-based glass has *two* major intrinsic absorption mechanisms at optical wavelengths:
 - (1) a *fundamental UV absorption edge*, the peaks are centered in the *ultraviolet wavelength region*. This is due to the *electron transitions* within the glass molecules. The tail of this peak may extend into the the shorter wavelengths of the fiber transmission spectral window.
 - (2) A fundamental *infrared and far-infrared absorption edge*, due to *molecular vibrations* (such as Si-O). The tail of these absorption peaks may extend into the longer wavelengths of the fiber transmission spectral window.

Fundamental fiber attenuation characteristics



Electronic and molecular absorption

- ***Electronic absorption:*** the bandgap of fused silica is about 8.9 eV (~140 nm). This causes strong absorption of light in the UV spectral region due to electronic transitions across the bandgap.

In practice, the bandgap of a material is not sharply defined but usually has ***bandtails*** extending from the conduction and valence bands into the bandgap due to a variety of reasons, such as *thermal vibrations of the lattice ions* and *microscopic imperfections of the material structure*.

An ***amorphous*** material like fused silica generally has very long bandtails. These bandtails lead to an absorption tail extending into the visible and infrared regions. Empirically, the absorption tail at photon energies below the bandgap falls off exponentially with photon energy.

Electronic and molecular absorption

- ***Molecular absorption:*** in the infrared region, the absorption of photons is accompanied by transitions between different *vibrational modes* of silica molecules.
- The *fundamental vibrational transition* of fused silica causes a very strong absorption peak at about 9 μm wavelength.
- *Nonlinear effects* contribute to important harmonics and combination frequencies corresponding to minor absorption peaks at 4.4, 3.8 and 3.2 μm wavelengths.
=> a long absorption tail extending into the near infrared, causing a sharp rise in absorption at optical wavelengths longer than 1.6 μm .

Extrinsic absorption

- Major extrinsic loss mechanism is caused by absorption due to water (*as the hydroxyl or OH⁻ ions*) introduced in the glass fiber during *fiber pulling by means of oxyhydrogen flame*.
- These OH⁻ ions are bonded into the glass structure and have absorption peaks (due to *molecular vibrations*) at 1.39 μm. The fundamental vibration of the OH⁻ ions appear at 2.73 μm.
- Since these OH⁻ absorption peaks are sharply peaked, narrow spectral windows exist around 1.3 μm and 1.55 μm which are essentially unaffected by OH⁻ absorption.
- The lowest attenuation for typical silica-based fibers occur at wavelength 1.55 μm at about 0.2 dB/km, approaching the *minimum possible attenuation* at this wavelength.

Impurity absorption

- ***Impurity absorption:*** most impurity ions such as OH⁻, Fe²⁺ and Cu²⁺ form absorption bands in the *near infrared* region where both electronic and molecular absorption losses of the host silica glass are very low.
- Near the peaks of the impurity absorption bands, an impurity concentration as low as *one part per billion* can contribute to an absorption loss as high as 1 dB km⁻¹.
- In fact, fiber-optic communications were not considered possible until it was realized in 1966 (Kao) that most losses in earlier fibers were caused by impurity absorption and then ultra-pure fibers were produced in the early 1970s (Corning).
- Today, impurities in fibers have been reduced to levels where losses associated with their absorption are negligible, with the exception of the OH⁻ radical.

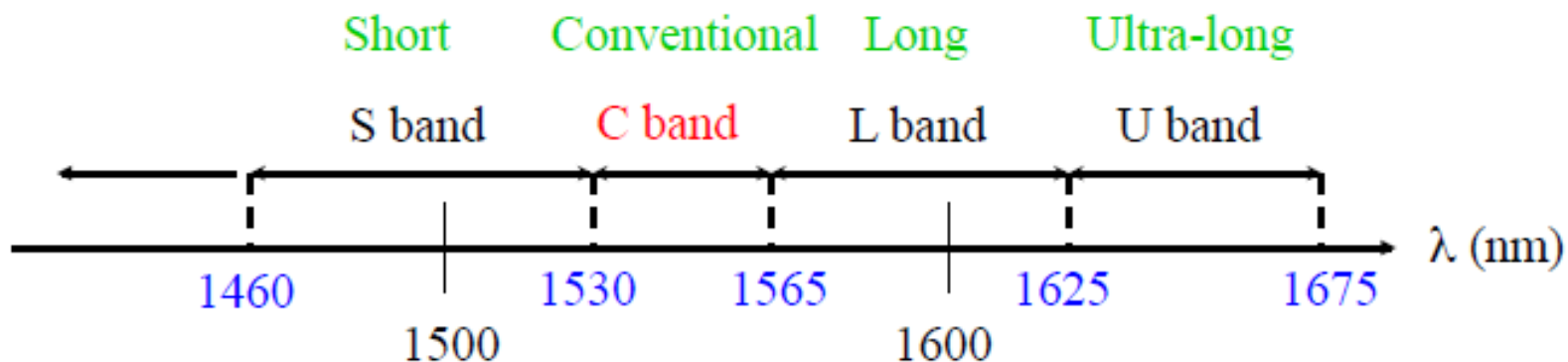
Three major fiber transmission spectral windows

The 1st window: 850 nm, attenuation 4 dB/km

The 2nd window: 1300 nm, attenuation 0.5 dB/km

The 3rd window: 1550 nm, attenuation 0.2 dB/km

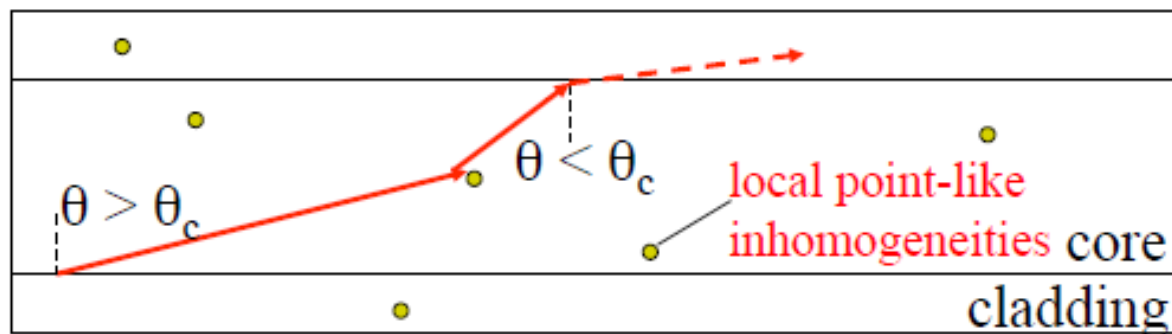
1550 nm window is today's standard **long-haul** communication wavelengths.



Scattering loss

Scattering results in attenuation (*in the form of radiation*) as the scattered light may not continue to satisfy the total internal reflection in the fiber core.

One major type of scattering is known as *Rayleigh scattering*.



The scattered ray can escape by refraction according to Snell's Law.

Rayleigh scattering

- *Rayleigh scattering* results from random *inhomogeneities* that are small in size compared with the wavelength.
 - $\bullet \ll \lambda$
- These inhomogeneities exist in the form of *refractive index fluctuations* which are frozen into the *amorphous* glass fiber upon fiber pulling. Such fluctuations *always exist and cannot be avoided !*

Rayleigh scattering results in an attenuation (dB/km) $\propto 1/\lambda^4$

Waveguide scattering

- ***Imperfections in the waveguide structure*** of a fiber, such as nonuniformity in the size and shape of the core, perturbations in the core-cladding boundary, and defects in the core or cladding, can be generated in the manufacturing process.
- Environmentally induced effects, such as stress and temperature variations, also cause imperfections.
- The imperfections in a fiber waveguide result in additional scattering losses. They can also induce coupling between different guided modes.

Nonlinear losses

- Because light is confined over long distances in an optical fiber, *nonlinear optical effects* can become important even at a relatively moderate optical power.
- Nonlinear optical processes such as *stimulated Brillouin scattering* and *stimulated Raman scattering* can cause significant attenuation in the power of an optical signal.
- Other nonlinear processes can induce *mode mixing* or *frequency shift*, all contributing to the loss of a particular guided mode at a particular frequency.
- Nonlinear effects are *intensity dependent*, and thus they can become very important at high optical powers.

Dispersion in fibers

Dispersion in fibers

- Dispersion is the primary cause of limitation on the optical signal transmission bandwidth through an optical fiber.

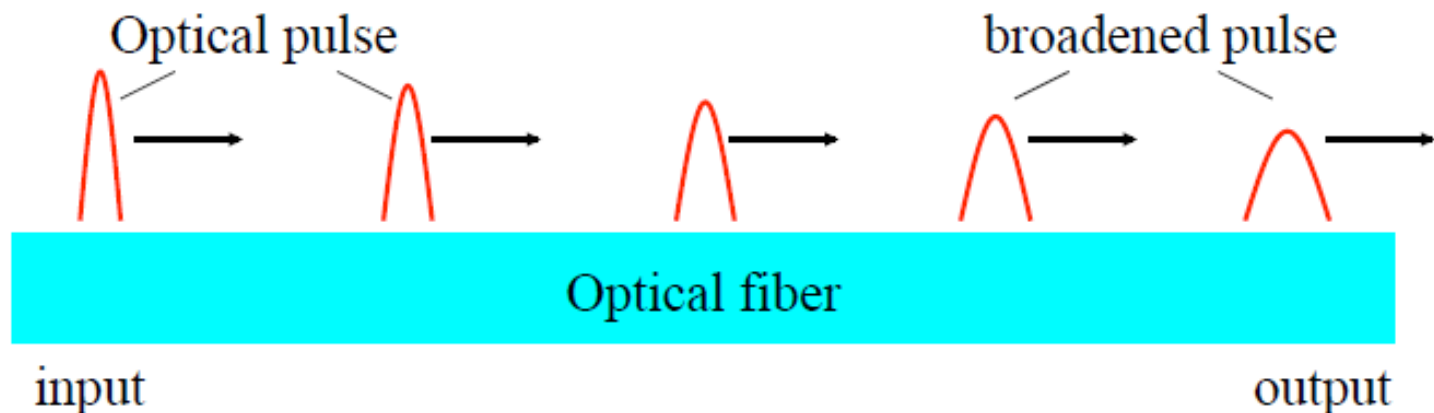
- Both material dispersion and waveguide dispersion are examples of *chromatic dispersion* because both are frequency dependent.
- *Waveguide dispersion* is caused by frequency dependence of the propagation constant β of a specific mode due to the waveguiding effect. (*recall the b vs. V plot of a specific mode*)
- The combined effect of material and waveguide dispersions for a particular mode alone is called *intramode dispersion*.

Modal dispersion

- ***Modal dispersion*** is caused by the variation in propagation constant between different modes; it is also called *intermode dispersion*. (*recall the b vs. V plot at a fixed V*)
- Modal dispersion appears only when *more than one* mode is excited in a multimode fiber. It exists even when chromatic dispersion disappears.
- *If only one mode is excited in a fiber*, only intramode chromatic dispersion has to be considered even when the fiber is a multimode fiber.

Fiber dispersion

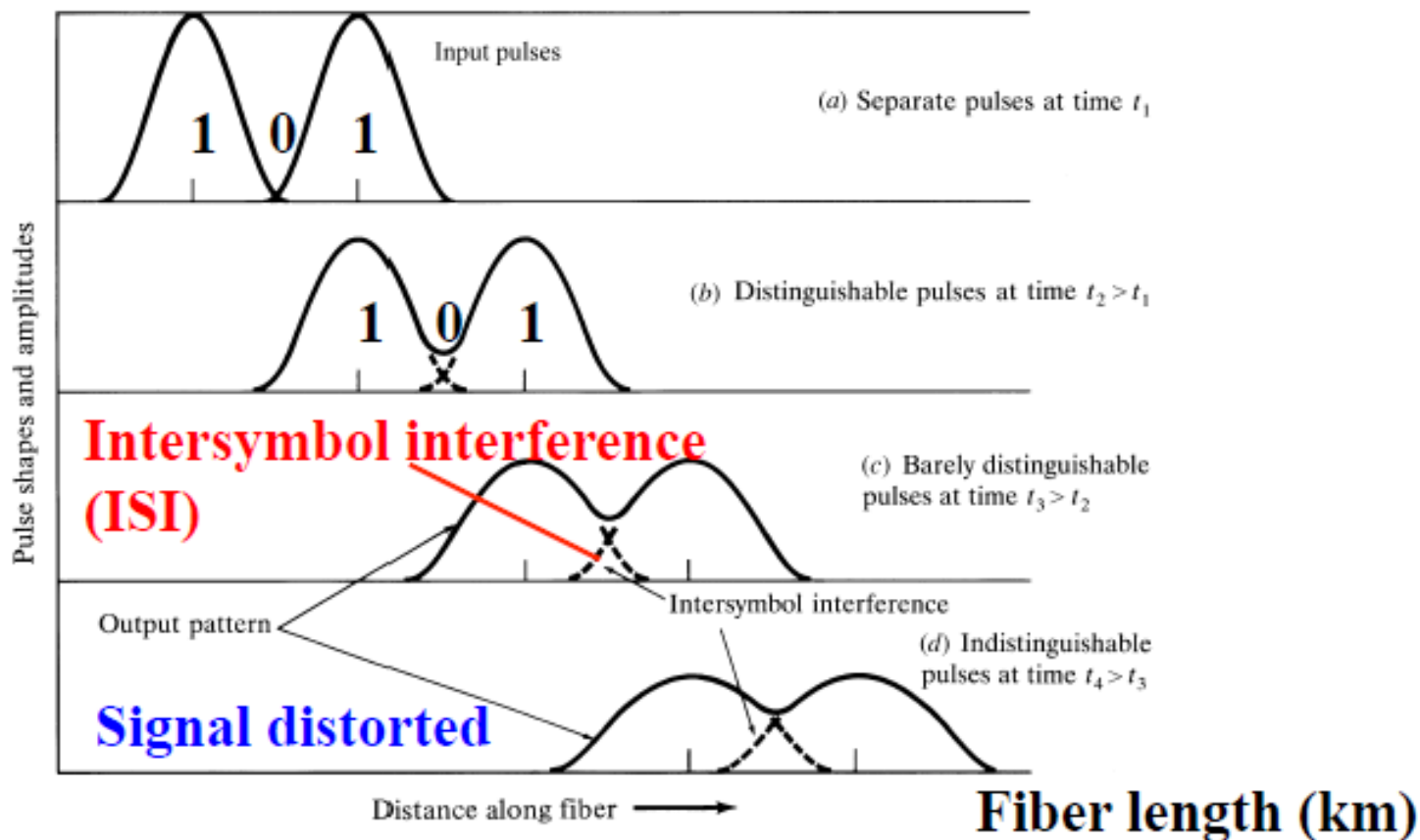
- Fiber dispersion results in *optical pulse broadening* and hence *digital signal degradation*.



Dispersion mechanisms:

1. Modal (or *intermodal*) dispersion
2. Chromatic dispersion (CD)
3. Polarization mode dispersion (PMD)

Pulse broadening limits fiber bandwidth (data rate)

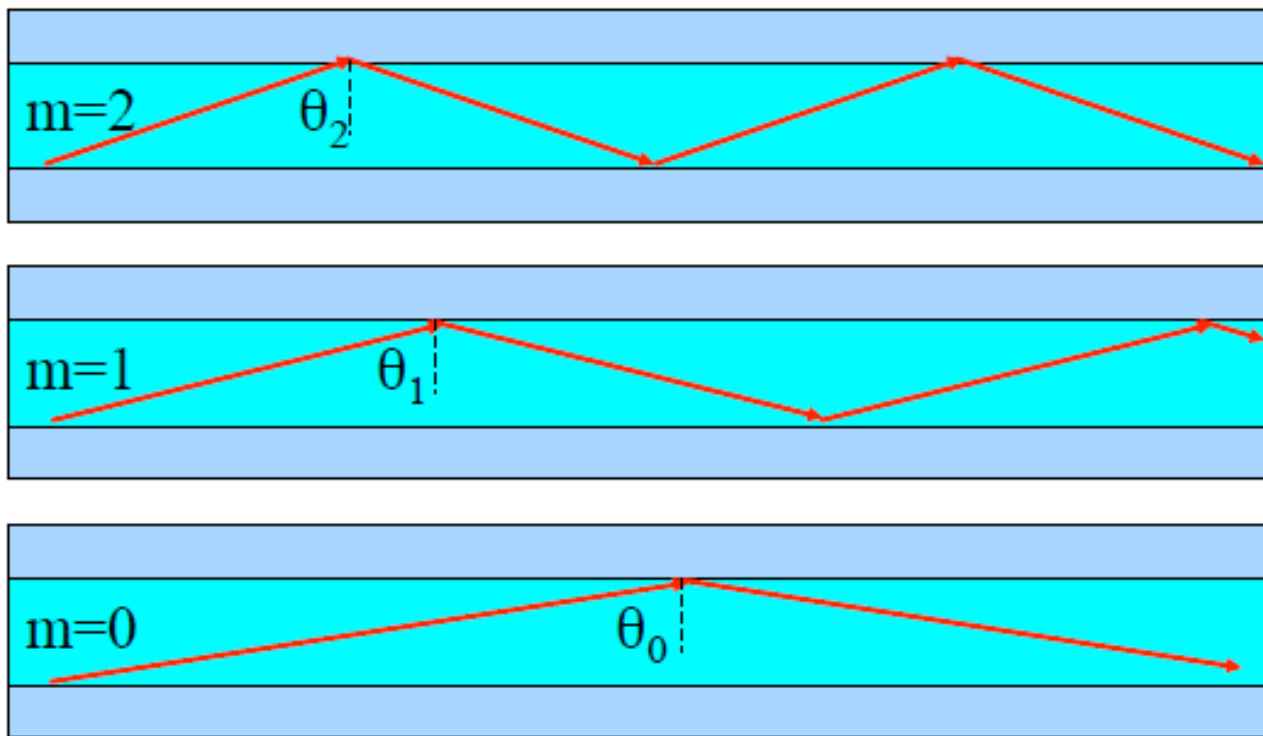


- An *increasing number of errors* may be encountered on the digital optical channel as the ISI becomes more pronounced.

Modal dispersion

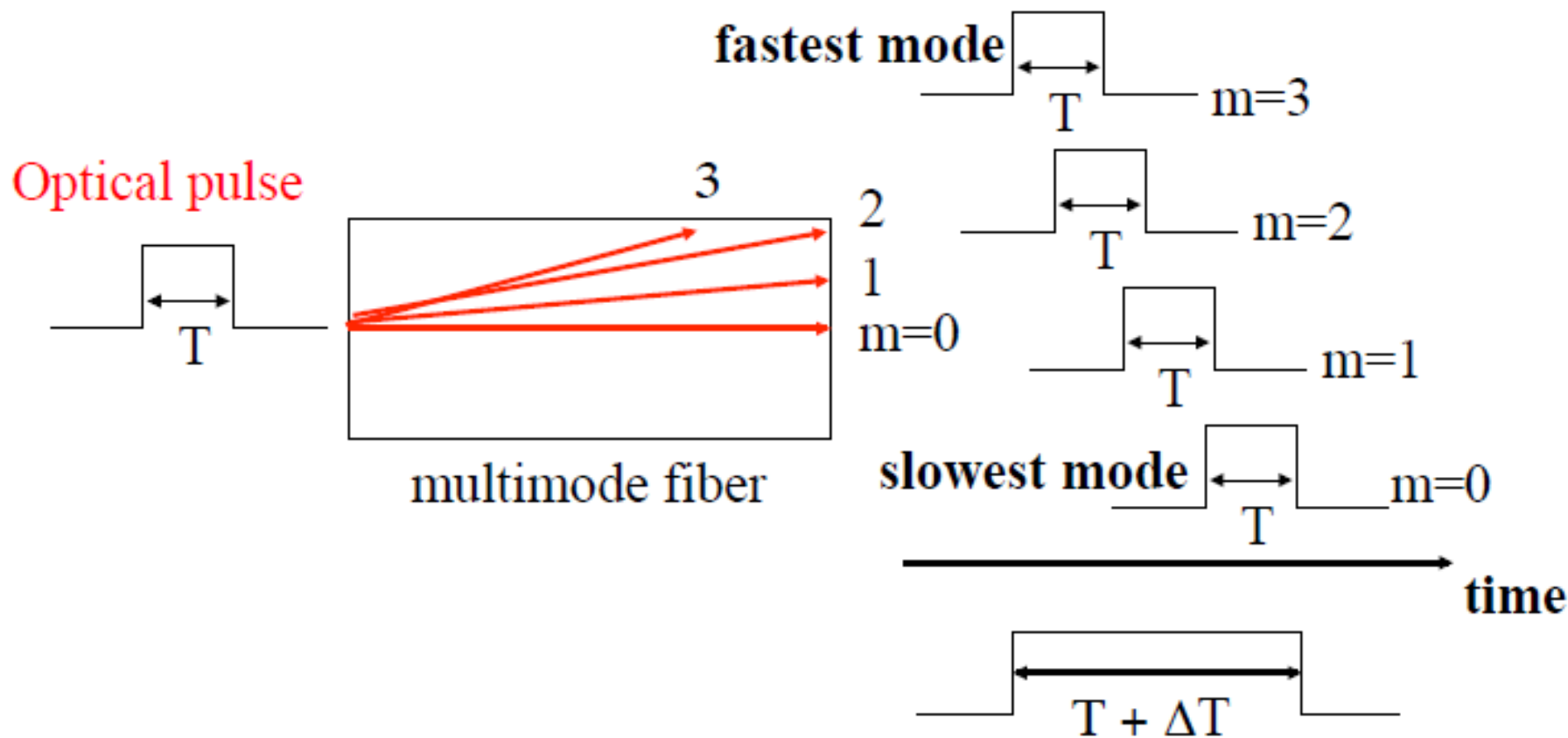
- When numerous waveguide modes are propagating, they all travel with different velocities with respect to the waveguide axis.
- An input waveform distorts during propagation because its energy is distributed among several modes, each traveling at a different speed.
- Parts of the wave arrive at the output before other parts, spreading out the waveform. This is thus known as **multimode (modal) dispersion**.
- Multimode dispersion does *not* depend on the source linewidth (even a *single* wavelength can be simultaneously carried by *multiple modes* in a waveguide).
- Multimode dispersion would *not* occur if the waveguide allows *only* one mode to propagate - the advantage of *single-mode* waveguides!

Modal dispersion in multimode waveguides



The carrier wave can propagate along all these different “zig-zag” ray paths of *different path lengths*.

Modal dispersion results in pulse broadening

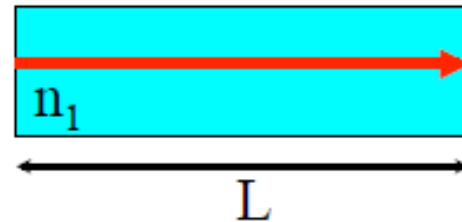


modal dispersion: different modes arrive at the receiver with different delays => pulse broadening

Estimate modal dispersion pulse broadening using phase velocity

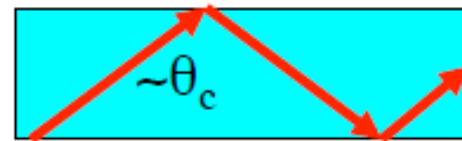
- A zero-order mode traveling near the waveguide axis needs time:

$$t_0 = L/v_{m=0} \approx L n_1/c \quad (v_{m=0} \approx c/n_1)$$



- The highest-order mode traveling near the critical angle needs time:

$$t_m = L/v_m \approx L n_2/c \quad (v_m \approx c/n_2)$$



=> the *pulse broadening* due to modal dispersion:

$$\Delta T \approx t_0 - t_m \approx (L/c) (n_1 - n_2)$$

$$\approx (L/2cn_1) NA^2 \quad (n_1 \sim n_2)$$

How does modal dispersion restricts fiber bit rate?

e.g. How much will a light pulse spread after traveling along 1 km of a step-index fiber whose NA = 0.275 and $n_{core} = 1.487$?

Suppose we transmit at a low bit rate of 10 Mb/s

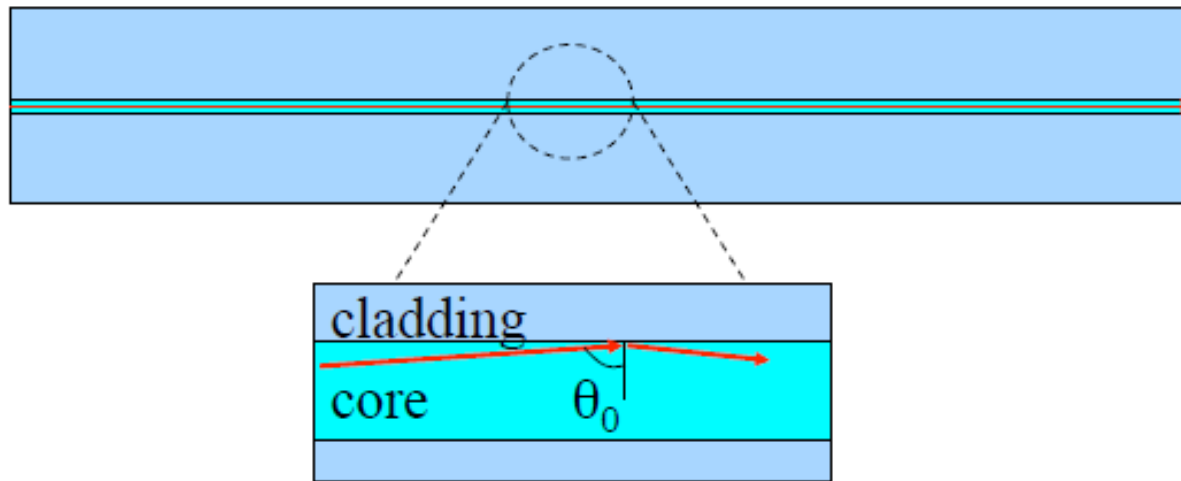
$$\Rightarrow \text{Pulse duration} = 1 / 10^7 \text{ s} = 100 \text{ ns}$$

Using the above e.g., each pulse will spread up to ≈ 100 ns (i.e. \approx pulse duration !) every km

\Rightarrow The broadened pulses overlap! (**Intersymbol interference (ISI)**)

*Modal dispersion limits the bit rate of a km-length fiber-optic link to ~ 10 Mb/s. (a coaxial cable supports this bit rate easily!)

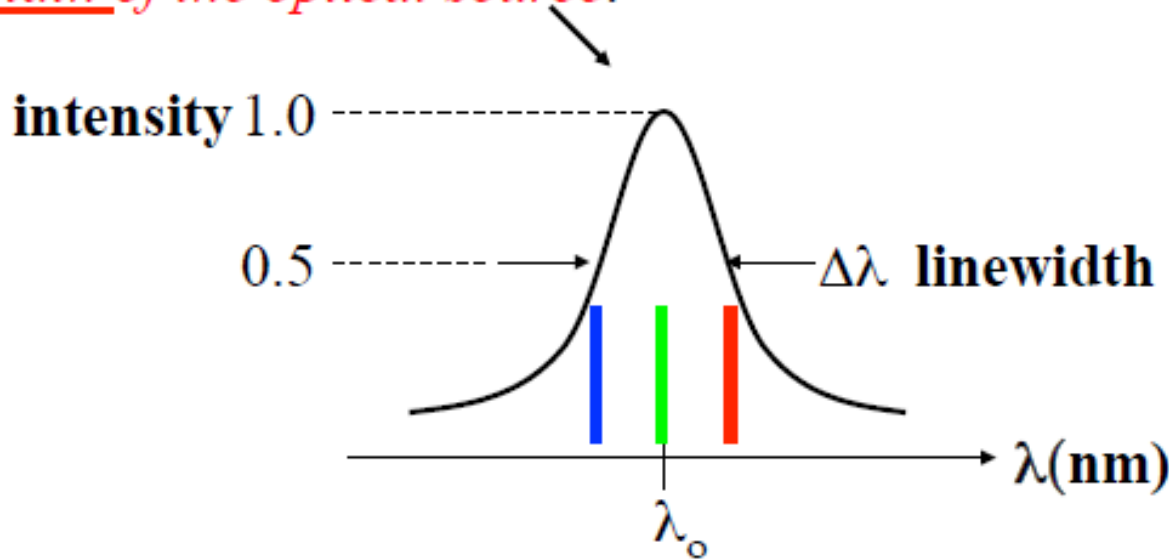
Single-mode fiber eliminates modal dispersion



- The main advantage of *single*-mode fibers is to propagate *only one mode* so that *modal dispersion is absent*.
- However, *pulse broadening does not disappear altogether*. The *group velocity* associated with the fundamental mode is *frequency dependent* within the pulse *spectral linewidth* because of chromatic dispersion.

Chromatic dispersion

- Chromatic dispersion (CD) may occur in *all* types of optical fiber. The optical pulse broadening results from the *finite spectral linewidth of the optical source*.



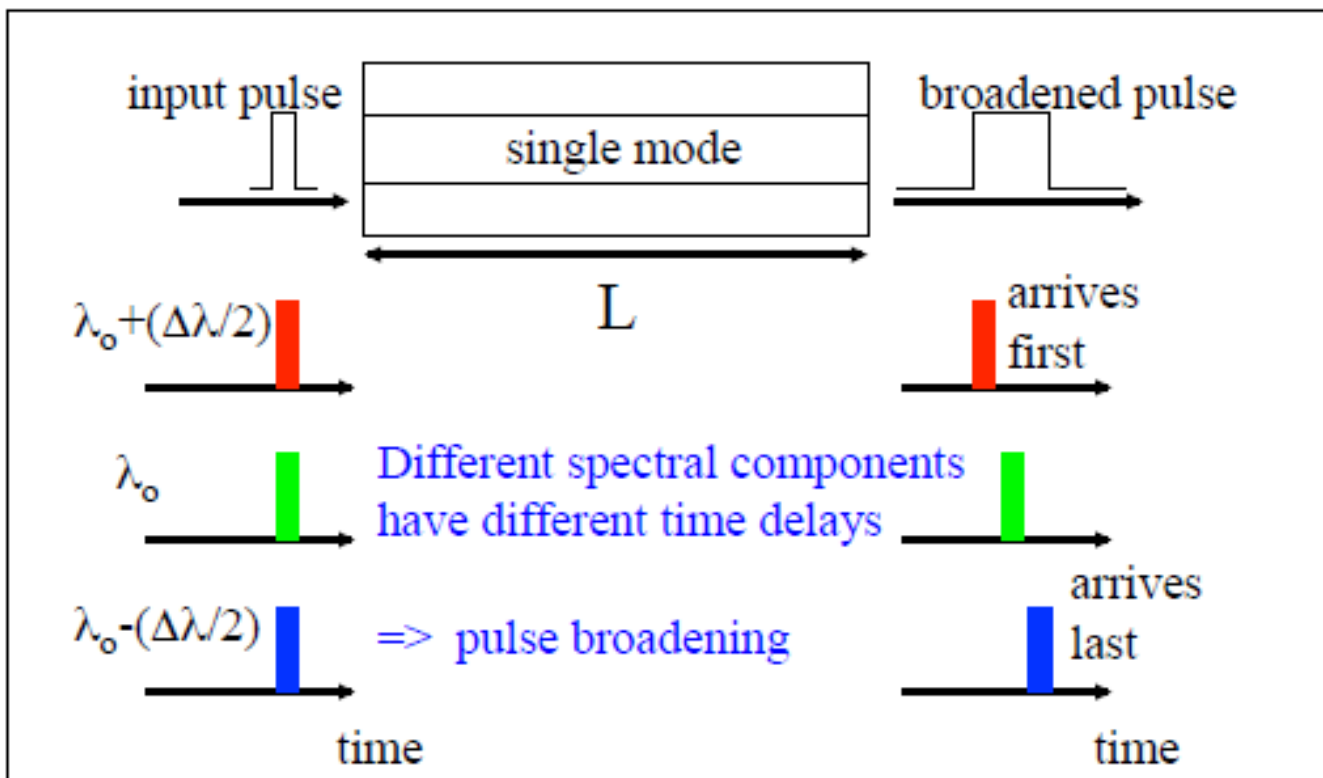
*In the case of the semiconductor laser $\Delta\lambda$ corresponds to only a fraction of % of the centre wavelength λ_o . For LEDs, $\Delta\lambda$ is likely to be a significant percentage of λ_o .

Spectral linewidth

- Real sources emit over a range of wavelengths. This range is the *source linewidth* or *spectral width*.
- The smaller is the linewidth, the smaller the spread in wavelength or frequencies, the more *coherent* is the source.
- A perfectly coherent source emits light at a single wavelength. It has *zero* linewidth and is perfectly monochromatic.

Light sources	Linewidth (nm)
Light-emitting diodes	20 nm – 100 nm
Semiconductor laser diodes	1 nm – 5 nm
Nd:YAG solid-state lasers	0.1 nm
HeNe gas lasers	0.002 nm

Chromatic dispersion



- Pulse broadening occurs because there may be *propagation delay differences* among the *spectral components* of the transmitted signal.
- Chromatic dispersion (CD):** Different spectral components of a *pulse* travel at different *group velocities*. This is also known as *group velocity dispersion (GVD)*.

Light pulse in a dispersive medium

When a *light pulse* with a spread in frequency $\delta\omega$ and a spread in propagation constant δk propagates in a *dispersive* medium $n(\lambda)$, the group velocity:

$$v_g = (d\omega/dk) = (d\lambda/dk) (d\omega/d\lambda)$$

$$k = n(\lambda) 2\pi/\lambda \quad \Rightarrow \quad dk/d\lambda = (2\pi/\lambda) [(dn/d\lambda) - (n/\lambda)]$$

$$\omega = 2\pi c/\lambda \quad \Rightarrow \quad d\omega/d\lambda = -2\pi c/\lambda^2$$

Hence $v_g = c / [n - \lambda(dn/d\lambda)] = c / n_g$

Define the **group refractive index** $n_g = n - \lambda(dn/d\lambda)$

Waveguide dispersion

In fact there are two mechanisms for chromatic dispersion:

(a) Silica refractive index *n is wavelength dependent* (i.e. $n = n(\lambda)$)

=> different wavelength components travel at different speeds in silica

This is known as material dispersion.

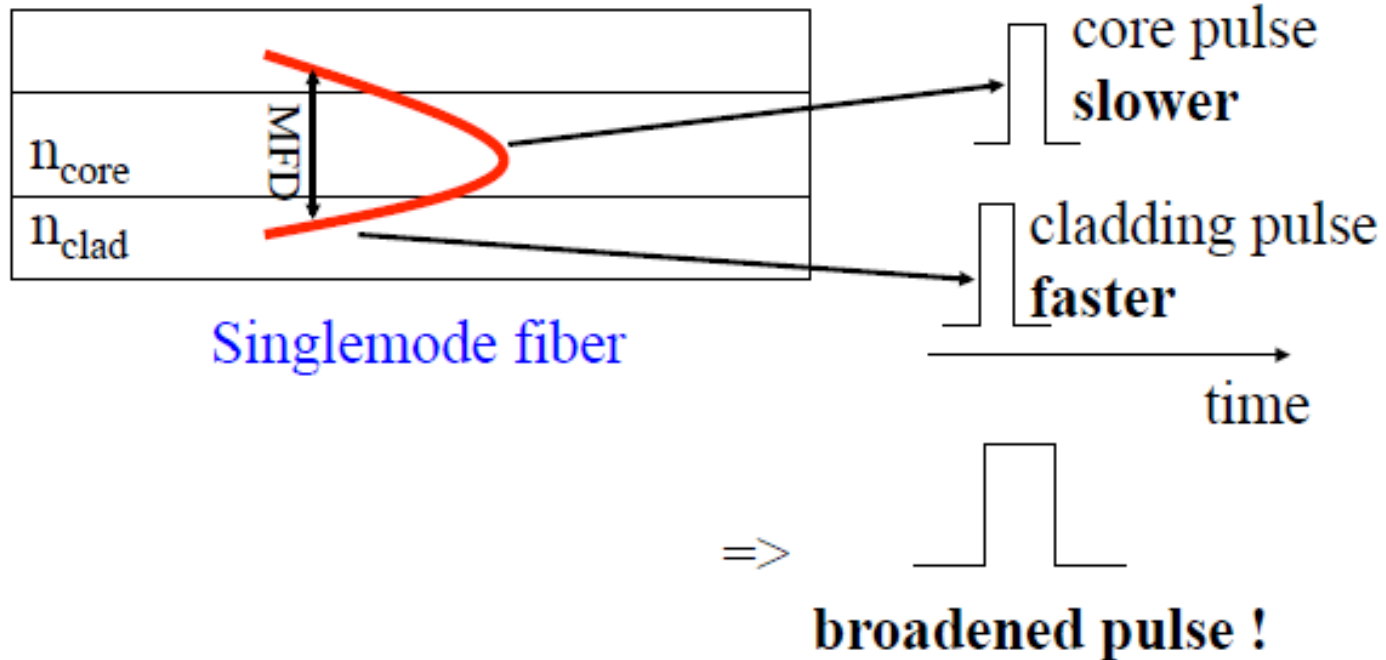
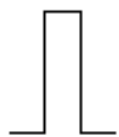
(b) Light energy of a mode propagates *partly in the core and partly in the cladding*. The mode power distribution between the core and the cladding *depends on λ* . (*Recall the mode field diameter*)

This is known as waveguide dispersion.

$$\Rightarrow D(\lambda) = D_{\text{mat}}(\lambda) + D_{\text{wg}}(\lambda)$$

Waveguide dispersion in a single-mode fiber

input pulse



Waveguide dispersion depends on the *mode field distribution in the core and the cladding*. (i.e. the fiber V number)

8

FIBER OPTICS

8.1 STEP-INDEX FIBERS

- A. Guided Rays
- B. Guided Waves
- C. Single-Mode Fibers

8.2 GRADED-INDEX FIBERS

- A. Guided Waves
- B. Propagation Constants and Velocities

8.3 ATTENUATION AND DISPERSION

- A. Attenuation
- B. Dispersion
- C. Pulse Propagation

Dramatic improvements in the development of low-loss materials for optical fibers are responsible for the commercial viability of fiber-optic communications. Corning Incorporated pioneered the development and manufacture of ultra-low-loss glass fibers.



C O R N I N G



An optical fiber is a cylindrical dielectric waveguide made of low-loss materials such as silica glass. It has a central **core** in which the light is guided, embedded in an outer **cladding** of slightly lower refractive index (Fig. 8.0-1). Light rays incident on the core-cladding boundary at angles greater than the critical angle undergo total internal reflection and are guided through the core without refraction. Rays of greater inclination to the fiber axis lose part of their power into the cladding at each reflection and are not guided.

As a result of recent technological advances in fabrication, light can be guided through 1 km of glass fiber with a loss as low as $\approx 0.16 \text{ dB} (\approx 3.6\%)$. Optical fibers are replacing copper coaxial cables as the preferred transmission medium for electromagnetic waves, thereby revolutionizing terrestrial communications. Applications range from long-distance telephone and data communications to computer communications in a local area network.

In this chapter we introduce the principles of light transmission in optical fibers. These principles are essentially the same as those that apply in planar dielectric waveguides (Chap. 7), except for the cylindrical geometry. In both types of waveguide light propagates in the form of modes. Each mode travels along the axis of the waveguide with a distinct propagation constant and group velocity, maintaining its transverse spatial distribution and its polarization. In planar waveguides, we found that each mode was the sum of the multiple reflections of a TEM wave bouncing within the slab in the direction of an optical ray at a certain bounce angle. This approach is approximately applicable to cylindrical waveguides as well. When the core diameter is small, only a single mode is permitted and the fiber is said to be a **single-mode fiber**. Fibers with large core diameters are **multimode fibers**.

One of the difficulties associated with light propagation in multimode fibers arises from the differences among the group velocities of the modes. This results in a variety of travel times so that light pulses are broadened as they travel through the fiber. This effect, called **modal dispersion**, limits the speed at which adjacent pulses can be sent without overlapping and therefore the speed at which a fiber-optic communication system can operate.

Modal dispersion can be reduced by grading the refractive index of the fiber core from a maximum value at its center to a minimum value at the core-cladding boundary. The fiber is then called a **graded-index fiber**, whereas conventional fibers

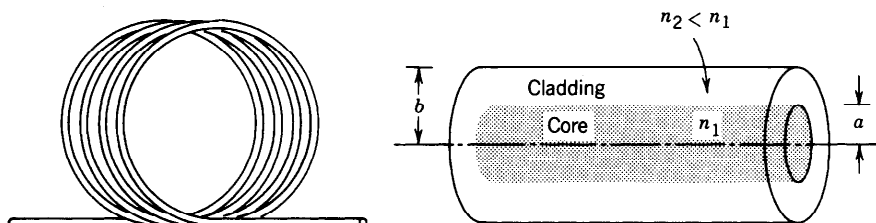


Figure 8.0-1 An optical fiber is a cylindrical dielectric waveguide.

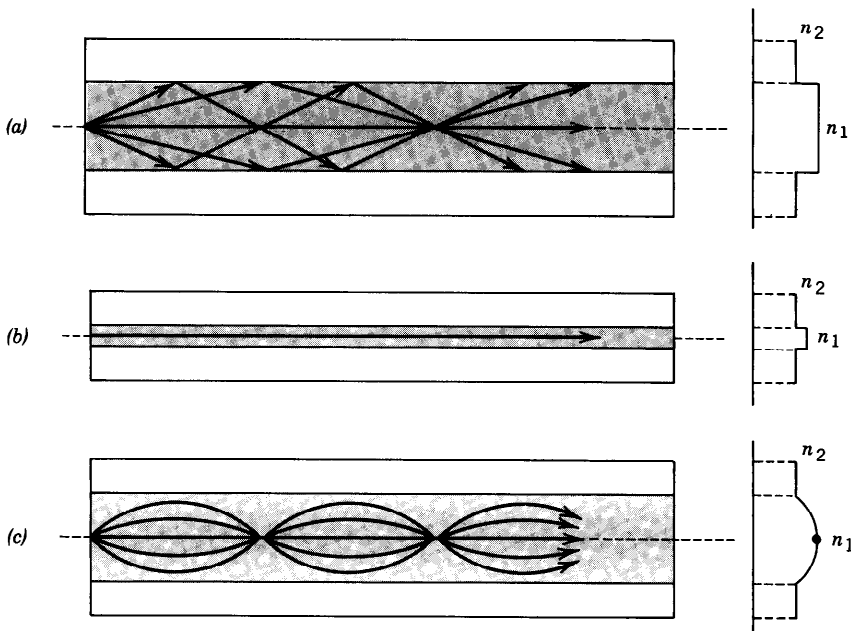


Figure 8.0-2 Geometry, refractive-index profile, and typical rays in: (a) a multimode step-index fiber, (b) a single-mode step-index fiber, and (c) a multimode graded-index fiber.

with constant refractive indices in the core and the cladding are called **step-index fibers**. In a graded-index fiber the velocity increases with distance from the core axis (since the refractive index decreases). Although rays of greater inclination to the fiber axis must travel farther, they travel faster, so that the travel times of the different rays are equalized. Optical fibers are therefore classified as step-index or graded-index, and multimode or single-mode, as illustrated in Fig. 8.0-2.

This chapter emphasizes the nature of optical modes and their group velocities in step-index and graded-index fibers. These topics are presented in Secs. 8.1 and 8.2, respectively. The optical properties of the fiber material (which is usually fused silica), including its attenuation and the effects of material, modal, and waveguide dispersion on the transmission of light pulses, are discussed in Sec. 8.3. Optical fibers are revisited in Chap. 22, which is devoted to their use in lightwave communication systems.

8.1 STEP-INDEX FIBERS

A step-index fiber is a cylindrical dielectric waveguide specified by its core and cladding refractive indices, n_1 and n_2 , and the radii a and b (see Fig. 8.0-1). Examples of standard core and cladding diameters $2a/2b$ are 8/125, 50/125, 62.5/125, 85/125, 100/140 (units of μm). The refractive indices differ only slightly, so that the fractional refractive-index change

$$\Delta = \frac{n_1 - n_2}{n_1} \quad (8.1-1)$$

is small ($\Delta \ll 1$).

Almost all fibers currently used in optical communication systems are made of fused silica glass (SiO_2) of high chemical purity. Slight changes in the refractive index are

made by the addition of low concentrations of doping materials (titanium, germanium, or boron, for example). The refractive index n_1 is in the range from 1.44 to 1.46, depending on the wavelength, and Δ typically lies between 0.001 and 0.02.

A. Guided Rays

An optical ray is guided by total internal reflections within the fiber core if its angle of incidence on the core-cladding boundary is greater than the critical angle $\theta_c = \sin^{-1}(n_2/n_1)$, and remains so as the ray bounces.

Meridional Rays

The guiding condition is simple to see for meridional rays (rays in planes passing through the fiber axis), as illustrated in Fig. 8.1-1. These rays intersect the fiber axis and reflect in the same plane without changing their angle of incidence, as if they were in a planar waveguide. Meridional rays are guided if their angle θ with the fiber axis is smaller than the complement of the critical angle $\bar{\theta}_c = \pi/2 - \theta_c = \cos^{-1}(n_2/n_1)$. Since $n_1 \approx n_2$, $\bar{\theta}_c$ is usually small and the guided rays are approximately paraxial.

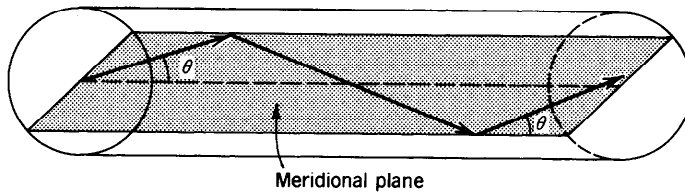


Figure 8.1-1 The trajectory of a meridional ray lies in a plane passing through the fiber axis. The ray is guided if $\theta < \bar{\theta}_c = \cos^{-1}(n_1/n_2)$.

Skewed Rays

An arbitrary ray is identified by its plane of incidence, a plane parallel to the fiber axis and passing through the ray, and by the angle with that axis, as illustrated in Fig. 8.1-2. The plane of incidence intersects the core-cladding cylindrical boundary at an angle ϕ with the normal to the boundary and lies at a distance R from the fiber axis. The ray is identified by its angle θ with the fiber axis and by the angle ϕ of its plane. When $\phi \neq 0$ ($R \neq 0$) the ray is said to be skewed. For meridional rays $\phi = 0$ and $R = 0$.

A skewed ray reflects repeatedly into planes that make the same angle ϕ with the core-cladding boundary, and follows a helical trajectory confined within a cylindrical shell of radii R and a , as illustrated in Fig. 8.1-2. The projection of the trajectory onto the transverse ($x-y$) plane is a regular polygon, not necessarily closed. It can be shown that the condition for a skewed ray to always undergo total internal reflection is that its angle θ with the z axis be smaller than $\bar{\theta}_c$.

Numerical Aperture

A ray incident from air into the fiber becomes a guided ray if upon refraction into the core it makes an angle θ with the fiber axis smaller than $\bar{\theta}_c$. Applying Snell's law at the air-core boundary, the angle θ_a in air corresponding to θ_c in the core is given by the relation $1 \cdot \sin \theta_a = n_1 \sin \theta_c$, from which (see Fig. 8.1-3 and Exercise 1.2-5) $\sin \theta_a = n_1(1 - \cos^2 \bar{\theta}_c)^{1/2} = n_1[1 - (n_2/n_1)^2]^{1/2} = (n_1^2 - n_2^2)^{1/2}$. Therefore

$$\theta_a = \sin^{-1} \text{NA}, \quad (8.1-2)$$

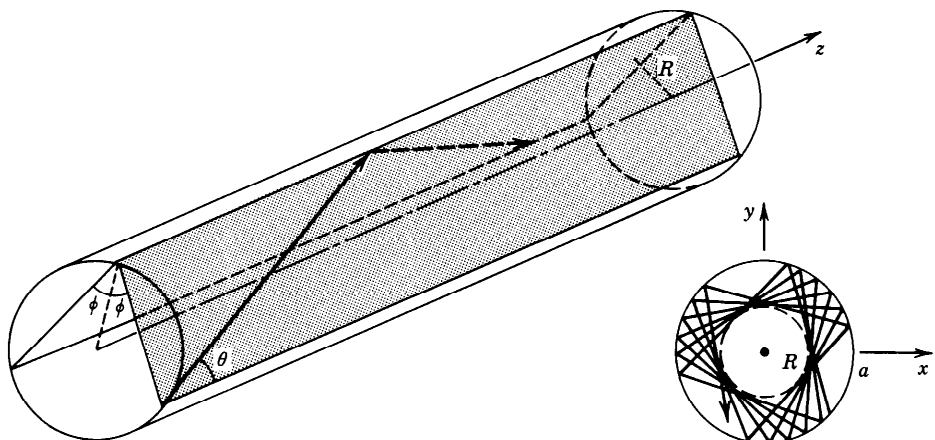


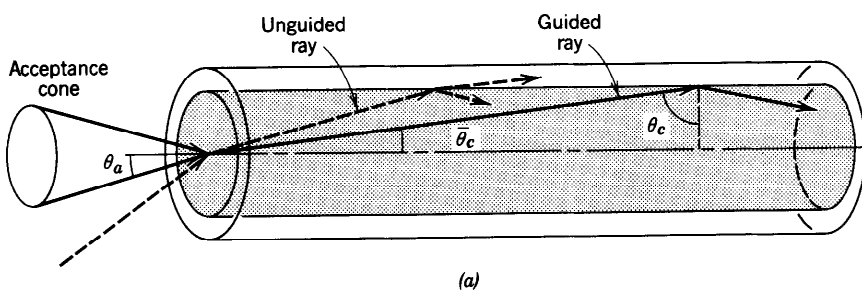
Figure 8.1-2 A skewed ray lies in a plane offset from the fiber axis by a distance R . The ray is identified by the angles θ and ϕ . It follows a helical trajectory confined within a cylindrical shell of radii R and a . The projection of the ray on the transverse plane is a regular polygon that is not necessarily closed.

where

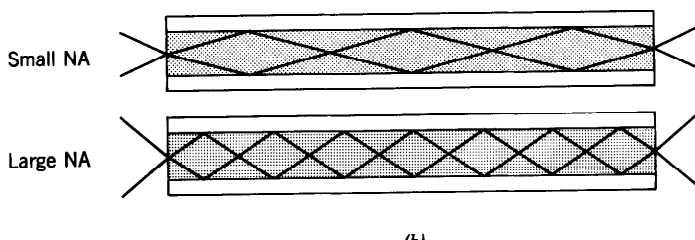
$$\text{NA} = (n_1^2 - n_2^2)^{1/2} \approx n_1(2\Delta)^{1/2}$$

(8.1-3)
Numerical Aperture

is the numerical aperture of the fiber. Thus θ_a is the acceptance angle of the fiber. It



(a)



(b)

Figure 8.1-3 (a) The acceptance angle θ_a of a fiber. Rays within the acceptance cone are guided by total internal reflection. The numerical aperture $\text{NA} = \sin \theta_a$. (b) The light-gathering capacity of a large NA fiber is greater than that of a small NA fiber. The angles θ_a and $\bar{\theta}_c$ are typically quite small; they are exaggerated here for clarity.

determines the cone of external rays that are guided by the fiber. Rays incident at angles greater than θ_a are refracted into the fiber but are guided only for a short distance. The numerical aperture therefore describes the light-gathering capacity of the fiber.

When the guided rays arrive at the other end of the fiber, they are refracted into a cone of angle θ_a . Thus the acceptance angle is a crucial parameter for the design of systems for coupling light into or out of the fiber.

EXAMPLE 8.1-1. Cladded and Uncladded Fibers. In a silica glass fiber with $n_1 = 1.46$ and $\Delta = (n_1 - n_2)/n_1 = 0.01$, the complementary critical angle $\bar{\theta}_c = \cos^{-1}(n_2/n_1) = 8.1^\circ$, and the acceptance angle $\theta_a = 11.9^\circ$, corresponding to a numerical aperture $NA = 0.206$. By comparison, an uncladded silica glass fiber ($n_1 = 1.46$, $n_2 = 1$) has $\bar{\theta}_c = 46.8^\circ$, $\theta_a = 90^\circ$, and $NA = 1$. Rays incident from *all* directions are guided by the uncladded fiber since they reflect within a cone of angle $\bar{\theta}_c = 46.8^\circ$ inside the core. Although its light-gathering capacity is high, the uncladded fiber is not a suitable optical waveguide because of the large number of modes it supports, as will be shown subsequently.

B. Guided Waves

In this section we examine the propagation of monochromatic light in step-index fibers using electromagnetic theory. We aim at determining the electric and magnetic fields of guided waves that satisfy Maxwell's equations and the boundary conditions imposed by the cylindrical dielectric core and cladding. As in all waveguides, there are certain special solutions, called modes (see Appendix C), each of which has a distinct propagation constant, a characteristic field distribution in the transverse plane, and two independent polarization states.

Spatial Distributions

Each of the components of the electric and magnetic fields must satisfy the Helmholtz equation, $\nabla^2 U + n^2 k_o^2 U = 0$, where $n = n_1$ in the core ($r < a$) and $n = n_2$ in the cladding ($r > a$) and $k_o = 2\pi/\lambda_o$ (see Sec. 5.3). We assume that the radius b of the cladding is sufficiently large that it can safely be assumed to be infinite when examining guided light in the core and near the core-cladding boundary. In a cylindrical coordinate system (see Fig. 8.1-4) the Helmholtz equation is

$$\frac{\partial^2 U}{\partial r^2} + \frac{1}{r} \frac{\partial U}{\partial r} + \frac{1}{r^2} \frac{\partial^2 U}{\partial \phi^2} + \frac{\partial^2 U}{\partial z^2} + n^2 k_o^2 U = 0, \quad (8.1-4)$$

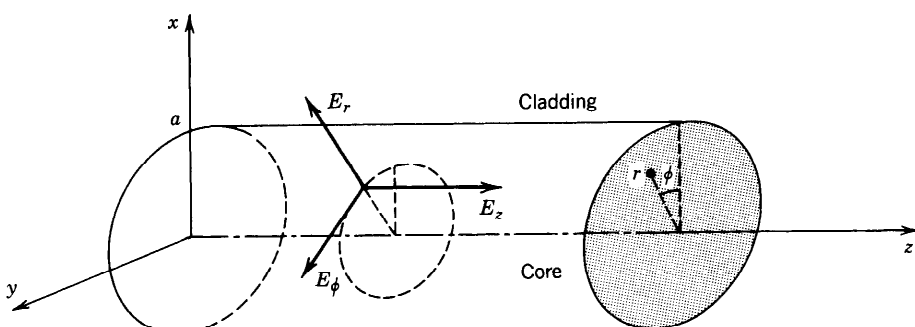


Figure 8.1-4 Cylindrical coordinate system.

278 FIBER OPTICS

where the complex amplitude $U = U(r, \phi, z)$ represents any of the Cartesian components of the electric or magnetic fields or the axial components E_z and H_z in cylindrical coordinates.

We are interested in solutions that take the form of waves traveling in the z direction with a propagation constant β , so that the z dependence of U is of the form $e^{-j\beta z}$. Since U must be a periodic function of the angle ϕ with period 2π , we assume that the dependence on ϕ is harmonic, $e^{-jl\phi}$, where l is an integer. Substituting

$$U(r, \phi, z) = u(r)e^{-jl\phi}e^{-j\beta z}, \quad l = 0, \pm 1, \pm 2, \dots, \quad (8.1-5)$$

into (8.1-4), an ordinary differential equation for $u(r)$ is obtained:

$$\frac{d^2u}{dr^2} + \frac{1}{r} \frac{du}{dr} + \left(n_1^2 k_o^2 - \beta^2 - \frac{l^2}{r^2} \right) u = 0. \quad (8.1-6)$$

As in Sec. 7.2B, the wave is guided (or bound) if the propagation constant is smaller than the wavenumber in the core ($\beta < n_1 k_o$) and greater than the wavenumber in the cladding ($\beta > n_2 k_o$). It is therefore convenient to define

$$k_T^2 = n_1^2 k_o^2 - \beta^2 \quad (8.1-7a)$$

and

$$\gamma^2 = \beta^2 - n_2^2 k_o^2, \quad (8.1-7b)$$

so that for guided waves k_T^2 and γ^2 are positive and k_T and γ are real. Equation (8.1-6) may then be written in the core and cladding separately:

$$\frac{d^2u}{dr^2} + \frac{1}{r} \frac{du}{dr} + \left(k_T^2 - \frac{l^2}{r^2} \right) u = 0, \quad r < a \text{ (core)}, \quad (8.1-8a)$$

$$\frac{d^2u}{dr^2} + \frac{1}{r} \frac{du}{dr} - \left(\gamma^2 + \frac{l^2}{r^2} \right) u = 0, \quad r > a \text{ (cladding)}. \quad (8.1-8b)$$

Equations (8.1-8) are well-known differential equations whose solutions are the family of Bessel functions. Excluding functions that approach ∞ at $r = 0$ in the core or at $r \rightarrow \infty$ in the cladding, we obtain the bounded solutions:

$$u(r) \propto \begin{cases} J_l(k_T r), & r < a \text{ (core)} \\ K_l(\gamma r), & r > a \text{ (cladding)}, \end{cases} \quad (8.1-9)$$

where $J_l(x)$ is the Bessel function of the first kind and order l , and $K_l(x)$ is the modified Bessel function of the second kind and order l . The function $J_l(x)$ oscillates like the sine or cosine functions but with a decaying amplitude. In the limit $x \gg 1$,

$$J_l(x) \approx \left(\frac{2}{\pi x} \right)^{1/2} \cos \left[x - \left(l + \frac{1}{2} \right) \frac{\pi}{2} \right], \quad x \gg 1. \quad (8.1-10a)$$

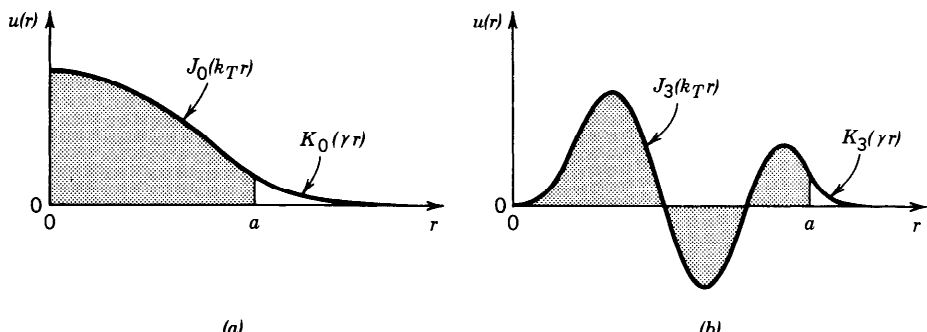


Figure 8.1-5 Examples of the radial distribution $u(r)$ given by (8.1-9) for (a) $l = 0$ and (b) $l = 3$. The shaded areas represent the fiber core and the unshaded areas the cladding. The parameters k_T and γ and the two proportionality constants in (8.1-9) have been selected such that $u(r)$ is continuous and has a continuous derivative at $r = a$. Larger values of k_T and γ lead to a greater number of oscillations in $u(r)$.

In the same limit, $K_1(x)$ decays with increasing x at an exponential rate,

$$K_l(x) \approx \left(\frac{\pi}{2x}\right)^{1/2} \left(1 + \frac{4l^2 - 1}{8x}\right) \exp(-x), \quad x \gg 1. \quad (8.1-10b)$$

Two examples of the radial distribution $u(r)$ are shown in Fig. 8.1-5.

The parameters k_T and γ determine the rate of change of $u(r)$ in the core and in the cladding, respectively. A large value of k_T means faster oscillation of the radial distribution in the core. A large value of γ means faster decay and smaller penetration of the wave into the cladding. As can be seen from (8.1-7), the sum of the squares of k_T and γ is a constant.

$$k_T^2 + \gamma^2 = (n_1^2 - n_2^2) k_o^2 = \text{NA}^2 \cdot k_o^2, \quad (8.1-11)$$

so that as k_T increases, γ decreases and the field penetrates deeper into the cladding. As k_T exceeds $NA \cdot k_o$, γ becomes imaginary and the wave ceases to be bound to the core.

The V Parameter

It is convenient to normalize k_T and γ by defining

$$X = k_T a, \quad Y = \gamma a. \quad (8.1-12)$$

In view of (8.1-11),

$$X^2 + Y^2 = V^2, \quad (8.1-13)$$

where $V = NA \cdot k_o a$, from which

$$V = 2\pi \frac{a}{\lambda_o} NA. \quad (8.1-14)$$

As we shall see shortly, V is an important parameter that governs the number of modes

280 FIBER OPTICS

of the fiber and their propagation constants. It is called the **fiber parameter** or **V parameter**. It is important to remember that for the wave to be guided, X must be smaller than V .

Modes

We now consider the boundary conditions. We begin by writing the axial components of the electric- and magnetic-field complex amplitudes E_z and H_z in the form of (8.1-5). The condition that these components must be continuous at the core-cladding boundary $r = a$ establishes a relation between the coefficients of proportionality in (8.1-9), so that we have only one unknown for E_z and one unknown for H_z . With the help of Maxwell's equations, $j\omega\epsilon_0n^2\mathbf{E} = \nabla \times \mathbf{H}$ and $-j\omega\mu_0\mathbf{H} = \nabla \times \mathbf{E}$, the remaining four components E_ϕ , H_ϕ , E_r , and H_r are determined in terms of E_z and H_z . Continuity of E_ϕ and H_ϕ at $r = a$ yields two more equations. One equation relates the two unknown coefficients of proportionality in E_z and H_z ; the other equation gives a condition that the propagation constant β must satisfy. This condition, called the **characteristic equation** or **dispersion relation**, is an equation for β with the ratio a/λ_0 and the fiber indices n_1, n_2 as known parameters.

For each azimuthal index l , the characteristic equation has multiple solutions yielding discrete propagation constants β_{lm} , $m = 1, 2, \dots$, each solution representing a mode. The corresponding values of k_T and γ , which govern the spatial distributions in the core and in the cladding, respectively, are determined by use of (8.1-7) and are denoted k_{Tlm} and γ_{lm} . A mode is therefore described by the indices l and m characterizing its azimuthal and radial distributions, respectively. The function $u(r)$ depends on both l and m ; $l = 0$ corresponds to meridional rays. There are two independent configurations of the \mathbf{E} and \mathbf{H} vectors for each mode, corresponding to two states of polarization. The classification and labeling of these configurations are generally quite involved (see specialized books in the reading list for more details).

Characteristic Equation for the Weakly Guiding Fiber

Most fibers are weakly guiding (i.e., $n_1 \approx n_2$ or $\Delta \ll 1$) so that the guided rays are paraxial (i.e., approximately parallel to the fiber axis). The longitudinal components of the electric and magnetic fields are then much weaker than the transverse components and the guided waves are approximately transverse electromagnetic (TEM). The linear polarization in the x and y directions then form orthogonal states of polarization. The linearly polarized (l, m) mode is usually denoted as the LP_{lm} mode. The two polarizations of mode (l, m) travel with the same propagation constant and have the same spatial distribution.

For weakly guiding fibers the characteristic equation obtained using the procedure outlined earlier turns out to be approximately equivalent to the conditions that the scalar function $u(r)$ in (8.1-9) is continuous and has a continuous derivative at $r = a$. These two conditions are satisfied if

$$\frac{(k_T a) J'_l(k_T a)}{J_l(k_T a)} = \frac{(\gamma a) K'_l(\gamma a)}{K_l(\gamma a)}. \quad (8.1-15)$$

The derivatives J'_l and K'_l of the Bessel functions satisfy the identities

$$J'_l(x) = \pm J_{l \mp 1}(x) \mp l \frac{J_l(x)}{x}$$

$$K'_l(x) = -K_{l \mp 1}(x) \mp l \frac{K_l(x)}{x}.$$

Substituting these identities into (8.1-15) and using the normalized parameters $X = k_T a$ and $Y = \gamma a$, we obtain the characteristic equation

$$X \frac{J_{l\pm 1}(X)}{J_l(X)} = \pm Y \frac{K_{l\pm 1}(Y)}{K_l(Y)}. \quad (8.1-16)$$

Characteristic
Equation

$$X^2 + Y^2 = V^2$$

Given V and l , the characteristic equation contains a single unknown variable X (since $Y^2 = V^2 - X^2$). Note that $J_{-l}(x) = (-1)^l J_l(x)$ and $K_{-l}(x) = K_l(x)$, so that if l is replaced with $-l$, the equation remains unchanged.

The characteristic equation may be solved graphically by plotting its right- and left-hand sides (RHS and LHS) versus X and finding the intersections. As illustrated in Fig. 8.1-6 for $l = 0$, the LHS has multiple branches and the RHS drops monotonically with increase of X until it vanishes at $X = V$ ($Y = 0$). There are therefore multiple intersections in the interval $0 < X \leq V$. Each intersection point corresponds to a fiber mode with a distinct value of X . These values are denoted X_{lm} , $m = 1, 2, \dots, M_l$ in order of increasing X . Once the X_{lm} are found, the corresponding transverse propagation constants k_{Tlm} , the decay parameters γ_{lm} , the propagation constants β_{lm} , and the radial distribution functions $u_{lm}(r)$ may be readily determined by use of (8.1-12), (8.1-7), and (8.1-9). The graph in Fig. 8.1-6 is similar to that in Fig. 7.2-2, which governs the modes of a planar dielectric waveguide.

Each mode has a distinct radial distribution. The radial distributions $u(r)$ shown in Fig. 8.1-5, for example, correspond to the LP_{01} mode ($l = 0, m = 1$) in a fiber with $V = 5$; and the LP_{34} mode ($l = 3, m = 4$) in a fiber with $V = 25$. Since the (l, m) and $(-l, m)$ modes have the same propagation constant, it is interesting to examine the spatial distribution of their superposition (with equal weights). The complex amplitude of the sum is proportional to $u_{lm}(r) \cos l\phi \exp(-j\beta_{lm}z)$. The intensity, which is proportional to $u_{lm}^2(r) \cos^2 l\phi$, is illustrated in Fig. 8.1-7 for the LP_{01} and LP_{34} modes (the same modes for which $u(r)$ is shown in Fig. 8.1-5).

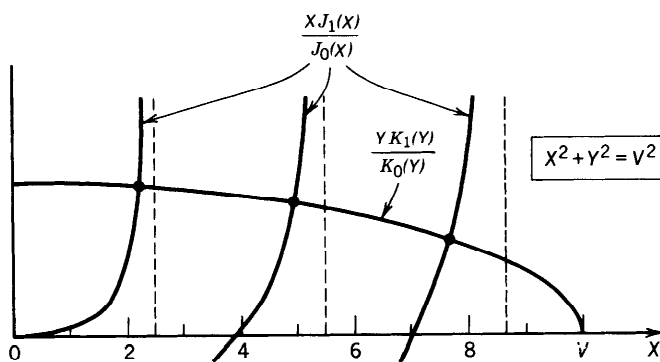


Figure 8.1-6 Graphical construction for solving the characteristic equation (8.1-16). The left- and right-hand sides are plotted as functions of X . The intersection points are the solutions. The LHS has multiple branches intersecting the abscissa at the roots of $J_{l\pm 1}(X)$. The RHS intersects each branch once and meets the abscissa at $X = V$. The number of modes therefore equals the number of roots of $J_{l\pm 1}(X)$ that are smaller than V . In this plot $l = 0$, $V = 10$, and either the $-$ or $+$ signs in (8.1-16) may be taken.

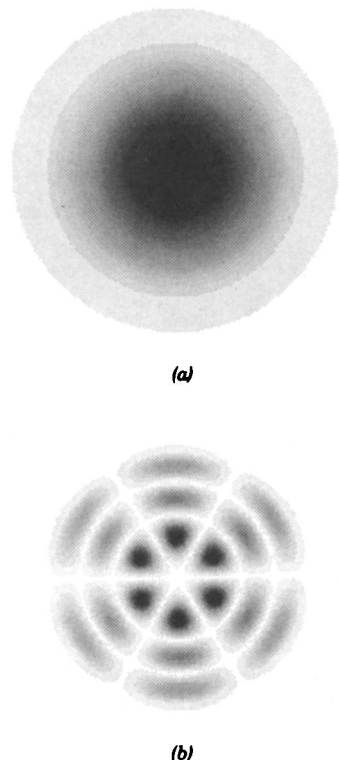


Figure 8.1-7 Distributions of the intensity of the (a) LP_{01} and (b) LP_{34} modes in the transverse plane, assuming an azimuthal $\cos l\phi$ dependence. The fundamental LP_{01} mode has a distribution similar to that of the Gaussian beam discussed in Chap. 3.

Mode Cutoff and Number of Modes

It is evident from the graphical construction in Fig. 8.1-6 that as V increases, the number of intersections (modes) increases since the LHS of the characteristic equation (8.1-16) is independent of V , whereas the RHS moves to the right as V increases. Considering the minus signs in the characteristic equation, branches of the LHS intersect the abscissa when $J_{l-1}(X) = 0$. These roots are denoted by x_{lm} , $m = 1, 2, \dots$. The number of modes M_l is therefore equal to the number of roots of $J_{l-1}(X)$ that are smaller than V . The (l, m) mode is allowed if $V > x_{lm}$. The mode reaches its cutoff point when $V = x_{lm}$. As V decreases further, the $(l, m - 1)$ mode also reaches its cutoff point when a new root is reached, and so on. The smallest root of $J_{l-1}(X)$ is $x_{01} = 0$ for $l = 0$ and the next smallest is $x_{11} = 2.405$ for $l = 1$. When $V < 2.405$, all modes with the exception of the fundamental LP_{01} mode are cut off. The fiber then operates as a single-mode waveguide. A plot of the number of modes M_l as a function of V is therefore a staircase function increasing by unity at each of the roots x_{lm} of the Bessel function $J_{l-1}(X)$. Some of these roots are listed in Table 8.1-1.

TABLE 8.1-1 Cutoff V Parameter for the LP_{0m} and LP_{1m} Modes^a

l	$m:$	1	2	3
0		0	3.832	7.016
1		2.405	5.520	8.654

^aThe cutoffs of the $l = 0$ modes occur at the roots of $J_{-1}(X) = -J_1(X)$. The $l = 1$ modes are cut off at the roots of $J_0(X)$, and so on.

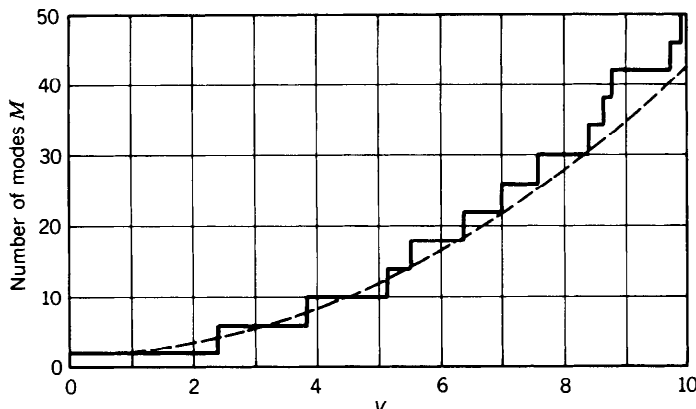


Figure 8.1-8 Total number of modes M versus the fiber parameter $V = 2\pi(a/\lambda_o)\text{NA}$. Included in the count are two helical polarities for each mode with $l > 0$ and two polarizations per mode. For $V < 2.405$, there is only one mode, the fundamental LP_{01} mode with two polarizations. The dashed curve is the relation $M = 4V^2/\pi^2 + 2$, which provides an approximate formula for the number of modes when $V \gg 1$.

A composite count of the total number of modes M (for all l) is shown in Fig. 8.1-8 as a function of V . This is a staircase function with jumps at the roots of $J_{l-1}(X)$. Each root must be counted twice since for each mode of azimuthal index $l > 0$ there is a corresponding mode $-l$ that is identical except for an opposite polarity of the angle ϕ (corresponding to rays with helical trajectories of opposite senses) as can be seen by using the plus signs in the characteristic equation. In addition, each mode has two states of polarization and must therefore be counted twice.

Number of Modes (Fibers with Large V Parameter)

For fibers with large V parameters, there are a large number of roots of $J_l(X)$ in the interval $0 < X < V$. Since $J_l(X)$ is approximated by the sinusoidal function in (8.1-10a) when $X \gg 1$, its roots x_{lm} are approximately given by $x_{lm} - (l + \frac{1}{2})(\pi/2) = (2m - 1)(\pi/2)$, i.e., $x_{lm} = (l + 2m - \frac{1}{2})\pi/2$, so that the cutoff points of modes (l, m) , which are the roots of $J_{l\pm 1}(X)$, are

$$x_{lm} \approx \left(l + 2m - \frac{1}{2} \pm 1\right) \frac{\pi}{2} \approx (l + 2m) \frac{\pi}{2}, \quad l = 0, 1, \dots; \quad m \gg 1, \quad (8.1-17)$$

when m is large.

For a fixed l , these roots are spaced uniformly at a distance π , so that the number of roots M_l satisfies $(l + 2M_l)\pi/2 = V$, from which $M_l \approx V/\pi - l/2$. Thus M_l drops linearly with increasing l , beginning with $M_l \approx V/\pi$ for $l = 0$ and ending at $M_l = 0$ when $l = l_{\max}$, where $l_{\max} = 2V/\pi$, as illustrated in Fig. 8.1-9. Thus the total number of modes is $M \approx \sum_{l=0}^{l_{\max}} M_l = \sum_{l=0}^{l_{\max}} (V/\pi - l/2)$.

Since the number of terms in this sum is assumed large, it may be readily evaluated by approximating it as the area of the triangle in Fig. 8.1-9, $M \approx \frac{1}{2}(2V/\pi)(V/\pi) = V^2/\pi^2$. Allowing for two degrees of freedom for positive and negative l and two polarizations for each index (l, m) , we obtain

$$M \approx \frac{4}{\pi^2} V^2.$$

(8.1-18)

Number of Modes
($V \gg 1$)

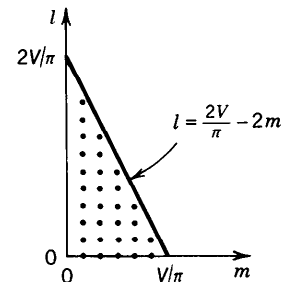


Figure 8.1-9 The indices of guided modes extend from $m = 1$ to $m \approx V/\pi - l/2$ and from $l = 0$ to $\approx 2V/\pi$.

This expression for M is analogous to that for the rectangular waveguide (7.3-3). Note that (8.1-18) is valid only for large V . This approximate number is compared to the exact number obtained from the characteristic equation in Fig. 8.1-8.

EXAMPLE 8.1-2. Approximate Number of Modes. A silica fiber with $n_1 = 1.452$ and $\Delta = 0.01$ has a numerical aperture $\text{NA} = (n_1^2 - n_2^2)^{1/2} \approx n_1(2\Delta)^{1/2} \approx 0.205$. If $\lambda_o = 0.85 \mu\text{m}$ and the core radius $a = 25 \mu\text{m}$, the V parameter is $V = 2\pi(a/\lambda_o)\text{NA} \approx 37.9$. There are therefore approximately $M \approx 4V^2/\pi^2 \approx 585$ modes. If the cladding is stripped away so that the core is in direct contact with air, $n_2 = 1$ and $\text{NA} = 1$. The V parameter is then $V = 184.8$ and more than 13,800 modes are allowed.

Propagation Constants (Fibers with Large V Parameter)

As mentioned earlier, the propagation constants can be determined by solving the characteristic equation (8.1-16) for the X_{lm} and using (8.1-7a) and (8.1-12) to obtain $\beta_{lm} = (n_1^2 k_o^2 - X_{lm}^2/a^2)^{1/2}$. A number of approximate formulas for X_{lm} applicable in certain limits are available in the literature, but there are no explicit exact formulas.

If $V \gg 1$, the crudest approximation is to assume that the X_{lm} are equal to the cutoff values x_{lm} . This is equivalent to assuming that the branches in Fig. 8.1-6 are approximately vertical lines, so that $X_{lm} \approx x_{lm}$. Since $V \gg 1$, the majority of the roots would be large and the approximation in (8.1-17) may be used to obtain

$$\beta_{lm} \approx \left[n_1^2 k_o^2 - (l + 2m)^2 \frac{\pi^2}{4a^2} \right]^{1/2}. \quad (8.1-19)$$

Since

$$M \approx \frac{4}{\pi^2} V^2 = \frac{4}{\pi^2} \text{NA}^2 \cdot a^2 k_o^2 \approx \frac{4}{\pi^2} (2n_1^2 \Delta) k_o^2 a^2, \quad (8.1-20)$$

(8.1-19) and (8.1-20) give

$$\beta_{lm} \approx n_1 k_o \left[1 - 2 \frac{(l + 2m)^2}{M} \Delta \right]^{1/2}. \quad (8.1-21)$$

Because Δ is small we use the approximation $(1 + \delta)^{1/2} \approx 1 + \delta/2$ for $|\delta| \ll 1$, and

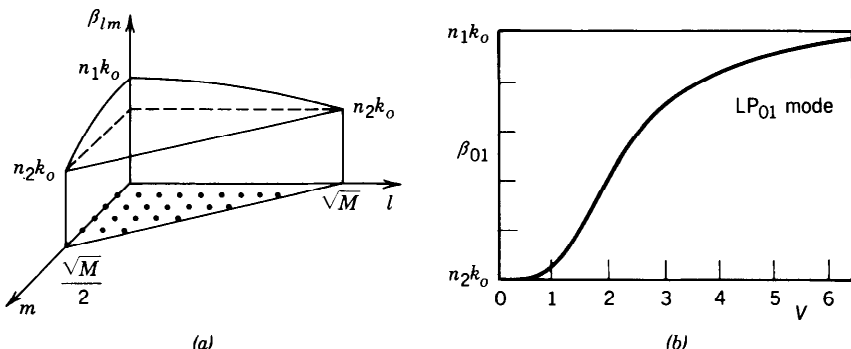


Figure 8.1-10 (a) Approximate propagation constants β_{lm} of the modes of a fiber with large V parameter as functions of the mode indices l and m . (b) Exact propagation constant β_{01} of the fundamental LP_{01} modes as a function of the V parameter. For $V \gg 1$, $\beta_{01} \approx n_1 k_o$.

obtain

$$\beta_{lm} \approx n_1 k_o \left[1 - \frac{(l + 2m)^2}{M} \Delta \right]. \quad (8.1-22)$$

Propagation Constants

$$l = 0, 1, \dots, \sqrt{M}$$

$$m = 1, 2, \dots, (\sqrt{M} - l)/2$$

$$(V \gg 1)$$

Since $l + 2m$ varies between 2 and $\approx 2V/\pi = \sqrt{M}$ (see Fig. 8.1-9), β_{lm} varies approximately between $n_1 k_o$ and $n_1 k_o(1 - \Delta) \approx n_2 k_o$, as illustrated in Fig. 8.1-10.

Group Velocities (Fibers with Large V Parameter)

To determine the group velocity, $v_{lm} = d\omega/d\beta_{lm}$, of the (l, m) mode we express β_{lm} as an explicit function of ω by substituting $n_1 k_o = \omega/c_1$ and $M = (4/\pi^2)(2n_1^2\Delta)c_1^2a^2 = (8/\pi^2)a^2\omega^2\Delta/c_1^2$ into (8.1-22) and assume that c_1 and Δ are independent of ω . The derivative $d\omega/d\beta_{lm}$ gives

$$v_{lm} \approx c_1 \left[1 + \frac{(l + 2m)^2}{M} \Delta \right]^{-1}.$$

Since $\Delta \ll 1$, the approximate expansion $(1 + \delta)^{-1} \approx 1 - \delta$ when $|\delta| \ll 1$, gives

$$v_{lm} \approx c_1 \left[1 - \frac{(l + 2m)^2}{M} \Delta \right].$$

$$(8.1-23)$$

Group Velocities
($V \gg 1$)

Because the minimum and maximum values of $(l + 2m)$ are 2 and \sqrt{M} , respectively, and since $M \gg 1$, the group velocity varies approximately between c_1 and $c_1(1 - \Delta) = c_1(n_2/n_1)$. Thus the group velocities of the low-order modes are approximately equal to the phase velocity of the core material, and those of the high-order modes are smaller.

286 FIBER OPTICS

The fractional group-velocity change between the fastest and the slowest mode is roughly equal to Δ , the fractional refractive index change of the fiber. Fibers with large Δ , although endowed with a large NA and therefore large light-gathering capacity, also have a large number of modes, large modal dispersion, and consequently high pulse spreading rates. These effects are particularly severe if the cladding is removed altogether.

C. Single-Mode Fibers

As discussed earlier, a fiber with core radius a and numerical aperture NA operates as a single-mode fiber in the fundamental LP₀₁ mode if $V = 2\pi(a/\lambda_o)NA < 2.405$ (see Table 8.1-1 on page 282). Single-mode operation is therefore achieved by using a small core diameter and small numerical aperture (making n_2 close to n_1), or by operating at a sufficiently long wavelength. The fundamental mode has a bell-shaped spatial distribution similar to the Gaussian distribution [see Figs. 8.1-5(a) and 8.1-7(a)] and a propagation constant β that depends on V as illustrated in Fig. 8.1-10(b). This mode provides the highest confinement of light power within the core.

EXAMPLE 8.1-3. Single-Mode Operation. A silica glass fiber with $n_1 = 1.447$ and $\Delta = 0.01$ (NA = 0.205) operates at $\lambda_o = 1.3 \mu\text{m}$ as a single-mode fiber if $V = 2\pi(a/\lambda_o)NA < 2.405$, i.e., if the core diameter $2a < 4.86 \mu\text{m}$. If Δ is reduced to 0.0025, single-mode operation requires a diameter $2a < 9.72 \mu\text{m}$.

There are numerous advantages of using single-mode fibers in optical communication systems. As explained earlier, the modes of a multimode fiber travel at different group velocities and therefore undergo different time delays, so that a short-duration pulse of multimode light is delayed by different amounts and therefore spreads in time. Quantitative measures of modal dispersion are determined in Sec. 8.3B. In a single-mode fiber, on the other hand, there is only one mode with one group velocity, so that a short pulse of light arrives without delay distortion. As explained in Sec. 8.3B, other dispersion effects result in pulse spreading in single-mode fibers, but these are significantly smaller than modal dispersion.

As also shown in Sec. 8.3, the rate of power attenuation is lower in a single-mode fiber than in a multimode fiber. This, together with the smaller pulse spreading rate, permits substantially higher data rates to be transmitted by single-mode fibers in comparison with the maximum rates feasible with multimode fibers. This topic is discussed in Chap. 22.

Another difficulty with multimode fibers is caused by the random interference of the modes. As a result of uncontrollable imperfections, strains, and temperature fluctuations, each mode undergoes a random phase shift so that the sum of the complex amplitudes of the modes has a random intensity. This randomness is a form of noise known as **modal noise** or **speckle**. This effect is similar to the fading of radio signals due to multiple-path transmission. In a single-mode fiber there is only one path and therefore no modal noise.

Because of their small size and small numerical apertures, single-mode fibers are more compatible with integrated-optics technology. However, such features make them more difficult to manufacture and work with because of the reduced allowable mechanical tolerances for splicing or joining with demountable connectors and for coupling optical power into the fiber.

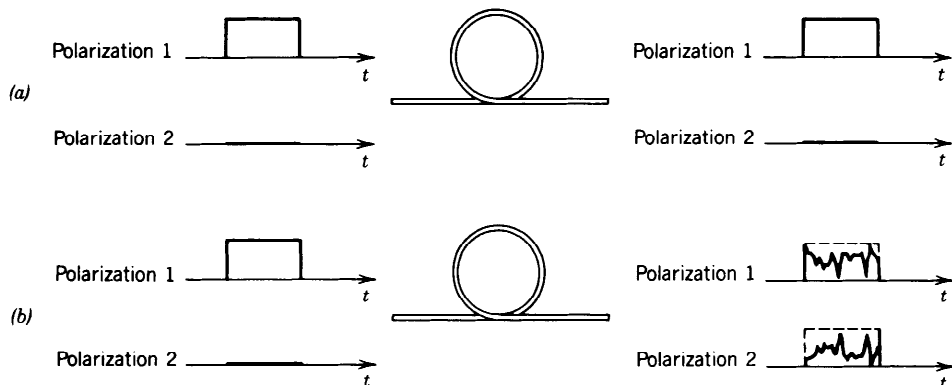


Figure 8.1-11 (a) Ideal polarization-maintaining fiber. (b) Random transfer of power between two polarizations.

Polarization-Maintaining Fibers

In a fiber with circular cross section, each mode has two independent states of polarization with the same propagation constant. Thus the fundamental LP_{01} mode in a single-mode weakly guiding fiber may be polarized in the x or y direction with the two orthogonal polarizations having the same propagation constant and the same group velocity.

In principle, there is no exchange of power between the two polarization components. If the power of the light source is delivered into one polarization only, the power received remains in that polarization. In practice, however, slight random imperfections or uncontrollable strains in the fiber result in random power transfer between the two polarizations. This coupling is facilitated since the two polarizations have the same propagation constant and their phases are therefore matched. Thus linearly polarized light at the fiber input is transformed into elliptically polarized light at the output. As a result of fluctuations of strain, temperature, or source wavelength, the ellipticity of the received light fluctuates randomly with time. Nevertheless, the total power remains fixed (Fig. 8.1-11). If we are interested only in transmitting light power, this randomization of the power division between the two polarization components poses no difficulty, provided that the total power is collected.

In many areas related to fiber optics, e.g., coherent optical communications, integrated-optic devices, and optical sensors based on interferometric techniques, the fiber is used to transmit the complex amplitude of a specific polarization (magnitude and phase). For these applications, polarization-maintaining fibers are necessary. To make a polarization-maintaining fiber the circular symmetry of the conventional fiber must be removed, by using fibers with elliptical cross sections or stress-induced anisotropy of the refractive index, for example. This eliminates the polarization degeneracy, i.e., makes the propagation constants of the two polarizations different. The coupling efficiency is then reduced as a result of the introduction of phase mismatch.

8.2 GRADED-INDEX FIBERS

Index grading is an ingenious method for reducing the pulse spreading caused by the differences in the group velocities of the modes of a multimode fiber. The core of a graded-index fiber has a varying refractive index, highest in the center and decreasing gradually to its lowest value at the cladding. The phase velocity of light is therefore minimum at the center and increases gradually with the radial distance. Rays of the

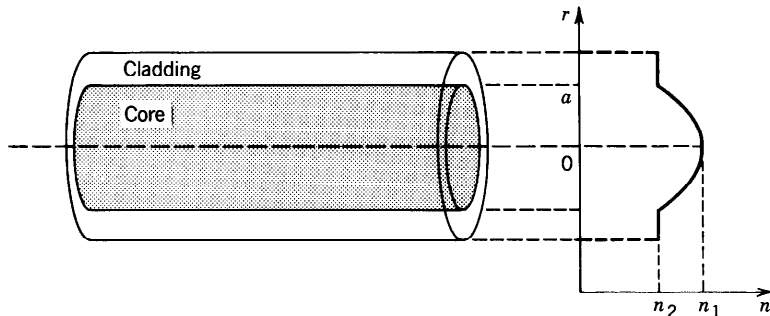


Figure 8.2-1 Geometry and refractive-index profile of a graded-index fiber.

most axial mode travel the shortest distance at the smallest phase velocity. Rays of the most oblique mode zigzag at a greater angle and travel a longer distance, mostly in a medium where the phase velocity is high. Thus the disparities in distances are compensated by opposite disparities in phase velocities. As a consequence, the differences in the group velocities and the travel times are expected to be reduced. In this section we examine the propagation of light in graded-index fibers.

The core refractive index is a function $n(r)$ of the radial position r and the cladding refractive index is a constant n_2 . The highest value of $n(r)$ is $n(0) = n_1$ and the lowest value occurs at the core radius $r = a$, $n(a) = n_2$, as illustrated in Fig. 8.2-1.

A versatile refractive-index profile is the power-law function

$$n^2(r) = n_1^2 \left[1 - 2 \left(\frac{r}{a} \right)^p \Delta \right], \quad r \leq a, \quad (8.2-1)$$

where

$$\Delta = \frac{n_1^2 - n_2^2}{2n_1^2} \approx \frac{n_1 - n_2}{n_1}, \quad (8.2-2)$$

and p , called the **grade profile parameter**, determines the steepness of the profile. This function drops from n_1 at $r = 0$ to n_2 at $r = a$. For $p = 1$, $n^2(r)$ is linear, and for $p = 2$ it is quadratic. As $p \rightarrow \infty$, $n^2(r)$ approaches a step function, as illustrated in Fig. 8.2-2. Thus the step-index fiber is a special case of the graded-index fiber with $p = \infty$.

Guided Rays

The transmission of light rays in a graded-index medium with parabolic-index profile was discussed in Sec. 1.3. Rays in meridional planes follow oscillatory planar trajec-

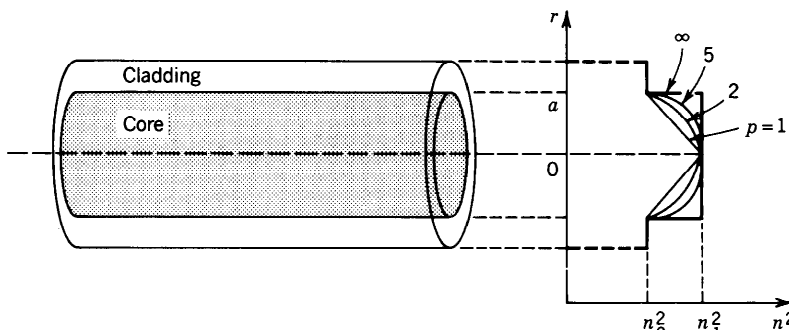


Figure 8.2-2 Power-law refractive-index profile $n^2(r)$ for different values of p .

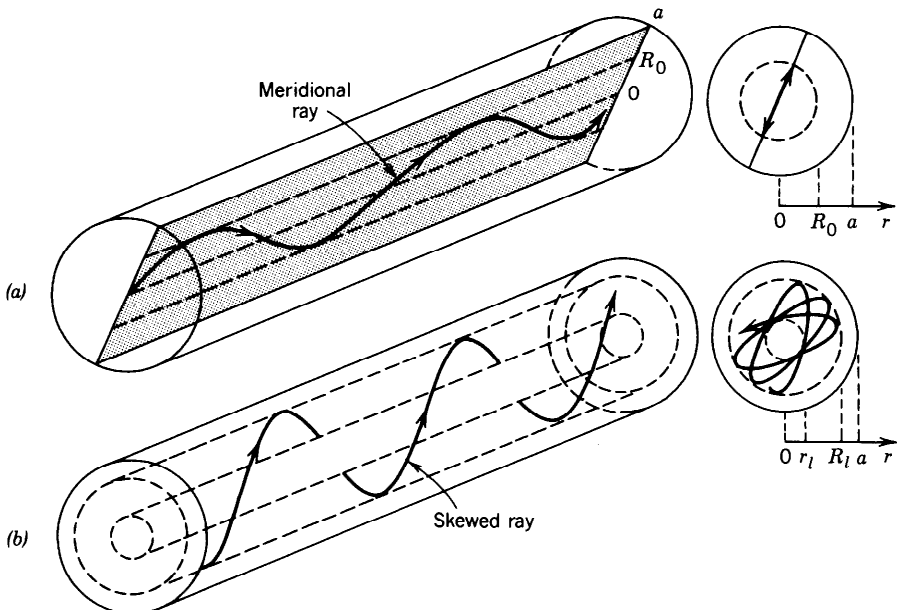


Figure 8.2-3 Guided rays in the core of a graded-index fiber. (a) A meridional ray confined to a meridional plane inside a cylinder of radius R_0 . (b) A skewed ray follows a helical trajectory confined within two cylindrical shells of radii r_i and R_i .

ries, whereas skewed rays follow helical trajectories with the turning points forming cylindrical caustic surfaces, as illustrated in Fig. 8.2-3. Guided rays are confined within the core and do not reach the cladding.

A. Guided Waves

The modes of the graded-index fiber may be determined by writing the Helmholtz equation (8.1-4) with $n = n(r)$, solving for the spatial distributions of the field components, and using Maxwell's equations and the boundary conditions to obtain the characteristic equation as was done in the step-index case. This procedure is in general difficult.

In this section we use instead an approximate approach based on picturing the field distribution as a quasi-plane wave traveling within the core, approximately along the trajectory of the optical ray. A quasi-plane wave is a wave that is locally identical to a plane wave, but changes its direction and amplitude slowly as it travels. This approach permits us to maintain the simplicity of rays optics but retain the phase associated with the wave, so that we can use the self-consistency condition to determine the propagation constants of the guided modes (as was done in the planar waveguide in Sec. 7.2). This approximate technique, called the WKB (Wentzel–Kramers–Brillouin) method, is applicable only to fibers with a large number of modes (large V parameter).

Quasi-Plane Waves

Consider a solution of the Helmholtz equation (8.1-4) in the form of a quasi-plane wave (see Sec. 2.3)

$$U(\mathbf{r}) = \alpha(\mathbf{r}) \exp[-jk_o S(\mathbf{r})], \quad (8.2-3)$$

where $\alpha(\mathbf{r})$ and $S(\mathbf{r})$ are real functions of position that are slowly varying in comparison with the wavelength $\lambda_o = 2\pi/k_o$. We know from Sec. 2.3 that $S(\mathbf{r})$ approximately

290 FIBER OPTICS

satisfies the eikonal equation $|\nabla S|^2 \approx n^2$, and that the rays travel in the direction of the gradient ∇S . If we take $k_o S(\mathbf{r}) = k_o s(r) + l\phi + \beta z$, where $s(r)$ is a slowly varying function of r , the eikonal equation gives

$$\left(k_o \frac{ds}{dr} \right)^2 + \beta^2 + \frac{l^2}{r^2} = n^2(r) k_o^2. \quad (8.2-4)$$

The local spatial frequency of the wave in the radial direction is the partial derivative of the phase $k_o S(\mathbf{r})$ with respect to r ,

$$k_r = k_o \frac{ds}{dr}, \quad (8.2-5)$$

so that (8.2-3) becomes

$$U(r) = \alpha(r) \exp\left(-j \int_0^r k_r dr\right) e^{-jl\phi} e^{-j\beta z}, \quad (8.2-6)$$

Quasi-Plane Wave

and (8.2-4) gives

$$k_r^2 = n^2(r) k_o^2 - \beta^2 - \frac{l^2}{r^2}. \quad (8.2-7)$$

Defining $k_\phi = l/r$, i.e., $\exp(-jl\phi) = \exp(-jk_\phi r\phi)$, and $k_z = \beta$, we find that (8.2-7) gives $k_r^2 + k_\phi^2 + k_z^2 = n^2(r) k_o^2$. The quasi-plane wave therefore has a local wavevector \mathbf{k} with magnitude $n(r)k_o$ and cylindrical-coordinate components (k_r, k_ϕ, k_z) . Since $n(r)$ and k_ϕ are functions of r , k_r is also generally position dependent. The direction of \mathbf{k} changes slowly with r (see Fig. 8.2-4) following a helical trajectory similar to that of the skewed ray shown earlier in Fig. 8.2-3(b).

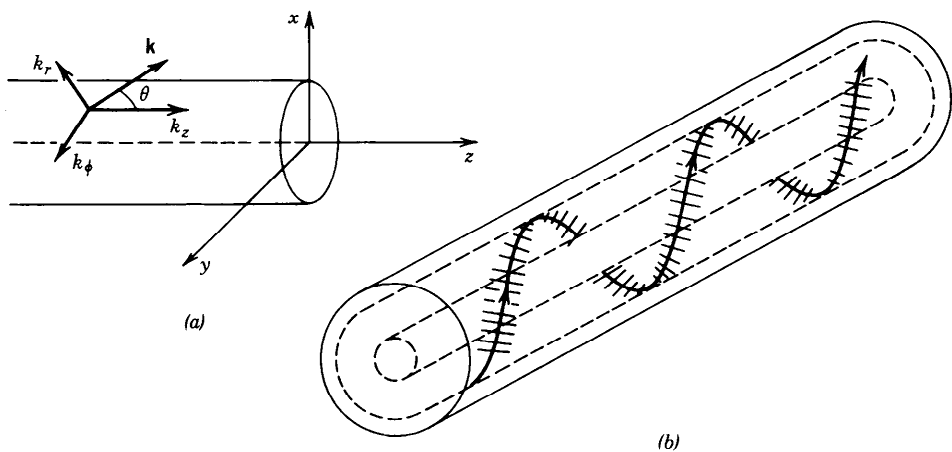


Figure 8.2-4 (a) The wavevector $\mathbf{k} = (k_r, k_\phi, k_z)$ in a cylindrical coordinate system. (b) Quasi-plane wave following the direction of a ray.

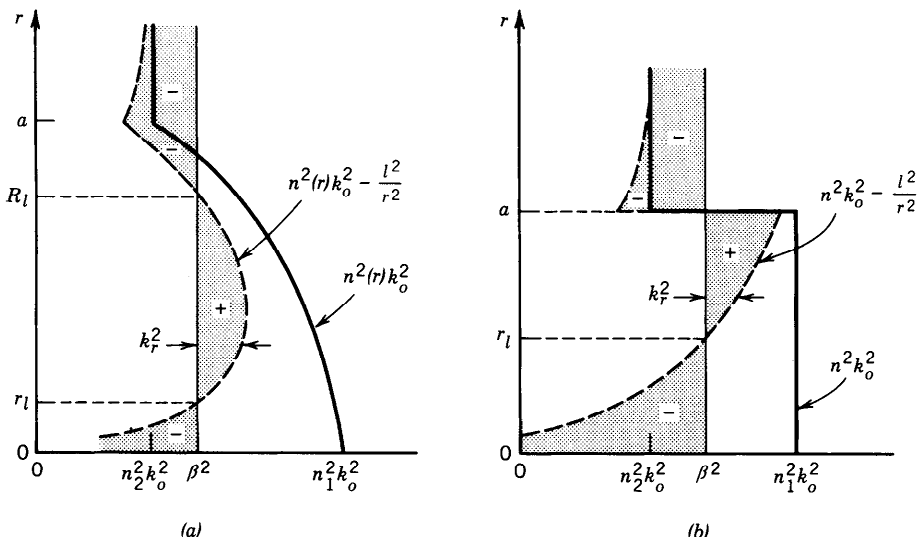


Figure 8.2-5 Dependence of $n^2(r)k_o^2$, $n^2(r)k_o^2 - l^2/r^2$, and $k_r^2 = n^2(r)k_o^2 - l^2/r^2 - \beta^2$ on the position r . At any r , k_r^2 is the width of the shaded area with the + and - signs denoting positive and negative k_r^2 . (a) Graded-index fiber; k_r^2 is positive in the region $r_l < r < R_l$. (b) Step-index fiber; k_r^2 is positive in the region $r_l < r < a$.

To determine the region of the core within which the wave is bound, we determine the values of r for which k_r is real, or $k_r^2 > 0$. For a given l and β we plot $k_r^2 = [n^2(r)k_o^2 - l^2/r^2 - \beta^2]$ as a function of r . The term $n^2(r)k_o^2$ is first plotted as a function of r [the thick continuous curve in Fig. 8.2-5(a)]. The term l^2/r^2 is then subtracted, yielding the dashed curve. The value of β^2 is marked by the thin continuous vertical line. It follows that k_r^2 is represented by the difference between the dashed line and the thin continuous line, i.e., by the shaded area. Regions where k_r^2 is positive or negative are indicated by the + or - signs, respectively. Thus k_r is real in the region $r_l < r < R_l$, where

$$n^2(r)k_o^2 - \frac{l^2}{r^2} - \beta^2 = 0, \quad r = r_l \quad \text{and} \quad r = R_l. \quad (8.2-8)$$

It follows that the wave is basically confined within a cylindrical shell of radii r_l and R_l just like the helical ray trajectory shown in Fig. 8.2-3(b).

These results are also applicable to the step-index fiber in which $n(r) = n_1$ for $r < a$, and $n(r) = n_2$ for $r > a$. In this case the quasi-plane wave is guided in the core by reflecting from the core-cladding boundary at $r = a$. As illustrated in Fig. 8.2-5(b), the region of confinement is $r_l < r < a$, where

$$n_1^2 k_o^2 - \frac{l^2}{r_l^2} - \beta^2 = 0. \quad (8.2-9)$$

The wave bounces back and forth helically like the skewed ray shown in Fig. 8.1-2. In the cladding ($r > a$) and near the center of the core ($r < r_l$), k_r^2 is negative so that k_r is imaginary, and the wave therefore decays exponentially. Note that r_l depends on β . For large β (or large l), r_l is large; i.e., the wave is confined to a thin cylindrical shell near the edge of the core.

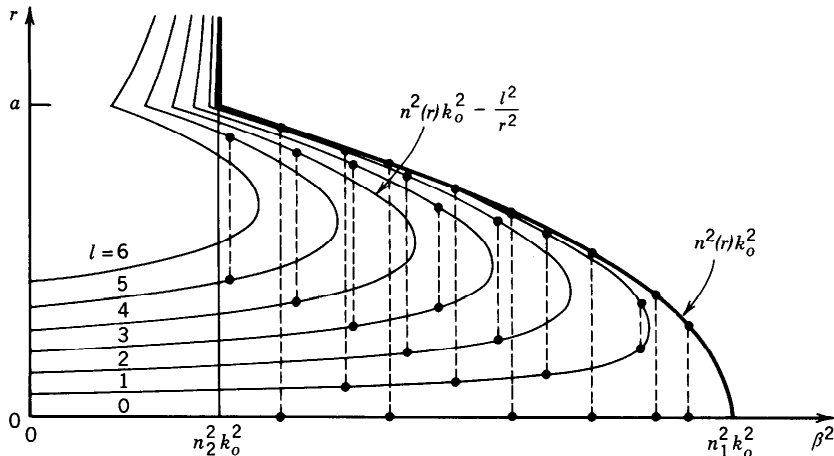


Figure 8.2-6 The propagation constants and confinement regions of the fiber modes. Each curve corresponds to an index l . In this plot $l = 0, 1, \dots, 6$. Each mode (representing a certain value of m) is marked schematically by two dots connected by a dashed vertical line. The ordinates of the dots mark the radii r_l and R_l of the cylindrical shell within which the mode is confined. Values on the abscissa are the squared propagation constants β^2 of the mode.

Modes

The modes of the fiber are determined by imposing the self-consistency condition that the wave reproduce itself after one helical period of traveling between r_l and R_l and back. The azimuthal path length corresponding to an angle 2π must correspond to a multiple of 2π phase shift, i.e., $k_\phi 2\pi r = 2\pi l$; $l = 0, \pm 1, \pm 2, \dots$. This condition is evidently satisfied since $k_\phi = l/r$. In addition, the radial round-trip path length must correspond to a phase shift equal to an integer multiple of 2π ,

$$2 \int_{r_l}^{R_l} k_r dr = 2\pi m, \quad m = 1, 2, \dots, M_l. \quad (8.2-10)$$

This condition, which is analogous to the self-consistency condition (7.2-2) for planar waveguides, provides the characteristic equation from which the propagation constants β_{lm} of the modes are determined. These values are marked schematically in Fig. 8.2-6; the mode $m = 1$ has the largest value of β (approximately $n_1 k_o$) and $m = M_l$ has the smallest value (approximately $n_2 k_o$).

Number of Modes

The total number of modes can be determined by adding the number of modes M_l for $l = 0, 1, \dots, l_{\max}$. We shall address this problem using a different procedure. We first determine the number q_β of modes with propagation constants greater than a given value β . For each l , the number of modes $M_l(\beta)$ with propagation constant greater than β is the number of multiples of 2π the integral in (8.2-10) yields, i.e.,

$$M_l(\beta) = \frac{1}{\pi} \int_{r_l}^{R_l} k_r dr = \frac{1}{\pi} \int_{r_l}^{R_l} \left[n^2(r) k_o^2 - \frac{l^2}{r^2} - \beta^2 \right]^{1/2} dr, \quad (8.2-11)$$

where r_l and R_l are the radii of confinement corresponding to the propagation constant β as given by (8.2-8). Clearly, r_l and R_l depend on β .

The total number of modes with propagation constant greater than β is therefore

$$q_\beta = 4 \sum_{l=0}^{l_{\max}(\beta)} M_l(\beta), \quad (8.2-12)$$

where $l_{\max}(\beta)$ is the maximum value of l that yields a bound mode with propagation constants greater than β , i.e., for which the peak value of the function $n^2(r)k_o^2 - l^2/r^2$ is greater than β^2 . The grand total number of modes M is q_β for $\beta = n_2 k_o$. The factor of 4 in (8.2-12) accounts for the two possible polarizations and the two possible polarities of the angle ϕ , corresponding to positive or negative helical trajectories for each (l, m) . If the number of modes is sufficiently large, we can replace the summation in (8.2-12) by an integral,

$$q_\beta \approx 4 \int_0^{l_{\max}(\beta)} M_l(\beta) dl. \quad (8.2-13)$$

For fibers with a power-law refractive-index profile, we substitute (8.2-1) into (8.2-11), and the result into (8.2-13), and evaluate the integral to obtain

$$q_\beta \approx M \left[\frac{1 - (\beta/n_1 k_o)^2}{2\Delta} \right]^{(p+2)/p}, \quad (8.2-14)$$

where

$$M \approx \frac{p}{p+2} n_1^2 k_o^2 a^2 \Delta = \frac{p}{p+2} \frac{V^2}{2}. \quad (8.2-15)$$

Here $\Delta = (n_1 - n_2)/n_1$ and $V = 2\pi(a/\lambda_o)NA$ is the fiber V parameter. Since $q_\beta \approx M$ at $\beta = n_2 k_o$, M is indeed the total number of modes.

For step-index fibers ($p = \infty$),

$$q_\beta \approx M \left[\frac{1 - (\beta/n_1 k_o)^2}{2\Delta} \right] \quad (8.2-16)$$

and

$$M \approx \frac{V^2}{2}.$$

(8.2-17)

Number of Modes
 (Step-Index Fiber)
 $V = 2\pi(a/\lambda_o)NA$

This expression for M is nearly the same as $M \approx 4V^2/\pi^2 \approx 0.41V^2$ in (8.1-18), which was obtained in Sec. 8.1 using a different approximation.

B. Propagation Constants and Velocities

Propagation Constants

The propagation constant β_q of mode q is obtained by inverting (8.2-14),

$$\beta_q \approx n_1 k_o \left[1 - 2 \left(\frac{q}{M} \right)^{p/(p+2)} \Delta \right]^{1/2}, \quad q = 1, 2, \dots, M, \quad (8.2-18)$$

where the index q_β has been replaced by q , and β replaced by β_q . Since $\Delta \ll 1$, the approximation $(1 + \delta)^{1/2} \approx 1 + \frac{1}{2}\delta$ (when $|\delta| \ll 1$) can be applied to (8.2-18), yielding

$$\boxed{\beta_q \approx n_1 k_o \left[1 - \left(\frac{q}{M} \right)^{p/(p+2)} \Delta \right].} \quad (8.2-19)$$

Propagation Constants
 $q = 1, 2, \dots, M$

The propagation constant β_q therefore decreases from $\approx n_1 k_o$ (at $q = 1$) to $n_2 k_o$ (at $q = M$), as illustrated in Fig. 8.2-7.

In the step-index fiber ($p = \infty$),

$$\boxed{\beta_q \approx n_1 k_o \left(1 - \frac{q}{M} \Delta \right).} \quad (8.2-20)$$

Propagation Constants
(Step-Index Fiber)
 $q = 1, 2, \dots, M$

This expression is identical to (8.1-22) if the index $q = 1, 2, \dots, M$ is replaced by $(l + 2m)^2$, where $l = 0, 1, \dots, \sqrt{M}$; $m = 1, 2, \dots, \sqrt{M}/2 - l/2$.

Group Velocities

To determine the group velocity $v_g = d\omega/d\beta_q$, we write β_q as a function of ω by substituting (8.2-15) into (8.2-19), substituting $n_1 k_o = \omega/c_1$ into the result, and evaluating $v_g = (d\beta_q/d\omega)^{-1}$. With the help of the approximation $(1 + \delta)^{-1} \approx 1 - \delta$ when

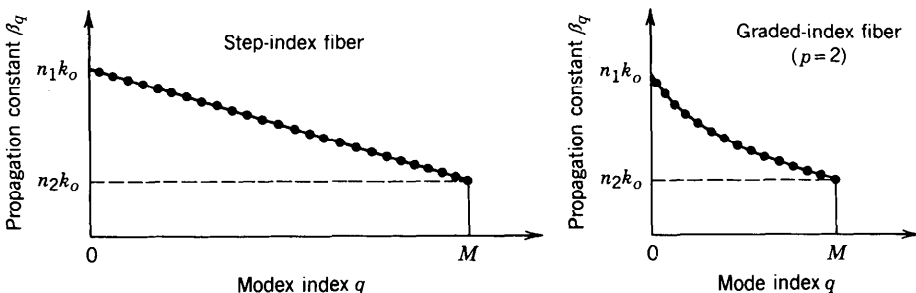


Figure 8.2-7 Dependence of the propagation constants β_q on the mode index $q = 1, 2, \dots, M$.

$|\delta| \ll 1$, and assuming that c_1 and Δ are independent of ω (i.e., ignoring material dispersion), we obtain

$$v_q \approx c_1 \left[1 - \frac{p-2}{p+2} \left(\frac{q}{M} \right)^{p/(p+2)} \Delta \right]. \quad (8.2-21)$$

Group Velocities
 $q = 1, 2, \dots, M$

For the step-index fiber ($p = \infty$)

$$v_q \approx c_1 \left(1 - \frac{q}{M} \Delta \right). \quad (8.2-22)$$

Group Velocities
(Step-Index Fiber)
 $q = 1, 2, \dots, M$

The group velocity varies from approximately c_1 to $c_1(1 - \Delta)$. This reproduces the result obtained in (8.1-23).

Optimal Index Profile

Equation (8.2-21) indicates that the grade profile parameter $p = 2$ yields a group velocity $v_q \approx c_1$ for all q , so that all modes travel at approximately the same velocity c_1 . The advantage of the graded-index fiber for multimode transmission is now apparent.

To determine the group velocity with better accuracy, we repeat the derivation of v_q from (8.2-18), taking three terms in the Taylor's expansion $(1 + \delta)^{1/2} \approx 1 + \delta/2 - \delta^2/8$, instead of two. For $p = 2$, the result is

$$v_q = c_1 \left(1 - \frac{q}{M} \frac{\Delta^2}{2} \right). \quad (8.2-23)$$

Group Velocities
($p = 2$)
 $q = 1, \dots, M$

Thus the group velocities vary from approximately c_1 at $q = 1$ to approximately $c_1(1 - \Delta^2/2)$ at $q = M$. In comparison with the step-index fiber, for which the group velocity ranges between c_1 and $c_1(1 - \Delta)$, the fractional velocity difference for the parabolically graded fiber is $\Delta^2/2$ instead of Δ for the step-index fiber (Fig. 8.2-8). Under ideal conditions, the graded-index fiber therefore reduces the group velocity

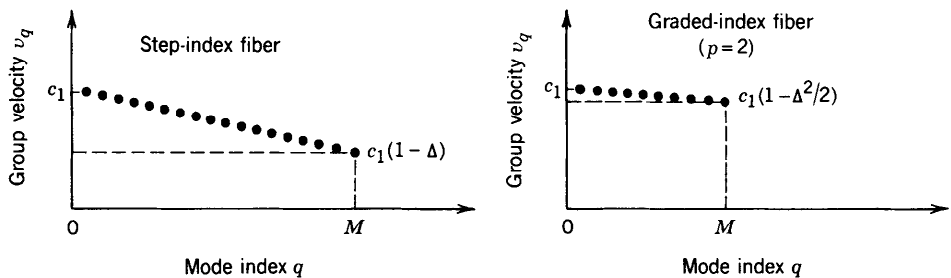


Figure 8.2-8 Group velocities v_q of the modes of a step-index fiber ($p = \infty$) and an optimal graded-index fiber ($p = 2$).

296 FIBER OPTICS

difference by a factor $\Delta/2$, thus realizing its intended purpose of equalizing the mode velocities. Since the analysis leading to (8.2-23) is based on a number of approximations, however, this improvement factor is only a rough estimate; indeed it is not fully attained in practice.

For $p = 2$, the number of modes M given by (8.2-15) becomes

$$M \approx \frac{V^2}{4}. \quad (8.2-24)$$

Number of Modes
(Graded-Index Fiber, $p = 2$)
 $V = 2\pi(a/\lambda_o)\text{NA}$

Comparing this with (8.2-17), we see that the number of modes in an optimal graded-index fiber is approximately one-half the number of modes in a step-index fiber of the same parameters n_1, n_2 , and a .

8.3 ATTENUATION AND DISPERSION

Attenuation and dispersion limit the performance of the optical-fiber medium as a data transmission channel. Attenuation limits the magnitude of the optical power transmitted, whereas dispersion limits the rate at which data may be transmitted through the fiber, since it governs the temporal spreading of the optical pulses carrying the data.

A. Attenuation

The Attenuation Coefficient

Light traveling through an optical fiber exhibits a power that decreases exponentially with the distance as a result of absorption and scattering. The attenuation coefficient α is usually defined in units of dB/km,

$$\alpha = \frac{1}{L} 10 \log_{10} \frac{1}{\mathcal{T}}, \quad (8.3-1)$$

where $\mathcal{T} = P(L)/P(0)$ is the power transmission ratio (ratio of transmitted to incident power) for a fiber of length L km. The relation between α and \mathcal{T} is illustrated in Fig. 8.3-1 for $L = 1$ km. A 3-dB attenuation, for example, corresponds to $\mathcal{T} = 0.5$, while 10 dB is equivalent to $\mathcal{T} = 0.1$ and 20 dB corresponds to $\mathcal{T} = 0.01$, and so on.

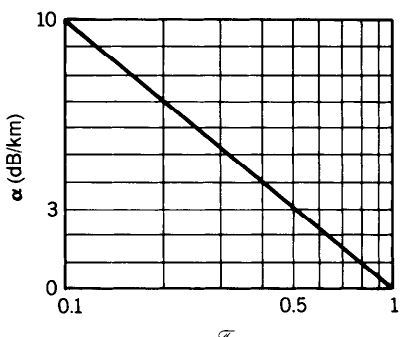


Figure 8.3-1 Relation between transmittance \mathcal{T} and attenuation coefficient α in dB units.

Losses in dB units are additive, whereas the transmission ratios are multiplicative. Thus for a propagation distance of z kilometers, the loss is αz decibels and the power transmission ratio is

$$\frac{P(z)}{P(0)} = 10^{-\alpha z/10} \approx e^{-0.23\alpha z}. \quad (\alpha \text{ in dB/km}) \quad (8.3-2)$$

Note that if the attenuation coefficient is measured in km^{-1} units, instead of in dB/km , then

$$P(z)/P(0) = e^{-\alpha z} \quad (8.3-3)$$

where $\alpha \approx 0.23\alpha$. Throughout this section α is taken in dB/km units so that (8.3-2) applies. Elsewhere in the book, however, we use α to denote the attenuation coefficient (m^{-1} or cm^{-1}) in which case the power attenuation is described by (8.3-3).

Absorption

The attenuation coefficient of fused silica glass (SiO_2) is strongly dependent on wavelength, as illustrated in Fig. 8.3-2. This material has two strong absorption bands: a middle-infrared absorption band resulting from vibrational transitions and an ultraviolet absorption band due to electronic and molecular transitions. There is a window bounded by the tails of these bands in which there is essentially no intrinsic absorption. This window occupies the near-infrared region.

Scattering

Rayleigh scattering is another intrinsic effect that contributes to the attenuation of light in glass. The random localized variations of the molecular positions in glass create random inhomogeneities of the refractive index that act as tiny scattering centers. The amplitude of the scattered field is proportional to ω^2 .[†] The scattered intensity is therefore proportional to ω^4 or to $1/\lambda_o^4$, so that short wavelengths are scattered more than long wavelengths. Thus blue light is scattered more than red (a similar effect, the

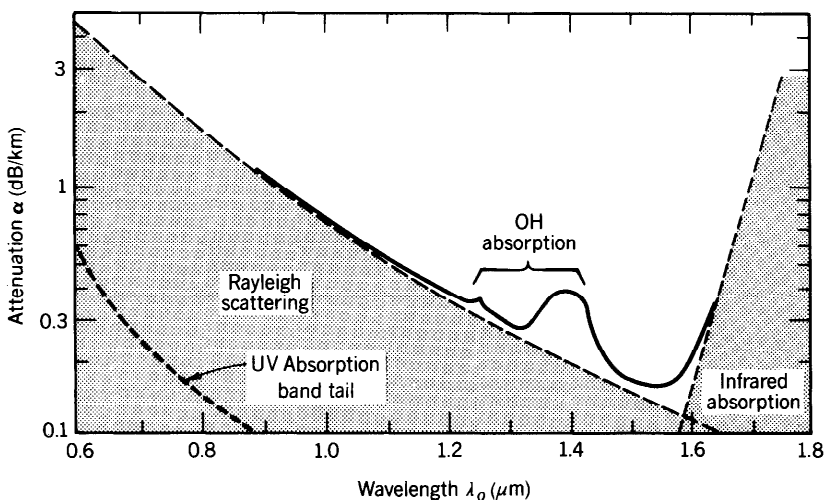


Figure 8.3-2 Dependence of the attenuation coefficient α of silica glass on the wavelength λ_o . There is a local minimum at $1.3 \mu\text{m}$ ($\alpha \approx 0.3 \text{ dB/km}$) and an absolute minimum at $1.55 \mu\text{m}$ ($\alpha \approx 0.16 \text{ dB/km}$).

[†]The scattering medium creates a polarization density \mathcal{P} which corresponds to a source of radiation proportional to $d^2\mathcal{P}/dt^2 = -\omega^2\mathcal{P}$; see (5.2-19).

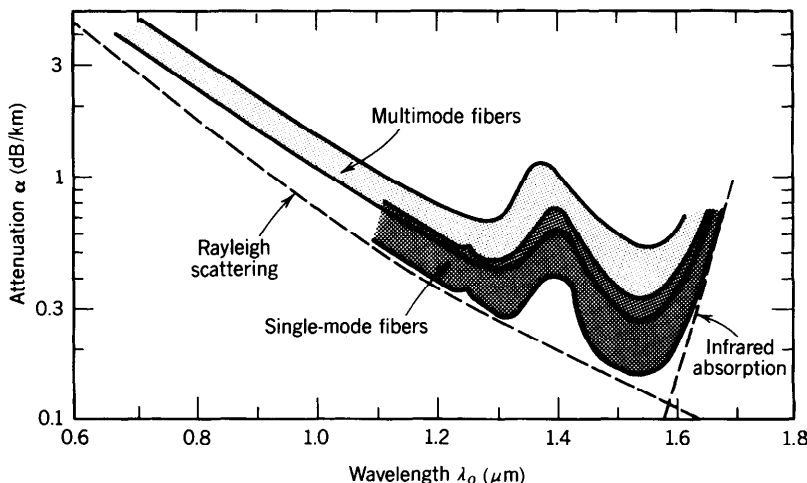


Figure 8.3-3 Ranges of attenuation coefficients of silica glass single-mode and multimode fibers.

scattering of sunlight from tiny atmospheric molecules, is the reason the sky appears blue). The attenuation caused by Rayleigh scattering therefore decreases with wavelength as $1/\lambda_0^4$, a relation known as **Rayleigh's inverse fourth-power law**. In the visible band, Rayleigh scattering is more significant than the tail of the ultraviolet absorption band, but it becomes negligible in comparison with infrared absorption for wavelengths greater than $1.6 \mu\text{m}$.

The transparent window in silica glass is therefore bounded by Rayleigh scattering on the short-wavelength side and by infrared absorption on the long-wavelength side (as indicated by the dashed lines in Fig. 8.3-2).

Extrinsic Effects

In addition to these intrinsic effects there are extrinsic absorption bands due to impurities, mainly OH vibrations associated with water vapor dissolved in the glass and metallic-ion impurities. Recent progress in the technology of fabricating glass fibers has made it possible to remove most metal impurities, but OH impurities are difficult to eliminate. Wavelengths at which glass fibers are used for optical communication are selected to avoid these absorption bands. Light-scattering losses may also be accentuated when dopants are added for the purpose of index grading, for example.

The attenuation coefficient of guided light in glass fibers depends on the absorption and scattering in the core and cladding materials. Since each mode has a different penetration depth into the cladding so that rays travel different effective distances, the attenuation coefficient is mode dependent. It is generally higher for higher-order modes. Single-mode fibers therefore typically have smaller attenuation coefficients than multimode fibers (Fig. 8.3-3). Losses are also introduced by small random variations in the geometry of the fiber and by bends.

B. Dispersion

When a short pulse of light travels through an optical fiber its power is “dispersed” in time so that the pulse spreads into a wider time interval. There are four sources of dispersion in optical fibers: modal dispersion, material dispersion, waveguide dispersion, and nonlinear dispersion.

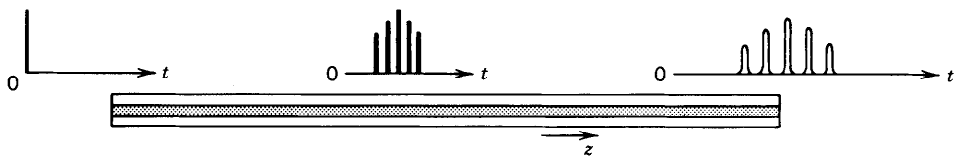


Figure 8.3-4 Pulse spreading caused by modal dispersion.

Modal Dispersion

Modal dispersion occurs in multimode fibers as a result of the differences in the group velocities of the modes. A single impulse of light entering an M -mode fiber at $z = 0$ spreads into M pulses with the differential delay increasing as a function of z . For a fiber of length L , the time delays encountered by the different modes are $\tau_q = L/v_q$, $q = 1, \dots, M$, where v_q is the group velocity of mode q . If v_{\min} and v_{\max} are the smallest and largest group velocities, the received pulse spreads over a time interval $L/v_{\min} - L/v_{\max}$. Since the modes are generally not excited equally, the overall shape of the received pulse is a smooth profile, as illustrated in Fig. 8.3-4. An estimate of the overall rms pulse width is $\sigma_\tau = \frac{1}{2}(L/v_{\min} - L/v_{\max})$. This width represents the response time of the fiber.

In a step-index fiber with a large number of modes, $v_{\min} \approx c_1(1 - \Delta)$ and $v_{\max} \approx c_1$ (see Sec. 8.1B and Fig. 8.2-8). Since $(1 - \Delta)^{-1} \approx 1 + \Delta$, the response time is

$$\boxed{\sigma_\tau \approx \frac{L}{c_1} \frac{\Delta}{2}}, \quad (8.3-4)$$

Response Time
(Multimode Step-Index Fiber)

i.e., it is a fraction $\Delta/2$ of the delay time L/c_1 .

Modal dispersion is much smaller in graded-index fibers than in step-index fibers since the group velocities are equalized and the differences between the delay times $\tau_q = L/v_q$ of the modes are reduced. It was shown in Sec. 8.2B and in Fig. 8.2-8 that in a graded-index fiber with a large number of modes and with an optimal index profile, $v_{\max} \approx c_1$ and $v_{\min} \approx c_1(1 - \Delta^2/2)$. The response time is therefore

$$\boxed{\sigma_\tau \approx \frac{L}{c_1} \frac{\Delta^2}{4}}, \quad (8.3-5)$$

Response Time
(Graded-Index Fiber)

which is a factor of $\Delta/2$ smaller than that in a step-index fiber.

EXAMPLE 8.3-1. Multimode Pulse Broadening Rate. In a step-index fiber with $\Delta = 0.01$ and $n = 1.46$, pulses spread at a rate of approximately $\sigma_\tau/L = \Delta/2c_1 = n_1\Delta/2c_o \approx 24$ ns/km. In a 100-km fiber, therefore, an impulse spreads to a width of $\approx 2.4 \mu\text{s}$. If the same fiber is optimally index graded, the pulse broadening rate is approximately $n_1\Delta^2/4c_o \approx 122$ ps/km, which is substantially reduced.

The pulse broadening arising from modal dispersion is proportional to the fiber length L in both step-index and graded-index fibers. This dependence, however, does not necessarily hold when the fibers are longer than a certain critical length because of mode coupling. Coupling occurs between modes of approximately the same propagation constants as a result of small imperfections in the fiber (random irregularities of the fiber surface, or inhomogeneities of the refractive index) which permit the optical power to be exchanged between the modes. Under certain conditions, the response time σ_τ of mode-coupled fibers is proportional to L for small L and to $L^{1/2}$ when a critical length is exceeded, so that pulses are broadened at a slower rate[†].

Material Dispersion

Glass is a dispersive medium; i.e., its refractive index is a function of wavelength. As discussed in Sec. 5.6, an optical pulse travels in a dispersive medium of refractive index n with a group velocity $v = c_o/N$, where $N = n - \lambda_o dn/d\lambda_o$. Since the pulse is a wavepacket, composed of a spectrum of components of different wavelengths each traveling at a different group velocity, its width spreads. The temporal width of an optical impulse of spectral width σ_λ (nm), after traveling a distance L , is $\sigma_\tau = |(d/d\lambda_o)(L/v)|\sigma_\lambda = |(d/d\lambda_o)(LN/c_o)|\sigma_\lambda$, from which

$$\sigma_\tau = |D_\lambda|\sigma_\lambda L, \quad (8.3-6)$$

Response Time
(Material Dispersion)

where

$$D_\lambda = -\frac{\lambda_o}{c_o} \frac{d^2n}{d\lambda_o^2} \quad (8.3-7)$$

is the material dispersion coefficient [see (5.6-21)]. The response time increases linearly with the distance L . Usually, L is measured in km, σ_τ in ps, and σ_λ in nm, so that D_λ has units of ps/km-nm. This type of dispersion is called **material dispersion** (as opposed to modal dispersion).

The wavelength dependence of the dispersion coefficient D_λ for silica glass is shown in Fig. 8.3-5. At wavelengths shorter than 1.3 μm the dispersion coefficient is negative,

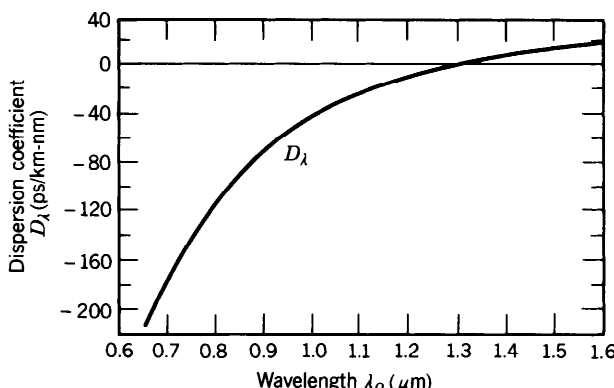


Figure 8.3-5 The dispersion coefficient D_λ of silica glass as a function of wavelength λ_o (see also Fig. 5.6-5).

[†]See, e.g., J. E. Midwinter, *Optical Fibers for Transmission*, Wiley, New York, 1979.

so that wavepackets of long wavelength travel faster than those of short wavelength. At a wavelength $\lambda_o = 0.87 \mu\text{m}$, the dispersion coefficient D_λ is approximately -80 ps/km-nm . At $\lambda_o = 1.55 \mu\text{m}$, $D_\lambda \approx +17 \text{ ps/km-nm}$. At $\lambda_o \approx 1.312 \mu\text{m}$ the dispersion coefficient vanishes, so that σ_τ in (8.3-6) vanishes. A more precise expression for σ_τ that incorporates the spread of the spectral width σ_λ about $\lambda_o = 1.312 \mu\text{m}$ yields a very small, but nonzero, width.

EXAMPLE 8.3-2. Pulse Broadening Associated with Material Dispersion. The dispersion coefficient $D_\lambda \approx -80 \text{ ps/km-nm}$ at $\lambda_o \approx 0.87 \mu\text{m}$. For a source of linewidth $\sigma_\lambda = 50 \text{ nm}$ (from an LED, for example) the pulse spreading rate in a single-mode fiber with no other sources of dispersion is $|D_\lambda|\sigma_\lambda = 4 \text{ ns/km}$. An impulse of light traveling a distance $L = 100 \text{ km}$ in the fiber is therefore broadened to a width $\sigma_\tau = |D_\lambda|\sigma_\lambda L = 0.4 \mu\text{s}$. The response time of the fiber is then $0.4 \mu\text{s}$. An impulse of narrower linewidth $\sigma_\lambda = 2 \text{ nm}$ (from a laser diode, for example) operating near $1.3 \mu\text{m}$, where the dispersion coefficient is 1 ps/km-nm , spreads at a rate of only 2 ps/km . A 100-km fiber thus has a substantially shorter response time, $\sigma_\tau = 0.2 \text{ ns}$.

Waveguide Dispersion

The group velocities of the modes depend on the wavelength even if material dispersion is negligible. This dependence, known as **waveguide dispersion**, results from the dependence of the field distribution in the fiber on the ratio between the core radius and the wavelength (a/λ_o). If this ratio is altered, by altering λ_o , the relative portions of optical power in the core and cladding are modified. Since the phase velocities in the core and cladding are different, the group velocity of the mode is altered. Waveguide dispersion is particularly important in single-mode fibers, where modal dispersion is not exhibited, and at wavelengths for which material dispersion is small (near $\lambda_o = 1.3 \mu\text{m}$ in silica glass).

As discussed in Sec. 8.1B, the group velocity $v = (d\beta/d\omega)^{-1}$ and the propagation constant β are determined from the characteristic equation, which is governed by the fiber V parameter $V = 2\pi(a/\lambda_o)\text{NA} = (a \cdot \text{NA}/c_o)\omega$. In the absence of material dispersion (i.e., when NA is independent of ω), V is directly proportional to ω , so that

$$\frac{1}{v} = \frac{d\beta}{d\omega} = \frac{d\beta}{dV} \frac{dV}{d\omega} = \frac{a \cdot \text{NA}}{c_o} \frac{d\beta}{dV}. \quad (8.3-8)$$

The pulse broadening associated with a source of spectral width σ_λ is related to the time delay L/v by $\sigma_\tau = |(d/d\lambda_o)(L/v)|\sigma_\lambda$. Thus

$$\sigma_\tau = |D_w|\sigma_\lambda L, \quad (8.3-9)$$

where

$$D_w = \frac{d}{d\lambda_o} \left(\frac{1}{v} \right) = -\frac{\omega}{\lambda_o} \frac{d}{d\omega} \left(\frac{1}{v} \right) \quad (8.3-10)$$

is the waveguide dispersion coefficient. Substituting (8.3-8) into (8.3-10) we obtain

$$D_w = -\left(\frac{1}{2\pi c_o}\right)V^2 \frac{d^2\beta}{dV^2}. \quad (8.3-11)$$

Thus the group velocity is inversely proportional to $d\beta/dV$ and the dispersion coefficient is proportional to $V^2 d^2\beta/dV^2$. The dependence of β on V is shown in Fig. 8.1-10(b) for the fundamental LP_{01} mode. Since β varies nonlinearly with V , the waveguide dispersion coefficient D_w is itself a function of V and is therefore also a function of the wavelength.[†] The dependence of D_w on λ_o may be controlled by altering the radius of the core or the index grading profile for graded-index fibers.

Combined Material and Waveguide Dispersion

The combined effects of material dispersion and waveguide dispersion (referred to here as **chromatic dispersion**) may be determined by including the wavelength dependence of the refractive indices, n_1 and n_2 and therefore NA, when determining $d\beta/d\omega$ from the characteristic equation. Although generally smaller than material dispersion, waveguide dispersion does shift the wavelength at which the total chromatic dispersion is minimum.

Since chromatic dispersion limits the performance of single-mode fibers, more advanced fiber designs aim at reducing this effect by using graded-index cores with refractive-index profiles selected such that the wavelength at which waveguide dispersion compensates material dispersion is shifted to the wavelength at which the fiber is to be used. **Dispersion-shifted fibers** have been successfully made by using a linearly tapered core refractive index and a reduced core radius, as illustrated in Fig. 8.3-6(a). This technique can be used to shift the zero-chromatic-dispersion wavelength from 1.3 μm to 1.55 μm , where the fiber has its lowest attenuation. Note, however, that the process of index grading itself introduces losses since dopants are used. Other grading profiles have been developed for which the chromatic dispersion vanishes at two wavelengths and is reduced for wavelengths between. These fibers, called **dispersion-flattened**, have been implemented by using a quadruple-clad layered grading, as illustrated in Fig. 8.3-6(b).

Combined Material and Modal Dispersion

The effect of material dispersion on pulse broadening in multimode fibers may be determined by returning to the original equations for the propagation constants β_q of the modes and determining the group velocities $v_q = (d\beta_q/d\omega)^{-1}$ with n_1 and n_2 being functions of ω . Consider, for example, the propagation constants of a graded-index fiber with a large number of modes, which are given by (8.2-19) and (8.2-15). Although n_1 and n_2 are dependent on ω , it is reasonable to assume that the ratio $\Delta = (n_1 - n_2)/n_1$ is approximately independent of ω . Using this approximation and evaluating $v_q = (d\beta_q/d\omega)^{-1}$, we obtain

$$v_q \approx \frac{c_o}{N_1} \left[1 - \frac{p-2}{p+2} \left(\frac{q}{M} \right)^{p/(p+2)} \Delta \right], \quad (8.3-12)$$

where $N_1 = (d/d\omega)(\omega n_1) = n_1 - \lambda_o (dn_1/d\lambda_o)$ is the group index of the core material. Under this approximation, the earlier expression (8.2-21) for v_q remains the same, except that the refractive index n_1 is replaced with the group index N_1 . For a step-index fiber ($p = \infty$), the group velocities of the modes vary from c_o/N_1 to

[†] For more details on this topic, see the reading list, particularly the articles by Gloge.

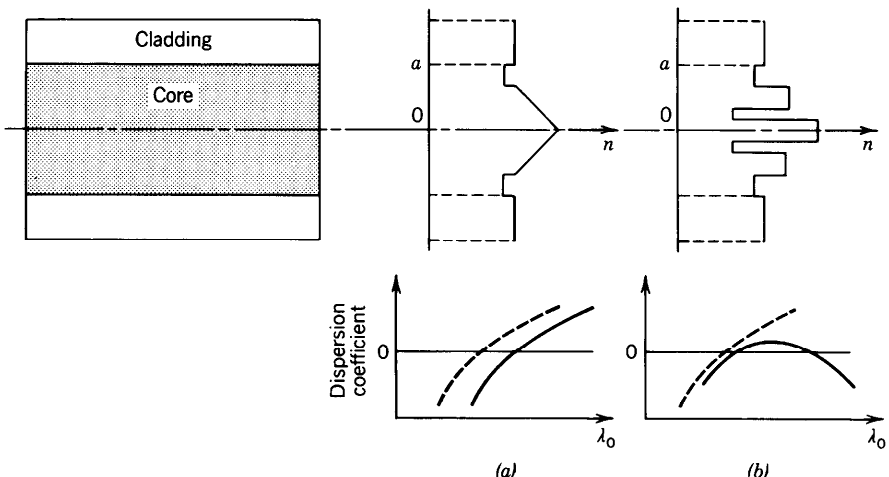


Figure 8.3-6 Refractive-index profiles and schematic wavelength dependences of the material dispersion coefficient (dashed curves) and the combined material and waveguide dispersion coefficients (solid curves) for (a) dispersion-shifted and (b) dispersion-flattened fibers.

$(c_o/N_1)(1 - \Delta)$, so that the response time is

$$\boxed{\sigma_\tau \approx \frac{L}{(c_o/N_1)} \frac{\Delta}{2}} \quad (8.3-13)$$

Response Time
(Multimode Step-Index Fiber
with Material Dispersion)

This should be compared with (8.3-4) when there is no material dispersion.

EXERCISE 8.3-1

Optimal Grade Profile Parameter. Use (8.2-19) and (8.2-15) to derive the following expression for the group velocity v_g when both n_1 and Δ are wavelength dependent:

$$v_g \approx \frac{c_o}{N_1} \left[1 - \frac{p - 2 - p_s}{p + 2} \left(\frac{q}{M} \right)^{p/(p+2)} \Delta \right], \quad q = 1, 2, \dots, M, \quad (8.3-14)$$

where $p_s = 2(n_1/N_1)(\omega/\Delta) d\Delta/d\omega$. What is the optimal value of the grade profile parameter p for minimizing modal dispersion?

Nonlinear Dispersion

Yet another dispersion effect occurs when the intensity of light in the core is sufficiently high, since the refractive indices then become intensity dependent and the material exhibits nonlinear behavior. The high-intensity parts of an optical pulse undergo phase shifts different from the low-intensity parts, so that the frequency is shifted by different amounts. Because of material dispersion, the group velocities are

304 FIBER OPTICS

modified, and consequently the pulse shape is altered. Under certain conditions, nonlinear dispersion can compensate material dispersion, so that the pulse travels without altering its temporal profile. The guided wave is then known as a solitary wave, or a soliton. Nonlinear optics is introduced in Chap. 19 and optical solitons are discussed in Sec. 19.8.

C. Pulse Propagation

As described in the previous sections, the propagation of pulses in optical fibers is governed by attenuation and several types of dispersion. The following is a summary and recapitulation of these effects, ignoring nonlinear dispersion.

An optical pulse of power $\tau_0^{-1}p(t/\tau_0)$ and short duration τ_0 , where $p(t)$ is a function which has unit duration and unit area, is transmitted through a multimode fiber of length L . The received optical power may be written in the form of a sum

$$P(t) \propto \sum_{q=1}^M \exp(-0.23\alpha_q L) \sigma_q^{-1} p\left(\frac{t - \tau_q}{\sigma_q}\right), \quad (8.3-15)$$

where M is the number of modes, the subscript q refers to mode q , α_q is the attenuation coefficient (dB/km), $\tau_q = L/v_q$ is the delay time, v_q is the group velocity, and $\sigma_q > \tau_0$ is the width of the pulse associated with mode q . In writing (8.3-15), we have implicitly assumed that the incident optical power is distributed equally among the M modes of the fiber. It has also been assumed that the pulse shape $p(t)$ is not altered; it is only delayed by times τ_q and broadened to widths σ_q as a result of propagation. As was shown in Sec. 5.6, an initial pulse with a Gaussian profile is indeed broadened without altering its Gaussian nature.

The received pulse is thus composed of M pulses of widths σ_q centered at time delays τ_q , as illustrated in Fig. 8.3-7. The composite pulse has an overall width σ_τ which represents the overall response time of the fiber.

We therefore identify two basic types of dispersion: **intermodal** and **intramodal**. Intermodal, or simply modal, dispersion is the delay distortion caused by the disparity among the delay times τ_q of the modes. The time difference $\frac{1}{2}(\tau_{\max} - \tau_{\min})$ between the longest and shortest delay constitutes modal dispersion. It is given by (8.3-4) and (8.3-5) for step-index and graded-index fibers with a large number of modes, respectively. Material dispersion has some effect on modal dispersion since it affects the delay times. For example, (8.3-13) gives the modal dispersion of a multimode fiber with material dispersion. Modal dispersion is directly proportional to the fiber length L , except for long fibers, in which mode coupling plays a role, whereupon it becomes proportional to $L^{1/2}$.

Intramodal dispersion is the broadening of the pulses associated with the individual modes. It is caused by a combination of material dispersion and waveguide dispersion

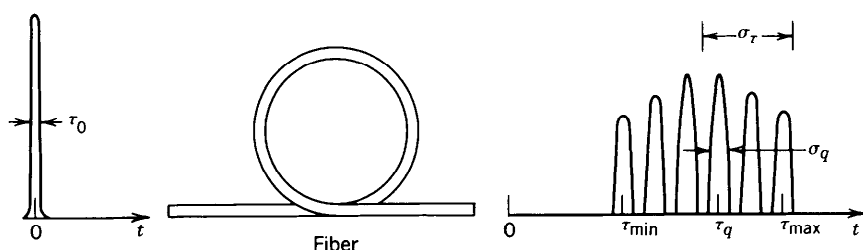


Figure 8.3-7 Response of a multimode fiber to a single pulse.

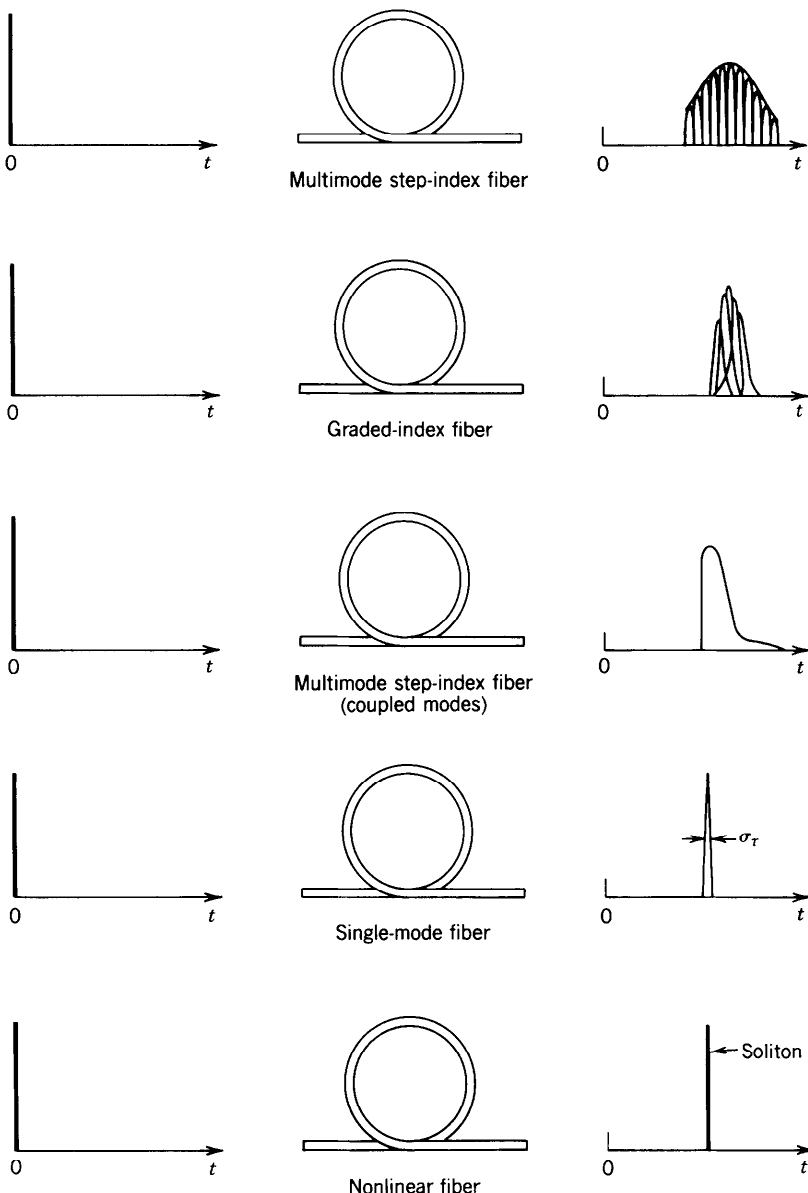


Figure 8.3-8 Broadening of a short optical pulse after transmission through different types of fibers. The width of the transmitted pulse is governed by modal dispersion in multimode (step-index and graded-index) fibers. In single-mode fibers the pulse width is determined by material dispersion and waveguide dispersion. Under certain conditions an intense pulse, called a soliton, can travel through a nonlinear fiber without broadening. This is a result of a balance between material dispersion and self-phase modulation (the dependence of the refractive index on the light intensity).

306 FIBER OPTICS

resulting from the finite spectral width of the initial optical pulse. The width σ_q is given by

$$\sigma_q^2 \approx \tau_0^2 + (D_q \sigma_\lambda L)^2, \quad (8.3-16)$$

where D_q is a dispersion coefficient representing the combined effects of material and waveguide dispersion for mode q . Material dispersion is usually more significant. For a very short initial width τ_0 , (8.3-16) gives

$$\sigma_q \approx D_q \sigma_\lambda L. \quad (8.3-17)$$

Figure 8.3-8 is a schematic illustration in which the profiles of pulses traveling through different types of fibers are compared. In multimode step-index fibers, the modal dispersion $\frac{1}{2}(\tau_{\max} - \tau_{\min})$ is usually much greater than the material/waveguide dispersion σ_q , so that intermodal dispersion dominates and $\sigma_\tau \approx \frac{1}{2}(\tau_{\max} - \tau_{\min})$. In multimode graded-index fibers, $\frac{1}{2}(\tau_{\max} - \tau_{\min})$ may be comparable to σ_q , so that the overall pulse width involves all dispersion effects. In single-mode fibers, there is obviously no modal dispersion and the transmission of pulses is limited by material and waveguide dispersion. The lowest overall dispersion is achieved in a single-mode fiber operating at the wavelength for which the combined material-waveguide dispersion vanishes.

READING LIST

Books

See also the books on optical waveguides in Chapter 7.

- P. K. Cheo, *Fiber Optics and Optoelectronics*, Prentice Hall, Englewood Cliffs, NJ, 1985, 2nd ed. 1990.
- F. C. Allard, *Fiber Optics Handbook for Engineers and Scientists*, McGraw-Hill, New York, 1990.
- C. Yeh, *Handbook of Fiber Optics: Theory and Applications*, Academic Press, Orlando, FL, 1990.
- L. B. Jeunhomme, *Single-Mode Fiber Optics*, Marcel Dekker, New York, 1983, 2nd ed. 1990.
- P. W. France, ed., *Fluoride Glass Optical Fibers*, CRC Press, Boca Raton, FL, 1989.
- P. Diament, *Wave Transmission and Fiber Optics*, Macmillan, New York, 1989.
- W. B. Jones, Jr., *Introduction to Optical Fiber Communication Systems*, Holt, Rinehart and Winston, New York, 1988.
- H. Murata, *Handbook of Optical Fibers and Cables*, Marcel Dekker, New York, 1988.
- E. G. Neuman, *Single-Mode Fibers—Fundamentals*, Springer-Verlag, New York, 1988.
- E. L. Safford, Jr. and J. A. McCann, *Fiberoptics and Laser Handbook*, Tab Books, Blue Ridge Summit, PA, 2nd ed. 1988.
- S. E. Miller and I. Kaminow, *Optical Fiber Telecommunications II*, Academic Press, Boston, MA, 1988.
- J. Gowar, *Optical Communication Systems*, Prentice Hall, Englewood Cliffs, NJ, 1984.
- R. G. Seippel, *Fiber Optics*, Reston Publishing, Reston, VA, 1984.
- ANSI/IEEE Standards 812-1984, *IEEE Standard Definitions of Terms Relating to Fiber Optics*, IEEE, New York, 1984.
- A. H. Cherin, *An Introduction to Optical Fibers*, McGraw-Hill, New York, 1983.
- G. E. Keiser, *Optical Fiber Communications*, McGraw-Hill, New York, 1983.
- C. Hentschel, *Fiber Optics Handbook*, Hewlett-Packard, Palo Alto, CA, 1983.
- Y. Suematsu and K. Iga, *Introduction to Optical Fiber Communications*, Wiley, New York, 1982.
- T. Okoshi, *Optical Fibers*, Academic Press, New York, 1982.
- C. K. Kao, *Optical Fiber Systems*, McGraw-Hill, New York, 1982.
- E. A. Lacy, *Fiber Optics*, Prentice-Hall, Englewood Cliffs, NJ, 1982.

- D. Marcuse, *Light Transmission Optics*, Van Nostrand Reinhold, New York, 1972, 2nd ed. 1982.
- D. Marcuse, *Principles of Optical Fiber Measurements*, Academic Press, New York, 1981.
- A. B. Sharma, S. J. Halme, and M. M. Butusov, *Optical Fiber Systems and Their Components*, Springer-Verlag, Berlin, 1981.
- CSELT (Centro Studi e Laboratori Telecomunicazioni), *Optical Fibre Communications*, McGraw-Hill, New York, 1981.
- M. K. Barnoski, ed., *Fundamentals of Optical Fiber Communications*, Academic Press, New York, 1976, 2nd ed. 1981.
- C. P. Sandbank, ed., *Optical Fibre Communication Systems*, Wiley, New York, 1980.
- M. J. Howes and D. V. Morgan, eds., *Optical Fibre Communications*, Wiley, New York, 1980.
- H. F. Wolf, ed., *Handbook of Fiber Optics*, Garland STPM Press, New York, 1979.
- D. B. Ostrowsky, ed., *Fiber and Integrated Optics*, Plenum Press, New York, 1979.
- J. E. Midwinter, *Optical Fibers for Transmission*, Wiley, New York, 1979.
- S. E. Miller and A. G. Chynoweth, *Optical Fiber Telecommunications*, Academic Press, New York, 1979.
- G. R. Elion and H. A. Elion, *Fiber Optics in Communication Systems*, Marcel Dekker, New York, 1978.
- H. G. Unger, *Planar Optical Waveguides and Fibers*, Clarendon Press, Oxford, 1977.
- J. A. Arnaud, *Beam and Fiber Optics*, Academic Press, New York, 1976.
- W. B. Allan, *Fibre Optics: Theory and Practice*, Plenum Press, New York, 1973.
- N. S. Kapany, *Fiber Optics: Principles and Applications*, Academic Press, New York, 1967.

Special Journal Issues

- Special issue on fiber-optic sensors, *Journal of Lightwave Technology*, vol. LT-5, no. 7, 1987.
- Special issue on fiber, cable, and splicing technology, *Journal of Lightwave Technology*, vol. LT-4, no. 8, 1986.
- Special issue on low-loss fibers, *Journal of Lightwave Technology*, vol. LT-2, no. 10, 1984.
- Special issue on fiber optics, *IEEE Transactions on Communications*, vol. COM-26, no. 7, 1978.

Articles

- M. G. Drexhage and C. T. Moynihan, Infrared Optical Fibers, *Scientific American*, vol. 259, no. 5, pp. 110–114, 1988.
- S. R. Nagel, Optical Fiber—the Expanding Medium, *IEEE Communications Magazine*, vol. 25, no. 4, pp. 33–43, 1987.
- R. H. Stolen and R. P. DePaula, Single-Mode Fiber Components, *Proceedings of the IEEE*, vol. 75, pp. 1498–1511, 1987.
- P. S. Henry, Lightwave Primer, *IEEE Journal of Quantum Electronics*, vol. QE-21, pp. 1862–1879, 1985.
- T. Li, Advances in Optical Fiber Communications: An Historical Perspective, *IEEE Journal on Selected Areas in Communications*, vol. SAC-1, pp. 356–372, 1983.
- I. P. Kaminow, Polarization in Optical Fibers, *IEEE Journal of Quantum Electronics*, vol. QE-17, pp. 15–22, 1981.
- P. J. B. Clarricoats, Optical Fibre Waveguides—A Review, in *Progress in Optics*, vol. 14, E. Wolf, ed., North-Holland, Amsterdam, 1977.
- D. Gloge, Weakly Guiding Fibers, *Applied Optics*, vol. 10, pp. 2252–2258, 1971.
- D. Gloge, Dispersion in Weakly Guiding Fibers, *Applied Optics*, vol. 10, pp. 2442–2445, 1971.

PROBLEMS

- 8.1-1 **Coupling Efficiency.** (a) A source emits light with optical power P_0 and a distribution $I(\theta) = (1/\pi)P_0 \cos \theta$, where $I(\theta)$ is the power per unit solid angle in the direction making an angle θ with the axis of a fiber. Show that the power collected

308 FIBER OPTICS

by the fiber is $P = (\text{NA})^2 P_0$, i.e., the coupling efficiency is NA^2 where NA is the numerical aperture of the fiber.

(b) If the source is a planar light-emitting diode of refractive index n_s bonded to the fiber, and assuming that the fiber cross-sectional area is larger than the LED emitting area, calculate the numerical aperture of the fiber and the coupling efficiency when $n_1 = 1.46$, $n_2 = 1.455$, and $n_s = 3.5$.

- 8.1-2 Modes.** A step-index fiber has radius $a = 5 \mu\text{m}$, core refractive index $n_1 = 1.45$, and fractional refractive-index change $\Delta = 0.002$. Determine the shortest wavelength λ_c for which the fiber is a single-mode waveguide. If the wavelength is changed to $\lambda_c/2$, identify the indices (l, m) of all the guided modes.
- 8.1-3 Modal Dispersion.** A step-index fiber of numerical aperture $\text{NA} = 0.16$, core radius $a = 45 \mu\text{m}$ and core refractive index $n_1 = 1.45$ is used at $\lambda_o = 1.3 \mu\text{m}$, where material dispersion is negligible. If a pulse of light of very short duration enters the fiber at $t = 0$ and travels a distance of 1 km, sketch the shape of the received pulse:
- Using ray optics and assuming that only meridional rays are allowed.
 - Using wave optics and assuming that only meridional ($l = 0$) modes are allowed.
- 8.1-4 Propagation Constants and Group Velocities.** A step-index fiber with refractive indices $n_1 = 1.444$ and $n_2 = 1.443$ operates at $\lambda_o = 1.55 \mu\text{m}$. Determine the core radius at which the fiber V parameter is 10. Use Fig. 8.1-6 to estimate the propagation constants of all the guided modes with $l = 0$. If the core radius is now changed so that $V = 4$, use Fig. 8.1-10(b) to determine the propagation constant and the group velocity of the LP_{01} mode. *Hint:* Derive an expression for the group velocity $v = (d\beta/d\omega)^{-1}$ in terms of $d\beta/dV$ and use Fig. 8.1-10(b) to estimate $d\beta/dV$. Ignore the effect of material dispersion.
- 8.2-1 Numerical Aperture of a Graded-Index Fiber.** Compare the numerical apertures of a step-index fiber with $n_1 = 1.45$ and $\Delta = 0.01$ and a graded-index fiber with $n_1 = 1.45$, $\Delta = 0.01$, and a parabolic refractive-index profile ($p = 2$). (See Exercise 1.3-2 on page 24.)
- 8.2-2 Propagation Constants and Wavevector (Step-Index Fiber).** A step-index fiber of radius $a = 20 \mu\text{m}$ and refractive indices $n_1 = 1.47$ and $n_2 = 1.46$ operates at $\lambda_o = 1.55 \mu\text{m}$. Using the quasi-plane wave theory and considering only guided modes with azimuthal index $l = 1$:
- Determine the smallest and largest propagation constants.
 - For the mode with the smallest propagation constant, determine the radii of the cylindrical shell within which the wave is confined, and the components of the wavevector \mathbf{k} at $r = 5 \mu\text{m}$.
- 8.2-3 Propagation Constants and Wavevector (Graded-Index Fiber).** Repeat Problem 8.2-2 for a graded-index fiber with parabolic refractive-index profile with $p = 2$.
- 8.3-1 Scattering Loss.** At $\lambda_o = 820 \text{ nm}$ the absorption loss of a fiber is 0.25 dB/km and the scattering loss is 2.25 dB/km . If the fiber is used instead at $\lambda_o = 600 \text{ nm}$ and calorimetric measurements of the heat generated by light absorption give a loss of 2 dB/km , estimate the total attenuation at $\lambda_o = 600 \text{ nm}$.
- 8.3-2 Modal Dispersion in Step-Index Fibers.** Determine the core radius of a multimode step-index fiber with a numerical aperture $\text{NA} = 0.1$ if the number of modes $M = 5000$ when the wavelength is $0.87 \mu\text{m}$. If the core refractive index $n_1 = 1.445$, the group index $N_1 = 1.456$, and Δ is approximately independent of wavelength, determine the modal-dispersion response time σ_r for a 2-km fiber.
- 8.3-3 Modal Dispersion in Graded-Index Fibers.** Consider a graded-index fiber with $a/\lambda_o = 10$, $n_1 = 1.45$, $\Delta = 0.01$, and a power-law profile with index p . Determine

the number of modes M , and the modal-dispersion pulse-broadening rate σ_r/L for $p = 1.9, 2, 2.1$, and ∞ .

- 8.3-4 **Pulse Propagation.** A pulse of initial width τ_0 is transmitted through a graded-index fiber of length L kilometers and power-law refractive-index profile with profile index p . The peak refractive index n_1 is wavelength-dependent with $D_\lambda = -(\lambda_o/c_o)d^2n_1/d\lambda_o^2$, Δ is approximately independent of wavelength, σ_λ is the source's spectral width, and λ_o is the operating wavelength. Discuss the effect of increasing each of the following parameters on the width of the received pulse: $L, \tau_0, p, |D_\lambda|, \sigma_\lambda$, and λ_o .

Optoelectronic Devices and Applications of Optical Fibers

Dr. C. Krishnamoorthi PhD
krishnamoorthi.c@vit.ac.in

Ceter for Nanotechnology Research, Vellore Institute of Technology

8/10/2018

1 Optical Transmitters

- For efficient light absorption and emission
- LED
- Laser Diode or Diode laser

2 Fiber Optical Receivers

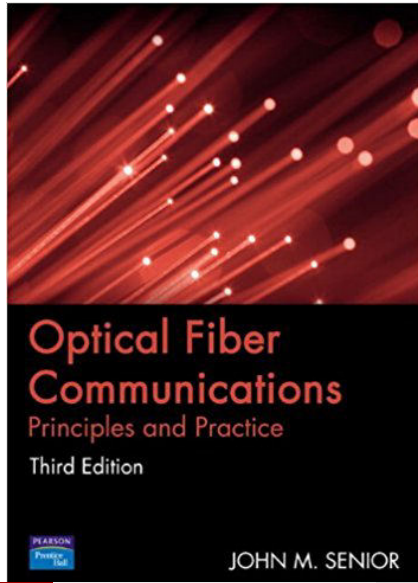
- Classical photodetectors
- Modern photodetectors

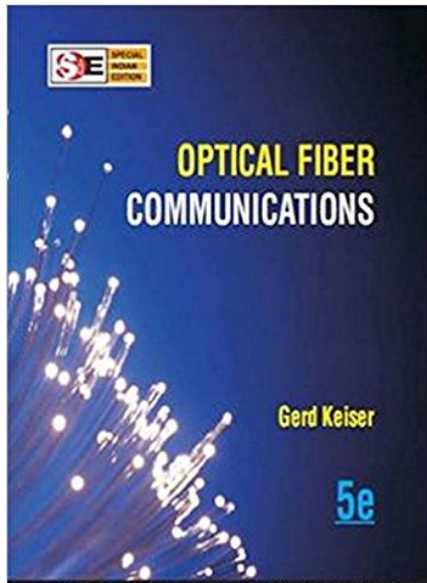
3 Applications

- Endoscopy
- In communication

Textbook 1

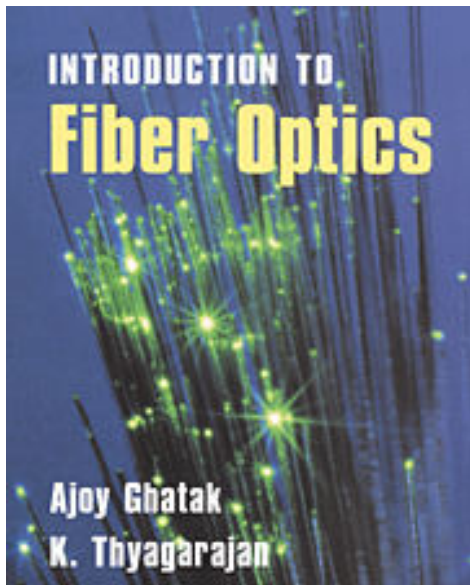
28.optoelectronic_devices_and_applications-CKM_08-Apr-2021_Reference





Textbook 3

28.optoelectronic_devices_and_applications-CKM_08-Apr-2021_Reference

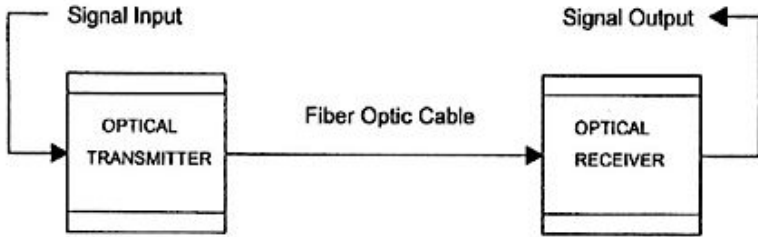


Syllabus of Module 7a

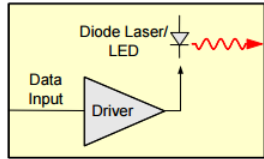
28 optoelectronic devices and applicaitons-CKM_08-Apr-2021_Reference

Module:7	Optoelectronic Devices & Applications of Optical fibers	9 hours	SLO: 2,4
Sources-LED & Laser Diode, Detectors-Photodetectors- PN & PIN - Applications of fiber optics in communication- Endoscopy.			

Components of fiber optic comm. networks



optical Transmitter



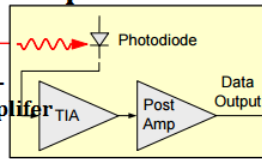
Optical Fiber

Booster Amplifier

Inline Amplifier

Pre-Amplifier

optical Receiver



Fiber optic comm. components

28 optoelectronic devices and applications CKM_08-Apr-2021_Reference

- We know that in fiber-optic communication, three key components are required: **Optical transmitters, optical fiber cable and Optical receiver.**
- We are familiar with the “rules for light (binary data) propagation” and “impediments for light (data) propagation” in OF cables.
- In fiber-optic communication information is transmitted from one point to another by sending short pulses of light through an optical fiber cable.
- The light forms an electromagnetic carrier-wave that is modulated to carry info.
- **“Optical transmitters”** are used to convert an electrical pulse signal into an optical pulse signal to launch into an OF cable.

Fiber optic comm. components

- “Optical receivers” are used to recover the signal as an electrical signal.

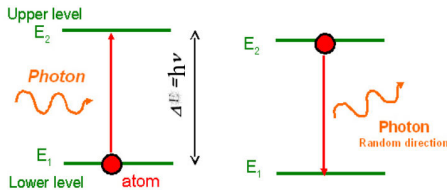
Optical Transmitters

28_optoelectronic_devices_and_applications-CKM_08-Apr-2021_Reference

- Optical transmitters are consists of optical source , electrical pulse generator and optical modulator .
- semiconductor devices such as LED and laser diode or diode laser are used as an optical sources.
- Semiconductor optical transmitters must be compact, efficient, and reliable while operating at optimal W/L or frequency.
- Ordinary electronic semiconductor diodes/transistors are activated by electrical potentials.
- Whereas optoelectronic devices (photodiodes and light emitting diodes) are designed to optimize light absorption and emission.

For efficient light absorption and emission

- It is known that incident photon with suitable energy generates e^- and h^+ pair in semiconductor. Similarly, e^- and h^+ pair recombination gives a photon emission.



- Light absorption and emission in semiconductor known to be heavily depend on detailed band structure of the semiconductor and charge carrier concentration in SC.
- Direct bandgap semiconductors**: $E = \frac{p^2}{2m} = \frac{\hbar^2 k^2}{2m}$; $k = \frac{2\pi}{\lambda}$. Hence, **E-k** diagram is important for band representation.

Working principle of light emission

- **Electron-hole pair recombination.**
- **High radiative recombination probability.**
- Radiative electron-hole recombination probability is high in direct bandgap SC, degenerate SC at depletion region of p-n junction.
- FB potential give sufficient electrical energy ($E = eV$) to inject carriers into depletion region.

Types of bandgap in semiconductors

26 optoelectronic devices and applications OKM 08 Apr-2021_Reference

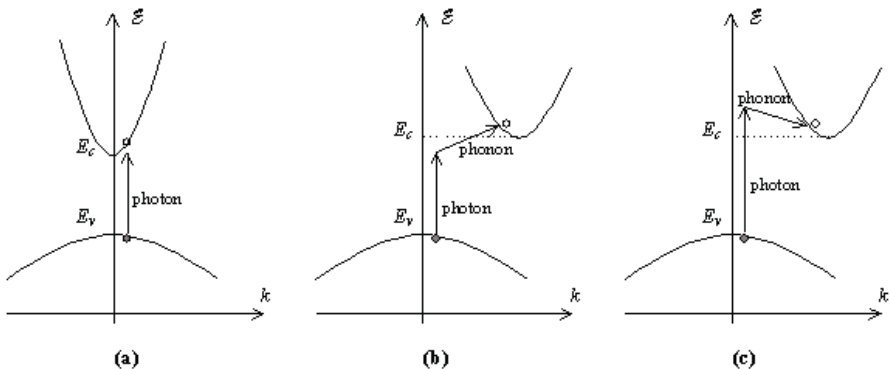


Figure: E-k diagram illustrating photon absorption in (a) direct bandgap (ii) indirect bandgap semiconductor assisted by phonon absorption and (c) indirect bandgap semiconductor assisted by phonon emission.

Direct bandgap semiconductor(DBSC)

- In electron-photon interaction, energy (E) and momentum ($p = \hbar k$) conservation is required.
- DBSC: the min. of CB and max. of VB are at the same k value. Whereas in indirect bandgap semiconductors (IBSC), the min. of CB is not at same k value of max. of VB.
- In SC, absorption of a photon occurs if an electron in the VB attains an energy and momentum of an empty state in CB.
- **Photons have little momentum relative their energy since they travel at the speed of light.** Therefore an electron makes almost a vertical transition on the E-k dia.
- Ref: Principles of Semiconductor devices by B Van Zeghbroeck ¹.

¹https://ecee.colorado.edu/~bart/book/book/chapter4/ch4_6.htm

//ecee.colorado.edu/~bart/book/book/chapter4/ch4_6.htm ↗ ↘ ↙ ↛

Indirect bandgap semiconductor (IBSC)

28 Optoelectronic devices and applications-CKW_08 Apr 2021_Reference

- If absorption of an incident photon directly provide an electron the correct energy and momentum equal to empty state in CB, it is DBSC. Ex.: GaAs, InP, and GaN. If does not provide, it is IBSC.Ex.: Si, Ge and SiC .
- Hence DBSC provide high e^- and h^+ radiative recombination probability than IBSCs.
- Phonon associate with lattice vibrations and has low velocity close to the speed of sound in a material. It has small energy and large momentum compared to that of a photon.
- Conservation of energy and momentum can therefore be obtained in absorption processes if phonon is created or existing phonon participates, as shown in Fig.

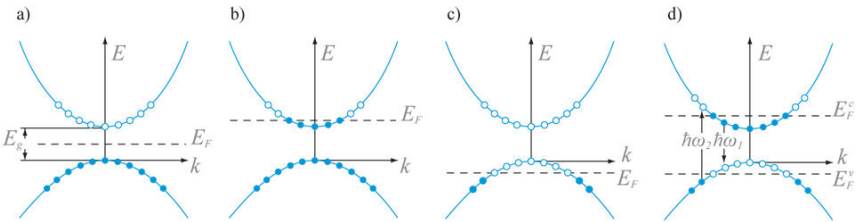
Degenerate SOs

28_optoelectronic_devices_and_applications-CKM_08-Apr-2021_Reference

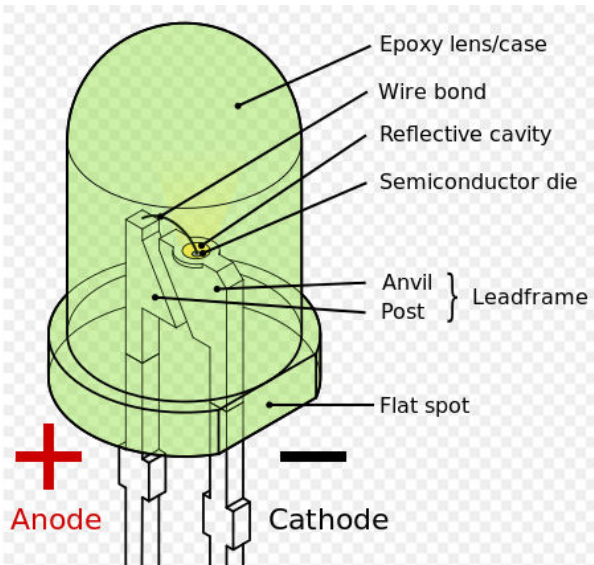
- **High radiative recombination probability is achievable at high minority-carrier densities at a region in a semiconductor.**
- Degenerate semiconductors provide high minority carrier densities in a p-n junction region.
- A degenerate semiconductor p-n junction provide high minority carrier densities at a metallurgical junction (p- & n-) at low current densities.

Degenerate SO

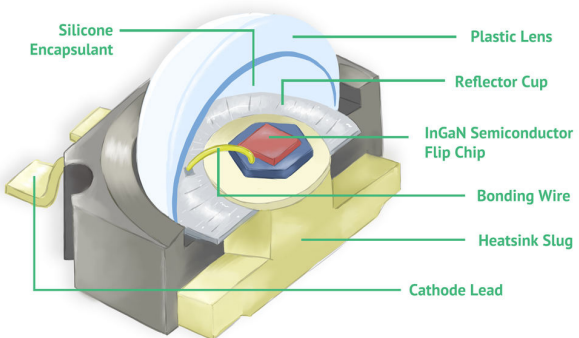
28_optoelectronic_devices_and_applications-CKM_08-Apr-2021_Reference



LED construction

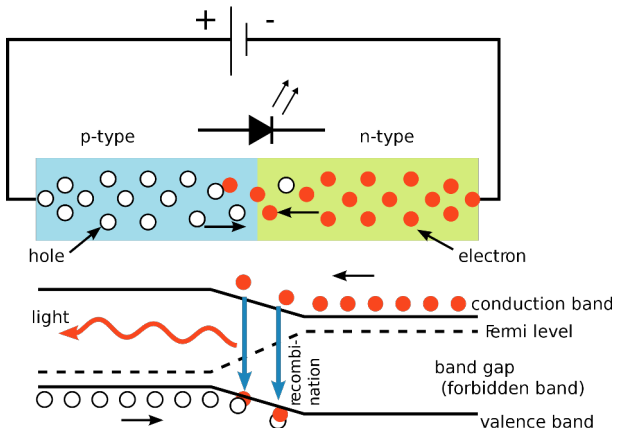


LED construction 2



LED construction 3

28.optoelectronic_devices_and_applications-CKM_08-Apr-2021_Reference

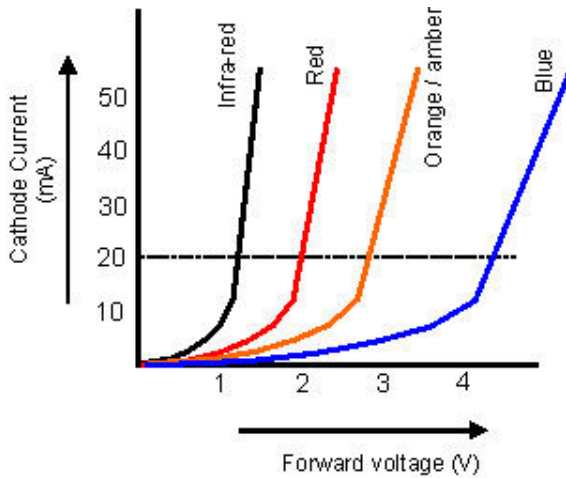


Working Principle

- In FB, flow of free electrons in the opposite direction of current and flow of holes in the direction of the current.
- Hence there will be high radiative recombination of these carriers at metallurgical junction region where minority carrier densities are high in VB.
- In p-region and n-region there are no high minority carrier densities and hence no radiative recombination.
- External electrical bias provides sufficient carriers motion across the Jn. region or injection into jn. region resulting in recombination process.

LED IV Characteristics

28.optoelectronic devices and applicaitons-CKM_08-Apr-2021_Reference



LED materials

28.optoelectronic devices_and_applications-CKM_08-Apr-2021_Reference

WAVELENGTH RANGE (NM)	COLOUR	V _F @ 20MA	MATERIAL
< 400	Ultraviolet	3.1 - 4.4	Aluminium nitride (AlN) Aluminium gallium nitride (AlGaN) Aluminium gallium indium nitride (AlGaN _x In _y N)
400 - 450	Violet	2.8 - 4.0	Indium gallium nitride (InGaN)
450 - 500	Blue	2.5 - 3.7	Indium gallium nitride (InGaN) Silicon carbide (SiC)
500 - 570	Green	1.9 - 4.0	Gallium phosphide (GaP) Aluminium gallium indium phosphide (AlGaInP) Aluminium gallium phosphide (AlGaP)
570 - 590	Yellow	2.1 - 2.2	Gallium arsenide phosphide (GaAsP) Aluminium gallium indium phosphide (AlGaInP) Gallium phosphide (GaP)
590 - 610	Orange / amber	2.0 - 2.1	Gallium arsenide phosphide (GaAsP) Aluminium gallium indium phosphide (AlGaInP) Gallium phosphide (GaP)
610 - 760	Red	1.6 - 2.0	Aluminium gallium arsenide (AlGaAs) Gallium arsenide phosphide (GaAsP)

LED

28.optoelectronic_devices_and_applications-CKM_08-Apr-2021_Reference

- LED sources are cheap and reliable. They emit only incoherent light with relatively wide spectral width of 30-60 nm. In view of this the signal will be subjected to chromatic dispersion.
- LED produce light through spontaneous emission and electroluminescence phenomenon.
- LED light transmission is also inefficient with only about 1% of I/P power eventually converted into launch power. Chromatic dispersion limits the data transmission distance.
- However, due to their relatively simple design, LEDs are very useful for low-cost apps.

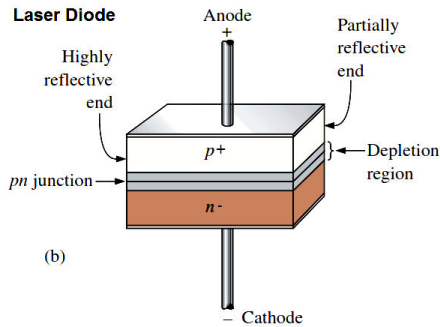
Laser Diode or Diode laser

28_optoelectronic_devices_and_applications-CKM_08-Apr-2021_Reference

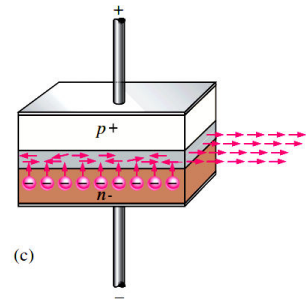
- LEDs produce incoherent light while laser diodes produce coherent light.
- Laser active medium formed by a p-n junction similar to that formed in LED.
- p-n junction is formed by degenerate (p^+ or n^-) direct band gap semiconductor (Al-doped GaAs).

Construction

Laser Diode



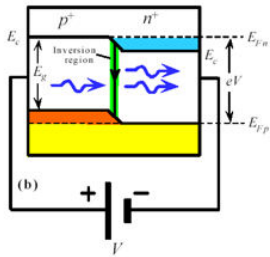
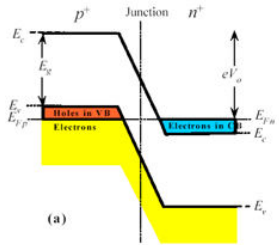
(b)



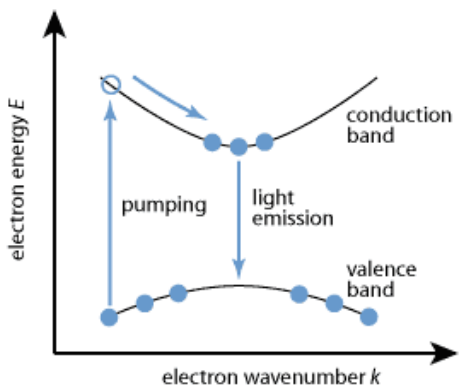
(c)

Diode Laser construction

28. optoelectronic devices and applications-CKM_08-Apr-2021_Reference



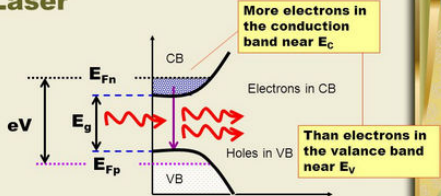
Diode Laser construction



Diode Laser construction

28. optoelectronic devices and applications-CKM_08-Apr-2021_Reference

Population Inversion in Diode Laser



$$E_{Fn} - E_{Fp} = eV$$

$$eV > E_g$$

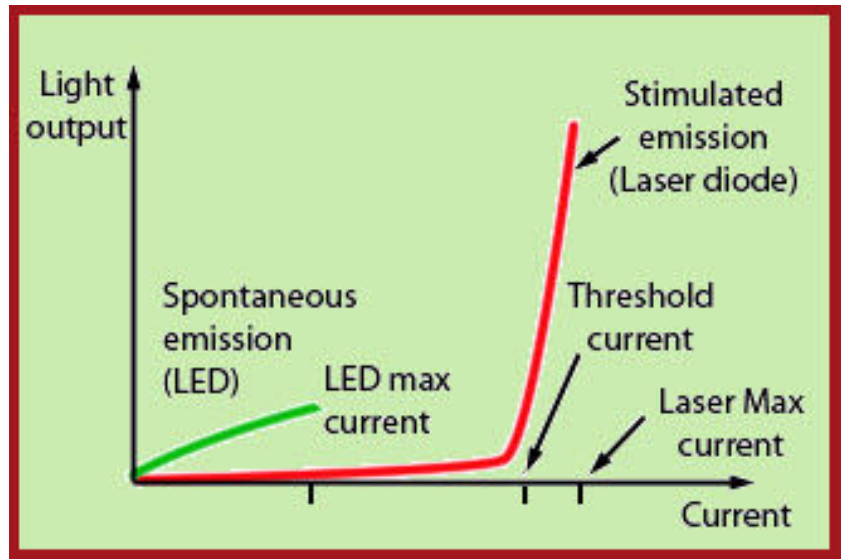
eV = forward bias voltage

Fwd Diode current pumping \rightarrow injection pumping

There is therefore a **population inversion** between energies near E_c and near E_v around the junction.

This is only achieved when degenerately doped p-n junction is forward bias with energy $> E_{gap}$

I-V characteristics



Working principle

- On applying FB connections, e^- and h^+ will inject into the opposite (minority) region through depletion (space charge) region.
- Radiative recombination occurs in the jn. region and emits suitable W/L radiation photons.
- The amount of recombination is determined by the current flowing across the junction.
- Emitted photons are oscillate to-and-pro between the mirrors, formed by smooth polishing, around the jn. region. Oscillating photons travel coherently in a particular, fixed direction.
- Laser O/P released through partially reflective mirror when energy is reached a threshold value.

Working principle

- Diode laser is 4-level laser. Hence efficiency is high.

LED vs Laser Diode

28.optoelectronic_devices_and_applications-CKM_08-Apr-2021_Reference

- LEDs are made from a very thin layer of fairly heavily doped SC material. Because of this thin layer a reasonable no. of photons leave the junction.
- Spontaneous emission predominates in LED. Hence it is incoherent. Whereas laser diode emits by stimulated emission and hence it is highly coherent.
-

Fiber Optic Receiver

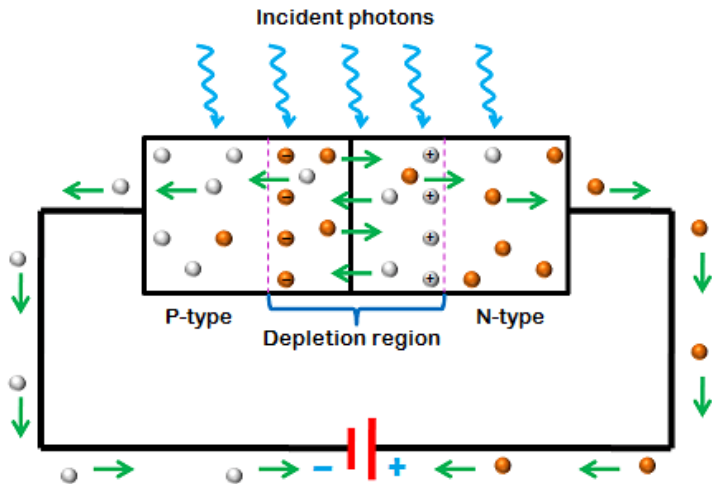
28 optoelectronic devices and applicaitons-CKM_08-Apr-2021_Reference

- They are used to receive the modulated light streams carrying data over fiber optic cables. The received light signals are converted into electrical pulses (square wave).
- Within the fiber optic receiver, photodetector is the key component. Major function of a photodetector is to convert an optical info signal back into an electrical signal (photocurrent) by photoelectric effect.
- Reliable photodetector is a semiconductor photo-diode. A variety of photodiodes such as **p-n photodiode, p-i-n photodiode, avalanche photodiodes, Schottky photodiodes**, etc., are used in fiber optic receivers.

Working principles of photodiode

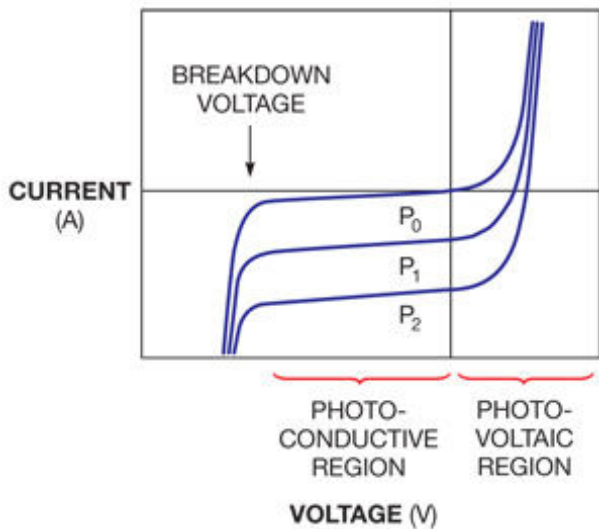
- Photodiode is basically a light detector semiconductor device, which converts light into electrical current or voltage.
- Separation and collection of electrical charge carriers (e^- and h^+) which are generated by absorbing a suitable energy (W/L) photon in SC.
- An e^- - h^+ pair was generated in depletion region of p-n junction and was efficiently separated under reverse bias configuration.
- $h\nu + e^0 \rightarrow e^- + h^+$.
- Photocurrent is proportional to light intensity falling on the photodiode.

p-n photodiode



PN Junction photodiode

I-V characteristics



Drawback of PN photodiode

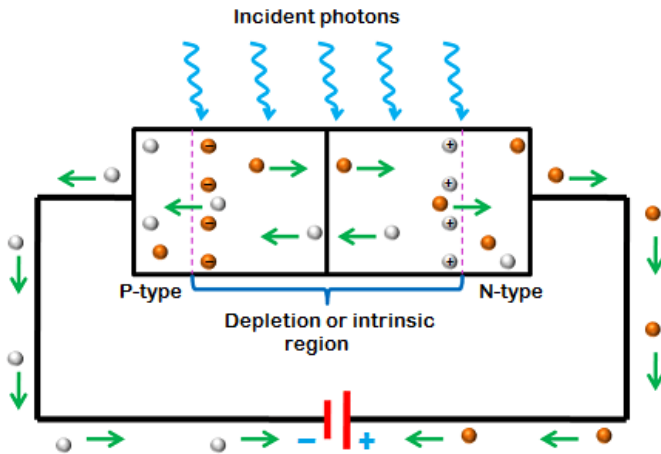
- The depletion region width in PN photodiode is limited. Hence the detection area is limited.
- High reverse bias voltage leads to p-n junction breakdown.
- Due to narrow depletion region, higher W/L radiation such as VIS and IR regions could not absorb completely.
- Higher W/L radiation travels deep into the device. Hence PN photodiode quantum efficiency is less.

p-intrinsic-n photodiode or PIN photodiode

- PIN photodiode is formed by a wide, intrinsic semiconductor sandwiched between p- and n-region of a diode.
- The p- and n- regions are typically heavily doped because they are used for ohmic contacts.
- when the reverse bias is applied, the space charge region must cover the intrinsic region completely.
- The wide intrinsic layer makes the PIN diode an inferior rectifier but makes it suitable for photodetector.
- The wider depletion width enables $e^- - h^+$ pair generation deep within the device. This increases the **quantum efficiency** of the photodiode.

PIN photodiode

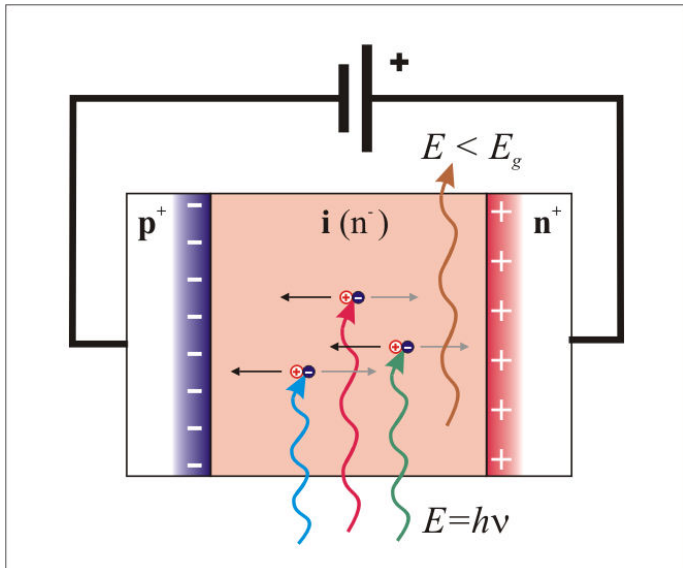
28 optoelectronic devices_and_applications-CKM_08-Apr-2021_Reference



PIN photodiode

PIN photodiode

28 optoelectronic devices_and_applications-CKM_08-Apr-2021_Reference



Quantum Efficiency of PIN photodiode

28 optoelectronic devices and applications-CKM_08-Apr-2021_Reference

- The electrical current produced by e^- and h^+ generated by incident photons are called as photocurrent (I_p). I_p is proportional to light power (P) (of suitable $h\nu$).
- $I_p \propto P$; $I_p = RP \implies R = \frac{I_p}{P}$, here R-responsivity of photodiode.
- $I_p = \frac{Q}{t} = \frac{N_e e}{t}$; here $\frac{N_e}{t}$ -no. of e^- generated per unit time.
- Light power $P = \frac{E}{t} = \frac{N_p E_p}{t}$; here $\frac{N_p}{t}$ - no. of photons incident on depletion region per unit time. E_p - average energy of incident photon.
-

$$R = \frac{I_p}{P} = \frac{\frac{N_e e}{t}}{\frac{N_p E_p}{t}} = \frac{N_e}{N_p} \frac{e}{E_p} = \frac{N_e}{N_p} \left(\frac{e \lambda_p}{hc} \right)$$

Endoscope

Self-study

In communication

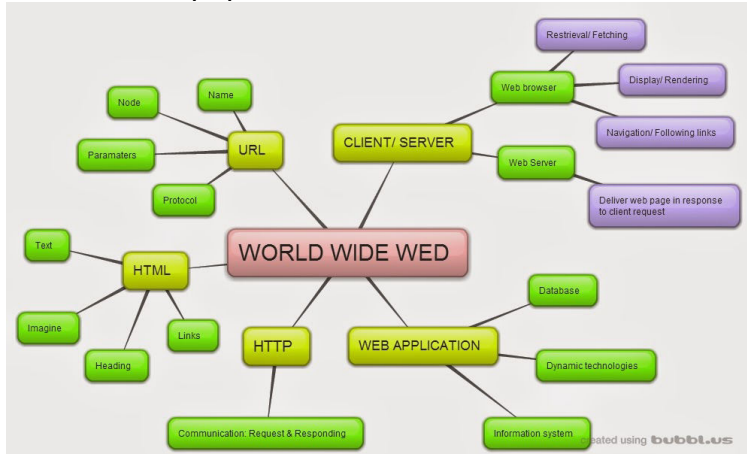
28_optoelectronic devices_and_applications-CKM_08-Apr-2021_Reference

Self-study

Assignment

28 optoelectronic_devices_and_applications-CKM_08-Apr-2021_Reference

Prepare Mind mapping of Module 7a (Optoelectronic devices and Applications of Optical fibers) content discussed in the class on a A4 size white paper.



28.optoelectronic_devices_and_applications-CKM_08-Apr-2021_Reference

THE END